

## PHASE EQUILIBRIA IN FATS

- theory and experiments -

## STELLINGEN BEHORENDE BIJ HET PROEFSCHRIFT 'LIQUID-MULTIPLE SOLID PHASE EQUILIBRIA IN FATS, theory and experiments'.

1. De complexe samenstelling van natuurlijke oliën en vetten maakt het gebruik van pseudocomponenten of triglyceride-groepen in berekeningen noodzakelijk. In vast-vloeistof evenwichtsberekeningen kunnen triglyceriden met een hoge mate van geometrische gelijkvormigheid en vergelijkbare smeltpunten als één (pseudo-)component worden beschouwd.

*Dit proefschrift, hoofdstuk 8*

2. Het voorkomen van meer dan één endotherme piek in een DSC-smeltcurve van een vet toont, in tegenstelling tot wat veelal wordt aangenomen, niet aan dat er in het vet verscheidene vaste fasen van verschillende samenstelling coëxisteren.

*R.E. Timms, Progr. Lipid Res. 23, 38 (1984)*

*Dit proefschrift, hoofdstuk 3.*

3. De door de Man et al. gevonden goede mengbaarheid van isobutanol met vloeibare triglyceriden is in strijd met de praktisch volledige onoplosbaarheid in isobutanol bij kamertemperatuur van vetkristallen uit normale margarines, die door hen is waargenomen.

*P. Chawla, J.M. de Man, JAOCS 67, 329 (1990)*

4. De smeltpieken van onstabiele polymorfe vormen van zuivere triglyceriden in de DSC-smeltcurven van Garti et al. vallen goeddeels samen met kristallisatiepieken van meer stabiele polymorfe vormen. Hierdoor zijn hun conclusies over het mechanisme van de polymorfe overgang en de hoeveelheid van een bepaalde polymorfe vorm onterecht.

*N. Garti, J. Schlichter, S. Sarig, Fat Sci. Technol. 90, 295 (1988)*

*N. Garti, J.S. Aronhime, S. Sarig, JAOCS 66, 1085 (1989)*

5. Bij modellering van de vermogensdissipatie in geschraapte warmtewisselaars mag het vermogen dat nodig is om het gekristalliseerde materiaal van de wand te schrapen niet worden verwaarloosd.

*T. Benezech, J. F. Maingonnat, J. of Food Engineering 7, 289 (1988)*

PHASE EQUILIBRIA IN FATS

- theory and experiments -

6. De hoeveelheid huishoudelijk afval in Nederland zal alleen afnemen indien alle betrokkenen naast een emotioneel een duidelijk economisch voordeel ervaren bij de productie van minder afval.
7. Een groot marktaandeel leidt tot risicomijdende en behoudzuchtige marketing. Dit werkt remmend op de technische innovativiteit.
8. Gelet op het belang ervan voor het dagelijks functioneren verdient toneelspelen een vaste plaats in het curriculum van het middelbaar onderwijs.

4/2084

7/2/773

7/2/773

**TR diss  
1846**

**LIQUID - MULTIPLE SOLID PHASE EQUILIBRIA  
IN FATS  
- theory and experiments -**

**LIQUID - MULTIPLE SOLID PHASE EQUILIBRIA  
IN FATS  
- theory and experiments -**



**EVENWICHTEN TUSSEN EEN VLOEIBARE EN VERSCHIEDENE  
VASTE FASEN IN SPIJSVETTEN  
- theorie en experimenten -**

**PROEFSCHRIFT**

ter verkrijging van de graad van doctor aan de Technische Universiteit Delft, op gezag van de Rector Magnificus Prof. drs. P.A. Schenck, in het openbaar te verdedigen ten overstaan van een commissie aangewezen door het College van Dekanen  
op donderdag 27 september 1990 te 14.00 uur, door

**Leendert Hendrik Wesdorp**

Chemicus

Geboren te Scheveningen



PHASE EQUILIBRIA IN FATS  
- theory and experiments -

*Dit proefschrift is goedgekeurd door de promotor:  
prof. dr. ir. J. de Swaan Arons.*

WOORD VOORAF

Dit proefschrift omvat een deel van de resultaten van een onderzoeksproject, dat wordt uitgevoerd bij het Unilever Research Laboratorium in Vlaardingen, in samenwerking met de Technische Universiteit Delft. De directie van Unilever Research ben ik zeer erkentelijk voor de gelegenheid die zij mij heeft geboden het hier beschreven werk uit te voeren en in deze vorm te publiceren.

Het proefschrift is tot stand gekomen dankzij de medewerking van velen, binnen en buiten Unilever Research. Ik wil met name noemen: Joke van Meeteren, om het vele experimentele werk dat zij heeft verzet en haar adviezen bij het gebruik van de Engelse taal, Paul Grootscholten, om zijn hulp bij het opzetten van dit onderzoek, Sijmen de Jong en Peter Overbosch, om hun grote bijdrage aan het vierde hoofdstuk,

Theo de Loos, Cor Peters en Iskander Gandasasmita, om hun belangrijke aandeel aan hoofdstuk 5,

Theo Struik, om de hulp bij hoofdstuk 6 en

Eli Royers, Ron v.d. Giessen, Aat Don en Aart van Beuzekom, om hun bijdragen aan diverse hoofdstukken.

Hun, en de vele anderen die aan dit proefschrift hebben meegewerkt, ben ik dank verschuldigd.

Mijn promotor, Jakob de Swaan Arons, dank ik voor de plezierige samenwerking en de stimulerende discussies die we hebben gevoerd.

Tenslotte, maar niet in de laatste plaats, dank ik mijn vrouw voor haar steun tijdens het schrijven van dit proefschrift.

PHASE EQUILIBRIA IN FATS  
- theory and experiments -

Table of Contents

1	INTRODUCTION AND PROBLEM DEFINITION .....	1
1.1	Solid-liquid phase equilibria and fats .....	1
1.2	Triacylglycerols: nomenclature .....	3
1.3	Triacylglycerols: polymorphism .....	4
	Basic polymorphic forms of TAGs .....	4
	Submodifications .....	7
	Stability .....	10
1.4	Methods for predicting solid phase composition and quantity .....	11
	Linear programming/multiple linear regression .....	12
	Excess contribution method .....	12
	TAGs inducteurs de cristallisation .....	13
	The CTG (classification of TAGs) method .....	14
1.5	Conclusion .....	15
2	APPROACH TO THE PROBLEM .....	17
2.1	Solid-liquid equilibrium thermodynamics .....	17
2.2	Kinetics of crystallization .....	19
	Polymorphism and kinetics of crystallization .....	20
	Shell formation .....	21
	Poor crystallinity .....	22
2.3	Conclusion and approach to the problem .....	23
3	FLASH CALCULATIONS .....	25
3.1	Introduction .....	25
3.2	Initial estimates and stability tests .....	26
	Splitting component method .....	27
	Michelsen's tangent plane criterion method .....	29
3.3	Iterating procedures .....	33
	Direct substitution .....	33
	Gibbs free energy minimisation .....	34
	Removal of phases .....	40
3.4	Comparison of methods .....	40
	Criteria .....	40
	Test results .....	41
3.5	Calculation of DSC-curves .....	43
3.6	Conclusion .....	45
4	PURE COMPONENT PROPERTIES .....	49
4.1	Literature data and correlations .....	49
	Correlating enthalpy of fusion and melting points of lipids .....	49
	Data and correlations for TAGs .....	51
4.2	Experimental .....	55
4.3	Development of the correlation .....	56
	Saturated TAGs .....	56
	Unsaturated TAGs .....	64
4.4	Conclusion .....	67
5	MIXING BEHAVIOUR IN THE LIQUID STATE .....	71
5.1	Literature .....	71
5.2	Model calculations .....	72
5.3	Experiments .....	74
	Method for determination of activity coefficients in mixtures of non-volatile liquids .....	74
	Experimental work .....	78

Results and discussion .....	79
5.4 Conclusion .....	84
6 MIXING BEHAVIOUR IN THE ALPHA MODIFICATION .....	87
6.1 Evidence for partial retained chain mobility .....	87
Supercooling of the alpha modification .....	90
Excess Gibbs energy in the alpha modification .....	90
6.2 Comparison of calculated and experimental alpha melting ranges .....	91
Experimental procedure .....	91
Calculations .....	95
Results .....	95
6.3 Conclusion .....	98
7 MIXING BEHAVIOUR IN THE BETA AND BETA' MODIFICATION .....	99
7.1 Excess Gibbs energy .....	99
Excess Gibbs energy models .....	100
Regular or athermal? .....	102
Phase diagrams .....	102
7.2 Experimental phase diagrams of TAGs .....	106
Measuring phase diagrams .....	106
Literature overview .....	111
Fitting experimental phase diagrams .....	113
Saturated TAGs .....	114
Saturated TAGs+ trans-containing TAGs .....	124
Saturated TAGs+ cis-unsaturated TAGs .....	127
Unsaturated TAGs .....	128
Summarizing .....	134
7.3 An alternative to phase diagram determination .....	136
How to proceed? .....	136
Formulation of an alternative method .....	137
DSC-curves of binary systems dissolved in a liquid TAG .....	139
What experiments? .....	141
7.4 Experimental .....	142
Principles of DSC .....	142
Thermal lag .....	143
Experimental procedure .....	144
7.5 Results .....	147
PSP and MPM with ESE and SEE .....	147
PSP and MPM with EPE and PEE .....	151
PSP and MPM with EEE .....	155
PSP and MPM with cis-unsaturated TAGs .....	157
7.6 Discussion .....	165
The use of DSC melting curves .....	165
Binary interaction parameters .....	165
Kinetics .....	166
7.7 Ternary solids .....	167
7.8 Conclusion .....	170
8 PREDICTING INTERACTION PARAMETERS .....	175
8.1 Are interaction parameters related to structural differences? .....	175
Degree of isomorphism .....	175
TAGs and the degree of isomorphism .....	178
8.2 Lattice distortion calculations .....	183
Equivalent distortions in the beta-2 modification ..	184
Beta-2A lattice distortion calculations .....	188
8.3 An empirical method .....	190

PHASE EQUILIBRIA IN FATS  
- theory and experiments -

The method .....	190
Discussion .....	193
8.4 Conclusion .....	194
9 PRACTICAL APPLICATIONS .....	197
9.1 Prediction of melting ranges .....	197
9.2 Fractional crystallization .....	200
9.3 Recrystallization phenomena .....	202
The influence of precrystallization and temperature cycling .....	202
Sandiness .....	205
9.4 Application outside edible oils and fats .....	207
Solid-liquid phase behaviour of n-alkanes .....	207
Petroleum waxes .....	211
Substituted naphthalenes .....	211
9.5 Conclusion of this work .....	212
SAMENVATTING .....	215
SUMMARY .....	219
APPENDIX 1. PURE COMPONENT DATA .....	223
APPENDIX 2. SPECIFIC RETENTION VOLUMES .....	243
APPENDIX 3. TAG PURITY .....	247
APPENDIX 4. PHASE DIAGRAMS .....	249
CURRICULUM VITAE .....	255

## CHAPTER 1 INTRODUCTION AND PROBLEM DEFINITION

*It is important for the production of fat containing food products to control the melting and solidification behaviour of edible oils and fats. The objective of this work is to develop a method to predict the melting range and solid phase composition of fats from their overall composition. Fats consist of triacylglycerols (TAGs), which show polymorphism in the solid phase. The polymorphic behaviour is reviewed. The nomenclature for TAGs and groups of TAGs used in this work is explained. Existing methods for solid phase prediction are discussed.*

### 1.1 SOLID-LIQUID PHASE EQUILIBRIA AND FATS

The fact that many languages have different words for the solid and liquid state of mixtures of triacylglycerols (triglycerides, TAGs) indicates that the solid-liquid phase behaviour of TAGs is something everyone encounters in daily life. Coconut 'oil' can be conveniently used as table oil in many tropical countries, while in N-W Europe it is considered a stone hard 'fat'.

Edible oils and fats usually consist for more than 95% of a complex mixture of triacylglycerols (TAGs). Typically an edible oil or fat can contain more than 500 different TAGs. Edible oils and fats therefore do not possess a distinct melting point, but exhibit a long melting range.

This melting range is one of the main factors determining the properties of fat containing food products, like fat spreads, dressings, chocolate, cakes, ice-cream and cookies. A fat spread, for example, must contain enough liquid fat at refrigerator temperature in order to make it a spreadable, soft solid. At ambient temperature it still must contain enough solid fat to prevent the spread from becoming pourable and oiling out. To give the spread a nice taste, the fat should be liquid at mouth temperature (1). (fig 1.1 and 1.2 ).

A fat with an optimal melting range for a particular application is obtained by carefully blending natural and modified oils and fats. Of course the edible fats industry likes to be able to blend fats

SOLID-LIQUID PHASE EQUILIBRIA  
AND FATS

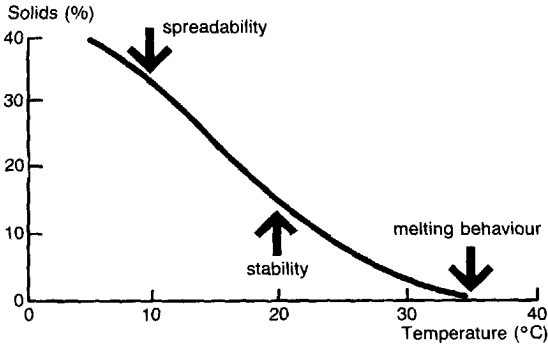


fig 1.1 Requirements for the melting range of a fat spread.

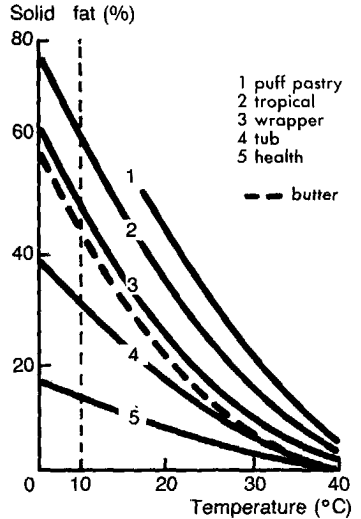


fig 1.2 Melting ranges of some types of fat spreads.

to a constant melting range regardless of the raw materials used. Other applications, like chocolate, require a fat with a very specific TAG-composition, which is often obtained by fractional crystallization of natural fats like palm oil. Simulation of this fractionation process requires calculation of the dependence of the crystal composition on process conditions. Both melting range and phase composition of a fat are primarily determined by the solid-liquid phase equilibrium in the fat. Describing the phase behaviour of edible oils and fats is therefore a necessity for the edible fats industry.

The objective of this work is to develop a method that enables prediction of the melting range and the solid phase composition of edible oils and fats.

## 1.2 TRIACYLGLYCEROLS: NOMENCLATURE

Edible oils and fats consist mainly of triacylglycerols (TAGs). For convenience TAGs will be identified by a 3-letter-code in this work. Each of the 3 characters in the code represents one of the fatty acids that is esterified with the glycerol. So glycerol-1-palmitate-2,3-distearate will be represented by PSS. The middle character always indicates the fatty acid that is esterified on the 2-position of the glycerol. The characters used to represent the fatty acids are given in table 1.1.

*table 1.1. Characters used for representing individual fatty acids.*

Code	Fatty acid	Code	Fatty acid
2	acetic acid	P	Palmitic acid (hexadecanoic acid)
4	butyric acid	S	Stearic acid (octadecanoic acid)
6	hexanoic acid	O	Oleic acid (cis-9-octadecenoic acid)
8	octanoic acid	E	Elaidic acid (trans-9-octadecenoic acid)
C	Capric acid (decanoic acid)	l	Linoleic acid (cis-cis-9,12-octadecadienoic acid)
L	Lauric acid (dodecanoic acid)	A	Arachidic acid (eicosanoic acid)
M	Myristic acid (tetradecanoic acid)	B	Behenic acid (docosanoic acid)

It is sometimes convenient to be able to refer to groups of TAGs. Therefore we have defined a set of letter-codes that represent a number of fatty acids. These codes are listed in table 2.2

*table 1.2 Letter-codes used for representing groups of fatty acids*

code	fatty acids
m	medium chain fatty acids ( 8+C+L+M )
h	long chain saturated fatty acids (P+S+A+B) ( 'hydrogenated' )
u	cis-C18 unsaturated fatty acids ( O+l+linolenic acid )

Hence the TAG-group  $h_3$  contains all TAGs that can be made from the four long chain fatty acids, like SSS, PPP, SPP, PPS, PSP, AAA, BBB, ASA, ASB etc., while  $h_0h$  stands for all TAGs having oleic acid on



TRIACYLGLYCEROLS: POLYMORPH-  
ISM

the 2-position and one of the four long chain fatty acids on the 1 and the 3 position of the glyceryl group like: SOS, POP, POS, AOS etc.

### 1.3 TRIACYLGLYCEROLS: POLYMORPHISM

The existence of a number of alternative crystal structures is a characteristic property of all lipids (alkanes, fatty acids, soaps, methyl esters of fatty acids and TAGs) (2). This is due to the fact that there are a number of different possibilities to pack the long hydrocarbon chains into a crystal lattice. This phenomenon called polymorphism and each different crystal structure is called a polymorphic form or modification of the lipid. Two types of polymorphism occur in lipids. When each form is thermodynamically stable in a definite range of temperature and pressure, it is called enantiotropic polymorphism. Each enantiotropic polymorph transforms into another polymorph at the transition temperature. The opposite case, when only one polymorphic form is thermodynamically stable, is called monotropic polymorphism. TAGs show monotropic polymorphism, while long chain odd alkanes show enantiotropic polymorphism (cf. chapter 9)

The polymorphism of TAGs was first observed in 1853 by Duffy (3), but only in the early 1960's some agreement was reached about the number, structure and nomenclature of the different polymorphic forms of TAGs (4,5). They occur in three different basic polymorphic forms,  $\alpha$ ,  $\beta'$  and  $\beta$ , which are characterized by a particular carbon chain packing and stability. Recent accurate experimental techniques, combined with better purity of the samples, has brought about a new controversy about the existence, number and nomenclature of submodifications of each polymorphic form (6-12).

It is not an objective of this work to enter into a discussion on submodifications. However the subject of this work, phase equilibria in TAGs, requires an opinion on TAG polymorphism.

### 1.3.1 Basic polymorphic forms of TAGs

In this work we will use the nomenclature proposed by Larsson (2,5) in the form applied by de Jong (13). Basically the fatty acid chains of TAGs can be packed into three main polymorphic forms, characterized by the short spacings in the X-ray diffraction pattern, namely:

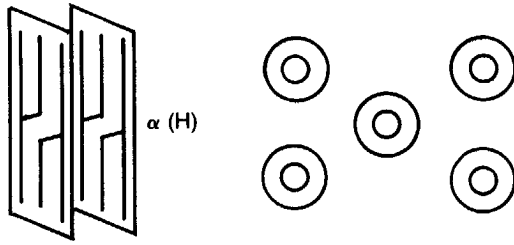
1. The  $\alpha$ -modification, characterized by only one strong short spacing line in the X-ray diffraction pattern near 0.415 nm. In the  $\alpha$ -modification the chains are arranged in a hexagonal chain packing, with no order of the zigzag chain planes. The chains have no angle of tilt. (fig 1.3a).

2. The  $\beta'$ -modification, characterized by two strong short spacing lines in the X-ray diffraction pattern near 0.38 nm and 0.42 nm. It also has a doublet in the  $720\text{ cm}^{-1}$  region of the infrared absorption spectrum. The chain packing in the  $\beta'$ -modification is orthorhombic, with a perpendicular arrangement of the zigzag chain planes. The chains have an angle of tilt between  $50^\circ$  and  $70^\circ$  (fig 1.3 b).

3. The  $\beta$ -modification, characterized by a strong short spacing line in the X-ray diffraction pattern near 0.455 nm and a number of other strong lines around 0.36-0.39 nm. The  $\beta$ -modification is the most densely packed polymorph. The chains are arranged in a triclinic chain packing, with a parallel arrangement of the zigzag chain planes. The chains have an angle of tilt between  $50^\circ$  and  $70^\circ\text{C}$  (fig 1.3c)

Based on the arrangement of the TAGs themselves in the crystal, two forms can be distinguished for each modification: a form with layers made up of two fatty acid chains and one with layers of three fatty acid chains (fig 1.4). These forms are characterized by their long spacing in the X-ray diffraction pattern. To distinguish between the two forms, a suffix is added to the symbol that indicates the modification, e.g.  $\beta$ -2 and  $\beta$ -3.

TRIACYLGLYCEROLS: POLYMORPHISM



$\alpha$  (H)

a:  $\alpha$ : unstable, lifetime < 60 s.  
present during process



$\beta'$  (O.L)

b:  $\beta'$ : metastable (>60 s --> years)  
present in products



$\beta$  ( $\tau//$ )

c:  $\beta$ : stable

fig 1.3 Schematic representation of orientation of the TAGs in their three basic polymorphic forms, together with the respective chain packing subcell. One zigzag is seen in the direction of the hydrocarbon chains, open circles are hydrogen, filled circles carbon (from 16).

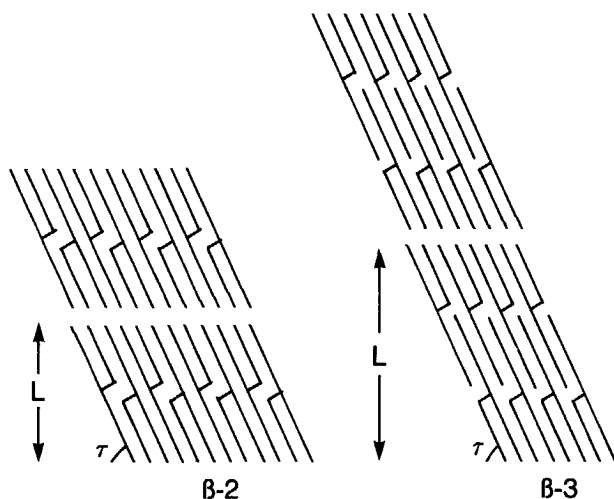


fig 1.4  $\beta$ -2 and  $\beta$ -3 arrangements of TAGs (from 13)

The -2 forms are the most stable and the -3 forms are therefore only found for TAGs of which the chain packing in the -2 form would be very unfavourable: in TAGs with *cis*-unsaturated fatty acids and in TAGs in which the fatty acid chains differ by 6 or more.

### 1.3.2 Submodifications

If submodifications exist, they will be indicated by a subscript in order of decreasing melting point, e.g.  $\beta_1$ -2 and  $\beta_2$ -2.

#### **Saturated TAGs**

De Jong (13) has done an excellent, extensive study of molecular packing possibilities in the  $\beta$ -modification. He shows that in theory a  $\beta$ -2 forming TAG can crystallize in at least 2 but often 3 different  $\beta$ -2 submodifications. For the  $\beta$ -3 modification 2 submodifications are possible. He found that in practice each TAG only occurs in one of these submodifications, although different TAGs crystallized in different submodifications.

Hagemann and Hernqvist (6,7) reported simultaneously the existence of two  $\beta'$ -submodifications for saturated TAGs, and somewhat later Hagemann (8) managed to distinguish even three  $\beta'$ -submodifications, two  $\alpha$  submodifications and two  $\beta$ -submodifications in his DSC thermograms. The submodifications were never obtained as pure solid phases on their own, but they rapidly transformed to the most stable submodification. Consequently, reliable melting points or heats of fusion could not be determined. The X-ray diffraction patterns of the submodifications show only very subtle differences. The pattern of a less stable submodification has much broader peaks and shows less details than that of the most stable submodification.

Rapid polymorphic transitions used to be hard to study by X-ray. The polymorphic transition takes 5 minutes, while one X-ray scan takes 15 minutes. This makes the unambiguous identification of very unstable submodifications difficult. Very recent experimental techniques allow so-called time resolved X-Ray diffraction studies (12,15). These new techniques need only 5 seconds for a scan, which means that the actual order of events during a polymorphic transition can be followed.

Kellens et al. (12) find that the polymorphic transitions take place in a very specific order. Re-ordering along the three different crystallographic axes is not achieved simultaneously but takes place sequentially. This is in agreement with computer simulation results of Hagemann (14), who showed that, due to sterical hindrance, the minimal energy path for the rearrangement in the crystal packing follows a very specific order of events. Also Sato (10) has observed this phenomenon. Kellens states that melting the crystal in a transitional state, where it has not yet reached full crystallinity, can very well result in DSC-thermograms similar to those from which Hagemann concluded the existence of unstable submodifications.

Kellens et al. also show that the melting entropies of Hagemann's and Hernqvist's submodifications are far too low to identify these submodifications as one of the differently packed  $\beta'$  and  $\beta$  forms of De Jong. Moreover, he found that the height of the shoulder or small pre-peak in the DSC-thermogram did not increase upon increasing scan rate, which is in contradiction to the existence of an unstable submodification that rapidly transforms into a more stable one.

Hagemann could not show that during all his experiments the recrystallization from  $\alpha$  to one of the  $\beta$ -forms was actually complete. The observed less stable  $\beta_2$ -form can therefore also be explained as the melting peak of the  $\beta$ -form in the presence of a little bit of liquid.

Kellens final conclusion is that these submodifications may very well not be separate polymorphic forms in a thermodynamic sense, but transitional variants with lower crystal perfection and crystallinity.

Due to the serious doubts that one may have on the actual occurrence of a large number of submodifications of saturated TAGs and the plausible alternative explanations available, we will in this work assume that only the three basic modifications occur.

#### Unsaturated TAGs

Only the polymorphism of hOh-type TAGs has been studied in more detail, because of their importance for explaining the phase behaviour of cocoa butter. As before, there is no agreement at all on the existence, properties and number of submodifications.

Perhaps the best results come from Sato (10). His X-ray diffraction results show very convincingly a fourth polymorph, the  $\gamma$ -modification, characterized by two strong short spacings, at 0.470 nm and 0.390 nm and a weaker one at 0.45 nm, characteristic for orthorhombic chain packing with parallel orientation of the chain zigzag planes. The thermodynamic properties are almost that of the perpendicular orthorhombic  $\beta'$ -modification. This  $\gamma$ -modification is of little practical importance, it is less stable than the  $\alpha$ -modification and converts readily into the  $\beta'$ -modification. It is not observed in mixtures. This  $\gamma$ -modification is also known under the names  $\beta''$ , sub- $\beta$ -3,  $L_2$  and form 4. We will use Sato's nomenclature.

Sato, and other authors, also found 2  $\beta'$  and 2  $\beta$ -submodifications, which hardly differ in X-ray pattern and stability. The existence and properties of  $\beta'$ -submodifications, which only occurred in POP and not in SOS and BOB, strongly depend on the level of impurities.

Therefore similar doubts arise for the existence of these submodifications as for Hagemann's submodifications of saturated TAGs. In this work we will only consider one  $\beta'$ -modification, having properties of the most stable of the  $\beta'$ -submodifications that are reported.

The existence of two  $\beta$ -submodifications is quite certain (23), as they can actually be obtained in pure form. The transition to the most stable form is extremely slow and takes several weeks. X-ray diffraction shows that the differences in structure must be minor. De Jong (13) suggests that the forms only differ in layer stacking. The most stable  $\beta_1$ -3 form has in this view a slightly higher symmetry and a heat of fusion that is only 1 kJ/mol more. This explains why the most stable form takes so long to form and why the 2  $\beta$ -forms are only observed in pure components and mixtures of hOh-TAGs that are nearly isomorphous, like cocoa butter. In more complex mixtures that contain high amounts of hOh-type TAGs, like palm oil (17) and the mixtures that Hernqvist used(16), only one  $\beta$ -form is observed. Therefore, for most practical purposes the possible existence of  $\beta$ -submodifications can be neglected. However, for systems with very high concentrations (>80%) of one single hOh-type TAG we need to be aware of the possible occurrence of  $\beta$ -submodifications.

## Conclusion

The discussion on submodifications is still very confusing and no clear evidence has been put forward for their existence, nor is there any agreement about their properties. In most cases alternative explanations, like those of Kellens(12) are possible for the observed changes in X-ray patterns and the shoulders and shifts in the DSC -thermograms. In this work it will therefore be assumed that each TAG crystallizes in three different polymorphic forms only.

### 1.3.3 Stability

The  $\alpha$  modification is the least stable and it converts within several minutes into the  $\beta'$ -modification. The  $\alpha$ -form is found in edible fat products during their preparation.

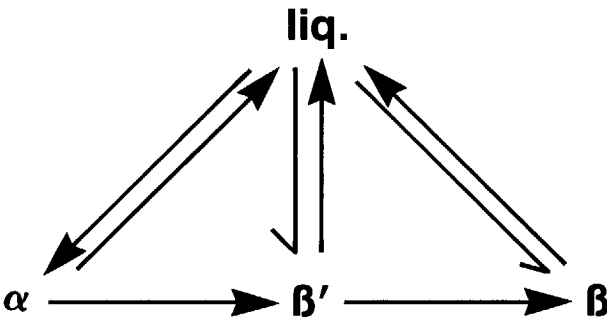


fig 1.5 Simple picture of the possible polymorphic transitions in TAGs.

The  $\beta'$ -modification is the stable modification for odd-chain TAGs and a number of even chain TAGs (like PSP). In other TAGs it converts into the  $\beta$ -modification within several minutes to hours. In mixtures this transition is often delayed to several months or years. It is therefore the modification that is encountered most frequently in normal edible fat products.

The  $\beta$ -modification is the stable modification. It only occurs in edible fat products during their lifetime, if the fat is composed of TAGs that are nearly isomorphous, like hardened rape-seed oils (16) and cocoa butter (17).

All three modifications can be obtained directly from the liquid, by varying the degree of supercooling. The transformation of  $\alpha$  to  $\beta$  however, always takes place via the  $\beta'$ -modification (12, 15, 16) (fig. 1.5).

#### 1.4 METHODS FOR PREDICTING SOLID PHASE COMPOSITION AND QUANTITY

The objective of this work is to develop a method to predict the melting range and composition of the solid phase of edible oils and fats from the overall composition of the fats. If the exact molecular composition of a fat is known, prediction of its properties is in principle possible. The vegetable oils and fats became only analytically accessible by the progress in high performance liquid chromatography (HPLC) techniques made during the last ten years,



METHODS FOR PREDICTING SOLID  
PHASE COMPOSITION AND QUAN-  
TITY

while the analysis of animal oils and fats is still troublesome. Besides, the theoretical understanding of solid-liquid phase equilibria in multicomponent systems was not at all adequate to deal with even very simple oils. Nevertheless, some (semi)-empirical methods for prediction of solid phase content were developed. They will be briefly discussed in this section.

1.4.1 Linear programming/multiple regression

This method is frequently used in industry (17). The composition of the fat blend is defined in terms of the natural and modified oils of which it is made (e.g. 50 % palm oil, 50 % bean oil). The solid phase content of the mixture is expressed as a linear function of the concentration of these components:

$$\%S = k_1 x_{oil1} + k_2 x_{oil2} + \dots$$

The coefficients  $k$  are obtained by multiple linear regression on the data of a number of mixtures. For limited ranges of compositions and solid phase contents this method is very useful. It does have disadvantages:

1. The predictive equation has no theoretical basis at all. Extrapolation outside the range of experimental data is not possible and gives dangerously erroneous results.
2. The equations cannot be easily extended to incorporate new component fats. The complete regression analysis and experimental work must be repeated and all coefficients will change.
3. No understanding at all is obtained about the actual phase behaviour, which implies that no solution can be found for undesired recrystallization phenomena and other crystallization phenomena that may be observed in practice. Polymorphism is neglected.

1.4.2 Excess contribution method.

Timms (17) shows the application of an empirical method developed by Nyvlt (18) to fats. The method is an extension of the multiple linear regression method of section 1.4.1. The solid phase content is expressed as:

PHASE EQUILIBRIA IN FATS  
- theory and experiments -

$$\%S = \sum_{i=1}^n \%S_i \cdot x_i + \sum_{j=1}^n \sum_{i=1}^{j-1} I_{ij} \cdot \frac{x_i x_j}{x_i + x_j}$$

The concentrations  $x$  are weight fractions of the constituting oils, the binary interactions  $I$  must be determined from measurements of a number of mixtures of the two oils concerned. The advantages over the linear method are twofold:

1. The equation is in principle valid over larger concentration ranges
2. If a new component fat is to be added, only the binary mixtures with all other component fats have to be measured in order to determine the interaction parameters. All other interactions remain unaffected.

Timms shows that the predictions are considerably worse than with the linear method, with deviations of 30% around the measured values. Again the model is totally empirical, the meaning of the parameters is unclear and it offers no real insight in the underlying crystallization phenomena.

#### 1.4.3 TAGs Inducteurs de Crystallisation -method (TGIC)

The first method that attempts to predict solid phase content from TAG-composition is the TGIC-method of Perron (19). He assumes that:

A crystallized fat consists of a number of solid phases in equilibrium with each other and with the liquid phase present.

Each solid phase consists mainly of one TAG, called the 'TAG Inducteur de Crystallization' (TGIC). All solid phases contain impurities, which modify its melting point and heat of fusion.

Upon heating each solid phase melts independently. The fraction of the solid phase that has disappeared at a certain temperature is given by a point on a Kessis-curve. A Kessis-curve is a general mathematical representation of a DSC or DTA melting peak of a single component in a liquid solvent. By adjustment of the parameters it can be used to describe a measured DSC-curve, including the thermal lag

METHODS FOR PREDICTING SOLID  
PHASE COMPOSITION AND QUAN-  
TITY

The solid phase content at a certain temperature can be obtained from an addition of all contributions from the Kessis-curves of each TGIC at that temperature.

Although Perron's notion of a number of coexisting solid phases is correct, the method he has developed is not sound at all:

1. His selection of the number and composition of the coexisting solid phases has no physical ground.
2. There is no reason why the solid phases should melt according to a Kessis curve. Moreover, the width of the Kessis curve is normally determined by the DSC apparatus and the scan rate selected. It is therefore not a property of the fat and any assumption about the width of such a curve is arbitrary.

The criticism Timms(17) applied to an earlier version of Perron's TGIC-method is still valid. Contrary to the two empirical methods mentioned above, the method is not even useful for practical purposes.

#### 1.4.4 The CTG (Classification of TAGs) method

Wieske (20) proposed a method in which he groups the TAGs into all possible TAG-groups that can be formed from elaidic acid (E) and the 3 fatty acid groups of section 1.2, h,m and u. These TAG-classes are supposed to form separate solid phases in a crystallized fat. The fraction of each class that has not crystallized is given by the Hildebrand-equation, assuming an average melting point and heat of fusion for each TAG-class. The Hildebrand equation reads:

$$\ln x_i^L = \frac{\Delta H_{f,i}}{R} \left( \frac{1}{T_{f,i}} - \frac{1}{T} \right)$$

This method has a physical background. It assumes that an oil can be considered as a mixture of a limited number of pseudo components that do not form mixed crystals. However, the predictions from this method are of a similar poor quality as those of the excess contribution method. Wieske's choice of the pseudo-components, as well as the assumption of solid immiscibility and the selection of melting points

and heats of fusion can be criticized. This method neither offers any understanding of the actual, underlying solid-liquid phase behaviour of TAGs.

#### 1.4.5 Other TAG-based methods

Several attempts have been made to find an empirical correlation between the TAG-composition of a fat and its solid phase content (20,21). None of these attempts was very successful. Moreover, the methods have the same disadvantages as the linear method of section 1.4.1.

### 1.5 CONCLUSION

The objective of this work is to develop a method that predicts the melting range and solid phase composition in an edible oil from the overall fat composition.

Existing predictive methods have no sound physical basis, are not generally applicable and offer no understanding at all of the actual solid-liquid phase behaviour of TAGs.

TAGs show polymorphism in the solid phase. In this work it will be assumed that each TAG crystallizes in three different polymorphs only: the unstable  $\alpha$ -modification, the  $\beta'$ -modification and the stable  $\beta$ -modification.

Due to their poor analytical accessibility, animal fats will not be considered in this work.

### LIST OF SYMBOLS

L	long spacing
R	gas constant (J/K,mol)
T	temperature (K)
$T_f$	melting point (K)
%S	solid phase content
x	mole fraction
$\Delta H_f$	heat of fusion (kJ/mol)
$\tau$	angle of tilt

## REFERENCES

### REFERENCES

1. C.Poot, G. Biernoth, *The Lipids Handbook*, F.B. Padley et al editors, Chapman & Hall, London (1986)
2. K. Larsson, *The Lipids Handbook*, F.B. Padley et al editors, Chapman & Hall, London (1986)
3. P. Duffy, *J. Chem Soc.* 5, 197 (1853)
4. D. Chapman, *Chem Rev* 62, 433 (1962)
5. K. Larsson, *Arkiv Kemi* 23, 35 (1964)
6. T.D. Simpson, J.W. Hagemann, *JAACS* 59, 118 (1982)
7. L. Hernqvist, K. Larsson, *Fette, Seife, Anstrichmittel* 84, 349 (1982)
8. J.W. Hagemann, J.A. Rothfuss, *JAACS* 60, 1123 (1983)
9. K. Sato, *Food Microstructure* 6, 151 (1987)
10. K. Sato et al., *JAACS* 66, 664 (1989)
11. V. Gibon, Thèse, Université Notre Dame de la Paix, Namur (1984)
12. M. Kellens, W.Meeussen, C. Riekel, H. Reynaers, *Chem. Phys. of Lipids* 52, 79 (1990)
13. S. de Jong, Thesis, Rijksuniversiteit Utrecht (1980)
14. J.W. Hagemann, J.A. Rothfuss, *JAACS* 65, 1493 (1988)
15. D. Cebula, to be published, *JAACS* (1990)
16. L. Hernqvist, Thesis, University of Lund (S) (1984)
17. R.E. Timms, *Progr. Lipid Res.* 23, 1 (1984)
18. J. Nyvlt, *J. Chem Prum.* 18/43, 260 (1967)
19. R. Perron, *Rev. Fr. Corps Gras* 33, 195 (1986) and *ibid.* 33, 253 (1986)
20. Th. Wieske, *Dev. Rep. Union Bahrenfeldt UDL BAH D 70/9* (1970)
21. Th. Wieske, K.Brown, private communication (1986)
22. J.B. Rosell et. al. *Leatherhead Food R.A. Research Report* 641 (1989)
23. K. Sato, *JAACS* 66, 1614 (1989)

## CHAPTER 2. APPROACH TO THE PROBLEM

*The ultimate amount and composition of the solid phase in a fat are determined by the position of the thermodynamic equilibrium solely, but the crystallization process may lead to significant deviations from the equilibrium composition in practical situations. Yet it appears that the starting point for any general predictive method of solid phase content in fats is a description of the solid-liquid phase equilibrium for all three polymorphic forms in which fats can crystallize. The thermodynamic equations that describe these equilibria are worked out. A number of steps is identified that need to be taken before a complete thermodynamic description can be obtained.*

### 2.1 SOLID-LIQUID EQUILIBRIUM THERMODYNAMICS

In the end the amount and the composition of the solid phase in a crystallized fat will be determined by the position of the solid-liquid phase equilibrium in that fat. Therefore a general method for prediction of the solid fat content and the fat crystal composition from the fat composition must be based on a description of the solid-liquid phase equilibrium thermodynamics in TAGs.

Fats are mixtures of many different TAGs. It is known that many pairs of TAGs only show limited miscibility in the solid phase (2). Therefore it is very likely that 'solid fat' often will consist of a number of different coexisting solid phases. These solid phases needn't necessarily have the same polymorphic form. A thermodynamic description of this complicated liquid-multiple solid equilibrium can be developed as follows:

Suppose a crystallized fat in equilibrium consists of  $N$  components and contains  $P$  phases (a liquid phase and  $P-1$  solid phases). The phase equilibrium must satisfy the following equations (1):

SOLID-LIQUID EQUILIBRIUM  
THERMODYNAMICS

1. The condition of thermodynamic equilibrium: the chemical potential of each component  $i$  in each phase must be equal to that in any other phase:

$$\text{eq. 2.1} \quad \mu_i^{\text{solid}} = \mu_i^{\text{liquid}}$$

for each solid phase.

This equation can be worked out for solid/liquid equilibria as:

$$\text{eq. 2.2} \quad \mu_i^{0,S} + RT \ln \gamma_i^S x_i^S = \mu_i^{0,L} + RT \ln \gamma_i^L x_i^L$$

$\gamma$  is the activity coefficient, and  $x$  the mol fraction.

$$\text{eq. 2.3} \quad \ln \left( \frac{\gamma_i^S x_i^S}{\gamma_i^L x_i^L} \right) = \frac{1}{RT} (\mu_i^{0,L} - \mu_i^{0,S})$$

$$\text{eq. 2.4} \quad \ln \left( \frac{\gamma_i^S x_i^S}{\gamma_i^L x_i^L} \right) = \frac{\Delta H_{f,i}}{R} \left( \frac{1}{T} - \frac{1}{T_f} \right) - \frac{\Delta c_{p,i}}{R} \left( \frac{T_{f,i} - T}{T} \right) + \frac{\Delta c_{p,i}}{R} \ln \frac{T_{f,i}}{T}$$

With  $\Delta c_p = 0.2$  kJ/mol and  $T_f - T$  never greater than 70 and usually between 0 and 20 the terms with  $\Delta c_p$  are comparatively small and tend to cancel due to their opposite sign. As an approximation they can therefore be neglected and there remains:

$$\text{eq. 2.5} \quad \ln \left( \frac{\gamma_i^S x_i^S}{\gamma_i^L x_i^L} \right) = \frac{\Delta H_{f,i}}{R} \left( \frac{1}{T} - \frac{1}{T_f} \right)$$

2. The mole balance : the sum of the amount of each compound  $i$  in each phase  $f$ , present in fraction  $\Phi^f$ , must be equal to the overall amount of  $i$ ,  $z_i$ : ( $P$  is the total number of phases)

eq. 2.6

$$\sum_{f=1}^P x_i^f \Phi^f = z_i$$

3. The stoichiometric condition : the sum of the concentrations of the components in each phase must be equal to 100%:

eq. 2.7

$$\sum_{i=1}^n x_i^f = 1$$

For  $P$  phases this results in  $PN+P$  equations with  $PN+P$  unknowns. ( $P*N$  mol fractions  $x$  and the quantity of  $P$  phases). This set of equations can in principle be solved to obtain the number of phases, the phase quantities and the composition of each phase from the overall composition and the temperature.

However, in order to solve these equations four things are needed:

1. Values for the pure component properties: the heat of fusion and the melting point.
2. Knowledge of the activity coefficients in the liquid phase.
3. Knowledge of the activity coefficients in the solid phase.
4. A method to solve this complex set of non-linear equations.

Each of these points will be handled in separate chapters of this work, so that in the end a full description of the liquid-multiple solid equilibrium in fats will evolve.

## 2.2 KINETICS OF CRYSTALLIZATION

Although the ultimate amount of solid phase and the solid phase composition are determined by thermodynamics solely, it is well known that due to the extremely slow diffusion rate in solids the equilibrium state is not always reached in practical situations (3). Hence both crystal composition and amount of solid phase that are observed may



deviate considerably from what is predicted by thermodynamics. To avoid possible pitfalls the effect of kinetic factors on the amount and composition of the solid phase of fats should be considered.

### 2.2.1 Polymorphism and kinetics of crystallization

When fats crystallize, they usually crystallize first in the most unstable polymorph, the  $\alpha$ -modification, followed by slow recrystallization to more stable polymorphs. Direct crystallization into the  $\beta'$  or  $\beta$ -modification only takes place under conditions where little or no supercooling of the less stable modification is present. Palm oil crystallizes into the  $\alpha$ -modification when supercooled to  $10^{\circ}\text{C}$ , into the  $\beta'$ -modification when cooled to  $25^{\circ}\text{C}$  and into the  $\beta$ -modification when crystallized at  $32^{\circ}\text{C}$  (4). In all three cases the thermodynamically most stable state is the  $\beta$ -modification.

Obviously solid fat content and crystal composition calculated for the  $\beta$ -modification using thermodynamics are poor predictions if the fat has crystallized in another polymorphic form. For a lot of practical situations the thermodynamically most stable state is irrelevant: the residence time in the process line after the onset of fat crystallization is only a few minutes for many edible fat products, so that in process calculations the unstable  $\alpha$ -modification is the solid fat phase that should be considered. During the life of most edible fat products, the recrystallization to the  $\beta$ -modification does not take place: the product is already consumed while it is still in the  $\beta'$ -modification.

In spite of their limited lifetime, the  $\beta'$ -modification and even the  $\alpha$ -modification may during their existence very well coexist in thermodynamic equilibrium with the liquid oil. Hence thermodynamics can be applied to predict the amount and composition of these intermediate solid phases. Application of equilibrium thermodynamics to unstable states is quite common: a mixture of benzene and air is not thermodynamically stable but should disintegrate into carbon dioxide and water, yet a vast amount of literature exists about vapour-liquid phase equilibria with benzene.

2.2.2 Shell formation

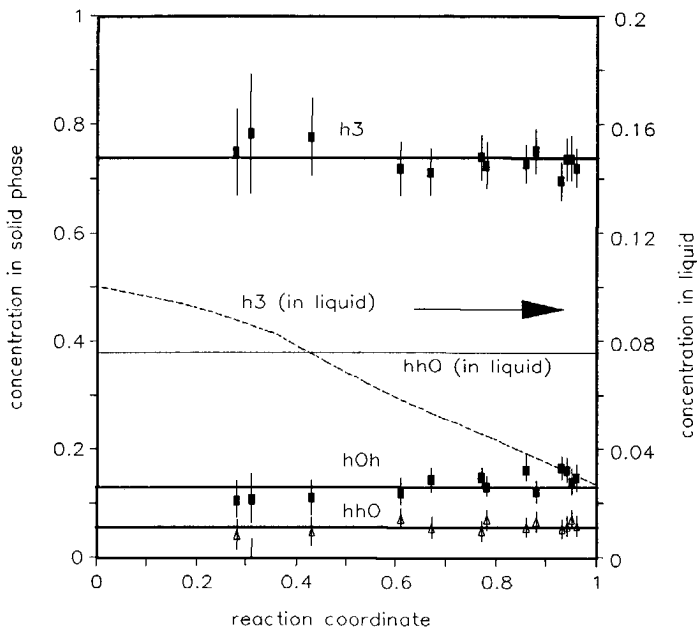


fig 2.1 Composition of fat crystals from palm oil against the reaction coordinate of crystallization at 30°C. (Overall palm oil composition:  $h_3$  - 0.1,  $hOh$  - 0.295,  $hhO$  - 0.075,  $h1h$  - 0.104,  $hOO$  - 0.246, liquid - 0.176. ). The palm oil was heated to 80°C, rapidly cooled to 30°C and stored in a stirred tank. At regular time intervals over totally 21 hrs samples were taken. The solid fat content of the sample was measured and a small amount of liquid phase was rapidly filtered off and analysed by  $AgNO_3$ -HPLC. Crystal composition is calculated from overall composition, solid fat content and the TAG analyses of the liquid phase of the samples. The error margin is indicated.

If a fat is slowly cooled while it is crystallizing, shell formation may occur. At each instant during the crystallization process the surface of the growing crystals has the equilibrium composition. As temperature decreases, the equilibrium composition changes, but the composition of the inner part of the crystal does not change due to the low solid state diffusion rate. An inhomogeneous solid phase

## KINETICS OF CRYSTALLIZATION

results, having a concentration gradient from the centre of the crystals outwards. The solid phase composition deviates from the equilibrium composition. It is reported that the solid fat content can decrease to only 80% of the equilibrium value (2) due to shell formation.

If no diffusion limitations occur during crystallization, shell formation can be prevented by crystallizing isothermally. The rate determining step in normal fat crystallization is the surface incorporation (4,5). Indeed, when the crystal composition of an isothermally crystallizing fat is plotted against the reaction coordinate, shell formation seems absent (fig 2.1)

Phase equilibrium thermodynamics will only give a reliable prediction of the solid phase composition and content if shell formation is absent. However, the effect of shell formation on solid phase content can be calculated from the equilibrium composition as a function of temperature, as will be shown in chapter 9.

### 2.2.3 Poor crystallinity

If fat is crystallizing rapidly, it may result in badly packed crystals. The clear point of such badly packed solid phases may be considerably lower than the clear point predicted by thermodynamics. By recrystallization these badly packed crystals can rearrange into well packed crystals. The results of Gibon (6) show that without the presence of a liquid phase badly packed crystal forms may persist for years. However recrystallization via the liquid phase can occur relatively easily (3). Norton (7) shows that partially hydrogenated palm oil initially crystallizes in a very badly packed  $\beta'$ -form, but that in the presence of about 50% of a liquid oil it only takes a few hours to rearrange into well packed crystals. Also the rate of polymorphic transitions was observed to be much larger in the presence of liquid (8).

Most fats, used in edible fat products only contain 0 - 40% of solid fat, that is purposely crystallized into very small ( $1 \mu$  and less) crystals. Deviations from thermodynamic predictions due to bad crystal packing will therefore be of minor influence.

### 2.3 CONCLUSION AND APPROACH TO THE PROBLEM

The ultimate amount and composition of the solid phase in a fat are determined by the position of the thermodynamic equilibrium solely. The set of equations that describe a solid liquid phase equilibrium can be solved, if a number of requirements is fulfilled.

For prediction of the amount and the composition of the solid phase that can crystallize from an oil in practical situations, calculation of the most stable state by solid-liquid phase equilibrium thermodynamics is insufficient. The solid-liquid phase equilibria of unstable polymorphic forms must be considered as well.

The crystallization route that is followed may lead to inhomogeneous solid phases, of which amount and composition can deviate significantly from the equilibrium composition. Yet in order to calculate the effect of the crystallization process on the solid phase composition the equilibrium solid phase composition as a function of temperature must be known.

From this it is clear that for a prediction of the amount and composition of the solid phase in fats as a function of temperature the first requirement is a good description of the solid-liquid phase equilibrium for all three modifications in which fats crystallize. This work will therefore concentrate upon the development of this description for liquid-multiple solid phase equilibria in fats. At the end of this work we will briefly come back to the influence of the crystallization process.

In section 2.1 it was shown that for the description of the solid liquid phase equilibrium four steps must be taken, namely:

1. Find a method to solve the complex set of non-linear equations that describe the liquid-multiple solid phase equilibrium
2. Find values for the pure component properties: the heat of fusion and the melting point for all of the hundreds of TAGs involved.
3. Predict the activity coefficients of TAGs in the liquid phase.
4. Predict the activity coefficients in all possible solid phases.

## LIST OF SYMBOLS

These steps, in the order in which they are listed, are the subjects of the next chapters of this work.

## LIST OF SYMBOLS

$c_p$	heat capacity (J/mol,K)
$g$	molar Gibbs free energy (J/mol)
$G$	Gibbs free energy (J)
$N$	number of components
$n$	number of moles (mol)
$P$	number of phases
$R$	gas constant (J/mol,K)
$T$	temperature (K)
$T_f$	normal melting point (K)
$x, y$	mole fractions
$z$	overall mole fraction
$\gamma$	activity coefficient
$\Delta H_f$	heat of fusion at $T_f$ . (kJ/mol)
$\phi$	phase fraction
$\mu$	chemical potential (J/mol)

## REFERENCES

1. J.M. Prausnitz Molecular Thermodynamics of Fluid Phase Equilibria. Prentice Hall 1986
2. R.E. Timms, Progr. Lip. Res. 23, 1 (1984)
3. M. Zief, W.R. Wilcox, Fractional Solidification, Marcel Dekker inc (New York) 1967.
4. K.P.A.M van Putte, B.H. Bakker, JAOCS 64, 1138 (1987)
5. M. Knoester, P. de Bruijne, M.v.d. Tempel, J. Crystal Growth 3, 776 (1968)
6. V. Gibon, Thèse, Université de Notre Dame de la paix, Namur (1984)
7. I.T. Norton, C.D. Lee-Tuffnell, D.W. Rowlands, P CW 85 1175 (Unilever Research Colworth House, 1985)
8. I.T. Norton et al., JAOCS 62, 1237 (1985)

### CHAPTER 3. FLASH CALCULATIONS

*Solving the set of nonlinear equations that describe the phase equilibrium between a liquid phase and a number of solid solutions, to obtain the number and amount of coexisting phases and the composition of each phase present from a given overall composition and temperature is called a 'solid flash' calculation. There exists no literature on such solid flash calculations. It is tried to alter the best existing algorithms for vapour /liquid flash calculations such that they can deal with polymorphism and a number of solid solutions.*

#### 3.1 INTRODUCTION

Solving the set of nonlinear equations that describe the phase equilibrium between a liquid phase and a number of solid solutions (eq. 2.5 - 2.7) to obtain the number of coexisting phases, the amount and the composition of each phase present from a given overall composition and temperature will be called a 'solid flash' calculation in this work. Unfortunately there exists no literature on such solid flashes for multicomponent, multiple mixed solid phase systems that can show polymorphism. In this chapter we will try to alter the best of the existing algorithms for multiphase vapour /liquid flash calculations such that they can deal with polymorphism and a number of coexisting solid solutions.

A flash calculation requires the simultaneous solution of the set of nonlinear equations 2.5, 2.6, 2.7. As this set cannot be solved analytically an iterating procedure has to be used, that involves the following steps:

1. Make a first estimate of the number of phases that will be present, the amount of phases and their composition.
2. Calculate the activity coefficients.
3. Make a new estimate, applying the equations 1-6, using the activity coefficients of 2.
4. Repeat step 2-3 until a convergence criterion is met.

INITIAL ESTIMATES AND STABIL-  
ITY TESTS

5. Perform a stability test to check whether the initial estimate of the number of phases is correct. If not, an extra phase is added with an estimate of its composition.
6. Repeat step 2 to 4 until convergence is obtained and a stability criterion is met.

Whether quick convergence is obtained in step 2-3 depends on the quality of the initial estimate and on the reliability of the stability test. If the initial estimate is poor, convergence may be slow, to a local, rather than a global minimum or to a trivial solution with two phases having the same composition. A poor stability test will lead to an incorrect number of phases. A robust convergence procedure leads to the solution, even with a poor initial estimate.

It follows that for composing a flash algorithm for fats, we need:

1. A procedure to test the phase stability and provide an initial estimate for the phase compositions.
2. An iterating procedure to solve the phase equilibrium and mass balance equations.

### 3.2 INITIAL ESTIMATES AND STABILITY TESTS

There exist no algorithms that directly give an estimate of the total number of phases that coexist. All methods start with assuming a single phase, either liquid or vapour. A simple calculation of the overall Gibbs energy learns which of the two is the most stable. For fats, the equivalent procedure is a comparison between the molar Gibbs energy of the fat in the liquid state and those in the  $\alpha$ ,  $\beta'$  and  $\beta$  polymorphic forms:

eq. 3.1

$$g^f = \sum_{i=1}^n z_i (\mu_i^{0,f} + RT \ln \gamma_i^f z_i)$$

For convenience we set in the remainder of this work the chemical potential in the pure liquid reference state arbitrary to 0, so that the above equation reduces for the liquid state to:

eq. 3.2

$$\frac{g^l}{RT} = \sum_{i=1}^n z_i (\ln z_i)$$

and for the 3 solid states to :

eq. 3.3

$$\frac{g^m}{RT} = \sum_{i=1}^n z_i \left( \frac{\Delta H_f^m}{R} \left( \frac{1}{T} - \frac{1}{T_f^m} \right) + \ln \gamma_i^m z_i \right)$$

(with  $m = \alpha, \beta'$  or  $\beta$  and neglecting all terms with  $\Delta c_p$  )

That phase out of the four that has the lowest molar Gibbs energy is the starting point for the stability test. The stability test checks whether addition of a new phase giving a decrease in the overall Gibbs energy is possible. Two types of stability tests for multicomponent, multiphase systems can be found in literature: methods using a 'splitting component' and methods based upon the tangent plane criterion of Gibbs.

### 3.2.1 Splitting component method

An example of this method is that of Gautam and Seider (for ASPEN, 2,3). Shah (8) uses a nearly similar procedure. Asselineau (14) proposes a simpler procedure where the 'splitting component' has to be known beforehand. That is not the case for fats.

Gautam and Seider first search all phases to locate the component with the highest activity. That component is named the 'splitting component'. Secondly the phase in which the splitting component is found, is searched for the component that has the highest activity in a binary mixture with the splitting component, taking concentrations proportional to those in the splitting phase. Next these two components are distributed over two trial phases by solving equations 2.5, 2.6 and 2.7 for this binary system using the well known two phase flash equation (1) (intermezzo 1), starting with two pure phases.

If this calculation results in a split then the remaining components are distributed over the two trial phases in order of decreasing binary activity with the splitting component. The distribution coefficients that are needed, are obtained using the composition of the trial phases calculated so far for getting the activity coefficients.



Intermezzo 1: If an initial amount  $S$  is assumed for the first trial phase, then equation 2.5, 2.6 and 2.7 (the material balance combined with the phase equilibrium equation) give:

eq. 3.4

$$x_i^B = \frac{z_i}{1 + S(K_i^{AB} - 1)}$$

and

eq. 3.5

$$x_i^A = \frac{z_i K_i^{AB}}{1 + S(K_i^{AB} - 1)}$$

$K$  is the distribution constant  $x^A/x^B$  that follows directly from equation 2.5.

Subsequently a function  $f(S)$  is defined:

$$f(S) = x_1^B + x_2^B - x_1^A - x_2^A = \sum_{i=1}^2 \frac{z_i(1 - K_i^{AB})}{1 + S(K_i^{AB} - 1)}$$

The equilibrium value for the phase split  $S$  is determined by calculating the zero of this function by a Newton Raphson iteration:

$$S_n = S_{n-1} - \frac{f(S)_{n-1}}{\left(\frac{df(S)}{dS}\right)_{n-1}}$$

When  $S$  is found, the mole fractions are calculated and next the values of the distribution constants  $K$  are recalculated, using the new values for  $x$ . If the new  $K$ -values differ too much from the old ones, the function  $f(S)$  is solved again, using the new values of  $K$ . If the value of  $S$  is not between 0 and 1, the split is considered unsuccessful.

eq. 3.6

$$K_i^{A,B} = \frac{x_i^A}{x_i^B} = \frac{\gamma_i^A}{\gamma_i^B}$$

This procedure is repeated, taking the component with the second highest activity as splitting component etc. The Gibbs energy of all these trial splits is compared and that one with the lowest Gibbs energy is taken as initial estimate for a subsequent iterating procedure. If none of the binary flashes is successful, no trial phases can be formed and the solution is considered stable.

This procedure can be easily extended to deal with polymorphism in the solid phase: Only the number of trial splits needs to be extended: in stead of one binary flash at each trial split four flashes need to be considered: e.g. if a component in a  $\beta$  phase had been selected as 'splitting' not only a  $\beta$ - $\beta$  split but also  $\beta$ - $\beta'$  split, a  $\beta$ - $\alpha$  split and a  $\beta$ -liquid split must be considered. For a P phase N component system maximally  $4P(N-1)$  trial splits must be evaluated.

### 3.2.2 Michelsen's tangent plane criterion method

The second approach is based on an extension of the well known tangent plane criterion of Gibbs(1) for phase stability to the multicomponent, multiphase situation. The tangent plane criterion says that if the tangent to the Gibbs free energy curve at the solution at no point lies above the Gibbs free energy curve then the Gibbs free energy is at a global minimum. The mixture is stable and will not show further demixing. In fig 3.1 the tangent to the Gibbs free energy curve at F lies partially above the curve: F is an unstable mixture and will demix in A and B. The tangent to the curve at G lies at no point above the curve and G represents a stable mixture.

The general formulation of the tangent plane criterion is presented by Michelsen( 4-6) and the parts of interest for this work will be given here:

The total Gibbs energy of an original P-phase system ( $P \geq 1$ ), apparently in equilibrium ( $\mu_i^A = \mu_i^B$ ) and to be tested for stability is

INITIAL ESTIMATES AND STABILITY TESTS

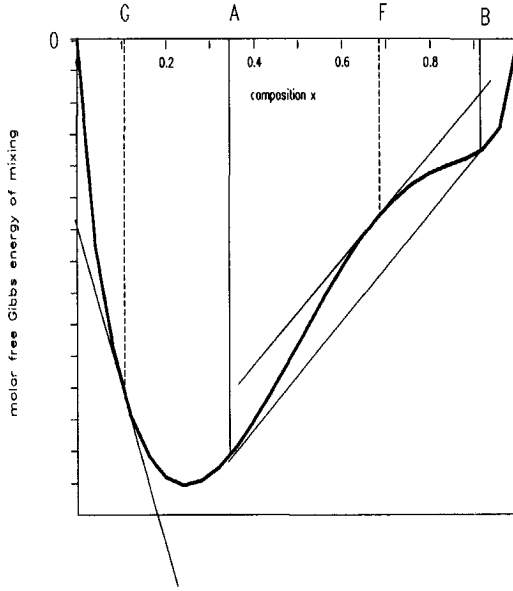


fig 3.1 Gibbs free energy of mixing as a function of composition

eq. 3.7

$$G^{(I)} = \sum_{j=1}^P \sum_{i=1}^n n_i^j \mu_i^j = \sum_{i=1}^n n_i \mu_i^{(I)}$$

A different phase split into  $L = P+1$  phases with mole fractions  $y_i^j$  and totally  $N_j$  mole in phase has a Gibbs energy of:

eq. 3.8

$$G^{(II)} = \sum_{j=1}^L \sum_{i=1}^n N_j y_i^j \mu_i^j$$

The energy difference between the two situations is:

eq. 3.9

$$\begin{aligned} G^{(II)} - G^{(I)} &= \sum_{j=1}^L \sum_{i=1}^n N_j y_i^j \mu_i^j - \sum_{i=1}^n n_i \mu_i^{(I)} \\ &= \sum_{j=1}^L \left( \sum_{i=1}^n y_i^j (\mu_i^j - \mu_i^{(I)}) \right) = \sum_{j=1}^L N_j F_j \end{aligned}$$

A phase split into L phases will occur if the Gibbs energy change is negative. That can only be so if at least one of the  $F_j$  is negative. Hence the stability criterion becomes: a system is stable if for any extra trial phase L with trial composition y

eq. 3.10

$$F_L = \sum_{i=1}^n y_i^L (\mu_i^L - \mu_i^{(I)}) \geq 0$$

This is the general form of the tangent plane criterion.

$F_L$  is positive for any composition y if the minimum of  $F_L$  is positive. The composition of the extra phase L at that minimum of  $F_L$  is found by simple differentiation of  $F_L$  to the n-1 independent mole fractions  $y_i$  and setting all derivatives to 0:

$$\frac{\partial F_L}{\partial y_i} = \frac{\partial \left( (\mu_n^L - \mu_n^{(I)}) + \sum_{i=1}^{n-1} y_i [(\mu_i^L - \mu_i^{(I)}) - (\mu_n^L - \mu_n^{(I)})] \right)}{\partial y_i} =$$

$$(\mu_i^L - \mu_i^{(I)}) - (\mu_n^L - \mu_n^{(I)}) = 0$$

which gives  $\mu_i - \mu_i^{(I)} = \mu_j - \mu_j^{(I)} = K$ , a constant. The minimum of F should be greater than zero for stability

$$F(\min) = \sum y_i K = K \geq 0$$

It is often simpler to deal with activity coefficients rather than chemical potentials. The activity coefficients of the trial phase L are introduced with the help of equation 2.2 :

eq. 3.11

$$k = \frac{K}{RT} = \frac{\mu_i^{0,L} - \mu_i^{(I)}}{RT} + \ln \gamma_i^L + \ln y_i^L$$

If addition of a trial phase L gives a negative value of k, then the addition of an infinitesimal amount of phase L (infinitesimal, in order not to change composition of the other phases and so  $\mu^{(I)}$ ) will lower the Gibbs energy. The original situation was unstable. The composition of the trial phase L with minimum value for k can be found from an initial estimate of L by iterating :

INITIAL ESTIMATES AND STABIL-  
ITY TESTS

eq. 3.12

$$\ln(y_i^L e^{-k}) = \frac{\mu_i^{(I)} - \mu_i^{0,L}}{RT} - \ln y_i^L$$

From the calculated values of  $y_i^L e^{-k}$  the composition of the new trial phase is obtained from  $y_i = \frac{y_i^L e^{-k}}{\sum_i y_i^L e^{-k}}$ . If the denominator in this equation

is smaller than 1, it corresponds to  $k > 0$  and so to stability.

If there is no minimum of  $K$  located on the plane between the initial estimate of the trial phase and one of the existing phases, the iteration procedure converges to a trivial solution, in which the trial phase has the same composition as one of the existing phases. Therefore a number of initial estimates is necessary, to ensure that the minimum of  $K$  is found if it exists.

Michelsen recommends to take a pure phase of each component as initial estimate plus a trial phase with a composition that is the average of the composition of all phases present. He has shown that the iterations needn't be continued to convergence: for each initial estimate four iterations suffice. The trial phase with the most negative value of  $K$  is used as the initial estimate for the new phase, that will form after the split. If no negative values of  $K$  are found for all initial estimates, then only the one with the least positive value of  $K$  is converged. If this trial phase still yields positive values of  $K$ , then the original situation is considered stable.

Sometimes we found in highly non ideal systems after 4 iterations a phase with a negative  $K$ , indicating instability. But upon continuing iterations to convergence, it occurred that  $K$  turned greater than 0, indicating stability. Stopping after 4 iterations would have led to a false conclusion. Therefore we always converged the trial phase that has the smallest  $K$  after four iterations.

Michelsen's stability test can be applied to solid liquid equilibria in TAGs simply by increasing the number of initial estimates for the trial phases: Pure  $\beta$ ,  $\beta'$  and  $\alpha$  phases of each component plus a  $\beta$ , a  $\beta'$ , an  $\alpha$  and a liquid phase (if not already present) with a composition being the average of all phases already present. In a N

component P phase system maximally  $3N+4$  trial phases must be considered, about a factor P less than with the splitting component approach.

Michelsen's stability test has the advantage of being derived from the proven thermodynamic tangent plane criterion and requiring only a small number of trial phases, while the method of Gautam and Seider and like methods have no fundamental guarantee that phase instability is always detected. However in Michelsen's procedure the true minimum of K may be overlooked because of the selection of starting values for the trial phases. The algorithm of Michelsen and a number of algorithms similar to that of Gautam and Seider have been tested on several different vapour liquid and vapour liquid-liquid-liquid equilibria (7). Generally Michelsen's algorithm proved to be the most reliable. In this work the performance of both methods with solid liquid equilibria in fats will be tested.

### 3.3 ITERATING PROCEDURES

Once a good initial estimate of the number of phases, their polymorphic form and their composition is obtained, the equilibrium composition and phase quantities can be calculated by solving equation 2.5 - 2.7. The iterating procedures to solve these phase equilibria and mass balance equations fall into two categories:

1. The direct substitution methods
2. Methods involving the minimisation of the Gibbs Free Energy.

#### 3.3.1 Direct substitution

This is the multiphase multicomponent analogue of the two-phase two component flash equation, described in section 3.2.1 (equation 3.4 and 3.5).

The function  $f(S)$  is redefined for the P phase analogue as a set of P-1 equations:

eq. 3.13

$$\sum_{i=1}^n \frac{z_i (K_i^{mP} - 1)}{1 + \sum_{f=1}^{P-1} \Phi_f (K_i^{fP} - 1)} = 0 \quad (m = 1, 2, \dots, P-1)$$

## ITERATING PROCEDURES

$m$  ranges from 1 to  $P-1$ .  $K_m^P$  is the distribution coefficient of a component over the phases  $m$  and  $P$ .

The solution of these sets of equations to obtain the  $P-1$  phase fractions is carried out by Newton Raphson iteration. Then using these phase fractions new compositions are obtained. Next new values for the distribution constants are calculated with the appropriate thermodynamic models. If these new values do not agree with the previous ones within a certain tolerance, the set equations is solved again for the  $P-1$  phase fractions, using the new values of  $K$ .

Direct substitution is a very fast and reliable method for phase equilibria where the values of the activity coefficients do not depend strongly on the phase composition. It seems therefore most suited for calculating  $\alpha$  phase equilibria, where all activity coefficients are 1 (see chapter 5) and the values of  $K$  only depend on temperature, so that only one iteration will be sufficient.

When the activity coefficients strongly depend on the phase composition and/or when phase envelopes are very narrow, like it is often the case in the  $\beta$  and  $\beta'$  modification, the direct substitution method converges very slowly. Examples of the need for several hundreds of iterations are known (5,9). Various acceleration procedures exist, the General Dominant Eigenvalue method (GDEM) of Crowe and Nishio (9) being recommended by Michelsen (5) and by Swank and Mullins (7). Even with these methods, convergence is not always obtained in the case of vapour-liquid equilibria, and other methods had to be used (5).

We found for our systems that 3 GDEM acceleration steps are sufficient, each after 5 iterations and that using more than two eigenvalues, even when more than 3 phases were present, offered no significant improvement in acceleration. This is in agreement with the findings of Michelsen and Swank & Mullins (5,7).

### 3.3.2 Gibbs free energy minimisation

The other method to solve the phase equilibrium and material balance equations is to minimize the Gibbs free energy. When the Gibbs energy

is at its minimum the requirement for equilibrium, equation 1, is satisfied. The problem can hence be reformulated for a N component, P phase system as:

Find the minimum of:

eq. 3.14

$$G_{\vec{n}} = \sum_{j=1}^P \sum_{i=1}^N n_i^j \mu_i^j = \vec{n} \cdot \vec{\mu}$$

subject to the constraints of the mass balance and the requirement of all  $n_i^j \geq 0$

The two vectors are defined as:

$$\vec{n} = \begin{pmatrix} n_1^1 \\ n_2^1 \\ \cdot \\ \cdot \\ n_N^P \end{pmatrix}, \quad \vec{\mu} = \begin{pmatrix} \mu_1^1 \\ \mu_2^1 \\ \cdot \\ \cdot \\ \mu_N^P \end{pmatrix}$$

The Gibbs free energy can be minimized by several variations on Newton's method (intermezzo 2).

Two things should be added to the standard Newton method:

1. The solution should be within the constraints imposed by the mass balance and not result in negative concentrations.
2. It should be verified that the extreme obtained is actually a minimum and not a maximum or a saddle point.

The mass balance equation 2.6 can be equivalently formulated for each component i as:

The elements i of the vector  $\overline{\Delta n}$  should obey



Intermezzo 2: The Gibbs free energy close to an initial estimate of the solution is given by a Taylor expansion :

eq. 3.15

$$G_{\bar{n}+\Delta\bar{n}} = G_{\bar{n}} + \overline{\nabla G_{\bar{n}}} \cdot \overline{\Delta n} + \frac{1}{2} \overline{\Delta n^T} \cdot \nabla^2 G_{\bar{n}} \cdot \overline{\Delta n}$$

$$= G_{\bar{n}} + \sum_{j=1}^P \sum_{i=1}^N \frac{\partial G_{\bar{n}}}{\partial n_i} \Delta n_i + \frac{1}{2} \sum_{j=1}^P \sum_{i=1}^N \sum_{k=1}^P \sum_{h=1}^N \frac{\partial^2 G_{\bar{n}}}{\partial n_i \partial n_h} \Delta n_i \Delta n_h$$

Since the first term of this equation is constant, the minimum Gibbs energy is obtained when the two right hand side terms  $\Phi_{\Delta\bar{n}} = \overline{\nabla G_{\bar{n}}} \cdot \overline{\Delta n} + \frac{1}{2} \overline{\Delta n^T} \cdot \nabla^2 G_{\bar{n}} \cdot \overline{\Delta n}$  have a minimum. The minimum of this quadratic function  $\Phi$  is easily calculated by setting its derivative to zero:

eq. 3.16

$$\nabla^2 G_{\bar{n}} \cdot \overline{\Delta n} = -\overline{\nabla G_{\bar{n}}}$$

This set of linear equations in  $\Delta n_i$  is readily solved and the resulting vector  $\overline{\Delta n}$  is called the Newton direction.  $\bar{n} + \overline{\Delta n}$  is an improved estimate of the composition at the minimum.

Next step would be to calculate new values for  $\overline{\nabla G}$  and  $\nabla^2 G$  at this improved estimate, determine the Newton direction from this point and repeat this until convergence is obtained

$$\sum_{j=1}^P \Delta n_j = 0$$

This set of N linear constraints can be used to eliminate N variables from equation 3.16, so that indeed the mass balance is satisfied. Intermezzo 3 following describes a general way of doing this.

Non negative values for the mole numbers can be assured by introduction of a so called step size  $\lambda$ . The new estimate for the composition is set to:  $\bar{n} + \lambda \overline{\Delta n}$ . The step size  $\lambda$  is taken as the largest possible value not exceeding 1 that:

- still results in a new estimate of the solution in which all mole numbers  $n_i$  are greater than a small positive number  $\delta$  and
- gives a decrease in Gibbs free energy.

Intermezzo 3: The set of linear mass balance constraints can be alternatively formulated as:

$$A \cdot \overline{\Delta n} = \vec{0} \quad , \quad A = (I_1 \quad I_2 \quad \dots \quad I_P)$$

The  $(P \times N) \times N$  matrix A consists of P identity matrices with dimension N.

If a second matrix Z of which its columns form a basis for the set of all vectors orthogonal to the rows of A is defined, then any vector  $\overline{\Delta n} = Z \cdot \overline{\Delta n}^Z$  will satisfy the mass balance constraints:  $A \cdot \overline{\Delta n} = A \cdot Z \cdot \overline{\Delta n}^Z = \vec{0} \cdot \overline{\Delta n}^Z = \vec{0}$ . Such a matrix Z of which the columns are orthogonal to the rows of A is:

$$Z = \begin{pmatrix} I_1 & I_2 & \dots & I_{P-1} \\ & & & -I_u \end{pmatrix}$$

in which I is an identity matrix of dimension N and  $I_u$  is an identity matrix of dimension  $(N-1) \times P$ .

If  $\overline{\Delta n}$  in equation 3.15 is substituted by  $\overline{\Delta n}^Z$ , then the solution to the constrained problem of equation 3.15 is given by :

eq. 3.17 
$$\nabla^2 G_{\bar{n}}^Z \cdot \overline{\Delta n}^Z = -\overline{\nabla G_{\bar{n}}^Z} \quad , \quad \nabla^2 G^Z = Z^T \cdot \nabla^2 G \cdot Z$$

$$\overline{\nabla G}^Z = Z^T \cdot \overline{\nabla G}$$

The solution  $\overline{\Delta n}^Z$  is transformed to the original  $\overline{\Delta n}$  by multiplication with Z.

The value that is chosen for  $\delta$  depends on the precision of the computer used. In this way is guaranteed, that no negative mole numbers will occur and that the calculations remain numerically stable.  $\lambda$  should differ from unity only in the first few Newton iterations.

A Newton direction that points to a minimum in the Gibbs energy is only obtained when the matrix of the second derivative of the Gibbs energy to all mole numbers,  $\nabla^2 G_{\bar{n}}$ , the so called Hessian, is positive definite, i.e. has only positive eigenvalues. In case of activity coefficients only slightly different from 1 this is so. However, in case of solid  $\beta$  and  $\beta'$  phases it is not necessarily true. If the Hessian is not positive definite, the iterations may converge to a maximum in the Gibbs energy or even not converge at all.

#### ITERATING PROCEDURES

Gautam and Seider (2,3) solve this problem by ignoring the second derivative of the excess Gibbs energy (= ignoring the compositional derivatives of the activity coefficients). This is called the 'Rand method'. The Hessian is in that case always positive definite. Because of the inaccurate Hessian used, the Rand method will converge slower than when the full second derivative had been used.

Michelsen (4-6) recommends the method of Murray (10). In cases where the Hessian is not positive definite an approximate Hessian is calculated that is positive definite and looks as much as possible like the original Hessian (intermezzo 4).

In stead of using the original Hessian, the modified Hessian is subsequently used when solving equation 3.16. Then the resulting Newton direction always points to smaller values of the Gibbs energy.

Intermezzo 4: The Hessian is decomposed by a so called Cholesky decomposition into a lower triangular matrix L and a diagonal matrix D:

$$\text{eq. 3.18} \quad \nabla^2 G = L \cdot D \cdot L^T$$

The j-th column of the L matrix is defined from the previous columns by the equations :

$$d_j = \nabla^2 G_{jj} - \sum_{s=1}^{j-1} d_s l_{js}^2$$

$$l_{ij} = \frac{1}{d_j} \left( \nabla^2 G_{ij} - \sum_{s=1}^{j-1} d_s l_{js} l_{is} \right)$$

If the Hessian is positive definite, all the elements of the diagonal of D are positive. In the other case the decomposition results in a matrix D with some negative elements and a matrix L with sometimes extremely large values. Murray's method modifies the elements of the L and D matrix during decomposition : if during decomposition an element  $d_j$  becomes smaller than a small positive number  $\delta$ ,  $d_j$  is replaced by  $\delta$ . The value of delta is determined by computer precision. If by using this value of  $d_j$  for the calculation of the next column of L one of the values of the elements of L next exceeds a certain maximum, the value of  $d_j$  is increased, such that the elements of L will be below that maximum. The maximum of the elements of the column of L to be calculated is given by

$$l_{ij}^2 \leq \frac{1}{d_j} \cdot \max \left( \gamma, \frac{\xi}{\sqrt{N^2 - 1}}, \epsilon_M \right)$$

$\gamma$  is the largest diagonal element of the Hessian,  $\xi$  is the largest off-diagonal element of the Hessian and  $\epsilon_M$  is the precision of the computer used.

Using the modified forms of the L and D matrices a modified Hessian is calculated. This modified Hessian is positive definite. The decomposition and recombination of the original Hessian is numerically stable. The resulting modified Hessian is a very close positive definite approximation of the original Hessian.

### 3.3.3 Removal of phases

Occasionally it is necessary to remove one of the phases during solving the flash equations. This can occur in cases where e.g. initially a liquid phase is most stable, next a phase split occurs into liquid and  $\beta$ , thereafter a second split into liquid,  $\beta$  and  $\beta'$  and during subsequent iterations the amount of liquid starts to approach zero. Calculations become increasingly inaccurate in that case. Therefore if the amount of one of the phases present drops below 5% during iterations, it is examined whether two phases can 'coalesce' such that a reduction in Gibbs energy is obtained. In that case iterations are continued with a reduced number of phases.

## 3.4 COMPARING METHODS

### 3.4.1 Criteria

The procedures that were outlined and modified in the previous section have to be compared on their performance with multicomponent multiphase solid-liquid flashes. Unfortunately no experimental data exist, in which the number of coexisting solid phases and their composition is known. It is probably impossible to obtain such data for TAG-systems. As an alternative the following procedure is adopted:

Both stability tests are applied and the initial estimates are converged using all three convergence methods. Criteria for performance of the stability tests are:

1. Indication of instability where this is not the case: the test indicates instability and results in a phase split while during subsequent convergence this phase is removed again.
2. Failure to predict instability: one test indicates instability, the other doesn't, while the resulting converged phase split indeed has a reduced Gibbs free energy.
3. Number of iterations needed to converge the initial estimate.

Performance criteria for the convergence methods are:

1. Convergence.
2. The total computing time to reach convergence.

As test cases the following systems were considered:

- A. Fully hardened palm oil (P058), a 6 component system containing all TAGS that can be formed from palmitic and stearic acid, at temperatures between 40 and 70 °C.
- B. A ternary system of SSS, PPP and SES, where two components that are completely immiscible in the solid phase are combined with a component that is partially miscible with both. Temperature is varied between 50 and 75 °C.

As description of the excess Gibbs energy both the 2-suffix and the 3-suffix Margules equation were used (see chapter 7 ). The necessary binary interaction coefficients were obtained by fitting the data of de Bruyne (15, 20, chapter 7). Calculations were performed three times, first only allowing the formation of the  $\alpha$ - modification, secondly only allowing the  $\beta'$ -modification and finally allowing all modifications.

Swank and Mullins(7) performed a similar exercise with a number of vapour - liquid phase equilibria. They judged Michelsen's stability test as the most reliable and direct substitution as the quickest convergence method. However not all problems could be solved by direct substitution.

A combination of Michelsen's stability test plus a Murray minimisation always lead to the correct solution.

### 3.4.2 Test Results

A computer program was written in Turbo Pascal 5.0 for MS-DOS PC's that implements the two initial estimate and stability test procedures and the three methods to solve the flash equations.

The stability test of Michelsen clearly performs better than the algorithm of Gautam and Seider: it is faster and more reliable: Especially in the ternary test system the splitting component approach indicates instability, where this is not the case.

Both tests where perfectly able to deal with polymorphism in the solid phase. The coexistence of a number of stable  $\beta$  and  $\beta'$  phases in P058 was obtained without problems.

COMPARING METHODS

The three convergence algorithms are compared in table 3.1.

table 3.1 : average time per flash (of 60 flashes) for the test systems. (on a Compaq 386/25 PC under MS DOS)

System	number of phases	Direct Substitution	Rand	Murray
P058 ( $\alpha$ form)	2	0.1 s	0.3 s	0.3 s
P058 ( $\beta'$ , 2 suffix)	3	0.5 s	no conv.	0.8 s
P058 ( $\beta'$ , 3 suffix)	3	no conv.	no conv.	1.4 s
P058 ( $\beta' + \beta$ , 2 suffix)	4	no conv.	no conv.	2.0 s
P058 ( $\beta' + \beta$ , 3 suffix)	5	no conv.	no conv.	2.7 s
(SSS/PPP/SES) $\alpha$	2	0.08 s	0.12 s	0.12 s
(SSS/PPP/SES) $\beta'$	2	0.16 s	0.3 s	0.12 s
(SSS/PPP/SES) $\beta$	3	0.16 s	0.2 s	0.24 s

No conv. in the table means that convergence to a gradient norm of  $10^{-12}$  was not obtained within 50 iterations. Except for the  $\alpha$  phase and cases where no convergence was obtained, direct substitution converged within 6 to 25 iterations, while the Murray method needed 2 to 6 iterations.

For  $\alpha$  phase calculations (in chapter 5 is shown that miscibility in the  $\alpha$ -modification is ideal, so only one solid phase plus a liquid phase are present) direct substitution is especially for larger systems ( $N= 6 - 50$ ) the quickest method that will converge safely.

The Rand Method has, as expected, problems with converging in highly non-ideal systems and in systems where the initial estimate contains concentrations close to zero. Performance is inferior to both other methods.

The Murray method always resulted in a reasonably fast and safe convergence and is therefore the best method to be used for the  $\beta'$  and  $\beta$  modifications, where demixing in the solid phase can occur. It is slower than the direct substitution method but more reliable.

These conclusions are in line with those of Michelsen: for vapour-liquid flashes with one liquid phase he advises the direct substitution method, while for VLL and VLLL flashes a Murray minimisation works out better.

For flash calculations in fats it is therefore recommended to use Michelsen's stability test for initial estimates and Murray minimisation of the Gibbs Free energy for obtaining the final solution. For the  $\alpha$  modification the direct substitution method should be used.

### 3.5 CALCULATION OF DIFFERENTIAL SCANNING CALORIMETRY CURVES

Differential Scanning Calorimetry (DSC) is one of the most frequently used techniques to study the solid phase behaviour of TAGs.

With DSC the apparent heat capacity of a sample is measured as a function of the temperature. It is often used as a tool to characterize a crystallized fat (16,17,18,21) and slowly replaces the more traditional methods for quality control of Cocoa Butter Equivalents and Replacers (19). Comparison of experimental and calculated DSC-curves enables a better interpretation of those curves.

If we make the simplifying approximation that the heat capacity of solid and liquid fat is equal, then the equilibrium DSC curve at infinitive slow scanning rate of any fat mixture can be calculated from:

$$\text{eq. 3.19} \quad C_p^{\text{apparent}} = C_p + \left( \frac{\partial H}{\partial T} \right)_n$$

$$H = H^E + \sum_{j=1}^P \sum_{i=1}^N n_i^j H_i^{0,j}$$

For convenience we set  $H(\text{liquid})$  to zero for each component, which implies that  $H^0$  becomes equal to the heat of fusion of the pure component in that modification. Another assumption is to neglect the excess entropy, which will be most likely comparatively small. The DSC curve can then be calculated from:

$$\text{eq. 3.20} \quad C_p^{\text{apparent}} = C_p + \frac{\partial G^E}{\partial T} + \sum_{j=1}^P \sum_{i=1}^N H_i^j \frac{\partial n_j^i}{\partial T}$$

The two partial derivatives in this formula are easily obtained by numerical differentiation, which requires two flash calculations for



CALCULATION OF DIFFERENTIAL  
SCANNING CALORIMETRY CURVES

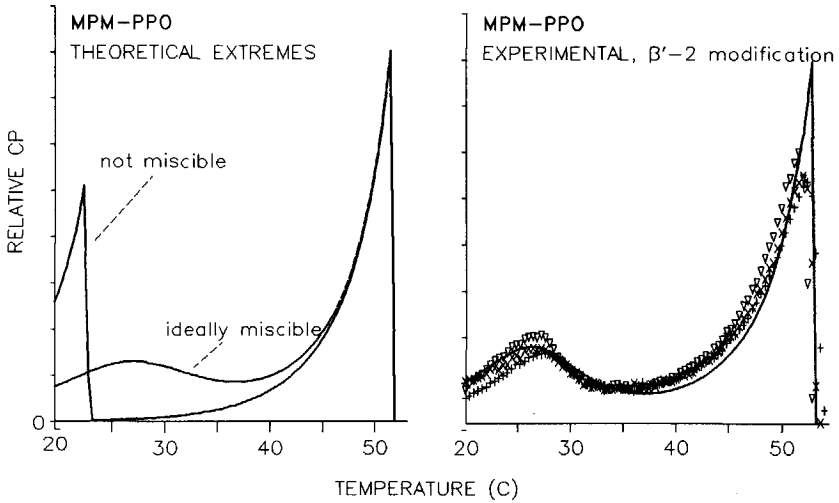


fig. 3.2 DSC - melting curves of a mixture of 25 MPM, 25 PPO and 50 000

left : theoretical extremes: ideal and no solid state miscibility  
right: experimental (points) and calculated (line) curves.

each point on a DSC curve. Calculations are speeded up considerably when the outcome of the flash calculation for one point is used as initial estimate for calculation of the next point.

Norton (12) constructs a DSC curve by using the Hildebrand equation for calculating the partial derivatives. The applicability of this approach is rather limited, because the Hildebrand equation describes only the phase behaviour of pure (=completely demixed) solid phases. Solid phase miscibility has a large influence on the shape of a DSC curve as is shown in figure 3.2 for the ternary system 25 MPM/ 25 PPO/ 50 000 in the  $\beta'$  form. This system cannot be described by the Hildebrand equation.

As will be shown in chapter 7, the ternary of fig 3.2 can be described by the two suffix Margules equation in which the binary interaction coefficient  $A_{MPM-PPO}$  is  $1.8 \pm 0.3$ . Although no demixing of the solid phase takes place, still two peaks occur in the DSC curve. In literature the appearance of two peaks in DSC-thermograms of a fat

is often used as indication for the presence of two solid phases (11,13,15,16). In fact it only indicates the presence of two groups of TAGs in the fat that have a clear difference in melting point, but may have cocrystallized.

Figure 3.2 also shows that DSC, together with the calculation procedures of this report form an elegant method for determination of binary interaction parameters and verification of excess Gibbs energy models.

### 3.6 CONCLUSION

A flash calculation consists of two parts: A stability test that gives an initial estimate of the phase compositions when it detects that a phase split can occur, and a convergence method that determines the phase compositions and phase quantities at equilibrium starting from the initial estimate. As no procedures for solid-liquid flashes were available, several existing methods for vapour-liquid flashes were adapted and tested for their performance with solid liquid flashes in fats.

1. The best stability test is the so called stability test of Michelsen, that, with some small changes, can perfectly handle solid fats and polymorphism.
2. Only in case of the  $\alpha$  modification (ideal solid miscibility) the normal direct substitution method for solving the flash equation gives a quick, reliable result.
3. For the  $\beta'$  and  $\beta$  modification (highly non-ideal solid phases) direct substitution is unreliable. The flash problem can better be solved with a Gibbs free energy minimisation using Murray's method (A modified Newton method). This method is somewhat slower but very reliable.
4. Flash calculations can be applied for simulation of DSC curves of fat blends.

LIST OF SYMBOLS

LIST OF SYMBOLS

$c_p$	Heat capacity (J/mol,K)
$g$	molar Gibbs free energy (J/mol)
$G$	Gibbs free energy (J)
$k, K$	A constant
$K^{AB}$	distribution constant
$N$	Number of components
$n$	Amount of material (mol)
$P$	Number of phases
$R$	Gas constant (J/mol,K)
$T$	Temperature (K)
$T_f$	Normal melting point (K)
$x, y$	mole fractions
$z$	overall mole fraction
$\gamma$	activity coefficient
$\Delta H_f$	Heat of fusion at $T_f$ . (kJ/mol)
$\phi$	phase fraction
$\mu$	chemical potential (J/mol)

REFERENCES

1. J.M. Prausnitz Molecular Thermodynamics of Fluid Phase Equilibria. Prentice Hall 1986
2. R. Gautam, W.D. Seider AIChE Journal 25, 991 (1979).
3. R. Gautam, W.D. Seider AIChE Journal 25, 999 (1979).
4. M. Michelsen, Fluid Phase Eq. 9, 1 (1982).
5. M. Michelsen, Fluid Phase Eq. 9, 21 (1982).
6. M. Michelsen Fluid Phase Eq. 16, to appear (1989)
7. D.J Swank, J.C. Mullins: Fluid Phase Eq. 30, 101 (1986)
8. V.B. Shah, Thesis, University of Toledo (1980)
9. C.M. Crowe, M.Nishio ,AIChE Journal 21, 528 (1975)
10. W. Murray, P.E. Gill, M.Wright, Practical Optimization p 108 Academic Press (London 1981).
11. P.H. Yap, J.M. de Man, L. de Man, JAOCS 66, 693 (1989)
12. I.T. Norton et al, JAOCS 62, 1237 (1985)
13. R.E. Timms, Progr. Lip. Res. 23, 1 (1984)
14. L. Asselineau, J. Jacq , 5th Int. Conf. on Fluid Properties and Phase Equilibria, Banff Canada, (May 1989)

PHASE EQUILIBRIA IN FATS  
- theory and experiments -

15. J.B. Rossell, Adv. Lip. Res. 5, 353 (1967)
16. L.H. Wesdorp, M. Struik, European patent EP 0 264 149 (1990)
17. A.C. Juriaanse, Butterlike Margarines, internal report Unilever Research R VD 85 6003 (1985)
18. M.J.N. Christophersen, Study of some fat blends with DSC, internal report Unilever Research P VD 86 3274 (1986)
19. K. Smith, Unilever Research Colworth, private communication (1988)
20. P. de Bruyne et al, Chem Phys Lipids 9, 309 (1972)
21. W. Ken Busfield, et al, JOACS 67, 171 (1990)



## CHAPTER 4 PURE COMPONENT PROPERTIES

For a thermodynamic description of the solid liquid phase equilibrium in a fat the enthalpy of fusion and melting point of each modification of each TAG in the mixture are needed. These pure component properties can impossibly be measured for all TAGs. Therefore correlations between structural characteristics and the properties must be developed. Existing correlations for heat of fusion and melting point are only reliable for mono-acid TAGs. Therefore, after having appended literature data with a set of experimental data, correlations for the heats of fusion and the melting points of TAGs in the  $\alpha$ ,  $\beta'$  and  $\beta$ -modification are developed.

### 4.1 LITERATURE DATA AND CORRELATIONS

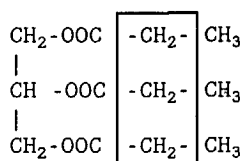
#### 4.1.1 Correlating enthalpy of fusion and melting points of lipids

It is often assumed (1-12) that the enthalpy and entropy of fusion of lipids (alkanes, fatty acids, methyl esters, TAGs) can be seen as the sum of a contribution of the hydrocarbon chains that depends linearly on the chain length and a contribution of the end and head groups that is independent of chain length.

$$\text{eq. 4.1} \quad \Delta H_f = hn + h_0$$

$$\text{eq. 4.2} \quad \Delta S_f = sn + s_0$$

$n$  is the carbon number of the component.



$n/3-2$

fig 4.1 Schematic representation of the head group, the hydrocarbon chain and the end group of a TAG.

In this view, the incremental hydrocarbon chain contributions  $h$  and  $s$  do not depend on the nature of the compound but only on the way the hydrocarbon chains are packed:  $h$  and  $s$  are universal lipid

LITERATURE DATA AND CORRELATIONS

constants that only depend on the polymorphic form in which the lipid has crystallized. This is experimentally confirmed (table 4.1). Only the values for h of Bailey (11) and de Bruyne (12) for the  $\alpha$ -modification of TAGs deviate. Perron(3) showed that these numbers were derived from very unreliable data.

table 4.1 Values for the incremental hydrocarbon chain contribution to the enthalpy of fusion (h) and the entropy of fusion (s). Numbers in superscript are references.

compound	polymorph	h (kJ/mol CH <sub>2</sub> )	s (J/K, mol CH <sub>2</sub> )
n-alkanes	$\alpha$	2.64 <sup>1</sup> , 2.5 <sup>2</sup> ,	6.4 <sup>1</sup> , 6.0 <sup>2</sup>
TAGs	$\alpha$	2.5 <sup>3</sup> , 3.4 <sup>11</sup> , 3.6 <sup>12</sup>	6.1 <sup>3</sup>
n-alkanes	$\beta'$	3.2 <sup>1</sup> , 3.8 <sup>2</sup> , 3.98 <sup>4</sup> , 3.86 <sup>5</sup>	7.7 <sup>1</sup> , 9.7 <sup>2</sup> , 9.52 <sup>4</sup> ,
methylesters	$\beta'$	3.78 <sup>6</sup>	9.2 <sup>6</sup>
TAGs	$\beta'$	3.87 <sup>3</sup> , 3.25 <sup>7</sup>	9.8 <sup>3</sup>
n-alkanes	$\beta$	4.11 <sup>1</sup> , 4.12 <sup>8</sup>	9.9 <sup>1</sup> , 9.89 <sup>8</sup>
methylesters	$\beta$	4.28 <sup>6</sup>	10.3 <sup>6</sup>
fatty acids	$\beta$	4.29 <sup>9</sup> , 4.3 <sup>7</sup>	11.1 <sup>7</sup>
diglycerids	$\beta$	4.28 <sup>7</sup>	10.5 <sup>7</sup>
monoglycerides	$\beta$	4.28 <sup>7</sup>	10.5 <sup>7</sup>
TAGs	$\beta$	4.28 <sup>7</sup> , 4.20 <sup>3</sup>	10.5 <sup>3</sup> , 10.6 <sup>7</sup>

The end group contributions  $h_0$  and  $s_0$  are specific to each class of lipids. Correlating the properties of alkanes and methylesters results in different values for  $h_0$  and  $s_0$  for these two groups of components.

The melting point T is simply given by the ratio of the enthalpy and entropy of fusion:

eq. 4.3

$$T_f = \frac{\Delta H_f}{\Delta S_f} = \frac{hn + h_0}{sn + s_0}$$

Expanding the denominator in this equation into a power series of  $1/n$  gives:

eq. 4.4

$$T_f = \frac{h}{s} \left( 1 + \left( \frac{h_0}{h} - \frac{s_0}{s} \right) \frac{1}{n} - \frac{s_0}{s} \left( \frac{h_0}{h} - \frac{s_0}{s} \right) \frac{1}{n^2} + \dots \right)$$

This equation can be cut off after the second or the third term:

eq. 4.5 
$$T_f = T_\infty \left( 1 + \frac{A}{n} - \frac{AB}{n^2} \right)$$

eq. 4.6 
$$T_f = T_\infty \left( 1 + \frac{A}{n} \right)$$

The constants  $T_\infty$ , A and B are given by:

eq. 4.7 
$$T_\infty = \frac{h}{s} \quad , \quad A = \frac{h_0}{h} - \frac{s_0}{s} \quad , \quad B = \frac{s_0}{s}$$

This implies that if the melting points of a class of lipids have been correlated, only one data point for the enthalpy of fusion is in principle sufficient to obtain a correlation for the enthalpy of fusion of the complete class of lipids.

Equation 4.6 has successfully been used by Zacharis (10) to correlate the melting points of a large number of lipids: n-alkanes, methyl-esters, ethylesters, fatty acids, mono-acid mono- di- and triacylglycerols, phosphoglycerides and dicarboxylic acids. He has found values for  $T_\infty$  that vary between 390 K and 410 K.

#### 4.1.2 Data and correlations for TAGs

The main difficulty in the development of correlations for the thermal properties of TAGs is that TAGs do not belong to one class of lipids in the sense of section 4.1.1. Not all TAGs share the same end-group. This becomes clear when a saturated TAG is formally denoted by the lengths p, q and r of its three fatty acid chains, i.e. p.q.r. P is always the shortest of the fatty acid chains on the 1- and 3-position of the glyceryl group. For example, myristoyl-stearoyl-palmitoyl-glycerol (MSP) is denoted as 14.18.16. The chain length differences x and y are defined as follows:

$$\begin{aligned} x &= q - p \\ y &= r - p \end{aligned}$$



LITERATURE DATA AND CORRELATIONS

Only TAGs having the same value of  $x$  and  $y$  belong to a family of TAGs that share the same end-group. For TAGs that differ in  $x$  and  $y$  the value of the head and end group contributions  $h_0$  and  $s_0$  from eq. 4.1 and 4.2 are different.

The dependency of the 'head and end group' contributions  $h_0$ ,  $s_0$ ,  $A$  and  $B$  from  $x$  and  $y$  and from the presence of unsaturation in the hydrocarbon chains must be accounted for in the development of general correlations for all TAGs. In this work this will be accomplished by the addition of two extra terms to equations 4.1 and 4.2.

$$\text{eq. 4.8} \quad \Delta H_f = h_n + h_0 + h_{xy} f_{xy} + h_{\text{unsat}} f_{\text{unsat}}$$

$$\text{eq. 4.9} \quad \Delta S_f = s_n + s_0 + s_{xy} f_{xy} + s_{\text{unsat}} f_{\text{unsat}}$$

The functions  $f_{xy}$  and  $f_{\text{unsat}}$  should account for the effects on the thermodynamic properties of differences in chain length and degree of unsaturation. Their functional form cannot a priori be established.

#### Literature

The literature on the enthalpy of fusion of TAGs was reviewed up to 1975 by R.E. Timms (7). Timms provided the enthalpy of fusion of 42 triglycerides, 19 saturated (16 beta and 3 beta') and 23 unsaturated TAGs. The data were correlated using equation 4.1:

$$\Delta H_f^\beta = 4.28n - 32.6 \text{ kJ/mol}$$

$$\Delta H_f^{\beta'} = 0.76\Delta H_f^\beta$$

For mixed acid saturated TAGs the enthalpy of fusion should be reduced by 18.3 kJ/mol. The enthalpy of fusion of unsaturated TAGs was described by setting an effective carbon number for each unsaturated fatty acid ( $O = 10.4$ ,  $E = 13.9$ ,  $Li = 8.9$ ). The root mean square error between experimental and predicted data is 4.3 kJ/mol. The values for  $h$  agree with those reported for other compounds (table 4.1).

Since 1975 various data on the enthalpy of fusion of the stable beta modification of saturated fatty acids were reported (3, 13, 14, 15, 16, 17, 18, 19, 20, 21, 22, 23, 24, 26). The majority of these data concern mono-acid TAGs. There is only one observation for the

PHASE EQUILIBRIA IN FATS  
- theory and experiments -

$\alpha$ -enthalpy of fusion of a mixed acid saturated TAG (PSP,16). The data for the  $\beta'$ -modification of saturated TAGs mainly concern PSP and LML. Some data on the mono-acid saturated TAGs are available, but they show large deviations (3,14,20), which are ascribed to the existence of a second, less stable  $\beta'$ -form. Only the data for the most stable  $\beta'$ -form were taken. The number of data for the lesser stable forms was too small and the data showed no consistency.

The data of Hagemann (14) for AAA to 30.30.30 for the  $\beta'$  form and for BBB to 26.26.26 for the  $\beta$ -form look very unreliable: the enthalpy of fusion levels off and starts to decrease with increasing carbon number, which is in contradiction to the generally observed trend in lipids. The same holds for the data of Perron (20) for the  $\beta'$ -form of AAA and BBB, which is also admitted by Perron in a later article (3).

The data reported by Garti, Schlichter and Sarig (19) for all modifications differ completely from all other values reported. Therefore they are disregarded in this report.

Perron (6) has carried out the most extensive work on development of correlations for the enthalpy of fusion and melting points of TAGs since Timms. His correlations for the enthalpy of fusion of mono-acid TAGs are:

$$\Delta H_f^\alpha = 2.5n - 27.5 \quad \text{kJ/mol}$$

$$\Delta H_f^{\beta'} = 3.87n - 19.2 \quad \text{kJ/mol}$$

$$\Delta H_f^\beta = 4.20n - 29.9 \quad \text{kJ/mol}$$

Perron modelled the enthalpy of fusion of an unsaturated TAG as that of the corresponding saturated TAG minus a contribution of the double bonds:

$$\Delta H_f(\text{unsat}) = \Delta H_f(\text{sat}) - 115(1 - e^{-0.706\Delta})$$

$\Delta$  = number of double bonds in the TAG.

LITERATURE DATA AND CORRELATIONS

Perron's values for  $h$  agree very well with those for other compounds given in table 4.1

Perron did not give relations for the enthalpy of fusion of mixed acid TAGs. However, he correlated the  $\alpha$  and  $\beta$ -melting points of 19 different TAG families using equation 4.6. It resulted, as expected, in large fluctuations of the constant  $A$ .

The total collection of data from literature and from the database of Unilever Research Vlaardingen resulted in 152 values for the enthalpy of fusion and 944 melting points. Many of these data are multiple measurements for the same TAG. The polymorphic form of the solid phase is not always given. The number of different TAGs for which data are available is much less (table 4.2)

table 4.2: Number of TAGs for which melting points and enthalpies of fusion are available in literature.

	$\Delta H_f$			$T_f$		
	$\alpha$	$\beta'$	$\beta$	$\alpha$	$\beta'$	$\beta$
saturated	10	10	30	65	54	87
unsaturated	8	11	16	50	47	49

### Conclusion

We found a disappointing number of data for the heat of fusion of TAGs. The heat of fusion data that are available for the unstable modifications are mainly for mono-acid TAGs. Consequently the correlations that have been developed are only valid for mono-acid TAGs. An experimental program is required before these correlations can be extended to mixed acid TAGs.

A considerable amount of melting points that is reasonably well spread over the modifications and TAG-families is available. Correlations have been developed for a number of individual TAG-families, but a general correlation is not available. This correlation will be developed in section 4.3.

#### 4.2 EXPERIMENTAL WORK

The enthalpy of fusion and melting points of 42 saturated mixed acid TAGs and 9 unsaturated TAGs were determined for all three polymorphic forms. The pure TAGs were taken from the stock of reference materials of Unilever Research Vlaardingen. Their purity exceeds 95%.

The experimental program was carried out on a Perkin Elmer Differential Scanning Calorimeter (DSC-7). This DSC-7 is equipped with a TAC 7/3 datalogger and a liquid nitrogen Cooling Accessory. Control of the apparatus is achieved by means of a PE computer. A more extensive description of DSC is given in chapter 7.

The thermal data for each modification were obtained by the following procedures:

The data for the  $\beta$ -modification were obtained from the melting curve of the samples as they were delivered, so after several months to years of storage at room temperature.

The  $\alpha$ -modification was obtained by rapidly quenching the TAGs from 10°C above the  $\beta$ -melting point to at least 20°C below the  $\alpha$ -melting point. The enthalpy of fusion was obtained from the cooling curves. The melting curves were normally not suited for determination of  $\alpha$ -thermal data, as the  $\alpha$ -melting peak interfered with the  $\beta'$  and  $\beta$ -crystallization peaks.

The  $\beta'$ -modification was most difficult to prepare as a pure substance; interference of the  $\beta'$ -melting peak with the  $\alpha$ - $\beta'$  or the  $\beta'$ - $\beta$  recrystallization peaks was often obtained. Although we did not always succeed in preparing pure  $\beta'$ , in general one of the two following methods gave good results:

- A. The TAG was crystallized into the  $\alpha$ -modification by quenching. Next it was heated till  $\alpha$ -melting set in and stabilised at that temperature for, depending on the TAG used, 1 minute to 1 hour. The melting curve was taken.

DEVELOPMENT OF THE CORRELATION.

B. If a  $\beta'$ - $\beta$ -transition interfered in procedure A, the TAG was melted to 10°C above the  $\beta$ -melting point, rapidly cooled to 1 or 2°C above the  $\alpha$ -melting point and stabilized for 30 minutes to 1 hour. The melting curve was taken.

The results are reported in appendix 1, marked by a \*.

#### 4.3 DEVELOPMENT OF THE CORRELATION.

In the development of the correlations, data for TAGs containing acetic acid, butyric acid and hexanoic acid are not used. The chain length of these fatty acids is so short, that they cannot be looked upon as long chain hydrocarbons.

##### 4.3.1 Saturated TAGs

###### Melting enthalpy

If the data for mono-acid TAGs are regressed against the carbon number  $n$  (equation 4.1), leaving out data that have a residual more than two times the root mean square error (RMSE) of the regression through all mono-acid data, we obtain:

$$\Delta H_f^a = 2.4 n - 17.6 \text{ kJ/mol, RMSE}=4.6, r^2=0.98$$

$$\Delta H_f^{\beta'} = 3.95 n - 59.2 \text{ kJ/mol, RMSE}=4.7, r^2=0.97$$

$$\Delta H_f^{\beta} = 4.13 n - 27.6 \text{ kJ/mol, RMSE}=6.1, r^2=0.97$$

The RMSE is in the order of magnitude of the experimental error (5-8 kJ/mol) and the values of the constants  $h$  agree with those of Perron(3) and those for other lipids, given in table 4.1.

If all data are used for a regression of  $\Delta H_f$  against the carbon number, the values of the incremental chain contribution  $h$  do not change significantly, but the RMSE goes up to 20 and the correlation coefficient decreases to 0.7. A RMSE of 20 is too large for a reliable correlation and a correction term for chain length differences must be introduced.

It can not a priori be assumed that the end group contribution and the variables  $x$  and  $y$  that define a TAG-family are neatly correlated. Neither is there any function  $f_{xy}$  that is self-evident for use. When

PHASE EQUILIBRIA IN FATS  
- theory and experiments -

Table 4.3. Parameters that result when equation 4.10 is fitted to the experimental melting enthalpy data of saturated TAGs. (s.e = standard error in estimate)

parameter	$\alpha$ -modification		$\beta^1$ -modification		$\beta$ -modification	
	estimate	s.e	estimate	s.e	estimate	s.e
h	2.39	0.1	4.17	0.2	4.03	0.1
h <sub>0</sub>	-16.3	5	-68.4	8	-24.4	4
h <sub>x</sub>	1.98	0.3	17.3	1.6	2.16	0.4
h <sub>x2</sub>	-0.54	0.07	-3.25	0.3	-0.63	0.07
h <sub>xy</sub>	-		-1.07	0.3	-	
h <sub>y</sub>	-		-9.03	1.2	-7.28	0.5
h <sub>y2</sub>	-0.64	0.08	-		-	
RMSE	5.2		6.0		7.1	

the residual error of data predicted by the mono-acid relation with the experimental data are plotted against x and y, it becomes clear that the end group contribution and (x,y) are correlated. The enthalpy of fusion drops more or less quadratically when the difference in chain lengths, represented by x and y, increases. X and y behave similarly and their effect seems additive. From the data for the  $\beta$ -modification it can be seen that the effect of x and y levels off at values of x or y of 6 and more. This is probably associated with the transition from the  $\beta$ -2 form to the  $\beta$ -3 form. At large x or y the -3 forms become more stable than the corresponding -2 forms.

A function that can describe the influence of chain length differences on the melting enthalpy that is observed is a general quadratic function:

$$\text{eq. 4.10} \quad \Delta H_f = hn + h_0 + h_x x + h_{x2} x^2 + h_{xy} xy + h_y y + h_{y2} y^2$$

In order to introduce the levelling-off at high x or y, we used a cut-off value of 6 in the calculations in stead of the real value of x or y when x or y exceeded 6. The resulting fit to the experimental data was very good: a RMSE nearly equal to that of a fit to the mono-acid data only was obtained. Melting enthalpies deviating more

DEVELOPMENT OF THE CORRELA-  
TION.

than 20 kJ/mol from the model predictions were rejected. The resulting values for h are in agreement with those of other lipids given in table 4.1.

**Melting points.**

If equation 4.5 is used to fit the mono-acid data, it results in a RMSE of 1.5°C for the  $\alpha$ - and  $\beta$ -modification and 3°C for the  $\beta'$ -modification. This compares very well to the experimental error in the melting points of 1-2°C. The RMSE increases to 7-10°C when equation 4.5 is fitted to all data of saturated TAGs. A closer look to the differences between experimental melting points and those predicted by the fit to the mono-acid data suggests a quadratic relationship between x and y and the model parameters A and B:

$$\text{eq. 4.11} \quad A = A_0 + A_x x + A_{x2} x^2 + A_{xy} xy + A_y y + A_{y2} y^2$$

$$B = B_0 + B_x x + B_{x2} x^2 + B_{xy} xy + B_y y + B_{y2} y^2$$

*Table 4.4. Parameters that result when equation 4.6 and 4.11 are fitted to the experimental melting points of even saturated TAGs*

parameter	$\alpha$	$\beta'$	$\beta$
A <sub>0</sub>	-9.0581	-8.4543	-8.0481
A <sub>x</sub>	0.00290	-0.10360	0.074130
A <sub>x2</sub>	-0.0619116	-0.018881	-0.0348596
A <sub>xy</sub>	0.115128	0.0739411	0.00771420
A <sub>y</sub>	-0.453461	-0.49721	-0.404136
A <sub>y2</sub>	-0.005827	0.0115995	0.0111938
B <sub>0</sub>	-4.4841	-0.26501	2.66923
B <sub>x</sub>	-0.00111	0.54997	-0.31675
B <sub>x2</sub>	0.148938	0.074136	0.085967
B <sub>xy</sub>	-0.365917	-0.340928	0.040642
B <sub>y</sub>	1.41154	2.34238	0.55040
B <sub>y2</sub>	-0.001766	-0.135735	-0.000945
T <sub>m</sub>	401.15	401.15	401.15
RMSE	2.3°C	2.9°C	3.0°C

If the model of equation 4.11 is fitted to the data, the RMSEs that result are most satisfying. A subdivision of the modifications into their -2 and -3 forms ( $\beta$ -2 and  $\beta$ -3 etc) does not give an improved fit.

The values for  $T_m$  are in agreement with the values that were found by Zacharis (10).

#### Simultaneous fit of melting points and melting enthalpies.

Although the empirical relations that were derived above are perfectly useful as such, a few unsatisfying aspects must be mentioned:

1. According to equation 4.7 the values for the parameters of relationship 4.10 for the melting enthalpy can be derived from the parameters values of relation 4.5 + 4.11 for the melting point. If this is actually done so, the resulting parameters for the melting enthalpy are completely different from those given in table 4.3. The melting enthalpies that are calculated in this way do not at all agree with the experimental data. Apparently the parameters of table 4.4 are not consistent with those in table 4.3.
2. The melting enthalpy data for the  $\beta$ -modification showed clearly that the influence of x and y levels off when x or y are greater than 6. The melting points did not seem to show such effect. However, if the correlation for the melting points extrapolated to extreme values of x or y, absurd results are obtained, indicating that levelling off of the influence of x and y should be introduced.

Therefore, in this section we will attempt to derive a unified model for both the enthalpies of melting, the entropies of melting and the melting points of saturated TAGs, by fitting the  $\Delta H_f$  and  $T_f$  data simultaneously.

The function  $f_{xy}$ , as defined in eq. 4.8 and 4.9 should account for the observed decrease in melting enthalpies and melting points as differences between the three chain lengths increase. It should be chosen in such a way that this effect does not grow indefinitely



DEVELOPMENT OF THE CORRELA-  
TION.

with increasing  $x$  and/or  $y$  but levels off. The general quadratic relations with cut-off value, which were previously used, did not perform well. The function finally arrived at is:

eq. 4.12

$$f_{xy} = 2 - \exp\left\{-\left(\frac{x-x_0}{k_x}\right)^2\right\} - \exp\left\{-\left(\frac{y}{k_y}\right)^2\right\}$$

which increases from 0 (for small values of both  $x$  and  $y$ ) via 1 (for a large absolute value of either  $x$  or  $y$ ) to 2 (for large values of both  $x$  and  $y$ ). We have investigated a more complex variation of this function, namely:

eq. 4.13

$$f'_{xy} = 2 - \left(1 + \frac{1}{2}\delta\right) \exp\left\{-\left(\frac{x'-x_0}{k_x}\right)^2\right\} - \left(1 - \frac{1}{2}\delta\right) \exp\left\{-\left(\frac{y'-y_0}{k_y}\right)^2\right\}$$

with

$$\begin{aligned} x' &= \cos \Theta x + \sin \Theta y \\ y' &= \cos \Theta y - \sin \Theta x \end{aligned}$$

The more general function [4.13] allows for a rotation over an angle  $\Theta$  of the  $(x,y)$ -axes to  $(x',y')$ -axes, a difference in scaling along these directions ( $k_x$  and  $k_y$  instead of a common  $k$ ), a non-zero offset  $y_0$ , and a relative difference in the maximal effects along the two directions expressed by the parameter  $\delta$ . It appeared, however, that equation 4.12, which is a special case of the more general equation 4.13 (viz.  $\Theta = 0$ ,  $k_x = k_y = k$ ,  $y_0 = 0$ ,  $\delta = 0$ ) gave a satisfactory fit to the data. Therefore, the results reported further on refer to this simpler model.

We must also take into account the possible effect of asymmetry on melting points. This is done by including an additional  $R\ln 2$  term in the expression for the melting entropy to distinguish symmetric ( $y=0$ ) from asymmetric ( $y \neq 0$ ) TAGs. The work of de Jong and van Soest has shown that for the  $\beta$ -phase the inclusion of such a term is appropriate (27, 28). In the  $\beta$ -modification random mixing of the two mirror images is not possible. For the loosely packed  $\alpha$ -phase we do not expect that this term is needed. The  $\beta'$ -phase takes an intermediate position and it is not clear beforehand whether the inclusion of the  $R\ln 2$  term will improve or worsen the fit.

Finally, we have to consider the phenomenon of melting point alternation: odd mono-acid TAGs tend to melt systematically lower than expected on the basis of interpolation from even mono-acid TAGs. Again we anticipate that allowance for this effect will improve the fit for melting points of  $\beta$ -phase TAGs. For the  $\alpha$ -phase TAGs we do not expect any benefit and for the  $\beta'$ -phase TAGs we do not know.

The full expressions for the enthalpy and entropy of melting then read:

$$\text{eq. 4.14} \quad \Delta H_f = hn + h_0 + h_{xy} f_{xy} + h_{odd} \cdot odd$$

$$\text{eq. 4.15} \quad \Delta S_f = sn + s_0 + s_{xy} f_{xy} + s_{odd} \cdot odd + R \ln 2 \cdot asym$$

Here 'asym' and 'odd' are indicator variables taking the value 1 ('true') when an asymmetric TAG or an odd TAG is involved and the value 0 ('false') otherwise. An TAG is considered 'odd' when at least one of the fatty acid chains has an odd number of carbon atoms.

The eight parameters  $h_0$ ,  $h_n$ ,  $s_0$ ,  $s_n$ ,  $h_{xy}$ ,  $s_{xy}$ ,  $k$  and  $x_0$  were estimated by simultaneously fitting the  $\Delta H_f$ -model (equations 4.12 and 4.14) to observed melting enthalpy data and the  $T_f$ -model based on equations 4.3, 4.12, 4.14 and 4.15 to observed melting points. The models were fit using weighted non-linear least-squares regression taking a factor 6 for the ratio of the variances of melting enthalpies and melting points.

Enthalpies of fusion deviating more than 20 kJ/mol from the model fit have been rejected. We also excluded all melting points which could not be fit well, i.e. that deviated more than 10 degrees. In all, the enthalpies of some 40 TAGs and the melting points of about 70 TAGs were fitted for the  $\alpha$ -,  $\beta'$ - and  $\beta$ -phase separately.

The main results are collected in appendix 1. Measured values are averaged over several observations with the number of independent observations given in the column labelled *FREQ*. Zero *FREQ* values refer to cases excluded from the estimation procedure. The heats of fusion that were measured in this work are separately listed. The estimated parameter values along with their standard errors are given in table 4.5.

DEVELOPMENT OF THE CORRELA-  
TION.

Table 4.5. Estimates and standard errors of the parameters from equation 4.14 and 4.15 when simultaneously fitted to melting points and melting enthalpies of all saturated TAGs.

parameter	$\alpha$ -modification		$\beta'$ -modification		$\beta$ -modification	
	estimate	s.e	estimate	s.e	estimate	s.e
h <sub>0</sub>	-31.95	3.00	-35.86	5.88	-17.16	4.83
h	2.70	0.07	3.86	0.13	3.89	0.10
s <sub>0</sub>	-19.09	10.56	-39.59	19.28	31.04	15.81
s	6.79	0.25	10.13	0.42	9.83	0.34
h <sub>xy</sub>	-13.28	2.42	-19.35	2.81	-22.29	2.08
s <sub>xy</sub>	-36.70	7.79	-52.51	8.76	-64.58	6.45
k	4.39	0.50	1.99	0.24	2.88	0.35
x <sub>0</sub>	1.25	0.27	2.46	0.19	0.77	0.27
T <sub>∞</sub>	397	4.1	381	3.6	395	3.3
h <sub>odd</sub>	-	-	-	-	2.29	0.44
RMSE ( $\Delta T_m$ )	8.6		9.2		10.3	
RMSE (T)	2.5		3.7		3.7	

It turned out that the inclusion of the symmetry/asymmetry term (Rln2) improved the fit for the  $\beta$ -phase in contrast to the  $\alpha$ -phase and the  $\beta'$ -phase where the fit became worse. A similar result was obtained for the even/odd term: no significant improvement for the  $\alpha$ - and  $\beta'$ -phase and a much better fit for the  $\beta$ -phase odd TAGs.

The resulting RMSEs for the melting points are only slightly more than those obtained by fitting the melting points solely. The RMSEs for the melting enthalpy have increased by 50%, but are still acceptable when compared to the experimental error of 5-7 kJ/mol. The values for h and s agree very well with those of other lipids, given in table 4.1. The values for h<sub>xy</sub>, which represent the maximum decrease in  $\Delta H_f$  that is caused by chain length differences and which are likely to be related to the enthalpy difference between the  $\beta$ -2 and  $\beta$ -3 form of a mono-acid TAG, compare well with the stability difference between the two forms that was calculated by de Jong (25) (10 -20 kJ/mol). The values of h<sub>xy</sub> and s<sub>xy</sub> increase from  $\alpha$  to  $\beta$ , in accordance with the expectation that the influence of chain length

PHASE EQUILIBRIA IN FATS  
- theory and experiments -

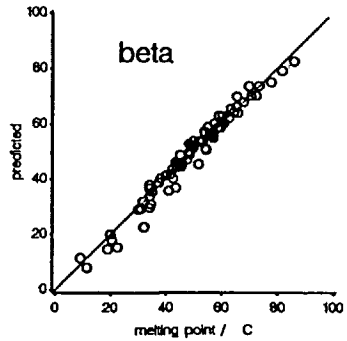
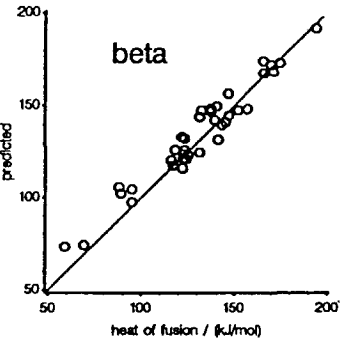
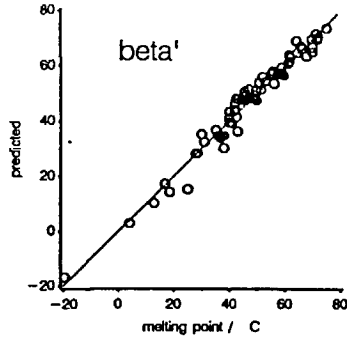
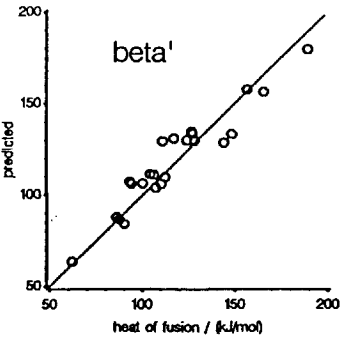
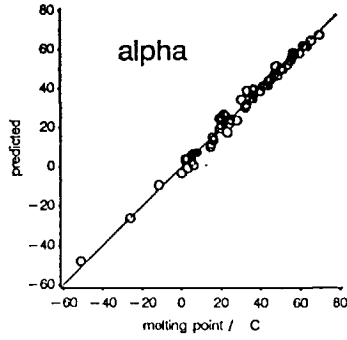
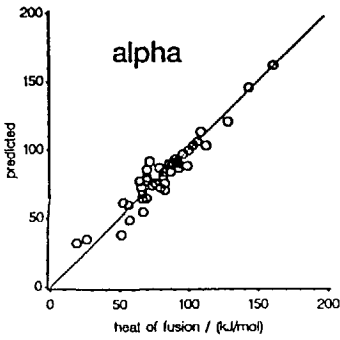


figure 4.2 Values of the melting enthalpy and the melting points of saturated TAGs, calculated using the relation 4.15 and 4.16 plotted against the experimental data.

differences is more pronounced in a more densely packed polymorph. In the  $\beta$ -modification the influence of  $x$  and  $y$  levels off at  $x$  or  $y = 6$  (2k), as was found previously.

A much more consistent correlation has been obtained at the expense of only a relatively small increase of the RMSEs.

#### 4.3.2 Unsaturated TAGs

##### melting enthalpy

We have chosen to model the effect of unsaturation on the melting enthalpy of a TAG as a correction to the melting enthalpy of the corresponding saturated TAG (eq. 4.8). The model proposed by Perron (6) did not perform very well; it resulted in a RMSE of more than 24 kJ/mol. After having investigated several other functions, the following model evolved:

$$\text{eq. 4.16} \quad \Delta H_f^{unsat} = \Delta H_f^{sat} + h_o n_o + h_e n_e + h_l n_l$$

Here  $n_o$  stands for the number of oleic chains,  $n_e$  stands for the number of elaidic chains and  $n_l$  for the number of linoleic chains in the TAG.  $\Delta H_f^{sat}$  is the melting enthalpy of the corresponding saturated TAG that can be obtained from the data in table 4.3 or table 4.5.

We have fitted this model for the  $\alpha$ ,  $\beta'$  and  $\beta$  modifications. The complete data set contained over 80 melting enthalpies of only 16 different TAGs: 20 observations for 12 TAGs in the  $\alpha$ -modification, 21 observations for 13 TAGs in the  $\beta'$ -modification, and 44 observations for 16 TAGs in the  $\beta$ -modification. We rejected data that deviated more than 30 kJ/mol from the predicted values. The data and the predictions are given in appendix 1. The resulting parameters are given in table 4.6

The values of the parameters that were obtained for the  $\beta$ -modification agree very well with the effective carbon numbers that Timms derived for the unsaturated fatty acids. The large RMSE for the  $\beta'$ -modification is solely due to the  $\beta'$ -melting enthalpy of POP (104 kJ/mol vs a predicted value of 128 kJ/mol). If POP is left out the RMSE decreases

PHASE EQUILIBRIA IN FATS  
- theory and experiments -

Table 4.6. Estimates and standard errors of the parameters of equation 4.16 fitted to the melting enthalpies of unsaturated TAGs. s.e = standard error. Values in brackets were guessed, due to lack of data.

parameter	$\alpha$ -modification		$\beta'$ -modification		$\beta$ -modification	
	estimate	s.e	estimate	s.e	estimate	s.e
$h_0$	-31.7	1.8	-28.3	1.8	-30.2	1.4
$h_E$	-11.7	1.3	(-15.9)		-15.9	0.9
$h_l$	(-37.7)		(-37.7)		-37.7	2.5
RMSE	8.3		22		11.1	

to 9.7, while the parameter values do not change. POP is the only cis-unsaturated TAG in the data set that crystallizes in the  $\beta'$ -2 form (26), which may explain its deviating behaviour.

There is a lack of data for the unstable modifications of TAGs with linoleic acid, so that the model parameter  $h_l$  for these modifications could not be calculated. The parameter that describes the effect of the fatty acid that is most similar to linoleic acid,  $h_0$ , is nearly independent from the modification. We have assumed that this also holds for  $h_l$ .

A good fit to the available data was altogether obtained; the RMSEs are nearly equal to those of the saturated TAGs. A better general model can only be developed if more experimental data are made available, over a wider range of carbon numbers, including linoleic acid and including mixed unsaturated fatty acid TAGs.

### melting point

An approach to model the melting points of unsaturated TAGs is start from a model for the saturated TAGs and add a correction term that accounts for the presence of O, E, l and linolenic acid (le) (eq. 4.8, 4.9). After exploring various simpler models we learned that it was necessary to model interactions between unsaturated chains. The final model giving the best results is equation 4.6 for which A is given by:

DEVELOPMENT OF THE CORRELA-  
TION.

$$\text{eq. 4.17} \quad A = A_{sat} + A_O n_O + A_E n_E + A_I n_I + A_{le} n_{le} \\ + A_{OO} n_{OO} + A_{EE} n_{EE} + A_{II} n_{II} + A_{lele} n_{lele} \\ + A_{OI} n_{OI} + A_{Ole} n_{Ole} + A_{Ile} n_{Ile}$$

and for which B is given by the much simpler expression:

$$\text{eq. 4.18} \quad B = B_{sat} + B_O n_O + B_I n_I + B_{le} n_{le}$$

Here, for example,  $n_O$  stands for the number of oleic chains in the TAG and  $n_{OI}$  for the number of O-I pairs.  $A_{sat}$  and  $B_{sat}$  can be obtained from table 4.4 and equation 4.11 or from table 4.5, using equations 4.13, 4,14 4,15 and 4.7.

We have fitted this model for the  $\alpha$ ,  $\beta'$  and  $\beta$  modifications. The complete data set contained over 120 melting points of cis-unsaturated TAGs, of which 18 were left out, because they involved unsaturated fatty acids other than O, I and le. Of the remaining 102 melting point data 13 were associated with the  $\alpha$ -modification, 16 with the  $\beta'$ -modification, 13 with the  $\beta$ -modification while for 60 data points the modification was not specified. The modification was not known for 13 of the 47 melting points of the trans containing TAGs.

In these cases we chose to assign the melting point to that modification, which gave the best fit. This assignment had to be done in an iterative manner using the results of the previous regression to determine the best modification input for the next regression analysis and carrying this process through till internal consistency was achieved. This laborious procedure can be viewed as a Maximum Likelihood estimation of both the melting point/ structure relationship and the unknown modifications. The data and the resulting assignments are given in appendix 1. Data deviating more than 10°C from the predicted value were disregarded. The parameters are given in table 4.7.

The standard deviations are only slightly larger than those for the saturated TAGs. We do not expect that these values can be substantially improved by another model. It should be realized that the reliability of the input data probably varies considerably. The data have been collected from literature spanning nearly a century. We have screened

PHASE EQUILIBRIA IN FATS  
- theory and experiments -

Table 4.7 Estimates and standard errors of the parameters in equations 4.17 and 4.18 fitted to the melting points of unsaturated TAGs

parameter	$\alpha$ -modification		$\beta'$ -modification		$\beta$ -modification	
	estimate	s.e	estimate	s.e	estimate	s.e
A <sub>0</sub>	3.46	0.39	2.20	0.36	2.93	0.24
A <sub>E</sub>	1.38	0.16	1.34	0.22	1.68	0.11
A <sub>I</sub>	3.35	0.66	2.5	1.1	4.69	0.50
A <sub>le</sub>	4.2	2.1	2.2	2.1	5.2	1.9
A <sub>00</sub>	0.11	0.16	-0.27	0.14	-0.89	0.10
A <sub>EE</sub>	0.01	0.19	-0.04	0.34	-0.40	0.13
A <sub>ll</sub>	3.68	0.87	-0.55	0.26	-1.21	0.17
A <sub>lele</sub>	1	1.9	-1.51	0.92	-1.38	0.60
A <sub>0l</sub>	-0.53	0.24	1.0	0.32	-0.71	0.15
A <sub>0le</sub>	-0.83	0.34	-0.76	0.22	-0.69	0.18
A <sub>lle</sub>	3.0	1.3	-1.12	0.36	-0.73	0.52
B <sub>0</sub>	0	1.6	-4.3	1.5	-3.7	0.8
B <sub>l</sub>	5.4	2.3	-7.8	5.3	-1.5	1.6
B <sub>le</sub>	2.6	8	-13.7	11.8	-1.8	7.0
RMSE	3.2°C		4.1°C		2.6°C	

the data to some extent and discarded a number of a priori very unlikely cases. In general, however, it is very difficult to assess the quality of the data reported. Thus, some of the input data may have a substantial error and this will cause some lack of fit.

In future work we will extend the number of available melting enthalpy data and attempt to correlate the melting enthalpy and melting points of unsaturated TAGs simultaneously.

#### 4.4 CONCLUSION

A compilation of literature data of melting points and melting enthalpies of TAGs was made. This data set was extended by measurements of melting enthalpies of 51 mixed acid saturated and unsaturated TAGs in all three modifications.



## LIST OF SYMBOLS

Reliable relations were developed that give the melting point and melting enthalpy as a function of the carbon number, chain length differences and degree of unsaturation for the  $\alpha$ ,  $\beta'$  and  $\beta$ -modification.

### LIST OF SYMBOLS

A, B, a, b, h, k, s	constants
f	a function
n	carbon number
$n_{o,l,e}$	number of O, l or E chains
p	shortest outer TAG-chain
q	middle TAG chain
r	longest outer TAG-chain
$T_m$	hypothetical melting point of polyethelyne (K)
$T_f$	melting point (K)
x	p - q
y	p - r
$\delta, \theta$	constants
$\Delta$	number of double bonds
$\Delta H_f$	melting enthalpy (kJ/mol)
$\Delta S_f$	melting entropy (J/K, mol)

### REFERENCES

1. M.G. Broadhurst, J. Res NBS-A 66A, 241 (1962)
2. A. Würflinger, Thesis, University of Bochum (BRD) (1972)
3. R.Perron, Rev. Fr. Corps Gras 31, 171 (1984)
4. P.J. Flory, A. Vrij, JACS 85, 3548 (1963)
5. F.W. Billmeyer jr, J. Appl Phys. 28, 115 (1975)
6. M.v.Bommel, Thesis, Rijksuniversiteit Utrecht (1986)
7. R.E. Timms, Chem. Phys. Lipids 21, 113 (1978)
8. W. Dollhopf, H.P.Grossmann, U.Leute, Colloid & Polymere Sci 259, 267 (1981).
9. K. Larsson, the Lipids Handbook, F.B.Padley et. al. ed., Chapman & Hall, London (1986)
10. H.M. Zacharis, Chem Phys Lipids 18, 221 (1977)
11. A.N. Bailey: Melting and Solidification of Fats, Interscience, New York (1950)

PHASE EQUILIBRIA IN FATS  
- theory and experiments -

12. P. de Bruyne, J.v. Eendenburg, Unilever Research Report PVD 83 3062 (1983)
13. H.W. Hagemann, JAOCs 52, 204 (1975).
14. H.W. Hagemann, J.A. Rothfus, JAOCs 60, 1123 (1983).
15. H. M. Zacharis, Ad X-Ray Anal 18, 535 (1975).
16. M.S. Gray, N.V. Lovegren, JAOCs 55, 601 (1978).
17. N.V. Lovegren, JAOCs 53, 519 (1976).
18. I. Norton, P CW 84 1065
19. N.V. Lovegren, M.S. Gray, JAOCs 55, 310 (1978).
20. M. Ollivon, R.Perron, Thermochimica Acta 53, 183 (1982).
21. M. Ollivon, R.Perron, Chem Phys Lipids 25, 395 (1979).
22. H.W. Hagemann, Crystallization and Polymorphism of fats, Surfactant Science series 31, 9, N. Garti, K Sato ed. Dekker NY (1988).
23. N. Garti, J. Schlichter, S.Sarig, Fat Sci Technol. 90, 295 (1988).
24. V. Gibon, These, Universite de Namur (1986).
25. S. de Jong, Thesis, Rijksuniversiteit Utrecht (1980).
26. K. Sato et al., JAOCs 66, 664 (1989)
27. S. de Jong and T.C. van Soest, Acta Cryst. B34, (1978)
28. T.C. van Soest, S. de Jong and E.C. Royers, JAOCs (1990)



## CHAPTER 5. MIXING BEHAVIOUR IN LIQUID STATE

*Before a study on solid TAG phases that are in equilibrium with a liquid TAG phase, can be started, knowledge of the mixing behaviour of TAGs in the liquid state is required. Although it is generally assumed that TAGs mix ideally in the liquid state, experimental evidence is lacking. Therefore the activity coefficients in mixtures of TAGs in the liquid state are measured using Gas-Liquid Chromatography with a liquid stationary TAG phase. The results are compared with activity coefficients calculated with the UNIFAC group contribution method.*

### 5.1 LITERATURE

It is generally stated in literature on the phase behaviour of TAGs that the miscibility of TAGs in the liquid state is ideal (1,2,3). Yet the experimental evidence on which this conclusion is based is only very minor:

1. In dilatation experiments on pure TAGs and binary mixtures of TAGs no volume effect was observed (3,4). However, although ideal miscibility implies a zero excess volume of mixing, the opposite is not necessarily true.
2. For liquid alkanes it was found that the heat of mixing is less than 0.1 kJ/mol (2,5), even for hydrocarbons considerably differing in chain length. Compared to the heat of fusion this heat of mixing is negligible. It was reasoned that if alkanes have almost no heat of mixing, then TAGs, which are chemically very similar to alkanes, will also have no heat of mixing. Again, ideal miscibility implies the absence of a heat of mixing, while the reverse is not necessarily true.
3. Mixtures of high melting saturated TAGs and liquid unsaturated TAGs were often found to obey the Hildebrand solubility equation (eqn 5.1).

eq. 5.1

$$\ln x_i^l = \frac{\Delta H_f}{R} \left( \frac{1}{T_f} - \frac{1}{T} \right)$$

## MODEL CALCULATIONS

It is stated that therefore liquid mixtures of TAGs are ideal and if the Hildebrand equation is not obeyed, it is often ascribed to liquid phase non-ideality (2,6). The Hildebrand equation assumes no solid phase miscibility and ideal liquid phase miscibility. In chapter 6 and 7 it will be shown that TAGs do show solid phase miscibility. Whether the Hildebrand equation is obeyed or not is therefore no indication for ideality of the liquid state, as the solid state behaviour may not be disregarded.

Summarizing it is clear that the evidence for ideal miscibility of liquid TAGs is not very convincing. Yet, before any description of solid-liquid phase behaviour and non-ideality in the solid phase can be given, the mixing behaviour of TAGs in the liquid state needs to be known. In the next sections measurements of activity coefficients of TAGs in the liquid state are reported and compared with activity coefficients that are estimated using the UNIFAC group contribution method

### 5.2 MODEL CALCULATIONS

In order to enable the estimation of activity coefficients in mixtures for which no experimental data are available, Fredenslund, Rasmussen and co-workers developed the UNIFAC method (7). The UNIFAC method was shown to perform quite well in phase equilibrium calculations for many hydrocarbon systems (8).

The basic idea of the UNIFAC method is that although there are thousands of different chemical components of interest for the chemical technology, the number of functional groups that constitute these compounds is much smaller. A natural oil contains thousands of different TAGs, but it only consists of  $\text{CH}_3$ -,  $-\text{CH}_2$ -,  $-\text{CH}$ -,  $-\text{CH}=\text{CH}$ -,  $-\text{OH}$  and  $\text{CH}_2\text{COO}$ - functional groups. UNIFAC assumes that the activity coefficient of each component in the mixture is a function of the individual contributions of the components' functional groups. Therefore activity coefficients can be calculated from a limited number of parameters for the functional groups. An excellent and clear description of the method is given by Fredenslund (7).

PHASE EQUILIBRIA IN FATS  
- theory and experiments -

The activity coefficients of TAGs in a set of TAG mixtures were calculated: in 3 binary mixtures of SSS and MMM, 3 binary mixtures of MMM and 8C8, 3 binary mixtures of SSS and 8C8 and in a mixture of the 6 main TAGs and the 2 main partial glycerides occurring in palm oil. We used a computer program and a database that were obtained from the department of prof. J.M. Prausnitz (University of California, Berkeley) for the calculations.

*table 5.1 Activity coefficients in the liquid phase for binary mixtures of SSS with MMM and 8C8, calculated with UNIFAC.*

SSS [1] and MMM [2]			SSS[1] and 8C8 [2]		
T (°C)	x <sub>1</sub>	γ <sub>i</sub>	T (°C)	x <sub>1</sub>	γ <sub>i</sub>
100	0.25	1.007	100	0.25	1.091
100	0.50	1.003	100	0.50	1.020
100	0.75	1.000	100	0.75	1.004
120	0.25	1.006	120	0.25	1.079
120	0.50	1.002	120	0.50	1.022
120	0.75	1.000	120	0.75	1.003

*table 5.2 Activity coefficients in the liquid phase for binary mixtures of MMM with 8C8, calculated with UNIFAC.*

MMM [1] and 8C8 [2]		
T (°C)	x <sub>1</sub>	γ <sub>i</sub>
100	0.25	1.046
100	0.50	1.015
100	0.75	1.003
120	0.25	1.041
120	0.50	1.014
120	0.75	1.002

The results confirm the assumption made in literature and show that the activity coefficients of all TAGs are unity, so ideal mixing of TAGs is predicted. In view of the chemical similarity between all components, this is not too surprising. The two partial glycerides are predicted to have activity coefficients considerably larger than unity, as may be expected for polar compounds in an a-polar solvent.

## EXPERIMENTS

table 5.3 Activity coefficients in the liquid phase for the 6 main TAGs and the 2 main partial glycerides of palm oil at 50°C, calculated with UNIFAC.

palm oil without partial glycerides			palm oil with partial glycerides		
component	x	γ	component	x	γ
PPP	0.08	0.9974	PPP	0.08	1.0005
POP	0.26	0.9997	POP	0.26	1.0018
PPO	0.14	0.9997	PPO	0.12	1.0018
PLP	0.10	1.0004	PLP	0.08	1.0008
POO	0.25	0.9998	POO	0.23	1.0009
OOO	0.17	0.9982	OOO	0.17	0.9982
mono-P	-	-	mono-P	0.01	4.2000
di-P	-	-	di-P	0.05	1.3518

### 5.3 EXPERIMENTS

#### 5.3.1 Method for determination of activity coefficients of mixtures of non-volatile liquids.

Activity coefficients in the liquid phase are often determined by measuring to what extent the vapour pressure of a liquid mixture deviates from Raoult's law.

eq. 5.2 
$$p_i = p_i^* x_i^L$$

However, the vapour pressure of TAGs is less than 1 Pa at temperatures between 0°C and 80°C, the temperature region in which solid fat crystallizes. This is unmeasurably small and therefore another method for determination of activity coefficients must be developed.

A well known method for determination of activity coefficients at infinite dilution of volatile compounds in non-volatile liquids is the use of gas-liquid chromatography (GLC). The non volatile liquid is used as stationary phase and the volatile component is injected into the carrier gas stream. The activity coefficient is calculated from the retention time. The GLC method is discussed in many textbooks on gas chromatography (e.g. 9,10, intermezzo 5).

INTERMEZZO 5: The net retention volume of a injected sample is defined as the product of the net retention time and the flow rate of carrier gas, corrected for the pressure drop over the chromatographic column:

eq. 5.3

$$V_R = t_n \Phi V \cdot \frac{3 \left( \frac{p_{in}}{p_{out}} \right)^2}{2 \left( \frac{p_{in}}{p_{out}} \right)^3}$$

The specific retention volume is defined as the net retention volume per unit mass of liquid stationary phase at 273.15 °C. It is given by:

eq. 5.4

$$V_g = \frac{273.15 V_R}{m_L T}$$

It is assumed that:

- the sample concentration in mobile and stationary phase always have the equilibrium values and
- that the sample volume is very small in comparison with mobile and stationary phase volume (infinite dilution).

In that case the mol fraction of the sample that is in the mobile phase must be equal to the ratio of the volume of the mobile phase and the retention volume (= net retention volume + mobile phase volume). The equilibrium distribution coefficient of the sample over mobile (L) and stationary phase (G) is therefore given by:

eq. 5.5

$$K_{LG} = \frac{x^L}{x^G} = \frac{V_R}{n_L} \cdot \frac{n_G}{V_G}$$

The condition for equilibrium between stationary and mobile phase for infinite sample dilution is (if the mixture of carrier gas and sample behaves ideally) :

eq. 5.6

$$p x^G = p^* \gamma^{\infty} x^L$$



EXPERIMENTS

By rearranging the latter two equations one obtains an expression for the activity coefficient at infinite dilution of the sample in the stationary phase as a function of net retention volume.

eq. 5.7

$$y^* = \frac{n_i}{p^* V_n} \cdot \frac{p V_c}{n_c}$$

The last term in this equation reduces to RT if the ideal gas law may be applied to a mixture of a carrier gas and a sample. When the influence of the pressure drop over the column and the non-ideality of the mobile gas phase are taken into account, a correction term must be added to eq. 5.7. Replacing the net retention volume by the specific retention volume and the vapour pressure by the corrected vapour pressure according to Barker (12), Desy (9) obtains the following corrected expression for the activity coefficient at infinite dilution:

eq. 5.8

$$\ln y^* = \ln \left( \frac{273.15R}{p^* V_s M_i} \right) - p^* \left( \frac{B_{11} - v}{RT} \right)$$

The second virial coefficient  $B_{11}$  and the molar volume  $v$  of the liquid probe at the measuring temperature can be obtained from one of the correlations based on the principle of corresponding states given in ref 12 and 13.

Although the correction term is significant for the activity coefficients at infinite dilution of the samples, that are used in this work, it is of no influence on the calculated interaction between the non-volatile components in the stationary phase, as will be clear from eq 5.12 and 5.16 in the next section. In that case the correction term can therefore be neglected.

Desphande and Patterson (11) have extended the use of this GLC method, using so-called 'probes' to measure the interaction between two non-volatile liquids:

PHASE EQUILIBRIA IN FATS  
- theory and experiments -

First two GLC columns are prepared, each containing a pure non-volatile liquid as stationary phase and the activity coefficient of a volatile 'probe' in these two pure stationary phases is determined by the method outlined above.

Next a number of GLC columns is prepared, containing mixtures of the two non-volatile components as stationary phase. The activity coefficients of the probe in these mixed stationary phases are determined.

The interaction between the two non-volatile components will affect their affinity for the probe, which will be expressed in the retention time of the probe. The interaction between the two liquid components can therefore be obtained by comparing the activity coefficients of the probe in the pure liquids with those in mixtures of the liquid components.

For simple regular solutions this can be worked out as follows: A system of two non-volatile components [1] and [2] and a probe [pr] are considered. The activity coefficient of the probe in a mixture of the two other components is given by: (12)

$$\text{eq. 5.9} \quad RT \ln \gamma_{pr,12} = A_{pr,1} x_1^2 + A_{pr,2} x_2^2 + (A_{pr,1} + A_{pr,2} - A_{1,2}) x_1 x_2$$

At infinite dilution we obtain for a binary system of the probe and one of the non-volatile components:

$$\text{eq. 5.10} \quad RT \ln \gamma_{pr,1}^{\infty} = A_{pr,1}$$

and for the complete ternary mixture:

$$\text{eq. 5.11} \quad RT \ln \gamma_{pr,12}^{\infty} = A_{pr,1} x_1 + A_{pr,2} x_2 - A_{1,2} x_1 x_2$$

The interaction between the two non-volatile components can now be determined from the experimental activity coefficients at infinite dilution of the probe by:

$$\text{eq. 5.12} \quad \frac{A_{1,2}}{RT} = \frac{x_1 \ln \gamma_{pr,1}^{\infty} + x_2 \ln \gamma_{pr,2}^{\infty} - \ln \gamma_{pr,12}^{\infty}}{x_1 x_2}$$

## EXPERIMENTS

It is clear that this elegant method can be applied straightforwardly to TAGs. The result should be independent from the probe used. If indeed TAGs mix ideally, the interaction coefficient  $A_{12}$  must turn out to be zero.

### 5.3.2 Experimental work

The mixing behaviour of the binary SSS-MMM and of the binary SSS-8C8 was studied. The TAGs were obtained from Dr. A. Fröhling of Unilever Research Vlaardingen and were GC-pure.

#### Experimental procedure

The stationary phases were prepared by mixing a predetermined amount of the carrier material Chromosorb W (80 -100 mesh, acid washed, DCMS treated) that was suspended in chloroform, with a predetermined amount of the TAG or TAG mixture, dissolved in chloroform. The chloroform was slowly evaporated at 60°C under occasional stirring. The last remnants of chloroform were removed by heating 3 hours at 80°C. It was checked by weighing whether no loss of carrier material or TAGs had occurred. The stationary phase was brought into a glass column of 1 m. length and 2 mm diameter and the column was conditioned for 10 hours at 150°C. Measurements were carried out at the Technical University of Delft (14) in a modified VARIAN 3700 gaschromatograph with a thermal conductivity detector. The retention times were determined with a VARIAN CDS-11 integrator. Helium was used as carrier gas.

In order to confirm that that the probe that is used has no influence indeed on the calculated TAG-TAG interaction, measurements were repeated using eight different probes:

- |                     |                     |
|---------------------|---------------------|
| 1. n-pentane        | 5. 3-methyl-pentane |
| 2. n-hexane         | 6. benzene          |
| 3. n-heptane        | 7. toluene          |
| 4. 2-methyl-pentane | 8. cyclohexane      |

All measurements were repeated at 2 carrier gas flow rates (17 and 38 ml/min) and with two columns, containing 10% and 20% of the stationary phase on carrier. About 0.1  $\mu$ l of the probe was injected.

PHASE EQUILIBRIA IN FATS  
- theory and experiments -

**Measurements**

The specific retention volumes of the 8 probes were determined at 82, 92, 102, 112, 123 and 133 °C for the following stationary phases: (concentrations in mol fractions)

SSS	0.4487 SSS, 0.5513 MMM	0.1557 SSS, 0.8443 8C8
MMM	0.7116 SSS, 0.2884 MMM	0.3593 SSS, 0.6407 8C8
8C8		0.6023 SSS, 0.3977 8C8

The results are given in appendix 2. The average experimental error in the retention volumes is 3%.

5.3.3 Results and discussion

The activity coefficients at infinite dilution of the probes can be calculated from the specific retention volumes with eq. 5.8. It turns out that they do not depend on temperature, as is illustrated for some of the probes and some stationary phases in the figures 5.1, 5.2, 5.3 and 5.4. The variation as a function of temperature is less than the experimental error of 3% in the activity coefficients. This indicates that the probe-TAG mixtures behave athermal, i.e that the excess Gibbs energy is nearly equal to the excess entropy of mixing.

*table 5.4. Average activity coefficients at infinite dilution of several probes in a number of liquid TAG mixtures determined by GLC. The experimental error in the activity coefficients is 3%. Concentrations in mol fractions.*

	x <sub>SSS</sub>	1	1	1	0.449 0.551	0.712 0.288	0.156 0.844	0.359 0.641	0.602 0.398
	x <sub>MMM</sub>								
	x <sub>8C8</sub>								
PROBE									
n-pentane	0.45	0.55	0.85	0.52	0.49	0.75	0.65	0.56	
n-hexane	0.47	0.57	0.87	0.52	0.50	0.75	0.66	0.57	
n-heptane	0.49	0.59	0.91	0.54	0.52	0.78	0.69	0.60	
2-methyl-pent.	0.49	0.59	0.90	0.54	0.52	0.77	0.68	0.59	
3-methyl-pent.	0.46	0.56	0.87	0.52	0.49	0.73	0.66	0.56	
benzene	0.28	0.32	0.43	0.30	0.29	0.39	0.36	0.32	
toluene	0.29	0.33	0.46	0.31	0.31	0.41	0.38	0.34	
cyclohexane	0.34	0.41	0.65	0.38	0.37	0.55	0.49	0.42	

EXPERIMENTS

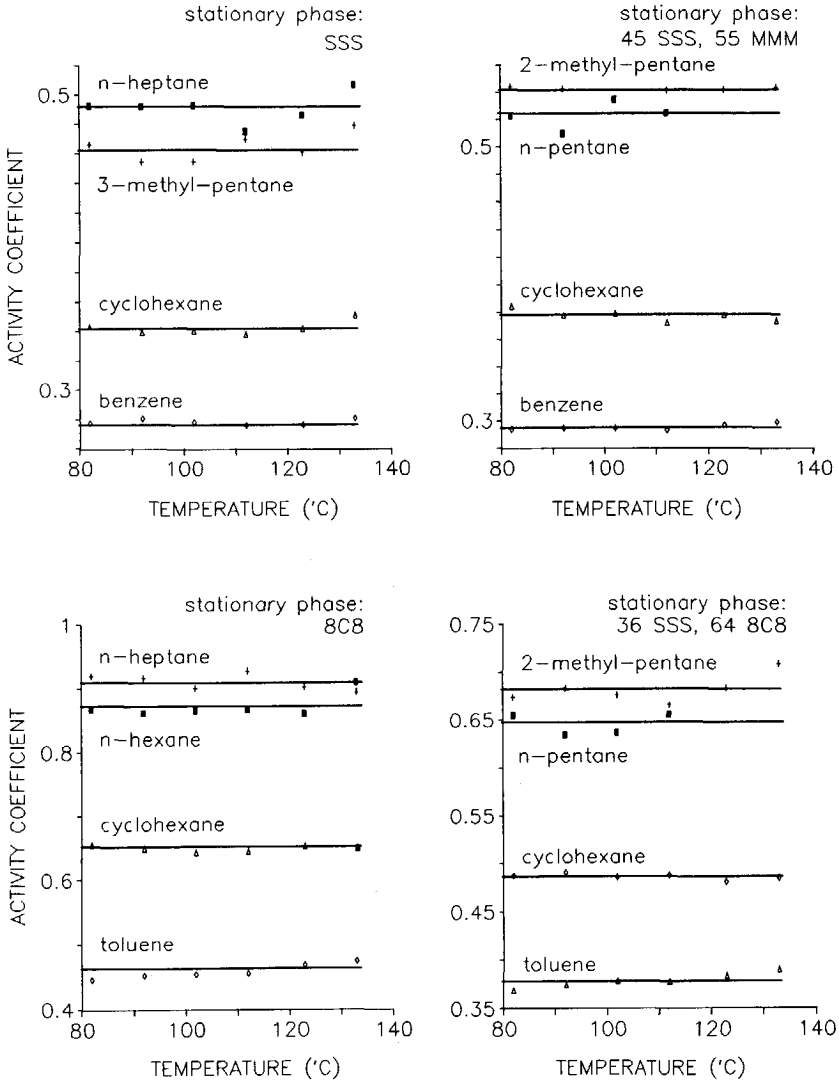


fig 5.1 - 5.4: Activity coefficients at infinite dilution of a number of different probes in stationary TAG phases as a function of temperature.

PHASE EQUILIBRIA IN FATS  
- theory and experiments -

Because no dependency on temperature was found, the averages over all temperatures of the activity coefficients are used in further discussions. They are given in table 5.4

The interaction coefficients between the TAGs for the regular solution theory can now be calculated using equation 5.12. The results are given in table 5.5.

*Table 5.5. Regular solution interaction parameters  $A_{12}/RT$  for the interaction between the TAGs determined from GLC results, using different probes. Experimental error in the parameters is 0.1. Concentrations in mol fractions.*

x <sub>SSS</sub>	0.449	0.712	0.156	0.359	0.602
x <sub>MMM</sub>	0.551	0.288			
x <sub>8C8</sub>			0.844	0.641	0.398
PROBE					
n-pentane	-0.15	-0.11	-2.61	-0.99	-0.58
n-hexane	0.03	-0.03	-2.23	-0.93	-0.47
n-heptane	0.01	-0.04	-2.29	-0.98	-0.50
2-methyl-pent.	-0.01	-0.02	-2.25	-0.94	-0.48
3-methyl-pent.	-0.02	-0.03	-2.29	-1.01	-0.47
benzene	0.05	-0.02	-1.69	-0.73	-0.36
toluene	0.02	-0.06	-1.77	-0.79	-0.41
cyclohexane	0.03	-0.05	-2.41	-0.99	-0.50
average	-0.01	-0.05	-2.19	-0.92	-0.47
stand. dev.	0.06	0.03	0.29	0.10	0.06

The results for the binary SSS-MMM clearly indicate that within experimental error these two TAGs mix ideally. The results are very consistent for both binary mixtures and all probes used.

The results for the binary SSS-8C8 clearly indicate that this binary does not mix ideally in the liquid phase. The interaction parameters significantly differ from zero. And even worse, they also depend on the concentration of the TAGs. The simple regular solution model is therefore not a correct description for the non-ideal behaviour of this binary pair.

## EXPERIMENTS

### Interpretation with the Flory-Huggins theory

The main difference between MMM and 8C8 is their difference in molecular size. This must be the cause of the large differences found in mixing behaviour with SSS. An excess Gibbs energy model that accounts for such size differences is the Flory-Huggins theory for polymer solutions (12). According to this theory the activity coefficient in the ternary system of probe [pr] and the two TAGs [1] and [2] is:

$$\text{eq. 5.13} \quad \ln \gamma_{pr,12} = \ln \left( \frac{v_{pr}}{x_{pr}v_{pr} + x_1v_1 + x_2v_2} \right) + \left( 1 - \frac{v_{pr}}{v_1} \right) \phi_1 + \left( 1 - \frac{v_{pr}}{v_2} \right) \phi_2 \\ + \chi_{pr,1} \phi_1^2 + \chi_{pr,2} \phi_2^2 + (\chi_{pr,1} + \chi_{pr,2} - \chi_{1,2}) \phi_1 \phi_2$$

The volume fraction  $\phi_i$  is defined as:

$$\phi_i = \frac{x_i v_i}{\sum_{j=1}^N x_j v_j}$$

in which  $v_i$  represents the molar volume.

At infinite dilution we obtain for a binary system of the probe and one of the TAGs:

$$\text{eq. 5.14} \quad \ln \gamma_{pr,1}^\infty = \ln \left( \frac{v_{pr}}{v_1} \right) + \left( 1 - \frac{v_{pr}}{v_1} \right) + \chi_{pr,1}$$

and for the complete ternary mixture:

$$\text{eq. 5.15} \quad \ln \gamma_{pr,12}^\infty = \ln \left( \frac{v_{pr}}{x_1 v_1 + x_2 v_2} \right) + \left( 1 - \frac{v_{pr}}{v_1} \right) \phi_1 + \\ \left( 1 - \frac{v_{pr}}{v_2} \right) \phi_2 + \chi_{pr,1} \phi_1 + \chi_{pr,2} \phi_2 - \chi_{1,2} \phi_1 \phi_2$$

The Flory-Huggins interaction parameter  $\chi_{12}$  for the two TAGs can be determined from the experimental activity coefficients at infinite dilution by:

PHASE EQUILIBRIA IN FATS  
- theory and experiments -

eq. 5.16

$$\chi_{12} = \frac{\phi_1 \left( \ln \gamma_{pr,1}^\infty - \ln \left( \frac{v_1}{x_1 v_1 + x_2 v_2} \right) \right) + \phi_2 \left( \ln \gamma_{pr,2}^\infty - \ln \left( \frac{v_2}{x_1 v_1 + x_2 v_2} \right) \right) - \ln \gamma_{pr,12}^\infty}{\phi_1 \phi_2}$$

When the molecular volumes of the 2 TAGs are equal, the Flory-Huggins interaction parameter  $\chi$  becomes equal to the regular solution interaction parameter  $A_{12}/RT$  and equation 5.16 reduces to equation 5.12 for the regular solution theory. The Flory-Huggins interaction parameters are given in table 5.6

*Table 5.6. Flory - Huggins interaction parameters  $\chi_{12}$  for the interaction between the TAGs determined from GLC results, using different probes. Experimental error in the parameters is 0.1. Concentrations in mol fractions.*

xSSS	0.449	0.712	0.156	0.359	0.602
xMMM	0.551	0.288			
x8C8			0.844	0.641	0.398
PROBE					
n-pentane	-0.17	-0.15	-0.07	-0.02	-0.08
n-hexane	0.01	-0.05	0.17	0.04	0.05
n-heptane	-0.01	-0.06	0.17	0.02	0.04
2-methyl-pent.	-0.02	-0.04	0.21	0.06	0.08
3-methyl-pent.	-0.04	-0.05	0.24	0.02	0.11
benzene	0.05	-0.03	0.14	0.04	0.09
toluene	0.01	-0.07	0.14	0.01	0.04
cyclohexane	0.01	-0.07	0.17	0.04	0.07
average	-0.02	-0.07	0.15	0.03	0.05
stand. dev.	0.06	0.03	0.09	0.02	0.06
total av.	-0.04		0.07		
stand. dev.	0.05		0.08		

The interaction parameters of both binaries do not depend on the probe used and not on the concentration of the two TAGs in the binary mixture. The values of interaction parameters,  $-0.04 \pm 0.1$  for SSS-MMM and  $0.07 \pm 0.1$  for SSS-8C8, do not differ significantly from zero, which implies that the TAGs have no specific interaction in



## CONCLUSION

the mixtures. The deviation from ideality that was found for SSS-8C8 is entirely explained by the extra entropy of mixing that arises from the large difference in molecular size of the two TAGs. The activity coefficients at infinite dilution of the 3 possible binary TAG mixtures, calculated with equation 5.14, and in agreement with measurements, are given in table 5.7

table 5.7 Activity coefficients at infinite dilution of the 3 TAGs studied, calculated using the Flory-Huggins theory for the excess entropy of mixing (eqn 5.14).

	$\ln \bar{\gamma}_{i,SSS}$	$\ln \bar{\gamma}_{i,MMM}$	$\ln \bar{\gamma}_{i,8C8}$	$\bar{\gamma}_{i,SSS}$	$\bar{\gamma}_{i,MMM}$	$\bar{\gamma}_{i,8C8}$
SSS	-	-0.02	-0.16	1	0.98	0.85
MMM	-0.03	-	-0.07	0.97	1	0.93
8C8	-0.24	-0.09	-	0.79	0.91	1

### Implications for natural edible oils.

The results imply that deviations from ideal miscibility only become noticeable when an oil contains reasonable amounts of TAGs that have a carbon number that differs more than about 10 with the average carbon number of the mixture. In normal vegetable oils and fats the differences in molecular size of the TAGs are of the order of the difference between MMM and SSS. For practical purposes liquid vegetable oils can therefore be treated as ideal mixtures of TAGs.

In animal oils and fats, like fish oil, butter fat and edible tallow, the spread in molecular size of the TAGs is much larger, although the concentrations of very small and very large TAGs are limited. Treating these oils as ideal mixtures may, depending on the situation, lead to errors of about 10%-15% in calculation results.

In this work we are considering the TAGs that occur in normal vegetable oils and fats. The liquid TAG phase may therefore safely be treated as an ideal mixture.

## 5.4 CONCLUSION

TAGs that differ not too much in molecular size mix ideally in the liquid state.

PHASE EQUILIBRIA IN FATS  
- theory and experiments -

The deviation from ideality that becomes noticeable at differences in carbon number greater than about 15-20, can entirely be ascribed to the extra entropy of mixing that occurs in mixtures of molecules that differ considerably in size. No specific TAG - TAG interactions were found.

In the liquid state the vegetable oils that are normally used in the edible fats industry may be treated as ideal mixtures of TAGs.

#### LIST OF SYMBOLS

A	Interaction parameter
$B_{11}$	Second virial coefficient
K	Molar distribution coefficient
m	mass (kg)
M	Molar weight (kg/mol)
n	Number of moles (mol)
N	Number of components
p	Pressure (Pa)
$p^*$	Vapour pressure of pure component
R	Gas constant (J/mol,K)
T	Temperature (K)
$T_f$	Normal melting point (K)
v	Liquid molar volume ( $m^3/mol$ )
V	Volume ( $m^3$ )
x	mol fraction (mol/mol)
$\gamma$	Activity coefficient
$\Delta H_f$	Heat of fusion (kJ/mol)
$\phi$	Volume fraction
$\phi_v$	Volume flow rate ( $m^3/s$ )
$\chi$	Interaction parameter

#### REFERENCES

1. R.E Timms, Progr Lipid Res. 23, 1 (1984).
2. P. de Bruijne, M v.d. Tempel, M. Knoester, Chem. Phys. Lipids 9, 309 (1972).
3. J. Hannewijk, A,J, Haighton, P.W. Hendrikse, Analysis and Characterization of Oils, Fats and Fat Products 1, 119 (H. Boekenooogen ed) Interscience, London (1964).

#### REFERENCES

4. P.W. Hendrikse, Dilatation of Fats, R VL Unilever Research Vlaardingen.
5. A. Würflinger, Thesis, University of Bochum (BRD, 1972).
6. I.T. Norton et al, JAOCS 62, 1237 (1985)  
ibid, P CW 87 1125, Unilever Research Colworth House (1987)
7. A. Fredenslund, J. Gmehling, P.Rasmussen, Vapor-Liquid equilibria using UNIFAC, Elsevier Scientific Publishing Company, Amsterdam (1977)
8. See the many articles on the use of UNIFAC in proceedings of the 5th Int. Conf. on Phase Equil. for Chem. Process Design, Banff, Canada (May 1989).  
J. Fluid Phase Equil. 52 ( dec 1989).
9. D.H. Desty et al., Gas Chromatography, Butterworths, London (1962)
10. R.L. Grob, Modern Practices of Gas Chromatography, J. Wiley, New York (1985)
11. D.D. Desphande, D. Patterson, H.P. Schreiber, C.S. Su, MAcromolecules 7, 530 (1974)
12. J.M. Prausnitz, Molecular Thermodynamics of Fluid Phase Equilibria, 2nd ed. John Wiley, New York (1986)
13. J.M. Smith, H.C. van Ness, Introduction to chemical engineering thermodynamics, 4th ed, Mc Graw-Hill, New York, 1987
14. I. Gandasmita, Afstudeerverslag, Technische Universiteit Delft (1987).

## CHAPTER 6. MIXING BEHAVIOUR IN THE ALPHA MODIFICATION

*Contrary to the  $\beta$  and  $\beta'$ -modification, in the  $\alpha$ -modification the fatty acid chains still appear to oscillate and rotate with considerable molecular freedom. The formation of mixed crystals will therefore hardly disturb the  $\alpha$ -crystal packing. As a consequence mixing in the alpha phase may be nearly ideal. With this assumption  $\alpha$ -melting ranges of a number of common fat blends are calculated and compared with experimental data.*

### 6.1 EVIDENCE FOR PARTIAL RETAINED CHAIN MOBILITY IN THE $\alpha$ -MODIFICATION.

Not only TAGs, but many lipids, like alkanes, n-alcohols and simple esters, solidify upon quick cooling from the melt in a crystal form with hexagonal chain packing, which for TAGs is called the  $\alpha$ -modification. Already in 1932 it was suggested by Müller (16) that the hexagonal polymorph of n-alkanes has complete rotational disorder of the chains in the crystal. Therefore the hexagonal polymorph of n-alkanes has been called the 'rotator phase'. At present the rotational disorder in the rotator phase of n-alkanes has been extensively studied and is well established (1,2,3,4). A curious property of lipid crystals in the rotator phase is their plasticity. Due to this property esters occurring in this form have been called waxes.

Contrary to n-alkanes, the chains in the  $\alpha$ -modification of TAGs cannot have complete freedom of rotation. For sterical reasons chain mobility near the glyceryl group must be restricted. Yet the heat of fusion and the entropy of fusion of the  $\alpha$ -modification of TAGs correspond closely to that of the rotator phase of alkanes. Moreover, the entropy of fusion is only 60% of that of the very crystalline  $\beta$  and 75% of that of the  $\beta'$ -modification, indicating that in the remaining part of the molecule still considerable disorder must exist. (table 6.1)

EVIDENCE FOR PARTIAL  
RETAINED CHAIN MOBILITY IN  
THE  $\alpha$ -MODIFICATION.

table 6.1 Enthalpy and entropy of fusion of some TAGs and some n-alkanes

TAG-name	$\Delta H_f$ kJ/mol			$\Delta S_f$ J/mol,K		
	$\alpha$	$\beta'$	$\beta$	$\alpha$	$\beta'$	$\beta$
MMM	84	107	145	275	334	440
PPP	98	132	169	309	399	501
SSS	113	156	193	343	464	561
n-C19	45	60	-	147	197	-
n-C21	48	63	-	153	203	-

The melting dilatation (the volume increase upon melting) of the  $\alpha$ -modification is only 60-70% of that of the  $\beta$ -modification (5). This clearly demonstrates a less dense packing of the TAG molecules in the  $\alpha$ -modification.

In pulse NMR for the determination of solid fat content (6) the so-called f-factor, which is inversely proportional to the relaxation time, is only 1.2 - 1.3 for the  $\alpha$ -modification, compared to 1.4-1.5 for the  $\beta'$ -modification and about 1.6 for the  $\beta$ -modification. This indicates a more disordered and liquid-like packing of the fatty acid chains in the  $\alpha$ -modification.

Hernqvist and Larsson (7) observed that the long spacing of the  $\alpha$ -modification of SSS depends on temperature. A temperature dependence of the same order of magnitude was one of the main arguments for V. Luzatti et al. in their classical work on liquid crystallinity (8) to suggest a liquid state of hydrocarbon chains in liquid crystals. Hernqvist and Larsson also measured RAMAN spectra of TAGs. The  $\beta'$  and  $\beta$ -modification showed sharp peaks at 1065 and 1130  $\text{cm}^{-1}$  (C-C stretching vibrations), while liquid TAGs have a broad band near 1090  $\text{cm}^{-1}$ . The RAMAN spectra of the  $\alpha$ -modification had a significant liquid-like character.

The most convincing evidence for chain mobility comes from Norton (13). He concludes from high resolution CP/MAS  $^{13}\text{C}$ -NMR spectra of the liquid state and the three polymorphs of SSS and PPP, that in the  $\alpha$ -modification, like in the liquid phase and contrary to the  $\beta'$

PHASE EQUILIBRIA IN FATS  
- theory and experiments -

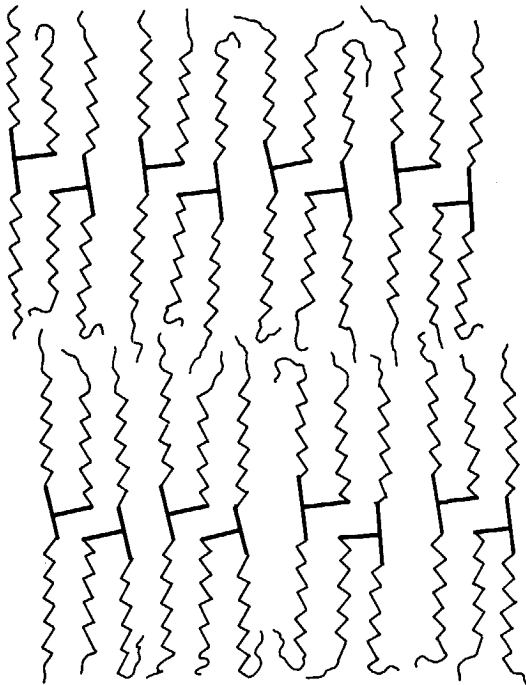


fig 6.1 Chain disorder in the  $\alpha$ -modification

and  $\beta$ -modification, the 1 and 3 position of the glycerol are equivalent. He was able to study molecular motion by application of 'interrupted decoupling' (switching of the  $^{13}\text{C}$ - $^1\text{H}$  decoupling for a short time, which suppresses the signal of immobile protonated carbons). The results clearly show that the mobility of the fatty acid chains near the glyceryl group is very limited in all three polymorphs. In the  $\alpha$ -modification the main hydrocarbon chain still possesses some mobility, while the carbons near the methyl end plane are very mobile. Main chain mobility is still present to some extent in the  $\beta'$ -modification, while the  $\beta$ -modification shows no main chain mobility. Even in the  $\beta$ -modification the methyl end group has retained some mobility.

The good correspondence with the rotator phase of alkanes and all facts that are mentioned above clearly support the view of Hernqvist (10) on the  $\alpha$ -modification. In the  $\alpha$ -modification, close to the methyl

EVIDENCE FOR PARTIAL  
RETAINED CHAIN MOBILITY IN  
THE  $\alpha$ -MODIFICATION.

end plane the fatty acid chains are disordered like in lamellar liquid crystalline phases. Close to the glyceryl group, chain mobility is absent. (fig 6.1)

6.1.1 Supercooling of the  $\alpha$ -modification

One of the other arguments that is often mentioned in favour of chain mobility in the  $\alpha$ -modification is the observation of van den Tempel (17) that the  $\alpha$ -modification, like lamellar liquid crystalline phase, cannot be supercooled (16).

To our observation this is not entirely correct. In oil-in-water emulsions with a relatively small average droplet size supercooling of the  $\alpha$ -modification could be obtained. Moreover we found a whole class of very slowly crystallizing fat blends with a specific TAG composition, in which even in a bulk phase under shear supercooling of the  $\alpha$ -modification could be obtained. Crystallization to equilibrium was extremely quick and took place in about 1 minute. A noticeable transition to the  $\beta'$ -modification only occurred after about 1 hour.

In all other fat blends that we investigated, we could not obtain supercooling of the  $\alpha$ -modification in sheared bulk phases. We will make use of this effect in the experiments described in section 6.2.

6.1.2 Excess Gibbs energy in the  $\alpha$ -modification

In normal crystalline phases ideal mixing is only found when the components that are mixed, are nearly isomorphous (11). In all other cases incorporation of a second component causes disturbances in the extremely regular crystal lattice, leading to non-ideal mixing. However, the  $\alpha$ -modification may be an exception. The large degree of liquid-like disorder that exists, especially in the methyl end-plane region, may very well enable the incorporation of TAGs with considerably longer or shorter fatty acid chains into the crystal 'lattice', without causing much extra disorder or misfittings. In other words, the excess Gibbs energy of mixing is likely to be very small, or even zero in the  $\alpha$ -modification.

There exists some evidence in literature, that indeed in the  $\alpha$ -modification of TAGs considerable solid solubility occurs (12, 14), but the data are too inaccurate and too scarce to allow any quantification. However, the phase diagrams of the rotational phase-liquid equilibrium of n-alkanes (4) indicate clearly that mixing in the rotational phase must be nearly ideal at atmospheric pressure. We will come back to the solid-liquid phase behaviour of n-alkanes in chapter 9.

In view of all above we assume that TAGs mix ideally in the  $\alpha$ -modification. With this assumption the  $\alpha$ -melting range of a fat can be predicted. In the next section it will be investigated whether such predicted  $\alpha$ -melting ranges agree with the experimental melting ranges.

## 6.2 COMPARISON OF EXPERIMENTAL AND CALCULATED $\alpha$ -MELTING RANGES.

### 6.2.1 Experimental procedure

The  $\alpha$ -modification is extremely unstable. In normal fats it transforms to the  $\beta'$ -modification within 3 to 20 minutes. This instability poses some problems in the determination of  $\alpha$ -phase equilibria. The normal thermal techniques for studying solid-liquid equilibria, like DSC and DTA, are too slow. A quicker method must be defined.

The fact that it is very hard to supercool the  $\alpha$ -modification in a bulk fat phase that is subjected to shear, while it is very easy to supercool the  $\beta'$ - and  $\beta$ -modification under those conditions, can be used to determine the  $\alpha$ -melting range of a fat blend. The following procedure takes advantage of this phenomenon:

1. About 2 kg, of the fat blend is heated in a stirred tank to a temperature at least 10 °C above the slip melting point of the fat. Next the fat is circulated through a gear pump, two lab-scale scraped surface heat exchangers (SSHE) for cooling and a tubular heat exchanger for remelting, in the set-up depicted in fig 6.2.

The volume of the SSHEs is 18 ml, the total cooling surface  $7.10^{-3}$  m<sup>2</sup>. As coolant ethanol is used at temperatures between 5 and -20°C. Samples can be taken directly after the SSHEs. The solid fat



COMPARISON OF EXPERIMENTAL  
AND CALCULATED  $\alpha$ -MELTING  
RANGES.

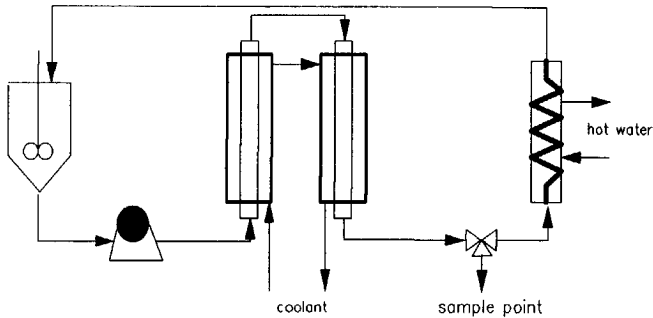


fig 6.2 Experimental set-up with two SSHEs and a remelter for measurements of  $\alpha$ -melting ranges.

content of these samples can be measured in a Bruker Minispec pl20i pulse NMR device. The NMR is operated with a  $90_x-\tau-90_y$  pulse sequence, that not only gives the solid fat content, but also the f-factor, a number that is characteristic for the modification in which the fat has crystallized (8).

2. The fat is cooled in the SSHEs to  $1^\circ\text{C}$  below its  $\alpha$ -cloud point. Next the throughput is increased, while keeping the SSHE exit temperature constant, until no decrease in solids content is observed upon further increase of throughput. Usually this is obtained at about 16 kg/hr (4.4 g/s). Thus is made sure that the transition to the  $\beta'$ -modification has not yet started in the SSHEs and that the solid phase is still completely in the  $\alpha$ -modification. Sample temperature and solid phase content are recorded.
3. Next the fat temperature is decreased in steps of about  $2^\circ\text{C}$ . When the solid phase content and temperature have stabilised, a sample is taken and the solid phase content and temperature are recorded. 8 data points are usually taken in duplo for each fat blend.
4. The plot of solids content against temperature is called an  $\alpha$ -line and represents the  $\alpha$ -melting range of the fat blend.

During experiments the pulse NMR always returned f-factors of about 1.25. A f-factor of 1.25 is indicative for the  $\alpha$ -modification.

PHASE EQUILIBRIA IN FATS  
- theory and experiments -

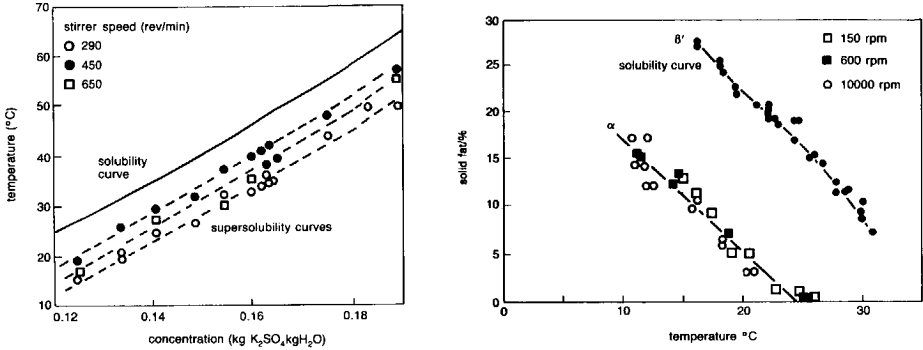


fig 6.3 Effect of crystallizer impeller speed on the position of the supersolubility curve.

a. Left : Potassium Sulphate (from ref 9)

b. Right: A mixture of soybean oil and hardened soybean oils.

It may be argued that the  $\alpha$ -line obtained in this way, is not a line representing the  $\alpha$ -liquid-phase equilibrium, but a line representing the maximum possible supercooling of the fat under the conditions used. Such lines of maximal supercooling usually depend strongly on the specific conditions, like impeller speed, that are applied (9, 15, fig 6.3a). However the  $\alpha$ -lines, which were measured, were found to be totally independent of the rotational shaft speed of the SSHEs, coolant temperature and throughput, once the throughput was high enough to prevent the formation a  $\beta'$ -phase in the SSHE (fig 6.3b).

9 fat blends were selected that cover the area of compositions and melting ranges normally occurring in household and industrial fat spreads. The TAG compositions of the fat blends were obtained by calculation from average TAG compositions of the fat blend components. The average TAG compositions of the fat blend components, like sunflower oil or hardened palm oils, were taken from the Edible Fats Database of Unilever Research Vlaardingen (table 6.2).

COMPARISON OF EXPERIMENTAL  
AND CALCULATED  $\alpha$ -MELTING  
RANGES.

*table 6.2 Summarized TAG compositions of 9 fat blends of commercial fat spreads.*

TAG	1	2	3	4	5	6	7	8	9
SSS				0.005	0.002			0.002	0.010
S2P				0.009	0.005	0.001		0.004	0.020
SP2	0.006	0.002	0.006	0.006	0.005	0.011	0.002	0.003	0.014
PPP	0.011	0.004	0.019	0.001	0.002	0.032	0.004		0.003
SES		0.001			0.007		0.002	0.004	0.025
PES	0.006	0.009			0.012	0.002	0.006	0.006	0.034
PEP	0.018	0.020			0.007	0.001	0.009	0.002	0.011
SSE		0.002			0.007		0.003	0.008	0.025
PSE	0.002	0.006			0.011	0.002	0.009	0.012	0.034
PPE	0.006	0.009			0.006	0.002	0.010	0.005	0.011
P2m	0.004		0.001	0.006	0.002	0.004			0.004
PSm	0.002			0.020	0.004				0.013
S2m				0.010	0.002				0.009
SOS	0.001	0.001	0.003	0.001	0.003	0.001	0.001	0.002	0.007
POS	0.020	0.015	0.052	0.002	0.007	0.021	0.004	0.004	0.010
POP	0.078	0.057	0.230	0.001	0.004	0.090	0.005	0.002	0.004
S1S			0.001	0.002	0.002			0.001	
PLS	0.008	0.005	0.009	0.004	0.004	0.008	0.003	0.003	0.002
PIP	0.027	0.014	0.035	0.003	0.003	0.029	0.004	0.002	0.002
SSO		0.001		0.002	0.003	0.001	0.002	0.005	0.007
PSO	0.010	0.007	0.008	0.004	0.008	0.013	0.006	0.009	0.010
PPO	0.033	0.016	0.031	0.003	0.005	0.052	0.007	0.004	0.004
SSL	0.001		0.001	0.003	0.002			0.002	0.001
PSL	0.011	0.005	0.005	0.008	0.005	0.007	0.005	0.006	0.003
PPL	0.030	0.009	0.009	0.006	0.004	0.020	0.007	0.005	0.004
SE2	0.002	0.018			0.041	0.010	0.031	0.027	0.084
PE2	0.009	0.034			0.036	0.014	0.050	0.021	0.056
Pm2	0.013			0.011	0.001				0.002
Sm2	0.003			0.018	0.001				0.004
EEE	0.003	0.037			0.059	0.020	0.063	0.021	0.047
mmm	0.014			0.007					
SmE					0.010				0.034
PmE					0.012				0.022
E2m					0.017			0.001	0.034
SEO	0.002	0.018			0.029	0.010	0.031	0.031	0.054
PEO	0.010	0.034			0.035	0.014	0.049	0.025	0.036
SEL		0.002			0.023	0.001	0.004	0.003	0.005
PEL	0.001	0.004			0.021	0.002	0.006	0.003	0.004
SmO	0.002			0.005					
PmO	0.012			0.003					
mOm	0.006								
mlm	0.001								
mmO	0.013			0.002					
mml	0.003			0.001					
E2O	0.004	0.055			0.049	0.030	0.094	0.037	0.053
E2l		0.007			0.058	0.004	0.012	0.004	0.005
SO2	0.020	0.007	0.009	0.008	0.021	0.013	0.004	0.012	0.009
PO2	0.120	0.039	0.049	0.012	0.028	0.101	0.011	0.014	0.010
liquid	0.485	0.560	0.530	0.836	0.437	0.481	0.557	0.706	0.272

### 6.2.2 Calculations

The  $\alpha$ -melting ranges were calculated using the standard multicomponent 2-phase flash algorithm and Michelsen's stability test for the initial estimate, both described in chapter 3. Ideal mixing in the solid and in the liquid phase was assumed, therefore all activity coefficients were unity. The TAG-compositions from table 8 were used, while all pure component properties were estimated using the correlations developed in chapter 4.

### 6.2.3 Results

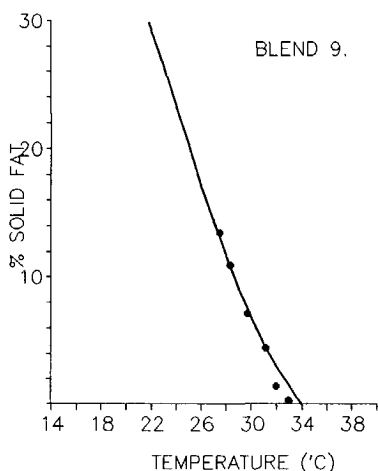


fig 6.4 Measured (points) and calculated (lines)  $\alpha$ -melting ranges of several commercial fat blends. The number corresponds to the composition given in table 6.2.

The results of the calculations and the measurements are given in figures 6.4, 6.5 and 6.6.

The outcome is very surprising: it appears possible to predict the behaviour of the extremely unstable  $\alpha$ -modification by phase equilibrium thermodynamics. The agreement between predictions and measurements is striking.

PHASE EQUILIBRIA IN FATS  
 - theory and experiments -

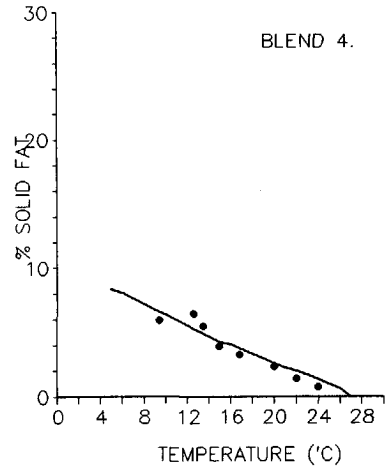
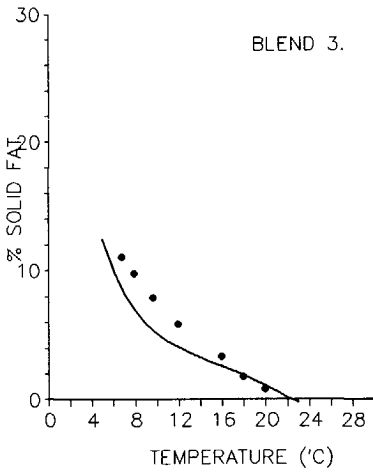
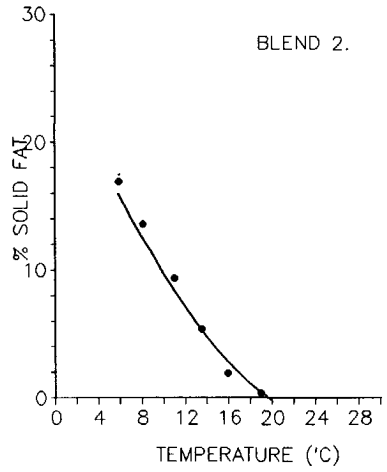
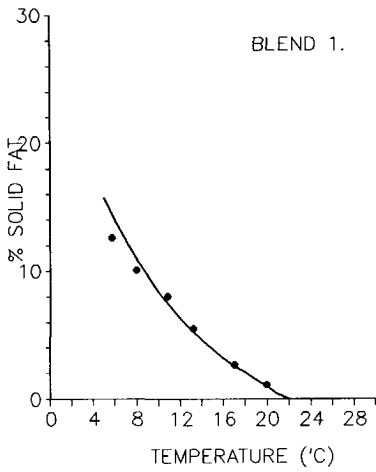


fig 6.5 Measured (points) and calculated (lines)  $\alpha$ -melting ranges of several commercial fat blends. The number corresponds to the composition given in table 6.2.

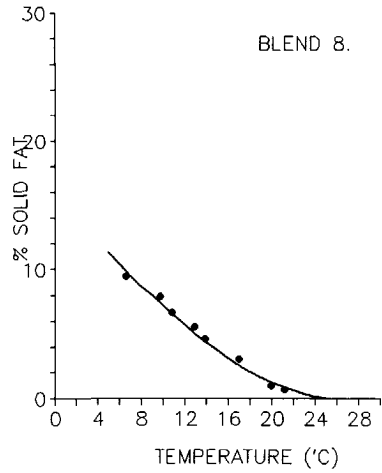
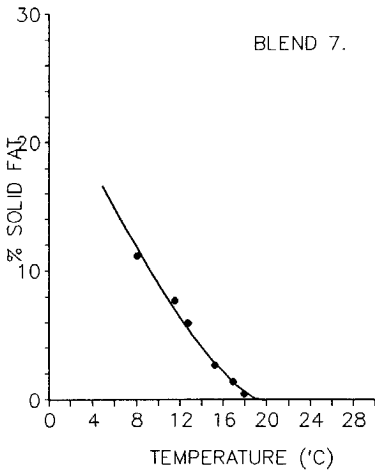
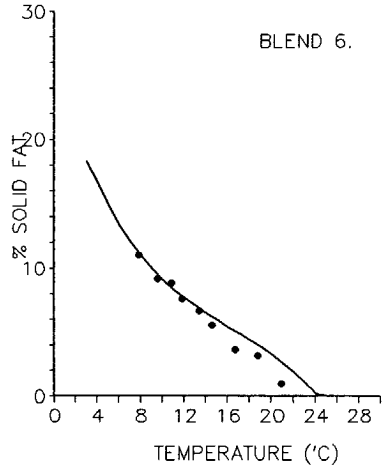
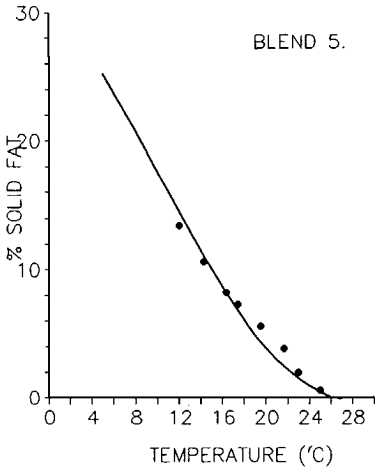


fig 6.6 Measured (points) and calculated (lines)  $\alpha$ -melting ranges of several commercial fat blends. The number corresponds to the composition given in table 6.2.

## CONCLUSION

### 6.3 CONCLUSION

A good description of the phase behaviour of TAGs in the very unstable  $\alpha$ -modification is obtained when it is assumed that TAGs form ideal solid solutions in the  $\alpha$ -modification.

### REFERENCES

1. K. Larsson in *The Lipid Handbook*, F.B. Padley et al editors, Chapman & Hall, London (1986)
2. P.J. Flory, A. Vrij, *JACS* 85, 3548 (1963)
3. M.G. Broadhurst, *J. Res. Nat. Bur. Standards A.* 66A, 241 (1962)
4. A. Würflinger, Thesis University of Bochum (1972)
5. D. M. Small et al. (editors), *The Physical Chemistry of Lipids, Handbook of Lipid Research* 4, Plenum Press, New York (1984)
6. H. Human, J.v.d Ende, L. Alderliesten, poster at AOCs meeting Maastricht, NL, (Sept 1989).
7. L. Hernqvist, K. Larsson, *Fette, Seife, Anstrichmittel* 84, 349 (1982)
8. V. Luzatti, H Mustacchi, A. Skoulios and F. Husson, *Acta Cryst.* 13, 660 (1960)
9. B.R. Pamplin, *Crystal Growth*, pp 526-530 Pergamon Press (1980)
10. L. Hernqvist, Thesis, University of Lund, Sweden (1984)
11. M. Zief, W.R. Wilcox, *Fractional Solidification*, M.Dekker Inc., New York (1967)
12. J.B. Rossel, *Adv. Lip. Res.* 5, 353 (1967)
13. I.T. Norton et al, *JAACS* 62, 1261 (1985)
14. I.T. Norton et al, *JAACS* 62, 1237 (1985)
15. P.A.M. Grootsholten, Jancic, *Industrial Crystallization*, (1986)
16. A. Müller, *Proc Roy. Soc.* 138 A, 514 (1932)
17. M. v.d. Tempel, *Physicochimie des Composés Amphiphiles, Colloques NAT. du CNRS* 938, p261 (1979)

## CHAPTER 7 MIXING BEHAVIOUR IN THE BETA' AND BETA MODIFICATIONS

*The miscibility of TAGs in the  $\beta'$  and  $\beta$ -modification is highly non ideal. It is attempted to describe this non ideal mixing with the simplest possible excess Gibbs energy models. A compilation of existing binary  $T, x, y$  solid-liquid phase diagrams is used to determine the binary interaction parameters that occur in these models. A new method is developed to determine binary interaction parameters from a single, complete DSC melting curve of ternary mixtures. Some ternary phase diagrams are considered.*

### 7.1 EXCESS GIBBS ENERGY

It is well known (12,20) that the mixing behaviour of TAGs in the  $\beta'$  and  $\beta$ -modification is highly non ideal. Therefore, in order to be able to solve the 'solid-flash' problem of chapter 3, we need to know the activity coefficient of each TAG in the  $\beta'$ - or  $\beta$ -solid phase as a function of the phase composition. Usually this is obtained from an excess Gibbs energy model:

The Gibbs energy of a phase is given by (1):

$$\text{eq. 7.1} \quad G = \sum_{i=1}^N n_i \mu_i = G^{\text{ideal}} + RT \sum_{i=1}^N n_i \ln \gamma_i$$

when eq. 2.2 is used for the chemical potential. The excess Gibbs energy of this phase is subsequently defined as:

$$\text{eq. 7.2} \quad G^E = G - G^{\text{ideal}} = RT \sum_{i=1}^N n_i \ln \gamma_i$$

As the chemical potential is by definition the partial molar Gibbs energy, it follows that an activity coefficient is a partial molar excess Gibbs energy:

$$\text{eq. 7.3} \quad \mu_i = \left( \frac{\partial G}{\partial n_i} \right)_{P, T, n_j} \Rightarrow RT \ln \gamma_i = \left( \frac{\partial G^E}{\partial n_i} \right)_{P, T, n_j}$$



## EXCESS GIBBS ENERGY

This implies that once a model for the excess Gibbs energy has been formulated, the activity coefficients, needed for solving the set of equilibrium equations eq. 2.1- 2.5 to obtain the number of phases and the amount and composition of each phase present, are readily obtained.

### 7.1.1 Excess Gibbs energy models

Hardly any literature on excess Gibbs energy models for solid mixtures is available. In thermodynamic calculations it is nearly always assumed that solid phases are pure phases. Deviations between experiments and calculations are explained with 'mixed crystal formation', but without any quantification.

Kitaigorodskii (5) and Haget (6,7) propose a parameter, the 'degré d'isomorphisme cristallin' that expresses how good a molecule will fit into the crystal of another compound. The parameter was successfully used for qualitatively predicting complete, partial or no miscibility in the solid phase of mixtures several substituted naphthalenes, but could not be used for quantitative predictions.

In a few cases existing liquid phase excess Gibbs energy models were applied to solid mixtures: a regular solution model for petroleum waxes (2,3,4), van Laar and Wilson equations (1) for sodium carbonate and sodium sulphate (10). No general guidelines can be distilled from literature.

The excess Gibbs energy of a pure phase is zero :  $G^E = 0$  (if  $x_i \rightarrow 1$ ). The simplest relation meeting this requirement is the regular solution or two suffix Margules model. For a binary system it is given by (1) :

$$\text{eq. 7.4} \quad g^E = A_{12}x_1x_2 \quad \Rightarrow \quad RT \ln \gamma_1 = A_{12}x_2^2$$

and for multicomponent systems by :

$$\text{eq. 7.5} \quad g^E = \sum_{i=1}^N \sum_{j=i+1}^N A_{ij}x_ix_j$$
$$RT \ln \gamma_i = -g^E + \sum_{j=1, j \neq i}^N A_{ij}x_j$$

It contains one interaction parameter per binary.

Usually the very regular crystal lattice of a pure component will be disturbed when a molecule of another size is incorporated. This results in a positive excess Gibbs energy. Therefore normally the interaction parameters  $A_{12}$  in the solid phase will be positive and the activity coefficients will be greater than unity.

The two suffix Margules equation is symmetric: A mixture of 10 % PPP and 90 % SSS would have the same excess Gibbs energy as a mixture of 10 % SSS with 90% PPP. However, symmetric behaviour in the solid phase is unlikely: the effect of incorporating a large molecule in a crystal lattice of smaller molecules probably differs from the effect of the reverse case. The two suffix Margules equation is therefore not the most obvious excess Gibbs energy model to be used for solid fats.

The simplest models, able to describe demixing, that can account for the expected asymmetric behaviour are the van Laar and the three suffix Margules equations. Both contain two interaction parameters per binary pair. More complex models are not justified (1) : they require very accurate and extensive data, which are not available for TAGs and in view of the experimental difficulties probably impossible to obtain. Because of its somewhat wider versatility (1) the three suffix Margules equation is used in this work. For a binary system it is given by:

$$\text{eq. 7.6} \quad g^E = (A_{21}x_1 + A_{12}x_2)x_1x_2$$

$$RT \ln \gamma_1 = x_2^2 [A_{12} + 2(A_{21} - A_{12})x_1]$$

$$\ln \gamma_1^\infty = \frac{A_{12}}{RT} \quad , \quad \ln \gamma_2^\infty = \frac{A_{21}}{RT}$$

The main disadvantage of 3-suffix Margules equation (and also of the van Laar equation) is its lack of a rational base for extension to multicomponent systems. An extra assumption has to be made. If we assume that an  $i, j$  pair in the multicomponent system gives the same

## EXCESS GIBBS ENERGY

contribution to  $g^E$  as in the binary mixture at the same relative concentrations (8), then the multicomponent 3-suffix Margules equation becomes:

eq. 7.7

$$g^E = \sum_{i=1}^N \sum_{j=i+1}^N \left( A_{ij} \frac{x_j}{x_i + x_j} + A_{ji} \frac{x_i}{x_i + x_j} \right) x_i x_j$$

$$RT \ln \gamma_i = -g^E + \sum_{j=1, j \neq i}^N x_j \left( \frac{A_{ji}(x_i^2 + 2x_i x_j) + A_{ij} x_j^2}{(x_i + x_j)^2} \right)$$

When both interaction parameters are equal, the equations reduce to the 2-suffix Margules equations.

### 7.1.2 Regular or athermal ?

The parameters in the Margules equations are usually taken to be independent of temperature. This is equivalent to assuming that the excess entropy equals zero. Mixtures with this behaviour are called 'regular'. The opposite case is assuming that the excess enthalpy is zero. Mixtures with this property are called 'athermal'. The interaction parameters are inversely proportional to temperature. In reality the situation lies usually in between: both excess enthalpy and entropy deviate from zero.

The data of Haget and Chanh (6,7) for substituted naphthalenes in the solid state as well as the data of Maroncelli (11) and Snyder for n-alkanes in the solid state suggest that these mixed solid phases of chemically very similar compounds show nearly regular behaviour. The temperature differences that are considered in this work, are probably too small to be able to discriminate between both extreme situations. We could not obtain any improvement of fit to binary phase diagrams of TAGs by replacing the assumption of regular behaviour with athermal mixing. Therefore it is arbitrarily assumed in this work that TAGs form regular mixtures.

### 7.1.3 Phase diagrams

The solid-liquid phase behaviour of two components is usually represented by a T,x,y phase diagram. Figures 7.1a and 7.1b on the following pages illustrate the types of binary T,x,y phase diagrams

PHASE EQUILIBRIA IN FATS  
 - theory and experiments -

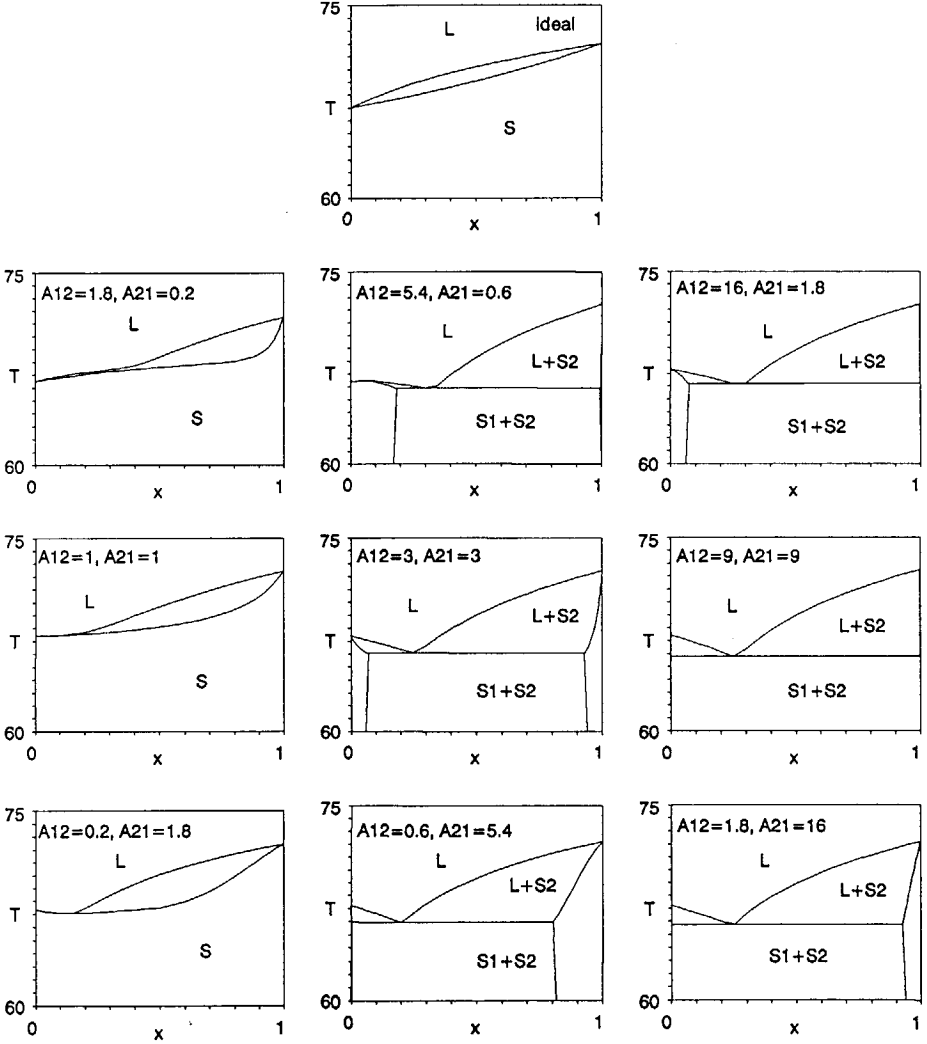


figure 7.1a Theoretically possible  $T, x, y$  solid-liquid phase diagrams of PSS-SSS calculated using the 3-suffix Margules equation. The values of the binary interaction parameters are indicated.

MASTER FIGURES

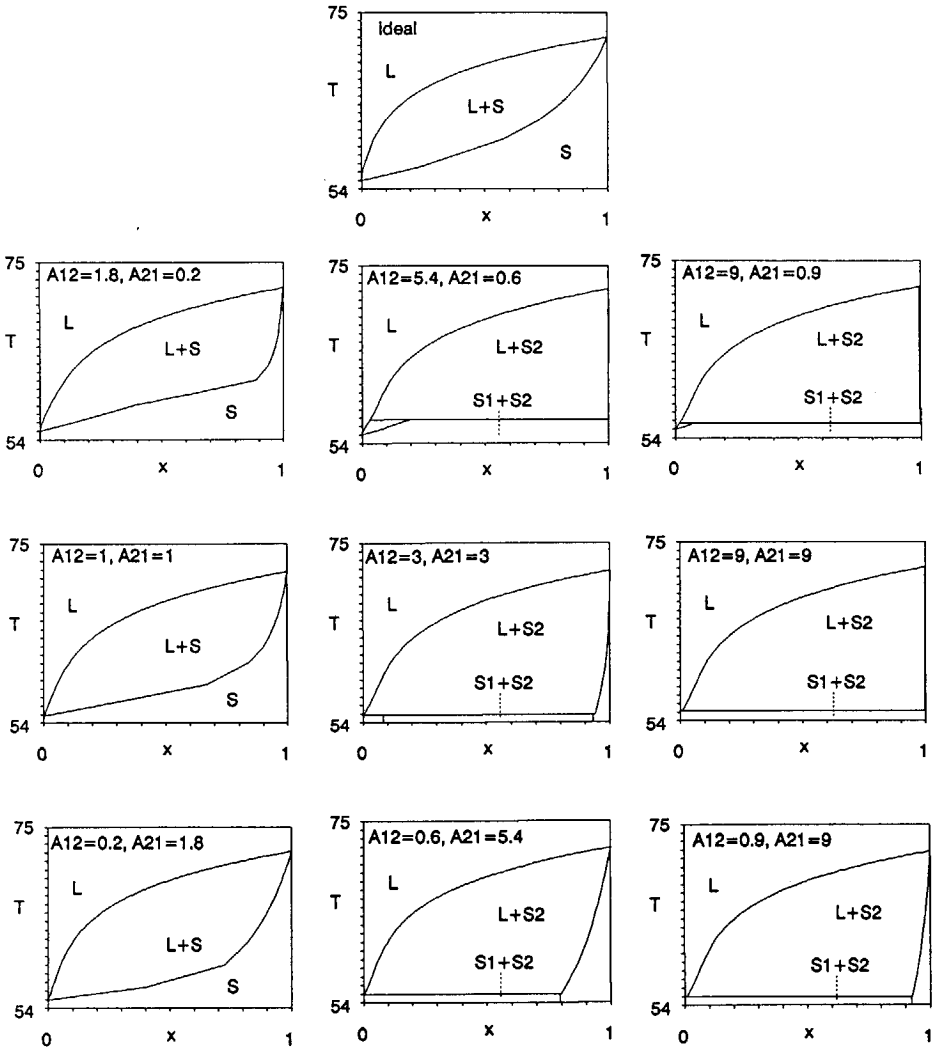


figure 7.1b Theoretically possible  $T, x, y$  solid-liquid phase diagrams of MMM-SSS calculated using the 3-suffix Margules equation. The values of the binary interaction parameters are indicated.

that can be obtained assuming an ideal liquid phase (chapter 4) and a non ideal solid phase that is described by the 2- or the 3- suffix Margules equation.

The following aspects feature:

1. The eutectic composition is determined almost completely by the difference in melting point of the two components when the 2-suffix Margules equation is used. Using the 3 suffix Margules equation the eutectic composition can still be shifted about 0.05 mol fraction in both directions.
2. Peritectic diagrams cannot be obtained using the 2 suffix Margules equation.
3. The position of the liquidus is hardly influenced by the magnitude of the interaction coefficients:
  - if the value of the interaction coefficients  $A/RT$  exceeds 4.
  - if the difference between the melting points of the components is more than about 15 °C.

In the first case, that of a eutectic diagram, the magnitude of the interaction coefficients only influences the position of the solidus at mole fractions less than 0.1 or greater than 0.9.

In the second case the position of the solidus hardly depends on the value of the interaction parameters at mole fractions of the lowest melting component  $\leq 0.5$ . Only at very low concentrations of the highest melting component there is influence of the interaction parameters on the liquidus. However in this region the experimental errors are normally most pronounced.

According to Timms (20) four types of phase diagrams are observed for TAGs: monotectic with continuous solid solubility, eutectic, monotectic with partial solid solubility and peritectic diagrams. Only the 3-suffix Margules equation is able to describe all these diagrams.

#### Nomenclature

Henceforth the liquidus and solidus that are obtained when ideal mixing in the solid phase is assumed will be called 'ideal liquidus' and 'ideal solidus'. The interaction parameters of the excess Gibbs

## EXPERIMENTAL PHASE DIAGRAMS OF TAGS

energy models are zero. The liquidus and the solidus that are obtained in the opposite case, when no mixing in the solid phase occurs, will be called 'eutectic liquidus' and 'eutectic solidus'. Then the interaction parameters of the  $G^E$  models are infinite, which is in practice equivalent to values of  $A/RT \geq 9$ .

The eutectic liquidus is also obtained from the well known Hildebrand equation, eq. 4.1, which assumes the absence of mixed solid phases. In literature this liquidus is often referred to as the 'ideal solubility line', in spite of the highly non-ideal solid phase behaviour that is implicitly assumed.

A point on the liquidus is called the 'clear point' and a point on the solidus will be referred to as the 'softening point' of a mixture.

### Use of phase diagrams to determine interaction parameters

Experimental binary phase diagrams of TAGs can be used to determine the interaction parameters that occur in an excess Gibbs energy model. Using a fitting procedure the interaction parameters are adjusted until the calculated and measured phase behaviour agree.

There is one important limitation: in the aforesaid cases where the position of the liquidus hardly depends on the magnitude of the interaction parameters, it will be very hard to obtain reliable values of those interaction parameters from a phase diagram. That would require a number of solidus points at mole fractions  $< 0.1$  and  $> 0.9$ . Such data points are seldom available.

Therefore the use of phase diagrams to determine interaction parameters is in practice limited to binaries of components that still show considerable solid miscibility and that differ less than about  $15^\circ\text{C}$  in melting point. It is possible to fit the phase diagram of other binaries, however without learning much of the performance of the  $G^E$  model that is applied.

## 7.2 EXPERIMENTAL PHASE DIAGRAMS OF TAGS

### 7.2.1 Measuring phase diagrams

Rossell (12) reviews all phase diagrams of TAGs that were published before 1967. Although he gives no quantitative interpretation of the

phase diagrams, he recognizes the main problems that occur when determining a binary solid-liquid T,x,y phase diagram:

1. Impurities,
2. Incomplete and incorrect stabilisation,
3. Other experimental errors.

#### Impurities

Impurities generally lead to an increase of the observed melting range and may cause an erroneous picture of mutual solid solubility. The position of both liquidus and solidus are affected by the presence of impurities. Good determination of TAG purity by GLC, TLC or HPLC is only possible since about 1965. Therefore older data may be suspect.

#### Stabilisation

Due to the extremely low diffusion rates in the solid phase lengthy stabilisation procedures are required to ensure that the solid phase composition has its equilibrium value. The polymorphic behaviour of TAGs complicates the stabilisation even more. Part of the solid phase may persist in an unstable polymorphic form with a deviating equilibrium composition. Except for the combination of very short stabilisation with very quick measurements, the position of the liquidus usually does not depend very strongly on the stabilisation procedure. The small amount of solid phase at temperatures just below the clear point can relatively easily recrystallize via the liquid phase to the equilibrium solid phase composition. Stabilisation strongly influences the position of the solidus.

Proper stabilisation requires lengthy schemes of temperature cycling between clear point and softening point. These can take several months to a year.

Often the mixtures are stabilised by long storage at a temperature several degrees below the softening point. This procedure is certainly not sufficient: in this way unstable polymorphic forms are 'frozen'. It was shown that they could persist several years (18).



EXPERIMENTAL PHASE DIAGRAMS  
OF TAGS

**Other experimental problems**

In older reports the technique usually applied for measuring phase diagrams is the thaw-melt technique with visual observation of softening and clear points. Visual observation of clear points and especially of softening points is very inaccurate and large errors both in liquidus and solidus may occur.

The method most applied at present is some form of thermal analysis, DTA (Differential Thermal Analysis) or DSC (Differential Scanning Calorimetry). Problems that can occur when using DSC are:

1. Thermal lag because of a too large sample size or scan rate. The softening point remains in place, but the observed clear point is shifted to a higher temperature. It becomes more difficult to detect small heat effects.
2. Failure to detect melting peaks. Combination of a large ( $> 15^{\circ}\text{C}$ ) difference in melting point, low concentration of one of the components and some solid solubility leads to broad, diffuse humps rather than sharp melting peaks in the DSC thermogram. The determination of the exact starting and end temperature of these humps is very difficult. The hump itself is easily overlooked. A set of false liquidus and solidus points results.

An alternative method, that is sometimes applied, is measurement of the solid phase content of a set of binary mixtures at different temperatures by wide range pulse NMR (or before 1970 by dilatometry (12) ). The phase diagram can be constructed from the resulting melting lines or solubility curves (14, 15). This method is much more time consuming than the thermal methods. Due to the inaccuracy of the measurements (0.7 % solids) the solidus and liquidus are obtained with a relatively large experimental error.

**An illustration**

The influence of the experimental problems on the quality of the phase diagram is illustrated in fig 7.2. Two sets of simulated (chapter 3) DSC curves of the binary POP-PEP are given. The first set was generated using the 2-suffix Margules equation with  $A/RT = 3$ , resulting in a mutual solid solubility of about 15%. For the

PHASE EQUILIBRIA IN FATS  
- theory and experiments -

second set the 3-suffix Margules equation was used with  $A_{POP-PEP}/RT = 0$  and  $A_{PEP-POP}/RT = 6$ , resulting in zero solubility of PEP in solid POP and 50% solubility of POP in solid PEP. Moreover 3% of impurities, a thermal lag of  $0.2^{\circ}\text{C}$  and 3% random noise were included. These levels of impurities, thermal lag and noise are quite normal for literature data on TAGs.

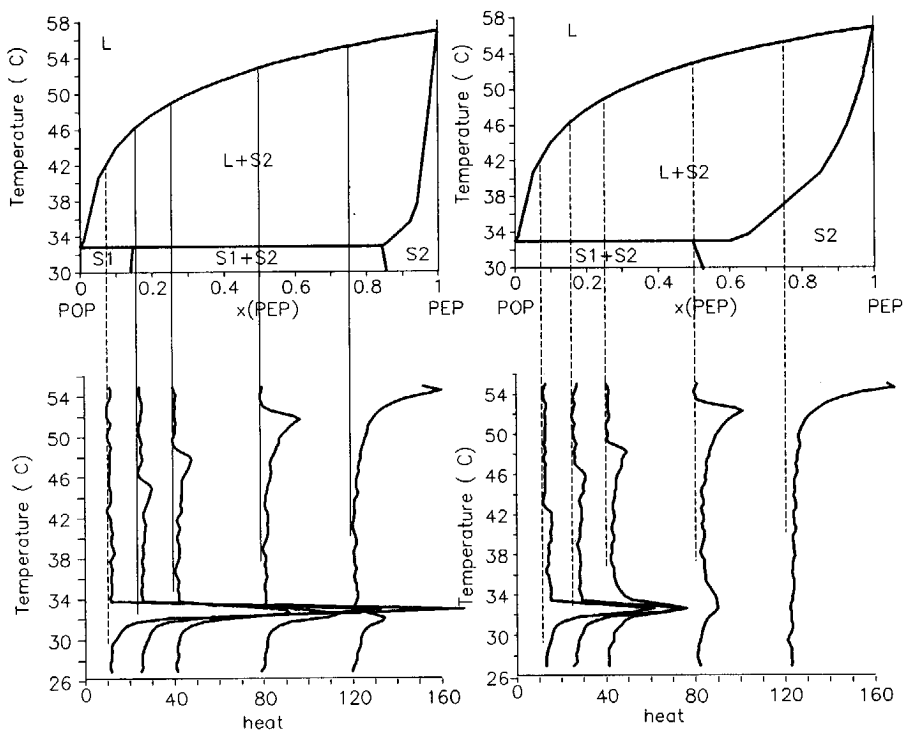


fig 7.2 Simulated DSC melting curves (bottom) and binary phase diagrams (top) for a number of different mixtures of POP and PEP. The trajectory through the binary phase diagram that is followed is indicated for each mixture.

left : Simulation with  $A_{12}=A_{21}=3$

right : Simulation with  $A_{12}=0$  and  $A_{21}=6$

EXPERIMENTAL PHASE DIAGRAMS  
OF TAGS

Perfect (i.e. in absence of thermal lag, impurities etc.) measurements on the first system would result in DSC curves with a sharp spike at the eutectic temperature followed by a broader hump that ends abruptly at the clear point. Due to the presence of impurities and thermal lag the eutectic 'spike' is broadened to 2-4 degrees. This causes an uncertainty in the position of the solidus of the same size, while the shape of the solidus remains correct.

In the second system the sharp spike at the eutectic temperature disappears and is replaced by a broad hump at PEP concentrations over 50%. The onset of this hump is hard to determine exactly. At 75% PEP, the hump becomes very broad. In the simulated curve it is no longer detectable. The softening point of this mixture is 36°C. However, the softening point that one would read from the simulated DSC-curve is the onset of the second melting peak, at about 46°C, a difference of 10°C!

The influence that the experimental errors can have the measured phase diagram becomes clear in figure 7.3. In this figure the simulated phase diagram is plotted together with pseudo-experimental solidus and liquidus points that are determined from the simulated 'experimental' DSC-melting curves of figure 9.2b. The original simulated liquidus and the 'experimental' liquidus points correspond very well, but the solidus points deviate considerably from the original solidus. At the POP side of the diagram the 'experimental' points lie far under the original solidus, while they are positioned above the ideal solidus at the PEP side of the phase diagram.

The POP-PEP binary was measured by Lovegren (28). As in the simulated DSC curve, it is impossible to detect a start melting point between 30 and 40°C in Lovegren's curve for 75% PEP. Whatever the solubility of POP in PEP would be, the start melting point would have to lie in this temperature range, which implies that the softening point that is read from this curve is wrong.

Solidus points that lie below the eutectic solidus at the side of lowest melting component and suddenly shift to values far above the ideal solidus on the other side of the phase diagram, are frequently reported for TAGs with a large difference in melting point (12). Often, in about half of the cases, contradicting reports exist,

PHASE EQUILIBRIA IN FATS  
- theory and experiments -

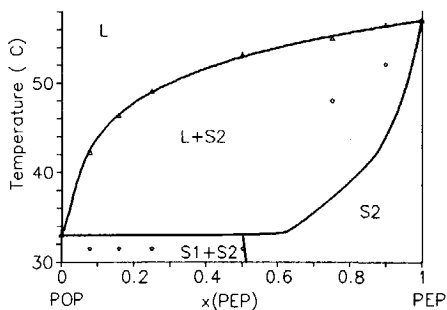


fig 7.3. Solidus and liquidus points read from the simulated DSC curves of fig 9.2b together with the phase diagram that formed the basis for the simulation of the DSC curves.

showing no solidus points that lie above the ideal solidus. An example from the data of Kerridge for SSS-LLL (12), that are in contradiction to the data of Lutton (29) (Diagram in figure 9.5).

A thermodynamic consistency test on the data is not possible. Heats of mixing, that are needed to check if the isobaric, non-isothermal Gibbs-Duhem equation is obeyed, are not available.

Compound formation, that would explain a solidus that lies above the ideal solidus is very unlikely: Compound formation is only known between pairs of TAGs made up of the same fatty acids, but attached to different positions of the glycerol group (like POP and PPO). The binaries for which deviating solidi are reported normally have a large difference in melting point, which stems from large differences in size or shape. It is therefore much more likely that the deviations are caused by impurities, improper stabilisation and failures in detecting the true softening point.

### 7.2.2 Literature overview

It is clear that the determination of solid-liquid T,x,y phase diagrams is a tedious and unrewarding job, which is probably the reason why since Rossell's review (12) so few phase diagrams were reported.

EXPERIMENTAL PHASE DIAGRAMS  
OF TAGS

De Bruyne and Knoester (13) have published the phase diagrams of all binary combinations of TAGs with palmitic(P) and stearic(S) acid. They put much effort in stabilisation and purification. Their data seem therefore of good quality. They always expected the sharp double peaked DSC-curve that is characteristic for eutectic behaviour. Therefore they missed the solidus in those cases where due to solid solubility the DSC melting curve had another shape.

De Bruyne also determined the phase diagrams of tribehenate (BBB) with tristearate (SSS) and tripalmitate (PPP) (17), and of POP with PPO in the  $\beta'$ -modification (18). Unfortunately these diagrams are only of little value as hardly any stabilisation was used.

Perron (24) and co-workers have also measured the systems of de Bruyne. They do not report any purity of their TAGs and did not stabilize the mixtures at all. Their DSC curves are full of polymorphic transitions, partially overlapping with melting peaks. They report  $\beta'$ - "stable" PSS and PPS while these TAGs are known to be beta stable (13,16). Consequently, the resulting diagrams can better be disregarded.

In later work Perron (25) again reports some of these phase diagrams (SSS-PSP, PSP-SPP, SSS-SPP), but now with very pure components and a longer stabilisation procedure.

Gibon (16) also measured the same systems and those of some of the TAGs occurring in palm oil (POP, PPO, OPO, POO). Although she worked with very pure samples, she put no effort at all in stabilisation. Most of her phase diagrams are therefore, like the early Perron work, useless for our purpose. Gibon's work is continued by de Smedt (19) with TAGs that contain elaidic acid (SES, SSE, PEP, PPE, EPE), but unfortunately in the same manner.

Krautwurst (26) gives the binary diagram of PPP-MMM and some data of the ternary PPP-MMM-LLL. He does not give purities and followed a reasonable stabilisation procedure.

The binary SSS-trioctanoate (888) was determined by Barbano (27) with a stabilisation of 23 months and very pure TAGs.

Grootscholten (14) determined the liquidus of SSS-SES, SSS-SSE, SSE-SES, SSS-SEE and of PPP and SSS with OOO using a reasonable stabilisation procedure.

Smith (15) reports the only known good quality ternary diagram: a well stabilised ternary diagram of POP/SOS/POS in their most stable polymorphic form determined by NMR.

Lovegren (28) gives the DSC melting curves of the binary POP-PEP after several stabilisation procedures, from which a diagram can be constructed.

Norton (22) gives some liquidus points of PPP and SSS with OOO determined by DSC. His end melting peaks show a strange tail for which the reason is not clear.

Only Grootscholten interpreted his phase diagrams applying an activity coefficient approach (21). All other authors only state, if something, whether their data deviate from the Hildebrand equation (eutectic liquidus and solidus).

Also outside the area of edible oils and fats phase diagrams of organic compounds that show similar phase behaviour as TAGs, like substituted naphthalenes (7) or sulfolane with compounds as dimethylsulfoxide and dioxane (9) are only interpreted with the Hildebrand equation for pure solids. Solid solutions have not been described quantitatively. Related phase diagrams, between a liquid crystalline phase and a gel phase of phospholipids (e.g. stearyl-palmityl-glycero-phosphocholine and dimyristyl-glycero-phosphocholine, 2 lecithins) have been described quantitatively with the 2-suffix Margules equation. In these systems stabilisation is considerably less important. Values of  $A/RT$  between 0 and 1.5 are found (31).

### 7.2.3 Fitting experimental phase diagrams

The ability of the 2-suffix and 3-suffix Margules equations to describe non ideal mixing in solid fats was tested by fitting these  $G^E$  models to the experimental binary phase diagrams. The Simplex method (23) was used for parameter adjustment.

EXPERIMENTAL PHASE DIAGRAMS  
OF TAGS

In section 7.3.1 it was concluded that solidus data may be very inaccurate. Therefore only the liquidus was fitted. Clear points were calculated using Michelsens' stability test (chapter 3). This guaranteed that the solid phase was in the right polymorphic form. Next the solidus data were used to fine-tune the interaction parameters within the error margin that resulted from the fit to the liquidus.

As pointed out in section 2.2.2, accurate values of binary interaction parameters can only be obtained from binaries of components that have a small difference in melting point and a reasonable mutual solid solubility. Typically the requirements are: an interaction parameter  $A/RT < 3$  and a difference in melting point  $< 15^{\circ}\text{C}$ . For all other cases only rough indications of the values of the interaction parameters can be given, using the solidus points that are available.

The phase diagram was rejected as a whole if:

- the reported melting points differ more than  $4^{\circ}\text{C}$  from the accepted values
- the reported liquidus lies on average more than  $2^{\circ}\text{C}$  above the ideal liquidus or more than  $2^{\circ}\text{C}$  below the eutectic liquidus.
- the eutectic composition differs 0.08 mol fraction or more from the composition that follows from the melting points alone.

Solidus points that lie more than  $3^{\circ}\text{C}$  above the ideal solidus were neglected: As is outlined in section 7.3.1, it is likely that the actual softening point was not detected in the experiments.

When published or when a lab journal was still available, the original data were used, but usually the data had to be read from the graphs in the publications. (Appendix 4)

#### 7.2.4 Saturated TAGs

SSS, SSP, PSP, SPS, PPS and PPP (fig 7.4-8)

These are the TAGs that occur in fully hydrogenated vegetable oils as palm oil, soybean oil, sunflower oil, rape seed oil and safflower oil. The interaction parameters and residual errors in predicted

PHASE EQUILIBRIA IN FATS  
- theory and experiments -

liquidus lines (the square root of the quotient of the sum of squared errors and the number of degrees of freedom) are given in table 7.1, the phase diagrams in fig 7.4-8.

table 7.1. Binary interaction parameters for the P/S TAGs and root mean square error between experimental points and fitted liquidus. (Standard error in the constants is 0.5, when two sets of constants are given, the first are values for the beta and the second set is for the beta' modification). Data from A = de Bruyne (15), B = Lutton (31), C = Perron (27).

binary	2-suffix Margules		3-suffix Margules			ref
	A/RT	rmse	A <sub>12</sub> /RT	A <sub>21</sub> /RT	rmse	
SSS-PSS	1.6	0.3	1.1	2.3	0.3	A
SSS-PSP	3 - 7	0.3	3 - 7	3 - 7	0.4	A/B
β'	3 - 7		3 - 7	3 - 7		
SSS-SPS	3 - 9	0.7	3 - 9	2 - 4	0.8	A
SSS-PPS	>2.2 ?	1.7	-	-	-	A
SSS-PPP	3	0.8	5.8	1.4	0.7	A/B
PSS-PSP	1.5?	1.2	-	-		A
β'	7?		-	-		
PSS-SPS	2.0	0.4	1.4	2.6	0.3	A
PSS-PPS	1.6	0.4	1.4	1.8	0.5	A
PSS-PPP	2.2	0.5	2.8	2.1	0.5	A
PSP-SPS	1.4	0.3	1.8	1 - 6	0.3	A
β'	1.0		2 - 7	0.3		
PSP-PPS	3 - 9	0.9	3 - 9	1 - 9	0.9	A
β'	2.2 - 9		1 - 9	2.2 - 9		
PSP-PPP	3 - 9	0.7	0 - 9	3 - 9	0.8	A
β'	0 - 9		0 - 9	0 - 9		
SPS-PPS	2.0	0.6	3 - 5	0.4	0.4	A
SPS-PPP	5 - 9	0.8	5 - 9	5 - 9	0.8	A
PPS-PPP	1.9	0.7	1.6	2.3	0.7	A
Perron:						
SSS-PSP	5 - 9	0.7	5 - 9	5 - 9	0.8	C
	5 - 9		5 - 9	5 - 9		
SSS-PPS	2.1 ?	2.4	-	-	2.4	C
PSP-PPS	-	-	3	0	-	C
			1.4	1.4		



EXPERIMENTAL PHASE DIAGRAMS  
OF TAGS

Taking into account that the experimental error that is claimed is 0.3-0.4 °C, the fit to the data is usually most satisfying. In spite of this good fit, the experimental error causes a rather large uncertainty in the interaction parameters. The uncertainty is even larger in the case of PSP. PSP crystallizes in the  $\beta'$  modification, and the phase diagrams are therefore mixed  $\beta$ - $\beta'$ . Consequently the 3 suffix Margules parameters determined from these diagrams that indicate the solubility in  $\beta$ -PSP and in the  $\beta'$  modification of the other TAG will show a very large error.

The data of Lutton (29) and the Bruyne(15) for SSS-PPP are in good agreement, while the data of the other authors mentioned by Rossell (Kerridge, Kung, Joglekar) disagree and cannot be fitted at all.

Lutton's and de Bruyne's data for SSS-PSP also agree very well. Both deviate from the data of Perron (25), which show a greater discrepancy between solidus and liquidus. When fitting the  $G^E$  models to Perron's data, the residual error is much larger, but similar interaction coefficients are obtained.

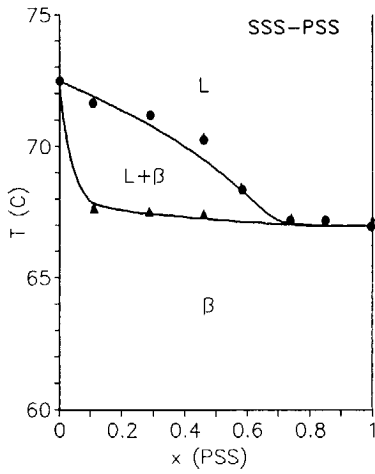
The diagrams of SSS-PSS, SSS-PSP, PSS-SPS, PSS-PPS, PSS-PPP, SPS-PSP and SPS-PPS are perfectly acceptable and are described rather well.

The 3 suffix-Margules parameter  $A_{SSS-SPS}$  is inaccurate, due to lack of data on the SPS side of the diagram. The same holds for the PPP side of the PSP-PPP diagram.

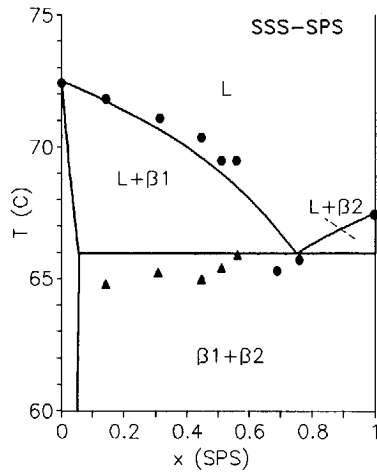
The data for SSS-PPS of de Bruyne are poor: part of the data lies above the ideal liquidus, while the data points on the PPS side of the diagram lie below the eutectic liquidus. The solidus points indicate that the 2 suffix Margules interaction parameter should exceed 2.2. The liquidus of Perron for this binary is somewhat better, although it still does not meet the acceptance criteria of section 3.3: on average the liquidus lies more 2°C below the eutectic liquidus.

At the PSP side of the PSS-PSP diagram the experimental clear points also lie far below the eutectic liquidus, indicating poor quality of the data. Best fit to the PSS side of the diagram gives an  $A(\beta)/RT$  of 1.5 for this system.

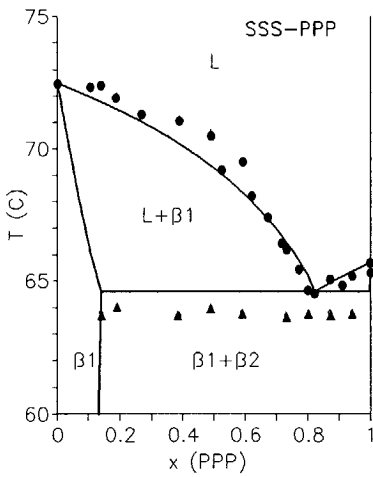
PHASE EQUILIBRIA IN FATS  
 - theory and experiments -



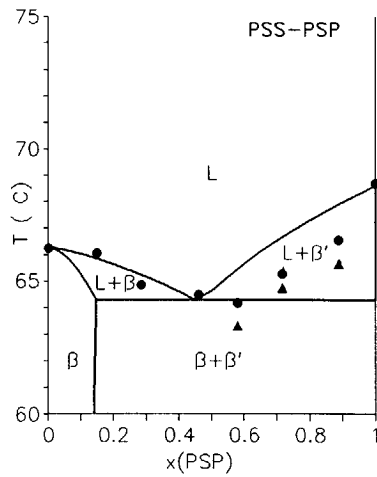
$\beta$ :  $a_{12} = 1.1, a_{21} = 2.3$



$\beta$ :  $a_{12} = 9, a_{21} = 3$



$\beta$ :  $a_{12} = 5.8, a_{21} = 1.4$

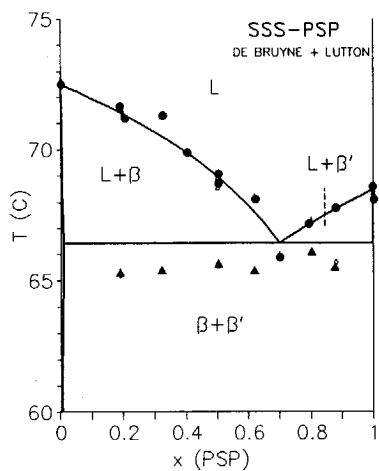


( $\beta$ :  $a = 1.5, \beta: a = 7$ )

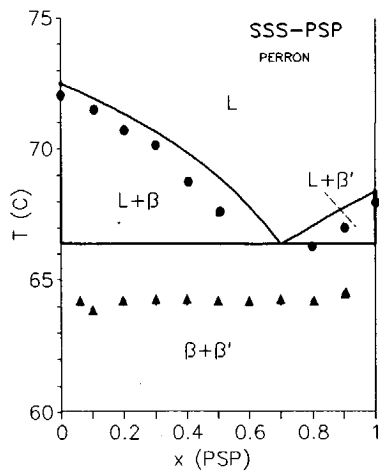
REJECTED

figure 7.4:  $T, x, y$  diagrams of TAGs from table 7.1. Experimental data (circles : clear points; triangles: softening points) and best fit (lines) with the 2- or 3-suffix Margules equation. ( $a = A/RT$ ).

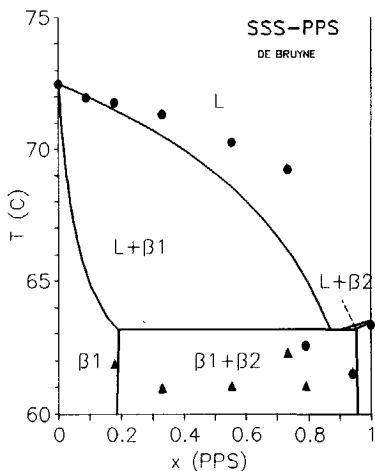
BINARY DIAGRAMS



$\beta: a = 5, \beta': a = 5$

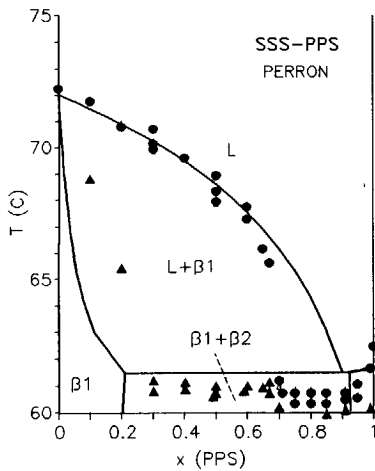


$\beta: a = 6, \beta': a = 6$



$(\beta: a_{12} = 2.8, a_{21} = 2.1)$

REJECTED

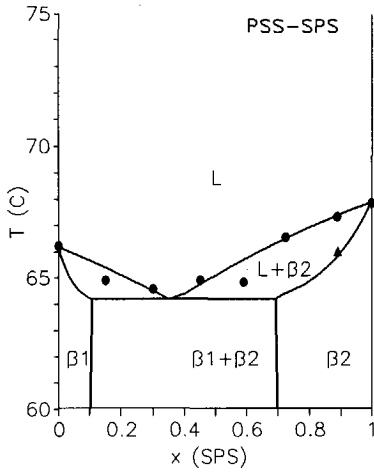


$(\beta: a_{12} = 2.8, a_{21} = 2.1)$

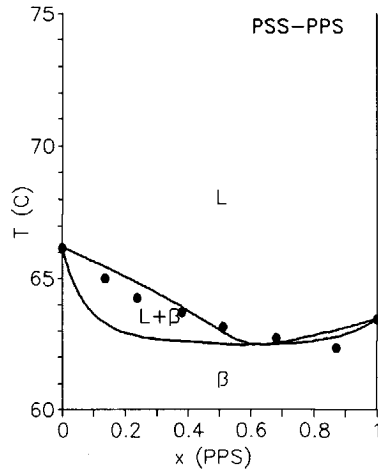
REJECTED

figure 7.5:  $T, x, y$  diagrams of TAGs from table 7.1. Experimental data (circles : clear points; triangles: softening points) and best fit (lines) with the 2- or 3-suffix Margules equation. ( $a = A/RT$ ).

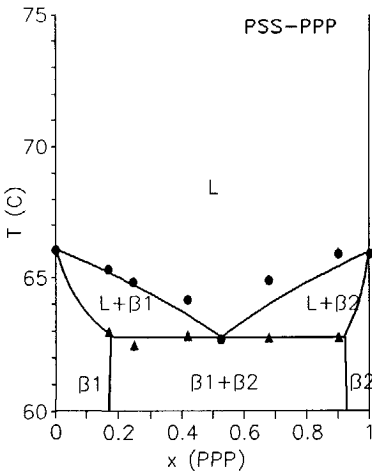
PHASE EQUILIBRIA IN FATS  
 - theory and experiments -



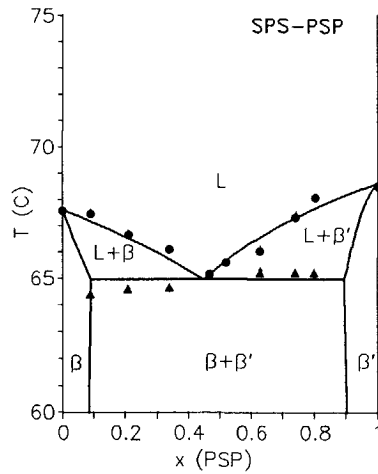
$\beta$ :  $a_{12} = 1.4$ ,  $a_{21} = 2.6$



$\beta$ :  $a_{12} = 1.4$ ,  $a_{21} = 1.8$



$\beta$ :  $a_{12} = 2.8$ ,  $a_{21} = 2.1$



$\beta$ :  $a_{12} = 4.1$ ,  $a_{21} = 1.8$

$\beta'$ :  $a_{12} = 0.3$ ,  $a_{21} = 7.3$

figure 7.6:  $T, x, y$  diagrams of TAGs from table 7.1. Experimental data (circles : clear points; triangles: softening points) and best fit (lines) with the 2- or 3-suffix Margules equation. ( $a = A/RT$ ).

BINARY DIAGRAMS

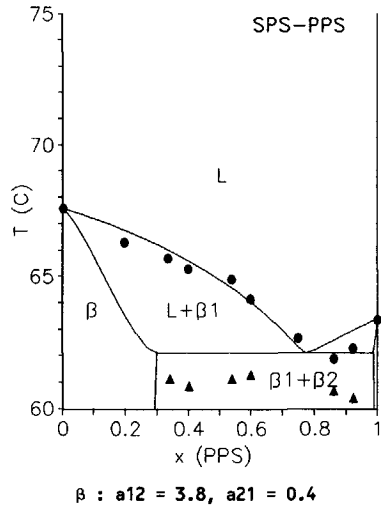
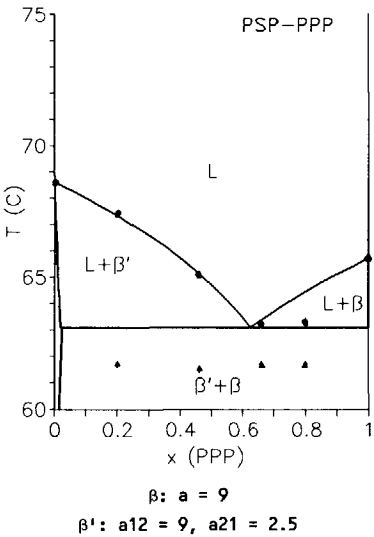
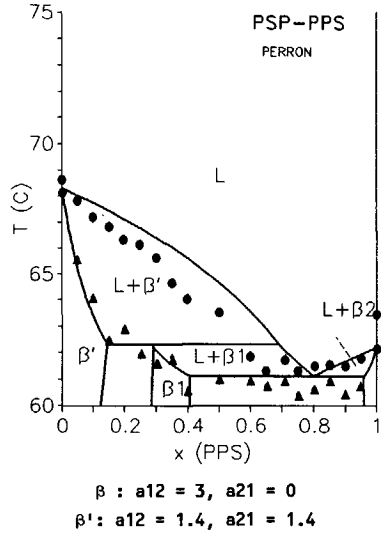
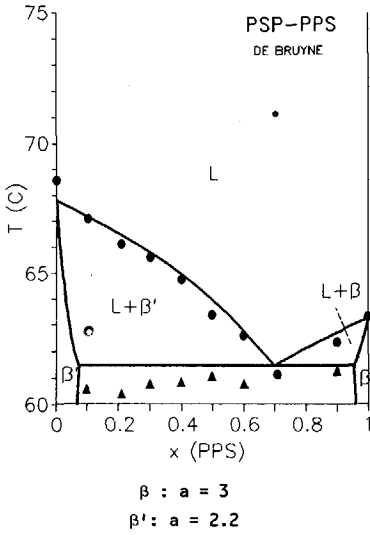


figure 7.7:  $T, x, y$  diagrams of TAGs from table 7.1. Experimental data (circles : clear points; triangles: softening points) and best fit (lines) with the 2- or 3-suffix Margules equation. ( $a = A/RT$ ).

PHASE EQUILIBRIA IN FATS  
- theory and experiments -

The liquidus of Perron and de Bruyne for the system PSP-PPS agree very well, the solidus are in complete disagreement. Best fit to the clear points results in a nearly eutectic solidus, in agreement with de Bruyne's results. The best fit to the complex solidus of Perron, that shows a peritectic and an eutectic, results in a liquidus that fits significantly worse to the data.

In the diagram of PPS-PPP there are two data points on the PPP side that lie more than 1 degree below the eutectic liquidus. Those points were given very low weight during fitting. The same occurs in the diagram of SPS-PPP, resulting in a very inaccurate 3-suffix Margules parameter for the solubility of SPS in PPP.

**Saturated mono acid TAGs (fig 7.8-9)**

The melting points most of these TAGs differ considerably. Therefore no exact values for the interaction parameters can be obtained. In this case fitting is merely a check whether the reported liquidus agree with expectations. (table 7.2, figures 7.8-9)

*table 7.2. Binary interaction parameters and root mean square error between experimental points and fitted liquidus for saturated mono acid TAGs. Data from A =De Bruyne (15,19), B= Lutton (31), C=Kerridge (14), D= Barbano (29), E= Krautwurst (28). Standard error in the parameters is 0.5, unless otherwise indicated.*

binary	2-suffix Margules		3-suffix Margules			ref
	A/RT	rmse	A <sub>12</sub> /RT	A <sub>21</sub> /RT	rmse	
BBB-SSS	3-9	1.0	4-9	2-9	1	A
BBB-PPP	3-9	0.5	3-9	2-9	0.5	A
SSS-PPP	3	0.8	5.8	1.4	0.7	A/B
SSS-LLL	3-9	0.9	3-9	3-9	0.9	B/C
SSS-888	3-9	2.4	3-9	0-9	2.4	D
PPP-MMM	3-9	0.3	3-9	2-9	0.3	E
PPP-LLL	3-9	0.3	5-9	2-9	0.3	B/C

Indeed all liquidus are described very well. The data of Kerridge and Barbano contain solidus points that lie far above the ideal solidus.

PHASE EQUILIBRIA IN FATS  
 - theory and experiments -

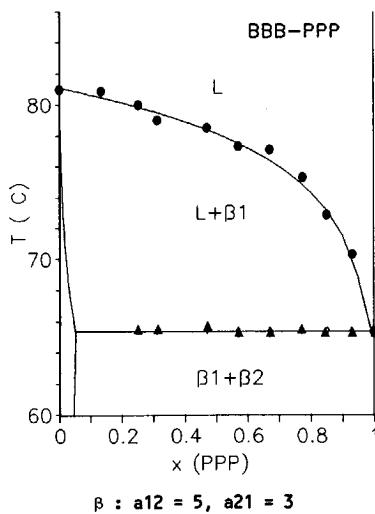
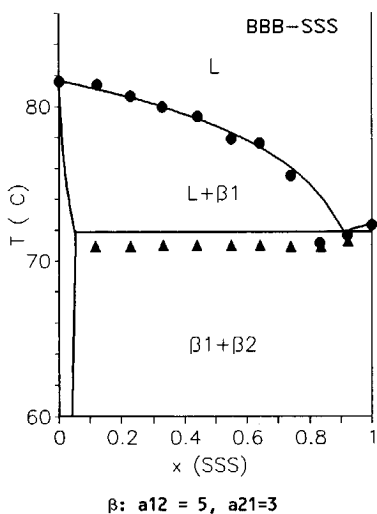
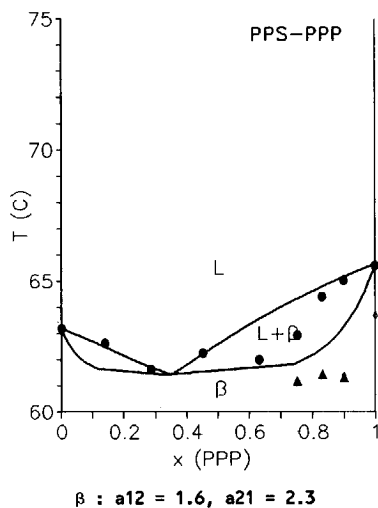
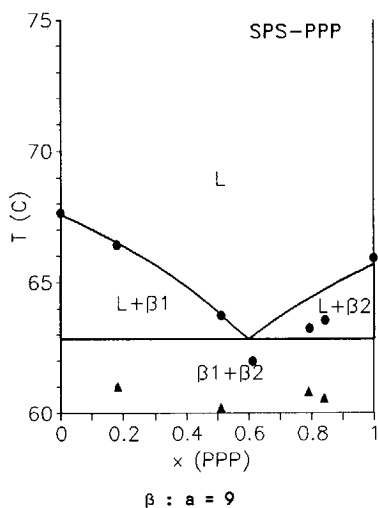


figure 7.8:  $T, x, y$  diagrams of TAGs from table 7.1 and 7.2. Experimental data (circles : clear points; triangles: softening points) and best fit (lines) with the 2- or 3-suffix Margules equation. ( $a = A/RT$ ).

BINARY DIAGRAMS

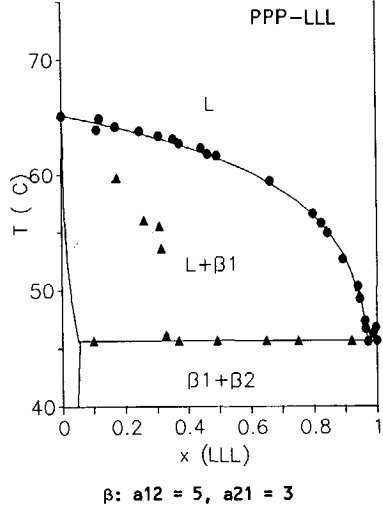
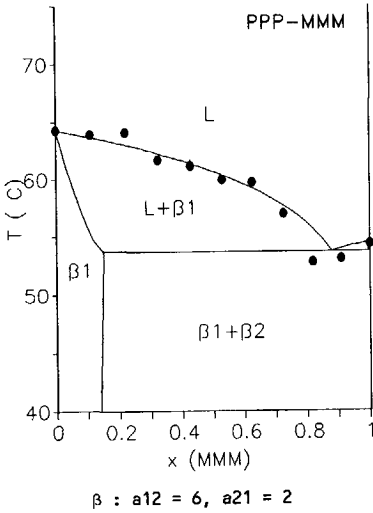
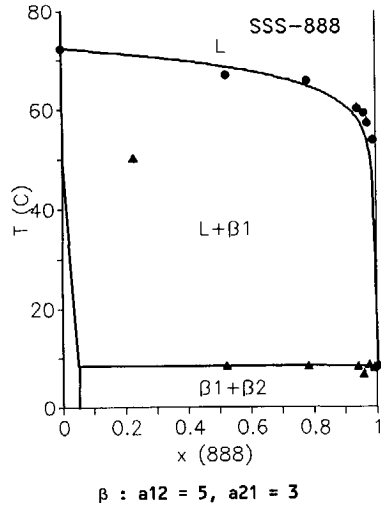
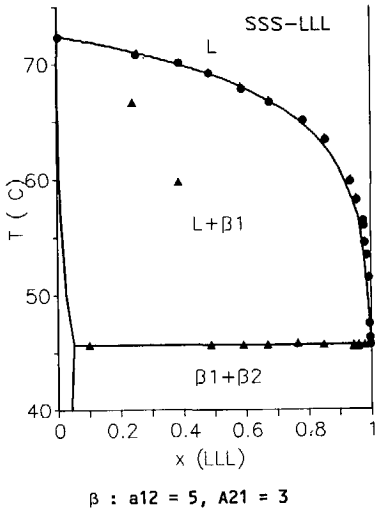


figure 7.9:  $T, x, y$  diagrams of TAGs from table 7.2. Experimental data (circles : clear points; triangles: softening points) and best fit (lines) with the 2- or 3-suffix Margules equation. ( $a = A/RT$ ).



EXPERIMENTAL PHASE DIAGRAMS  
OF TAGS

Lutton's data for the systems with LLL confirm that these solidus points are indeed not right. The available solidus points indicate that in all systems solid solubility is only very limited.

7.2.5 Saturated TAGS + trans TAGs (fig 7.10-11)

table 7.3. Binary interaction parameters and root mean square error between experimental points and fitted liquidus for saturated+trans containing TAGs. Data from A=Grootscholten (16), B=Kung (14), C=Clements(14). Standard error in the constants is 0.5, unless otherwise indicated.

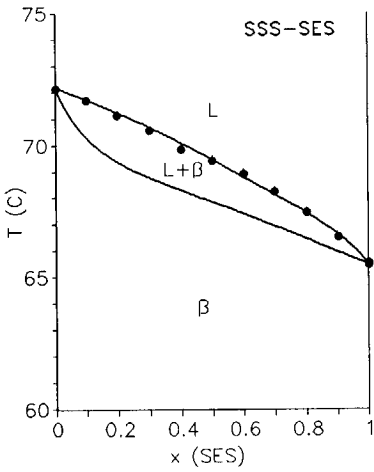
binary	2-suffix Margules		3-suffix Margules			ref
	A/RT	rmse	A <sub>12</sub> /RT	A <sub>21</sub> /RT	rmse	
SSS-SES	0.4	0.2	0	0.8	0.2	A
SSS-SSE	0.4	0.7	0.1	0.7	0.5	A/B
PPP-SSE	-	-	1?	9?	0.9	B
PPP-EEE	-	-	-	-	-	C
LLL-EEE	-	-	2.8?	0?	-	C

The similarity between elaidic acid and stearic acid is reflected in the nearly ideal miscibility of SSE and SES with SSS.

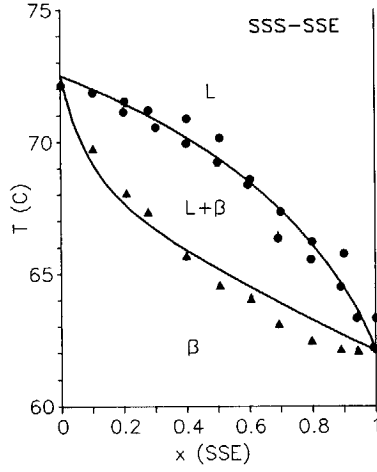
The interaction parameters for PPP-SSE are very similar to that of PPP and SSS. However, the data of Kung for this system look unreliable : there is a very poor correspondence between liquidus and solidus and the liquidus lies well below the eutectic liquidus near the eutectic point. Therefore the interaction parameters cannot be very reliable either.

Clement's data for PPP-EEE had to be disregarded: the liquidus and solidus lie too far above the ideal liquidus and solidus. Simultaneously Clements measured the system LLL-EEE, using the same technique and batch of EEE. The data are therefore suspect. The fit to these data is with a residual error of 20% rather poor. The interaction coefficients for EEE-LLL should therefore not be taken too seriously.

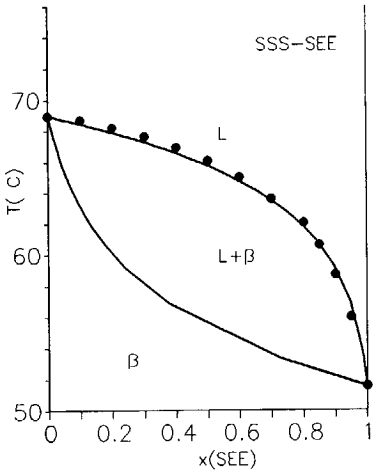
PHASE EQUILIBRIA IN FATS  
 - theory and experiments -



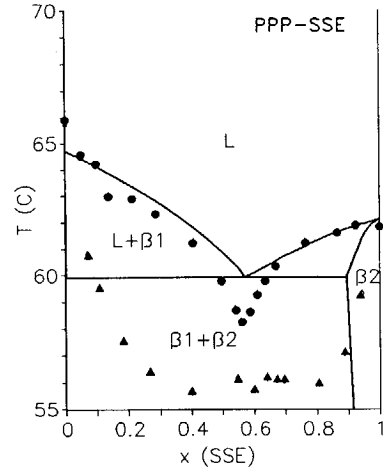
$\beta : a_{12} = 0, A_{21} = 0.8$



$\beta : a_{12} = 0.1, a_{21} = 0.7$



$\beta : a = 0$

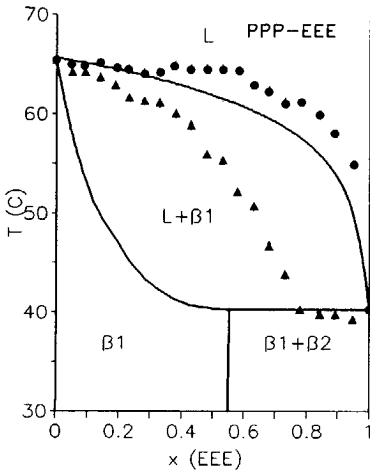


$(\beta : a_{12} = 1, a_{21} = 9)$

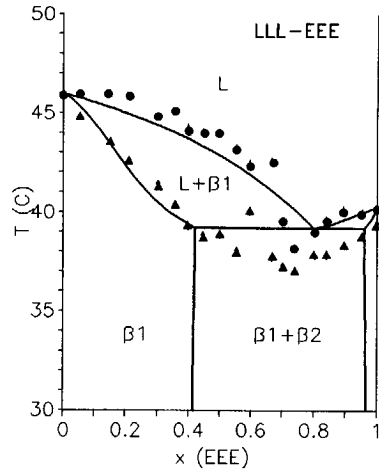
REJECTED

figure 7.10:  $T, x, y$  diagrams of TAGs from table 7.3. Experimental data (circles : clear points; triangles: softening points) and best fit (lines) with the 2- or 3-suffix Margules equation. ( $a = A/RT$ ).

BINARY DIAGRAMS

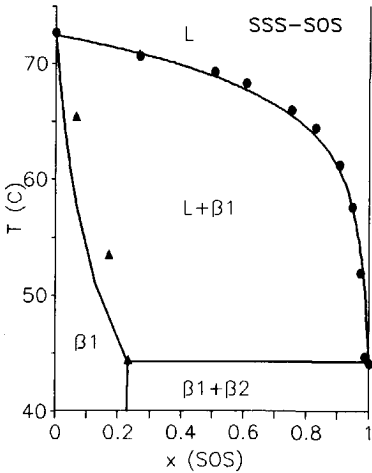


REJECTED



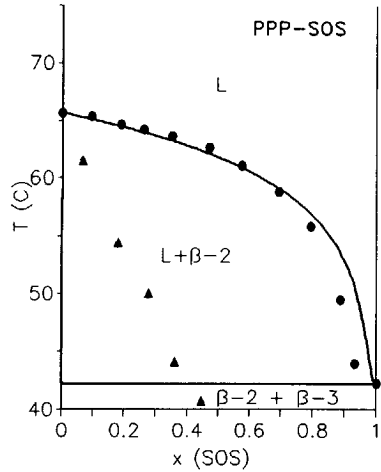
( $\beta$  :  $a_{12} = 0$ ,  $a_{21} = 2.8$ )

REJECTED



$\beta$ -2 :  $a = 1.5$

$\beta$ -3 :  $a = 1.5$



$\beta$ -2:  $a = 1.5$

$\beta$ -3:  $a = 3$

REJECTED

figure 7.11:  $T,x,y$  diagrams of TAGs from table 7.3 and 7.4. Experimental data (circles : clear points; triangles: softening points) and best fit (lines) with the 2- or 3-suffix Margules equation. ( $a = A/RT$ ).

7.2.6 Saturated TAGs + mono- and di-unsaturated TAGs (fig 7.11-12)

Due to the large differences in melting points, it will only be possible to get a coarse indication of the magnitude of the interaction parameters.

*table 7.4. Binary interaction parameters and root mean square error between experimental points and fitted liquidus for the saturated + unsaturated TAGs. Data from A=Lutton (31), B= Kung(14),C=Kerridge(14), D=Gibon(18).Standard error in the constants is 0.5, unless otherwise indicated.*

binary	2-suffix Margules			ref
	$A\beta-2/RT$	$A\beta-3/RT$	rmse	
SSS-SOS	>1.5	>1	2	A
PPP-SOS	>1	>1	4	B
PPP-POP	>1.3	>1	3.6	C
PPP-POO	1.5	4 ( $\beta'-3$ )	1	D

A complicating factor in the interpretation of these phase diagrams is the fact that the saturated TAGs crystallize in the  $\beta-2$  modification, while the cis-unsaturated TAGs crystallize in the  $\beta-3$  modification. Complete miscibility of a saturated and a cis-unsaturated TAG is impossible: an intermediate  $\beta'-2/\beta'-3$  structure is not feasible. In thermodynamic calculations the two  $\beta'$ -forms must therefore be treated as separate modifications, just like the  $\beta'$  and  $\beta$ -modification. This requires  $\beta-3$  melting points and enthalpies of fusion of  $\beta-2$  stable TAGs and vice versa. In line with the findings of de Jong (30) and our own observations in chapter 4, we assume that the melting point of the  $\beta$ -form that does normally not occur in the pure substance lies 3°C below the normal  $\beta$ -melting point, while the enthalpy of fusion is 90% of that of the normal  $\beta$ -enthalpy of fusion.

The liquidus of SSS-SOS (Lutton) and of PPP-POO (Gibon) are described very well. In those cases also good correspondence with the solidus could be obtained.

EXPERIMENTAL PHASE DIAGRAMS  
OF TAGS

The liquidus of PPP-SOS (Kung), PPP-POP (Kerridge) and also the data for PPP-POO of Moran (12) are rejected: do not meet the criteria of section 7.3.3 : the liquidus lines lie too far below the eutectic liquidus and large parts of the solidus lines are found far above the ideal solidus.

7.2.7 Unsaturated TAGs

Mono unsaturated TAGs (fig 7.12-13)

table 7.5. Binary interaction parameters and root mean square error between experimental points and fitted liquidus for mono-unsaturated TAGs. Data from A = Grootcholten (23), B= Freeman (14), C=Smith(17), D= Lovegren(30), E = Moran(14). Standard error in the constants is 0.5, unless otherwise indicated.

binary	2-suffix Margules		3-suffix Margules			ref
	A/RT	rmse	A <sub>12</sub> /RT	A <sub>21</sub> /RT	rmse	
SES-SSE	0	0.2	0	0	0.2	A
SOS-SSO	-	-	-	-	-	B
SOS-POS	1.3	0.2	1.5	1.1	0.2	C
SOS-POP	3.6 - 6	0.3	5	1.5	0.3	C
POS-POP	1.6	0.5	2.2	1.0	0.4	C
POP-PPD	-	-	-	-	-	E
POP-PEP	0.4 ± 1	0.9	-	-	-	D
β-3:	1 ± 0.8					

SSE and SES show ideal miscibility, in line with the good solid solubility of both components in SSS. Elaidic acid behaves like stearic acid.

Smith determined solidus and liquidus in independent experiments using NMR. His liquidus of POS-POP, SOS-POP and SOS-POS, which he obtained after extensive temperature cycling, could be fitted very well. Smith's cycling procedure was less suited for obtaining a reliable solidus, and consequently the correspondence between the solidus and liquidus data is not perfect. The very inaccurate data of Rek and Stip (12) for these systems agree only qualitatively.

PHASE EQUILIBRIA IN FATS  
 - theory and experiments -

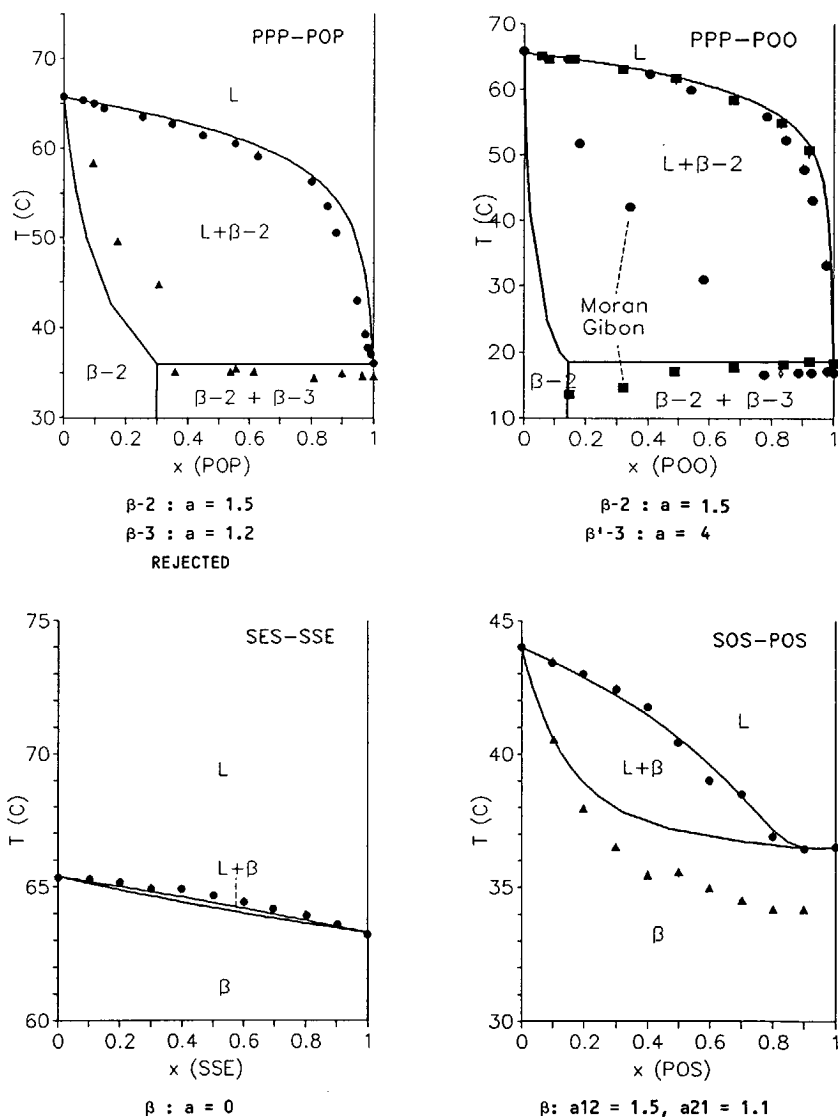
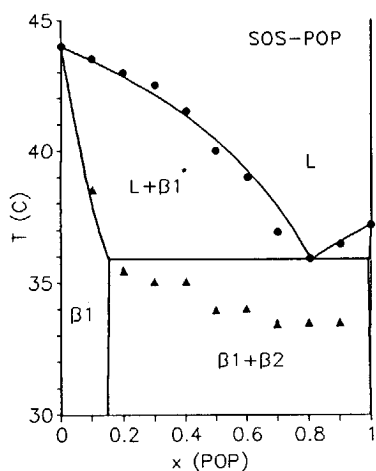
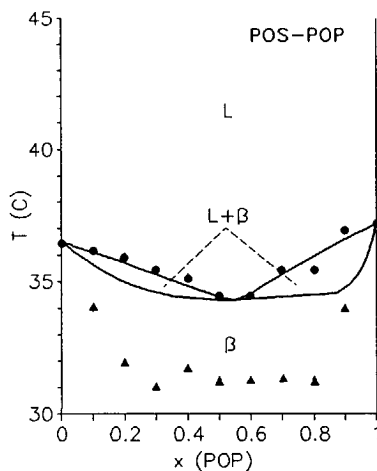


figure 7.12:  $T, x, y$  diagrams of TAGs from table 7.4 and 7.5. Experimental data (circles : clear points; triangles: softening points) and best fit (lines) with the 2- or 3-suffix Margules equation. ( $a = A/RT$ ).

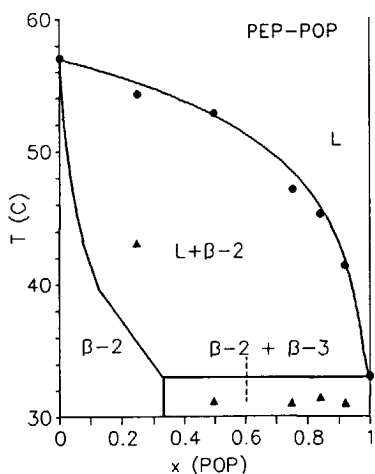
BINARY DIAGRAMS



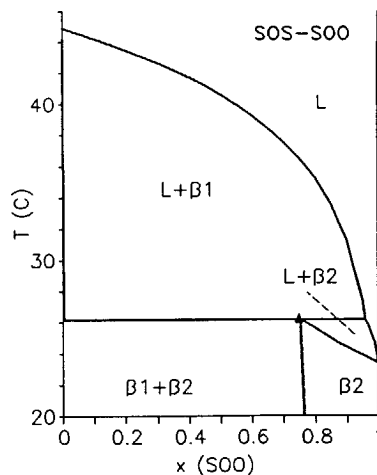
$\beta$ :  $a_{12} = 5, a_{21} = 1.5$



$\beta$ :  $a_{12} = 2.2, a_{21} = 1.0$



$\beta-2$ :  $a = 0.4$   
 $\beta-3$ :  $a = 1$



$(\beta$ :  $a_{12} = 0, a_{21} = 5)$   
 REJECTED

figure 7.13:  $T, x, y$  diagrams of TAGs from table 7.5 and 7.6. Experimental data (circles : clear points; triangles: softening points) and best fit (lines) with the 2- or 3-suffix Margules equation. ( $a = A/RT$ ).

PHASE EQUILIBRIA IN FATS  
- theory and experiments -

The diagrams of SOS-SSO and POP-PPO could not be fitted. For both systems there is evidence for formation of a 50-50 compound (20), leading to a maximum in the liquidus lines. The  $\beta'$ -liquid phase diagrams for POP-PPO given by Moran (12) and de Bruyne (18) are in complete disagreement. Moran obtained an eutectic at 15% POP, while de Bruyne found an eutectic near 50% POP, in agreement with the eutectic composition that is expected from calculations. Phase diagrams in the unstable  $\beta'$ -modification are suspect: during slow scanning in the DTA or DSC equipment a transition to a more stable modification will occur very easily when a large amount of liquid phase is present. Consequently not all clear points may be those of the unstable modification.

The binary POP-PEP is another example of a phase diagram of two TAGs, that crystallize in different  $\beta$ -forms: PEP crystallizes into the  $\beta$ -2 form, while POP crystallizes into the  $\beta$ -3 form.

Other unsaturated TAGs (fig 7.13-14)

All phase diagrams reported for these TAGs seem very unreliable.

table 7.6. Binary interaction parameters and root mean square error between experimental points and fitted liquidus for unsaturated TAGs. Data from A = Rossell (14), B= Moran(14), C= Gibon(18).

binary	2-suffix Margules		3-suffix Margules			ref
	A/RT	rmse	A <sub>12</sub> /RT	A <sub>21</sub> /RT	rmse	
SOS-SOO	-		0?	5?	-	A
PPO-POO( $\beta'$ )	1-9?	1.7	1-9?	1-9?	1.7	C
PPO-OPO( $\beta'$ )	5-9 ?	0.6	4-9 ?	2-9 ?	0.6	B
POO-OPO( $\beta'$ )	2.0 ?	0.3	1.6 ?	2.4 ?	0.3	B

Rossell (12) gives 3 diagrams of SOS-SOO, from McGowan, Moran and Rossell. The three diagrams all disagree and have liquidus far below the eutectic liquidus. Therefore they are unreliable. There is one similarity: all diagrams have peritectic point at 24% SOS and about 27°C. This peritectic point can be obtained using the values of the interaction parameters given in table 7.6.



EXPERIMENTAL PHASE DIAGRAMS  
OF TAGS

The liquidus data of Gibon for PPO-POO are described by the eutectic liquidus. The data were obtained after a stabilisation at room temperature for a year. The mixtures are still partially liquid at room temperature and it may be assumed that sufficient recrystallization had occurred to render a reasonable liquidus. The solidus was obtained directly after crash cooling and is therefore unreliable. Moran gives for PPO-POO a liquidus far below the eutectic liquidus. His data were therefore not further used.

Both diagrams of Moran for POP-POO also have a liquidus below the eutectic liquidus and were therefore disregarded. In Gibon's DSC curves for POP-POO the final melting peak overlapped with a  $\beta'$ - $\beta$  transition. Stabilisation has been insufficient.

The data of Moran for PPO-OPO are very well described by the eutectic liquidus, but the solidus again lies far above the ideal solidus.

Moran reported two diagrams for POO-OPO, of which the one given in figure 14 has an eutectic composition where it is expected, at about 50% POO. Strangely enough Moran judged his other diagram, with a eutectic at 17% POO, more reliable. The correspondence with the solidus is poor in both cases.

Moran's diagram for POP-OPO has to be disregarded: the liquidus lies far below the eutectic liquidus. Moran explained this by assuming compound formation, but if a compound would have formed, part of the liquidus certainly had to be situated above the eutectic liquidus.

It seems that most of Moran's data are not reliable, which arouses doubts about the two diagrams of Moran (PPO-OPO and POO-OPO) that did meet the acceptance criteria of section 7.3.3.

#### Triolein (fig 7.14-15)

Indeed, all data lie reasonably well on the calculated liquidus, the data of Grootcholten being slightly better than those taken from Rossell.

PHASE EQUILIBRIA IN FATS  
 - theory and experiments -

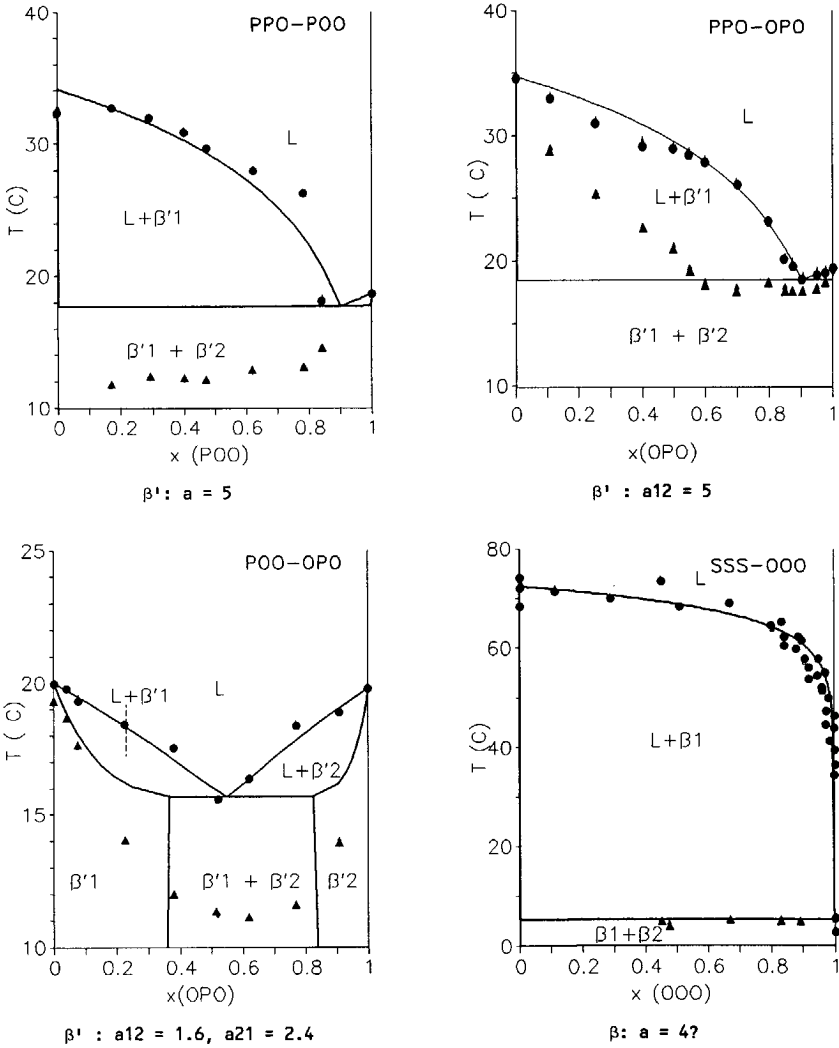


figure 7.14:  $T, x, y$  diagrams of TAGs from table 7.6 and 7.7. Experimental data (circles : clear points; triangles: softening points) and best fit (lines) with the 2- or 3-suffix Margules equation. ( $a = A/RT$ ).

PHASE EQUILIBRIA IN FATS  
- theory and experiments -

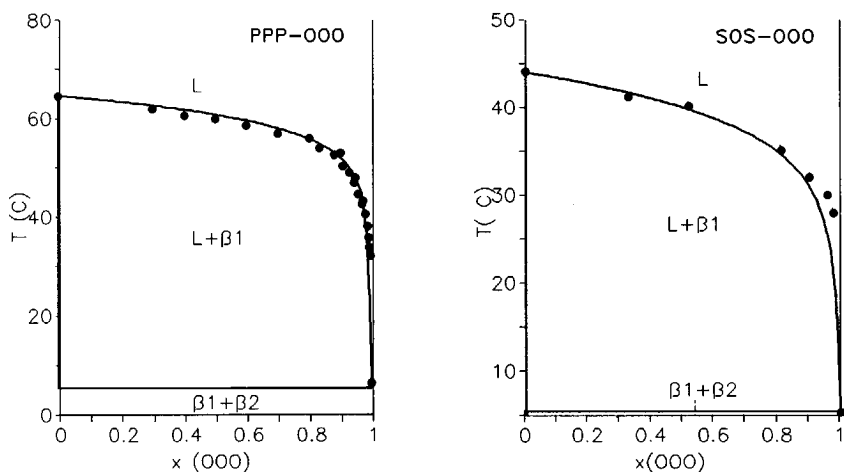


fig 7.15.  $T, x, y$  diagrams of TAGs from table 7.7. Experimental data (circles: clear points, triangles: softening points) and calculated lines.

In these diagrams, the difference in melting points is so large that the ideal and eutectic liquidus and solidus almost coincide. Fitting is in this case merely a test of the quality of the data and does not give much information about the extent of non-ideal mixing.

table 7.7 Binary interaction parameters and root mean square error between experimental points and fitted liquidus for triolein. Data from A = Rossell (14) and B = Grootcholten (16).

binary	2-suffix Margules		3-suffix Margules			ref
	A/RT	rmse	A <sub>12</sub> /RT	A <sub>21</sub> /RT	rmse	
SSS-000	0.9	4	-	-		A/B
PPP-000	0.9	3	-	-		A/B
SOS-000	0.9	2	-	-		A

### 7.2.8 Summarizing

Nearly 120 phase diagrams were considered:

- 84 had to be rejected because they were clearly not correct.

EXPERIMENTAL PHASE DIAGRAMS  
OF TAGS

- The liquidus lines were fitted very well for 34 of the remaining 36 phase diagrams. The average deviation from the experimental curves was only 7% of the difference between maximal and minimal liquidus temperature.
- In 2 cases no fit could be obtained, which was attributed to compound formation that was not accounted for in the thermodynamic modelling.
- The experimental softening points lay far above the ideal solidus at the side of the higher melting component in 5 of the 34 remaining diagrams. These five binaries all concerned TAGs with a large difference in melting point. It was made plausible that this deviation was due to an experimental error. Experimental evidence that confirmed this exists for two of the five binaries.
- The difference between the melting points of two components was less than 15°C in 24 of the 34 binaries that remained. Eleven of these 24 diagrams were almost completely eutectic. This implies that only in 13 diagrams the interaction parameters have a clear influence on the shape of the liquidus. Therefore these 13 diagrams are the most demanding test cases for the performance of the excess Gibbs energy models.

The average root mean square error between measured and fitted liquidus for these 13 remaining diagrams is 0.4°C. This is approximately the experimental error that is claimed. It is impossible to obtain very accurate values of the interaction parameters with an experimental error of this magnitude.

Based on the available data it is not possible to express a preference for one of the 2 excess Gibbs energy models used. Hardly any improvement in fit was obtained when the 3-suffix Margules equation was used. Peritectic diagrams that could not be described using the 2-suffix Margules equation, had to be disregarded. Generally the experimental softening points were better described with the 3-suffix Margules equation.

### 7.3 AN ALTERNATIVE TO PHASE DIAGRAM DETERMINATION.

#### 7.3.1 How to proceed?

The evaluation of all available phase diagrams of TAGs in section 7.3 has resulted in interaction coefficients for only 35 binaries. The uncertainty in these interaction parameters is considerable, due to the large experimental error in the diagrams.

Interaction parameters were almost exclusively obtained for the  $\beta$ -modification. However, it is of much greater importance to know the parameters for the polymorph that is normally found in edible fat products, the  $\beta'$ -modification.

The determination of binary interaction parameters that occur in an excess Gibbs energy model by fitting this model to experimental binary T,x,y solid liquid phase diagrams has a number of very serious drawbacks:

- It is extremely troublesome, time-consuming and probably almost impossible to determine accurate phase diagrams: it takes months to years before the samples have been stabilized properly, minor impurities have large effects and the true start and end melting point of a mixture are very hard to determine.
- Relatively small experimental errors in the position of the liquidus and solidus lead to large uncertainty in the interaction parameters that are determined from the diagrams. It is questionable whether more accurate  $\beta$ -data can be obtained by determining binary solid-liquid phase diagrams.
- It is not possible to measure reliable phase diagrams of unstable modifications, like a binary  $\beta'$ -phase diagram of  $\beta$ -stable TAGs.
- Determination of binary interaction parameters from phase diagrams is only feasible for TAGs that differ less than about 15°C in melting point. At larger melting point differences the position of liquidus and solidus becomes too insensitive to the value of the interaction parameters.

AN ALTERNATIVE TO PHASE DIAGRAM DETERMINATION.

Determining phase diagrams of TAGs to obtain binary interaction parameters is therefore not practical and another method has to be defined.

7.3.2 Formulation of an alternative method

The problem of the extremely long stabilization times can probably be solved:

In a solid binary system, diffusion rates are extremely low, so that unstable modifications and crystals with a non equilibrium composition have been shown to persist for years (16). But if a surplus of a liquid TAG is added to the binary system, things become different. The phase diagram of such a ternary system (PSP/SEE/OO0) is shown in figure 7.16. When the temperature is sufficiently above the melting point of the liquid component (OO0), the solidus surface in the diagram coincides with the binary side plane of the two crystallizing TAGs (PSP and SEE), even when ideal mixing in the solid phase occurs. The concentration of the liquid component in the solid phase is then negligible. The solid phase in this ternary system is still a binary mixture.

If the fat is crystallized in very small ( $< 1 \mu\text{m}$ ) crystals, to create a large exchange surface with the liquid phase, then the solid fat can recrystallize relatively easily via the liquid phase to its equilibrium composition and modification (22,36).

Phase diagrams are usually determined by measuring the softening and clear point of a set of mixtures using DSC. Due to impurities and thermal lag that occur both points can only be determined with an accuracy of about 0.2 - 1 °C.

In fact this application of DSC does not use all available information: a DSC-curve of a mixture is taken and next the two most undefined points on the curve, its start- and end-point, are used, while everything in between, that contains lots of information about the phase behaviour of the binary system, is wasted. If the complete DSC curve is used for determination of the interaction parameters, rather than only 2 points, it should be possible to increase the accuracy of results with considerably less measurements. In chapter 3 we

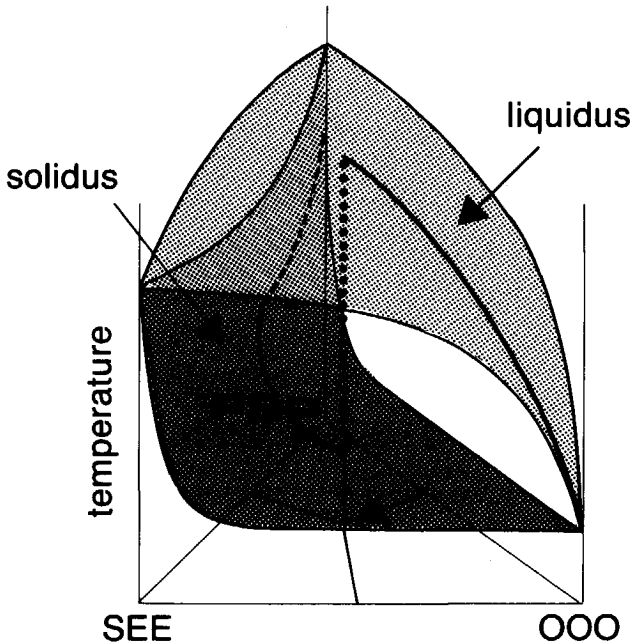


figure 7.16. Schematic ternary phase diagram of the system PSP/SEE/OO in the  $\beta'$ -modification. The softening point surface is dark shaded, while the clear point surface is light shaded. The lines indicated with solidus and liquidus represent the composition of the solid and liquid phase of a mixture with composition A while it is being melted.

defined a method to simulate the effect of non-ideal mixing in the solid phase on the shape of DSC-curves. This method can be applied to fit a complete DSC curve by adapting the binary interaction parameters.

The method for determination of interaction parameters that evolves, is the fitting of the complete DSC-curve of a binary mixture to which a surplus of a liquid TAG is added. The liquid TAG assures shorter and better stabilization. The use of the complete curves reduces experimental error, reduces the number of measurements and removes the limitation to binary pairs that have a difference in melting point less than 15 °C.

### 7.3.3 DSC curves of binary systems dissolved in a liquid TAG.

Figure 7.17 on the following page gives the types of DSC-curves that can be obtained for TAGs that differ considerably in melting point by application of the 3-suffix Margules equation. Although in this situation the position of liquidus and solidus in the binary phase diagram are nearly invariant, still considerable differences in curve shape are obtained.

The following aspects feature:

1. All curves contain two melting peaks. The shape of the final melting peak and the start of the first melting peak are hardly influenced by the values of the interaction parameters. This is in line with the invariance of the phase diagram. However, the shape of the first melting peak and the height of the plateau in between the two peaks depend very much on the values of the interaction parameters.
2. The first melting peak ends sharply if demixing in the solid state occurs.
3. If no demixing occurs, the complete shape of the first melting peak is indicative for the value of the interaction parameters, which implies that the interaction parameters can be determined very accurately.
4. If demixing occurs, the height of the plateau just after the first peak is indicative for the magnitude of the interaction parameters. This implies that in these cases the interaction parameters can be determined less accurately, due to the influence of noise and the uncertainty in the baseline.
5. Above values of  $A/RT=4$  the curve shape does not depend on the magnitude of the interaction parameters any more. However, as at  $A/RT=4$  already nearly complete solid phase immiscibility occurs, this is not a real problem.
6. For the 2-suffix Margules equation peak shape and peak position are closely related: upon increasing magnitude of the interaction parameters the first melting peak becomes sharper and shifts towards lower temperatures. Therefore 2-suffix Margules parameters



PHASE EQUILIBRIA IN FATS  
 - theory and experiments -

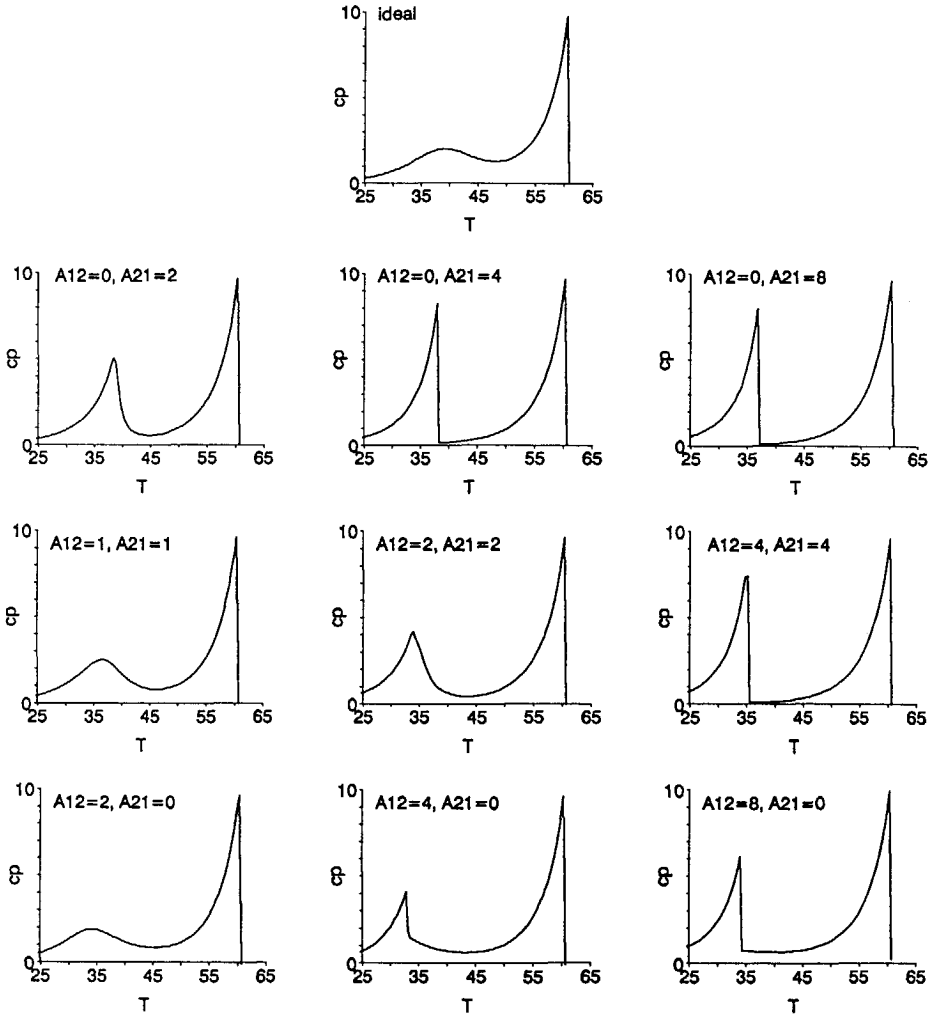


figure 7.17 Theoretically possible DSC-melting curves of a ternary mixture of 25% PSP, 25% SOS and 50% OOO crystallized in the B'-2 modification. The curves are calculated using the 3-suffix Margules equation. The values of the binary interaction parameters are indicated.

can be determined very easily. Bringing in asymmetric behaviour with the 3 suffix Margules equation allows shifting of sharp peaks to higher temperatures and of broad humps towards lower temperatures. In fact, if the component with the highest melting point is [1] and the other [2], then the shape of the first melting peak is mainly determined by  $A_{21}$  and its position mainly by  $A_{12}$ . The 3-suffix Margules parameters determined from the curves will necessarily have a larger error, as the uncertainty in the melting points of 1-1.5°C has to be taken into account now.

#### 7.3.4 What experiments ?

In most edible fat products the fat has crystallized into the  $\beta'$  modification. There are no reliable data available about miscibility in the  $\beta'$  modification.

For fat fractionation calculations it is important to know the solubility of mono-unsaturated TAGs in the solid phase of saturated TAGs both in the  $\beta'$  and in the  $\beta$  modification. It was shown in section 7.3 that the scarce information that exists is unreliable.

In edible fat products mostly hydrogenated fats, which are rich in elaidic acid, are used. Except for  $S_2E$  in SSS there is no information available about the phase behaviour of TAGs that contain elaidic acid.

Of the many systems that can be studied, it seems therefore most relevant to determine interaction parameters for the  $\beta'$ -modification of systems where mono-unsaturated and trans-containing TAGs are combined with saturated TAGs.

In order to enable the determination of  $\beta'$ -interaction parameters, we must assure that during determination of the DSC-curve, which must be taken at low scan rates in order to reduce thermal lag, no transition to the  $\beta$ -modification will occur. Near the clear point the solid phase usually almost completely consists of the component with the highest melting point. If this component is  $\beta$ -stable, than a transition is very likely. However, if for this component a  $\beta'$ -stable TAG is taken, the chances of keeping the system sufficiently long into the  $\beta'$ -modification to allow a measurement are much higher.

## EXPERIMENTAL

Moreover, even if in this case a solid phase in the  $\beta$ -modification, rich in the crystallizing component with the lower melting point, comes about, the DSC curve will still contain a melting peak of a mixed  $\beta'$ -phase that holds information about the miscibility in the  $\beta'$ -modification.

In view of this, we have selected a number of systems, of a  $\beta'$  stable saturated TAG and a number of mono- and di-unsaturated TAGs, including some that contain elaidic acid :

PSP with SOS, SSO, POP, PPO, PEE, EPE, SEE, ESE and EEE.

MPM with SOS, SSO, POP, PPO, PEE, EPE, SEE, ESE and EEE.

These systems allow the study of the influence of a difference in size as well as the influence of position and nature of the unsaturated chains. The data themselves are relevant for normal edible fat products.

### 7.4 EXPERIMENTAL

#### 7.4.1 Principles of DSC

With DSC (Differential Scanning Calorimetry) two cups, one containing a few mg's of the sample to be investigated and the other containing an inert reference material, are placed in two identical micro-furnaces. Both furnaces are mounted in cavities of a large aluminium block or 'heat sink'. The aluminium block is kept at a constant temperature, well below the temperature range of the experiment. In the base of each furnace are 2 identical platinum resistance elements. One is used to provide heat to the furnace, the other that is mounted directly under the furnace base, serves as temperature sensor. (fig. 7.18)

The equipment is controlled by two control loops: An average temperature control or scan loop that enables simultaneous heating of both micro-furnaces at a constant heating rate (in °C/min). The other loop is a differential temperature control loop from which the instrument output signal is obtained. This loop adjusts the heat flow to one of the furnaces if a process in one of the samples takes place that gives out or takes up heat, such that the temperature difference between the two cups always remains zero.

The difference in the amount of energy that must be supplied to the

PHASE EQUILIBRIA IN FATS  
- theory and experiments -

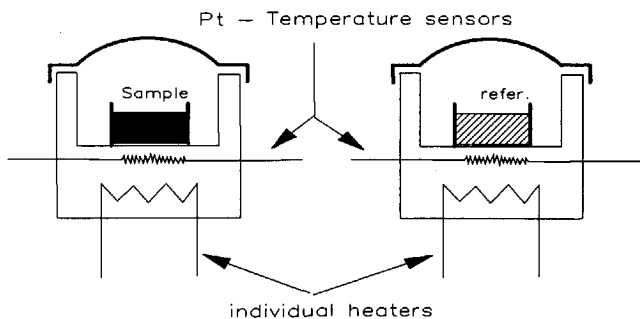


fig 7.18. Schematic view of a DSC apparatus

samples to heat both at the same rate plotted as a function of temperature is the DSC-curve. It is directly proportional to the apparent heat capacity of the sample as a function of temperature.

DSC is often confused with DTA, Differential Thermal Analysis. In DTA both samples are heated in the same micro-furnace with a constant heat flow. The temperature difference that occurs between the samples, when the sample gives out or takes up heat, is recorded, the DTA-curve. The DTA-curve contains essentially the same information as DSC-curves. With DTA fast heating and cooling rates as well as isothermal measurements are not possible and heat effects are derived quantities rather than directly measured quantities. However DTA is technically less complex.

#### 7.4.2 Thermal lag

The main problem in the use of DSC-curves is the thermal lag that occurs. During scanning the temperature of the inner part of the sample lags behind that of the apparatus. This thermal lag can completely disturb the shape of the DSC curve at too large sample sizes and scan rates (fig 7.19).

## EXPERIMENTAL

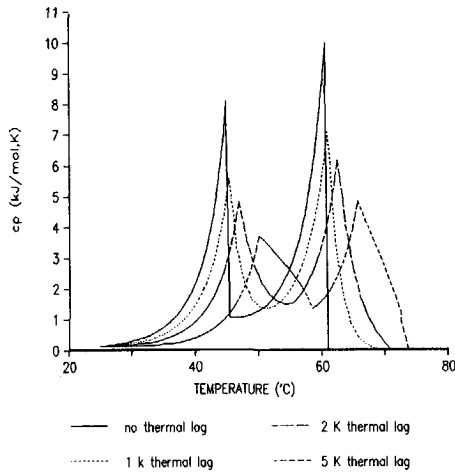


fig 7.19. Influence of thermal lag on the curve shape of the system 25% PSP, 25% SEE, 50% OOO. (simulated curves)

Best check for the presence of thermal lag is obtained from the steepness of the peak at the end melting point. Ideally this should be a straight line perpendicular to the temperature axis. At very low scanning rate or small sample size thermal lag is negligible, but the DSC signal becomes very weak, leading to noisy DSC curves. In the experimental procedure the right balance between thermal lag and sensitivity must be found by trial and error.

### 7.4.3 Experimental procedure

The work was largely carried out using a Perkin Elmer DSC-2, equipped with an IBM-AT for data-acquisition and control of the apparatus by means of software developed at the Department for Thermal Analysis of the Unilever Research Vlaardingen. Some work was done on a Perkin Elmer DSC-7, which is mechanically equivalent, but equipped with more advanced Perkin Elmer machinery for data-acquisition and control, making it more sensitive. The heat sink was cooled with a solid CO<sub>2</sub>/acetone mixture (DSC-2) or liquid nitrogen (DSC-7). The equipment was calibrated using pure Indium ( $T_f = 156.6$  °C) and Gallium ( $T_f = 29.8$  °C).

PHASE EQUILIBRIA IN FATS  
 - theory and experiments -

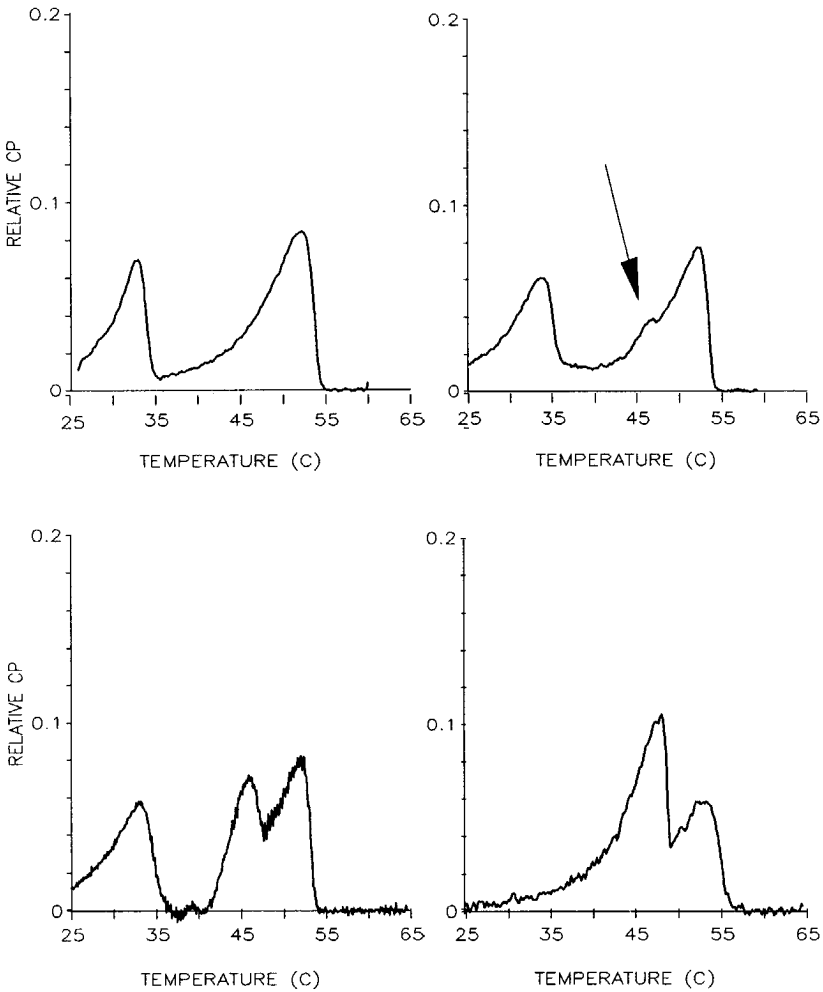


fig 7.20. Measured DSC-curves of ternary mixtures of 25% MPM with  $\pm 25\%$  ESE and  $\pm 50\%$  OOO. Note the appearance of a melting peak of a separate ESE-rich  $\beta$ -phase at  $46^\circ\text{C}$  and the disappearance of the melting peak of an ESE-rich  $\beta'$ -phase at  $34^\circ\text{C}$  upon increasing stabilisation time.

top left = 1 min  $20^\circ\text{C}$   
 bottom left = 60 min  $20^\circ\text{C}$

top right = 15 min  $20^\circ\text{C}$   
 bottom right = 7 days  $20^\circ\text{C}$

## EXPERIMENTAL

About 10 mg of a sample was weighed into an aluminium cup, that was closed and sealed. The sample was inserted into the apparatus, melted at 80 °C and kept for 10 minutes at that temperature to prevent possible memory effects. Next the sample was cooled at 20°C/min to 5°C below the temperature where the melting of a fully eutectic  $\beta'$ -phase would take place. The sample was stabilised for 1 minute at that temperature and subsequently heated at 1-2°C/min. The melting curve was recorded. This procedure is repeated several times with varying stabilisation time: 1 minute stabilisation, 5 minutes, 15 minutes, 1 hour, 3 hours, 24 hours, a week and a month.

Usually stabilisation times less than 1 hour resulted in melting curves of the  $\beta'$  modification, sometimes disturbed by a transition to the  $\beta$  modification. Longer stabilisation times mostly lead to a 3 phase  $\beta$ - $\beta'$ -Liquid system.

Stabilisation longer than a week usually did not result in changes any more. To verify that indeed crystallization had taken place in the right polymorphic form X ray diffractograms were taken after the same cooling and stabilization procedure for some of the mixtures.

The influence of stabilisation time on the polymorphic form in which crystallization has taken place is illustrated in figure 7.20 for the system PSP/SEE/000. The shortest stabilisation time only shows melting peaks of  $\beta'$ -crystal phases. After somewhat longer stabilisation a  $\beta$ -melting peak starts to appear as a shoulder, while in the completely stabilised sample a sharp melting peak of a SEE-rich  $\beta$ -phase is present next to a melting peak of a PSP-rich  $\beta'$  phase.

At the sample size and scan rate used thermal lag may be neglected: the curve shape does not change significantly when the scan rate is further decreased, while the noise increases. Normally a scan rate of 2.5 °C/min was used, sometimes, if no  $\beta'$ - $\beta$  transition occurred and the noise level was acceptable a scan rate of 1.25 °C/min was used.

The TAGs were obtained from Dr. A. Fröhling of the section Organic Chemistry of Unilever Research Vlaardingen. They were pure on TLC. To remove oxidation products and partial glycerides the unsaturated TAGs were treated over a silica column. The TAGs were as extra purification recrystallized from hexane. To prevent oxidation during

measurements and storage 0.01 % of BHA was added as anti-oxidant. The GLC and HPLC analysis results of the TAGs are given in Appendix 3.

#### determination of interaction parameters

The interaction parameters were determined from the measured curves by adapting the parameters using a Simplex procedure until the sum of squared errors between the calculated and measured curve are minimal. Heats of fusion and melting points are obtained from the correlations of chapter 4. As the melting points from the correlations, as well as experimental melting points, have an accuracy of about 1°C, we allowed the fitting procedure to vary the melting point maximally  $\pm 1^\circ\text{C}$  around the value from the correlation. Both calculated as well as measured curves are normalized such, that the area under the curves from 25 °C up to the clear point equals unity. To reduce calculation time the number of data points was reduced to one per 0.4 °C. One iteration required about 40-60 s on a Compaq 386/25 PC under MS-DOS.

## 7.5 RESULTS

### 7.5.1 PSP and MPM with ESE and SEE.

The measurements that were carried out and the results of the fitting procedure are given in table 7.8 and figures 7.21 and 7.22

The fit to the measured curves is most satisfactory. The minor overshoot of the calculated curves at the top of sharp peaks must be ascribed to the inertness of the measuring technique, due to factors like thermal lag and the sampling time of the A/D converter in the DSC-2.

Only the 2-suffix Margules parameters are given, as no improvement of fit could be obtained by application of the 3-suffix Margules equation. While the interaction parameters for the  $\beta'$ -modification are indeed very accurate, the interaction parameters for the  $\beta$ -modification are only rough estimates. In combination with a  $\beta'$ -stable TAG a solid phase split, leading to a DSC-curve with 2



RESULTS

table 7.8. DSC measurements and 2-suffix Margules parameters for the highest melting binary pair determined from these measurements. (composition in mole fractions, temperatures in °C, time in minutes, unless otherwise indicated : d = days)

modification	PSP	MPM	SEE	ESE	000	scan rate (K/min)	stabilisation time (min)	stabilisation temp. (°C)	A/RT
$\beta'$	0.26		0.25		0.49	2.5	15 - 180	20	$0 \pm 0.2$
$\beta'$		0.28	0.24		0.48	2.5	1 - 15	20	$3.0 \pm 0.2$
$\beta'$	0.26			0.24	0.50	2.5	1 - 180	20 - 25	$0 \pm 0.2$
$\beta'$		0.27		0.23	0.50	2.5	1 - 15	20	$3.0 \pm 0.2$
$\beta$	0.26		0.25		0.49	2.5	14d	20	$\geq 2.5$
$\beta$		0.28	0.24		0.48	2.5	1d - 3d	20	$\geq 2.5$
$\beta$	0.26			0.24	0.50	1.25	5d - 28d	20 - 25	$\geq 2.0$
$\beta$		0.27		0.23	0.50	1.25	60 - 7d	20	$2 \pm 1$

sharp peaks, will always occur. Only the position of the peak at the lower temperature end of the curve is indicative for the magnitude of  $\beta$ -interaction parameter, while its shape does not change.

The behaviour of ESE and SEE is exactly the same, which is in correspondence to the close similarity of elaidic and stearic acid. Both mix ideally with PSP in the  $\beta'$ -modification, but show a solid solubility less than 15% in the  $\beta$ -modification. With MPM the solubility in the  $\beta'$ -modification is reduced to only 7%, showing the influence of the increased difference in molecular size.

X-ray diffractograms for PSP-SEE-000 are in line with these DSC observations: initially a typical  $\beta'$  diffraction pattern is obtained, with two strong maxima at 3.80 Å and 4.20 Å, which are characteristic for the  $\beta'$ -modification and a single long spacing, indicating the existence of only one crystalline phase. The diffraction pattern differs from that of pure PSP, indicating that a single mixed  $\beta'$ -phase indeed exists, in agreement with the complete miscibility derived from the DSC results. (fig 7.23)

After one day the diffraction pattern has changed. The  $\beta'$ -short spacings are still present, but also a short spacing at 4.55 Å has come up, which is characteristic for the  $\beta$ -modification. The long

PHASE EQUILIBRIA IN FATS  
 - theory and experiments -

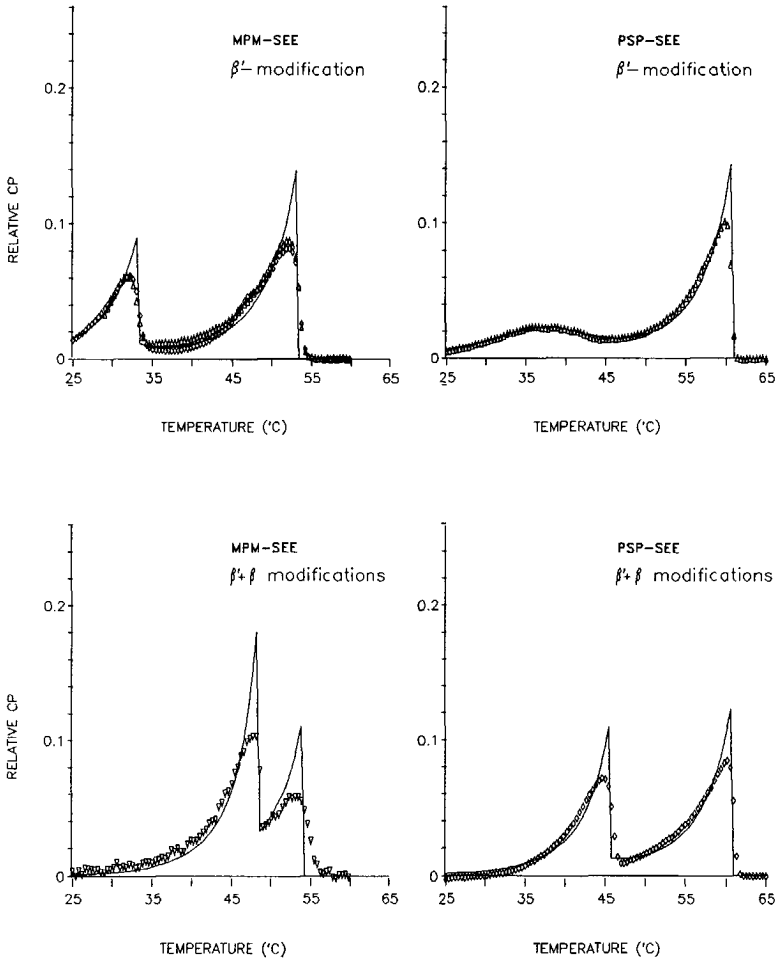


fig 7.21. Measured (dots) and fitted (lines) DSC-curves of ternary mixtures of  $\pm 25\%$  PSP or MPM% with  $\pm 25\%$  SEE and  $\pm 50\%$  OOO. The modification(s) in which crystallization has taken place is indicated.

DSC-CURVES

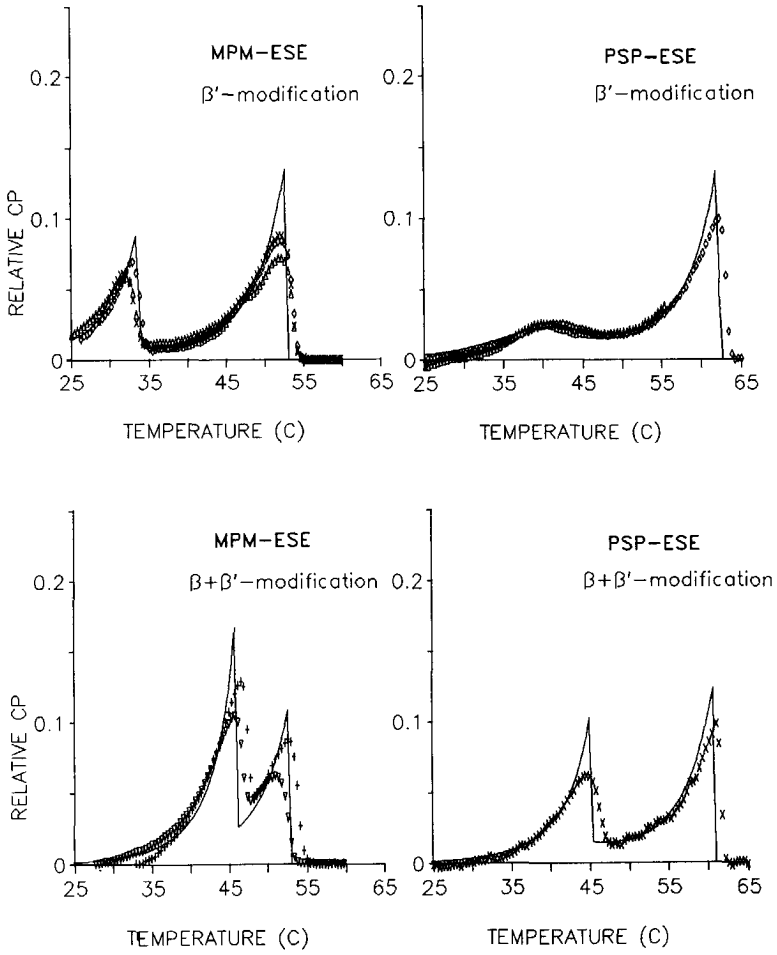


fig 7.22. Measured (dots) and fitted (lines) DSC-curves of ternary mixtures of  $\pm 25\%$  PSP or MPM% with  $\pm 25\%$  ESE and  $\pm 50\%$  OOO. The modification(s) in which crystallization has taken place is indicated.

PHASE EQUILIBRIA IN FATS  
- theory and experiments -

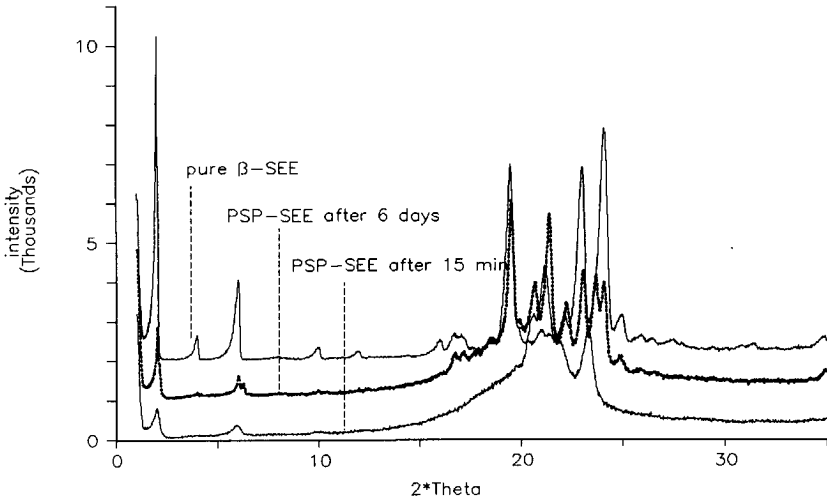


figure 7.23: X-ray diffractograms of the mixture 25 PSP- 25 SEE- 50 000, after 15 minutes and 6 days of stabilisation at 20°C. The diffractogram of pure  $\beta$ -SEE is also given.

spacing has doubled, indicating the presence of a second crystalline phase. The DSC-results are confirmed again: after long stabilisation a  $\beta$ -phase coexists with a  $\beta'$ -phase. The positions of the extra  $\beta$ -diffraction peaks correspond closely to those of pure SEE, in agreement with the prediction of a nearly pure  $\beta$ -SEE phase, which can be derived from the DSC curve.

#### 7.5.2 PSP and MPM with EPE and PEE.

The measurements that were carried out and the results of the fitting procedure are given in table 7.9 and figures 7.24 and 7.25.

Naturally palmitic and elaidic acid do not show the similarity in behaviour that elaidic and stearic acid do. Consequently PEE and EPE can be expected to show differences in mixing behaviour. This is indeed observed: while PEE shows a complete miscibility with both PSP and MPM in the  $\beta'$ -modification, EPE shows only limited solubility.

RESULTS

table 7.9. DSC measurements and 2-suffix Margules parameters for the highest melting binary pair determined from these measurements. (composition in mole fractions, temperatures in °C, time in minutes, unless otherwise indicated : d = days)

modification	PSP	MPM	PEE	EPE	OOO	scan rate (K/min)	stabilisation time (min)	stabilisation temp. (°C)	A/RT
β'	0.26		0.25		0.49	0.62	14d	15	0 ± 0.2
β'		0.28	0.24		0.48	2.5	1 - 5	5 - 15	1.8 ± 0.5
β'	0.26			0.25	0.49	2.5	7d	15	2.0 ± 0.5
β'		0.27		0.25	0.48	1.25	3d	20	2.3 ± 0.5
β	0.26		0.25		0.49	0.62	30d	15	no β
β		0.28	0.24		0.48	2.5	15 - 10d	15	≥ 2.5
β	0.26			0.25	0.49	2.5	7d	15	≥ 2.5
β		0.27		0.25	0.48	1.25	3d	20	≥ 3

PEE shows a very interesting behaviour. The system PSP/PEE/OOO has remained in the β'-modification, even after a month of stabilisation. This is confirmed by the X-ray results for this system. Looking at the results obtained for SEE, ESE and EPE, a realistic estimate for the PSP-PEE β-interaction parameter is A/RT = 3. In that case, calculations show that this system is β'-stable at all temperatures, although PEE itself is β-stable: the extra stability of the β-modification is not enough to compensate for the large excess Gibbs energy of a solid phase in that modification. A nearly pure β-PEE phase will only crystallize when the ratio PSP/PEE in the system drops below 0.5. But even for such mixtures the driving force to β is very low, making quick recrystallization unlikely. After one week of stabilisation of such a mixture only a minor broadening of the first β'-melting peak at the position where a β melting peak would occur, was observed.

The system MPM/PEE/OOO does crystallize into the β-modification. Contrary to PSP and PEE, MPM and PEE show non-ideal mixing in the β'-modification, and therefore the difference in excess Gibbs energy between the two modifications is not large enough to counterbalance the stability difference. The same holds for the PSP/EPE/OOO system that was studied.

PHASE EQUILIBRIA IN FATS  
 - theory and experiments -

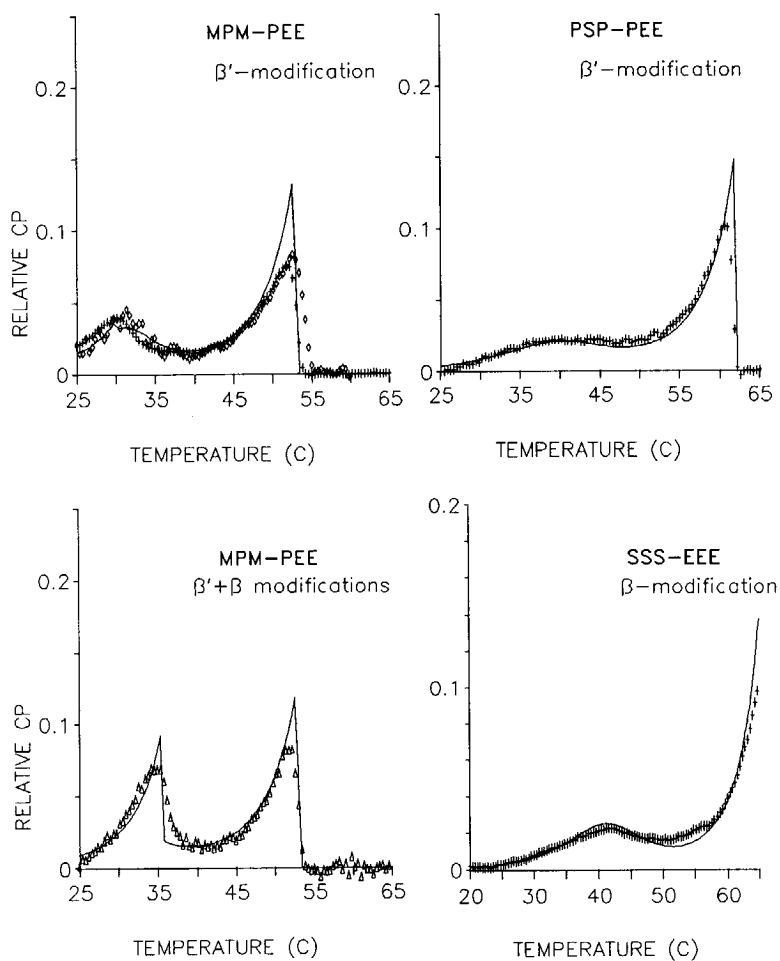


fig 7.24. Measured (dots) and fitted (lines) DSC-curves of ternary mixtures of  $\pm 25\%$  PSP or MPM% with  $\pm 25\%$  PEE and  $\pm 50\%$  OOO and of a mixture of 25% SSS, 25% EEE and 50% OOO. The modification(s) in which crystallization has taken place is indicated.

DSC-CURVES

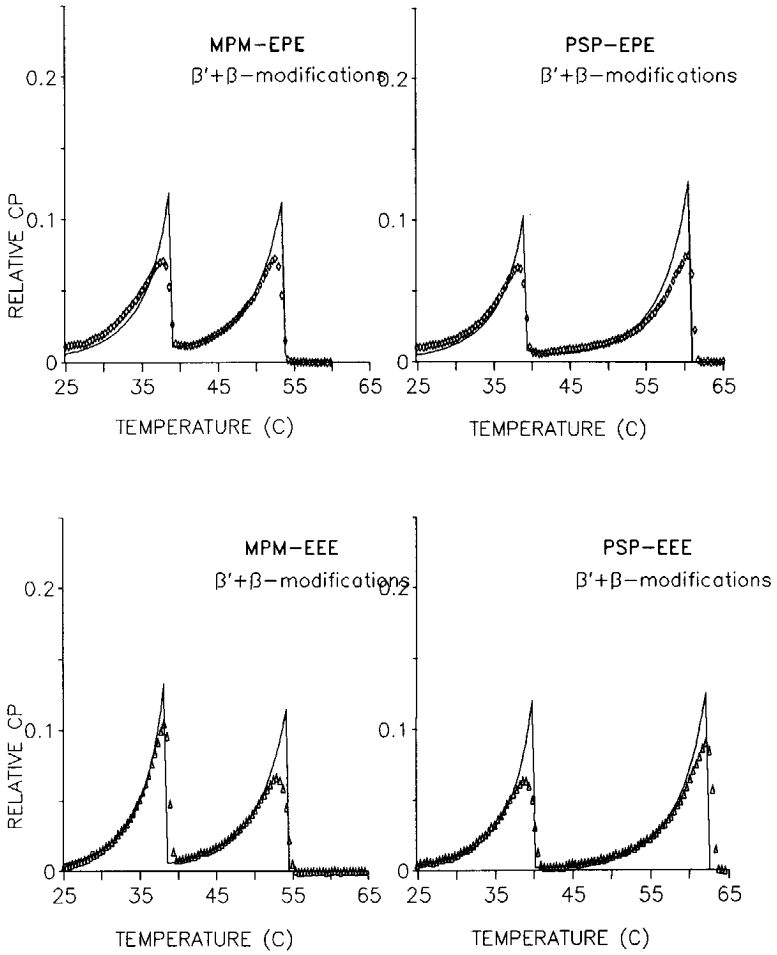


fig 7.25. Measured (dots) and fitted (lines) DSC-curves of ternary mixtures of  $\pm 25\%$  PSP or MPM% with  $\pm 25\%$  EPE or EEE and  $\pm 50\%$  OOO. The modification(s) in which crystallization has taken place is indicated.

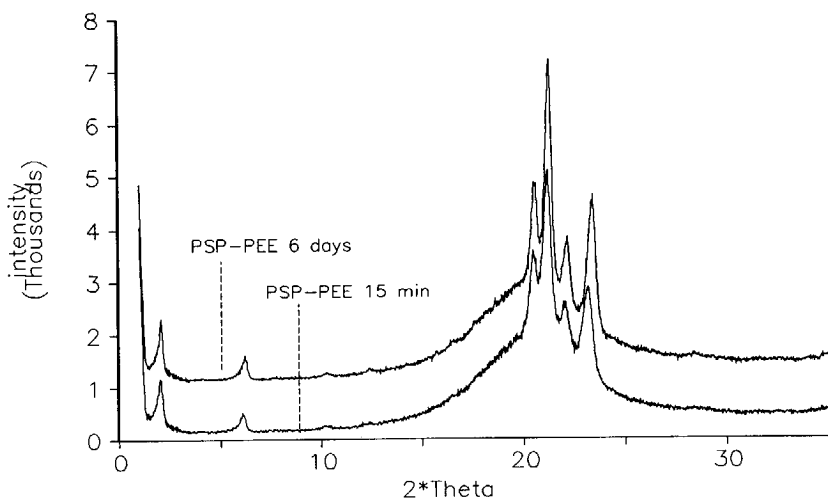


figure 7.26: X-ray diffractograms of the mixture 25 PSP- 25 PEE- 50 000, after 15 minutes and 6 days of stabilisation at 20°C.

Even without stabilisation the DSC-curves of the systems with EPE showed exothermic peaks of the  $\beta'$ - $\beta$ -transition. A complete  $\beta'$ -melting curve can therefore not be obtained. The estimate for the  $\beta'$ -interaction parameter is based on the shape and height of the plateau just after the first melting peak in the curve of a completely stabilised sample.

### 7.5.3 PSP and MPM with EEE.

The measurements that were carried out and the results of the fitting procedure are given in table 7.10 and fig 7.24 and 7.25.

These systems all recrystallized extremely quickly into the  $\beta$ -modification. Even without stabilisation, the melting curves of the  $\beta'$ -modification were disturbed by exothermic peaks of the  $\beta'$ - $\beta$ -transition. Therefore the values of the  $\beta'$ -interaction parameters had to be estimated from the height of the plateau just after the first melting peak. The plateau height is nearly zero.



RESULTS

table 7.10. DSC measurements and 2-suffix Margules parameters for the highest melting binary pair determined from these measurements. (composition in mole fractions, temperatures in °C, time in minutes, unless otherwise indicated : d = days)

modi- fication	PSP	MPM	EEE	OOO	scan rate (K/min)	stabil- isation time (min)	stabil- isation temp. (°C)	A/RT
$\beta'$	0.26		0.25	0.49	2.5	1 - 7d	15	$0 \pm 1$
$\beta'$		0.27	0.25	0.48	2.5	30 - 70	15 - 20	$\geq 2 ?$
$\beta$	0.26		0.25	0.49	2.5	1- 7d	20	$\geq 2.0$
$\beta$		0.27	0.25	0.48	2.5	30 - 70	15 - 20	$\geq 2.0$

For a reliable determination of the  $\beta'$ -interaction parameter the  $\beta'$ -melting point of EEE is required. We were not able to determine a  $\beta'$ -melting point of our EEE sample, only an  $\alpha$  and a  $\beta$ -melting point were found. This is in line with the findings of Hagemann (34) and earlier authors (33), who also could not detect a  $\beta'$ -melting point of EEE. A very old report of Malkin (35) gives 37°C for the  $\beta'$ -melting point. This value does not compare well with the data of Hagemann (34) for a number of glycerol tri-trans-octadecenoates. Hagemann found a steady decrease in the  $\beta'$ -melting point from 43°C for trans-17-octadecenoic acid to 28°C for trans-11-octadecenoic acid. Extrapolating the data of Hagemann to trans-9-octadecenoic acid (E) results in a  $\beta'$ -melting point of 27-28°C for EEE.

If 37°C is used as  $\beta'$ -melting point of EEE, than the 2 suffix Margules interaction parameter for PSP-EEE in the  $\beta'$ -modification must be greater than 2.5 in order to explain a zero plateau height. If a melting point of 27°C is used,  $A/RT(\text{PSP-EEE}) = 0 \pm 1$ .

From binary phase diagrams we concluded that SSS mixes nearly ideally with SES, SSE and SEE in the  $\beta$ -modification (section 7.3). In addition to the DSC-curve of PSP-EEE -OOO we also determined the curve of SSS-EEE-OOO in the  $\beta$ -modification (fig 7.24). The result is not very surprising: SSS and EEE also mix ideally in the  $\beta$ -modification. Clearly the elaidic and stearic acid chains behave more or less equivalent, which is confirmed by our findings for PSP-SEE and PSP-ESE for both  $\beta'$ - and  $\beta$ -modification.

If S and E behave equivalent, then the interaction parameter for the binary PSP-EEE should be equal to those of PSP-SEE and PSP-ESE. As the latter parameters both equal zero, we expect that  $A/RT(\text{PSP-EEE})$  will also be zero. This implies that the  $\beta'$ -melting point of EEE must be  $27 \pm 2^\circ\text{C}$ , and that Malkins' value for the  $\beta'$ -melting point of EEE,  $37^\circ\text{C}$ , is not right.

#### 7.5.4 PSP and MPM with cis-unsaturated TAGs

The measurements of mixtures of PSP and MPM with SSO, PPO, SOS and POP resulted in more complicated curves than those of the previous mixtures. Contrary to the previous TAGs, which all crystallized into the  $\beta'$ -2 and  $\beta$ -2 modification, most cis-unsaturated TAGs crystallize into the  $\beta'$  and  $\beta$ -3 modification. Only POP crystallizes into the  $\beta'$ -2 form (table 7.11)

table 7.11. Polymorphic forms of the cis unsaturated TAGs (32,33)

PSP	$\beta'$ -2		MPM	$\beta'$ -2	
SOS	$\beta'$ -3	$\beta$ -3	PPO	$\beta'$ -3	
SSO	$\beta'$ -3		POP	$\beta'$ -2	$\beta$ -3

The formation of a continuous solid solution between a component that crystallizes into the  $\beta'$ -2 form and a component that crystallizes into the  $\beta'$ -3 form seems on structural grounds impossible: an intermediate  $\beta'$ -2/ $\beta'$ -3 structure is not feasible. In thermodynamic calculations the two  $\beta'$ -forms must therefore be treated as separate modifications, just like the  $\beta'$  and  $\beta$ -modification.

This has two implications:

1. The DSC curve of the  $\beta'$ -modification of a mixture of a  $\beta'$ -2 and a  $\beta'$ -3 forming TAG must always contain 2 sharp peaks, because demixing in the solid phase will occur even when the components mix ideally both in the  $\beta'$ -2 as in the  $\beta'$ -3 phase.
2. For calculation of the interaction parameters the heat of fusion and the melting point of a hypothetical  $\beta'$ -2 form of the  $\beta'$ -3 forming TAG and of the hypothetical  $\beta'$ -3 form of the  $\beta'$ -2 forming TAG must be known. These hypothetical pure component properties

RESULTS

cannot be measured. They must be estimated, which will cause a considerable uncertainty in the value of the interaction parameters.

Quite surprisingly, we obtained after short stabilisation of the MPM-SSO-000 and MPM-PPO-000 mixtures DSC curves in which the first melting peak is a broad hump, rather than the sharp peak that was expected for these  $\beta'$ -2 /  $\beta'$ -3 mixtures. After prolonged stabilisation a clear polymorphic transition was observed, and finally the expected DSC curves with two sharp peaks were obtained. The final melting peak remained in place during this transition. The broad hump indicates that initially crystallization must have taken place into a single, mixed solid phase, which has to be in the  $\beta'$ -2 modification. The final, stable, separate PPO- or SSO-rich  $\beta'$ -3 phase is only formed later. This behaviour confirms the assumption that the -2 and -3 forms must be treated as separate, independent modifications, that needn't always occur in pure components. The order of the polymorphic transitions that is observed is therefore:

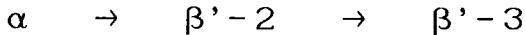


table 7.12. DSC measurements and 2-suffix Margules parameters for the highest melting binary pair determined from these measurements. (composition in mole fractions, temperatures in °C, time in minutes, unless otherwise indicated : d = days)

modi- fication	PSP	MPM	SOS	SSO	000	scan rate (K/min)	stabil- isation time (min)	stabil- isation temp. (°C)	A/RT
$\beta'$ -2	0.32		0.19		0.49	2.5	15	5	0 ± 0.3
$\beta'$ -2		0.29	0.23		0.48	2.5	1	5	2 ± 0.7
$\beta'$ -2	0.26			0.24	0.50	2.5	1 - 7d	10	no fit
$\beta'$ -2		0.28		0.24	0.48	1.25	1 - 60	15	2 ± 0.2
$\beta'$ -3	0.32		0.19		0.49	2.5	15	5	0 ± 0.5
$\beta'$ -3		0.29	0.23		0.48	1.25	8d	10	1.7 ± 0.7
$\beta'$ -3		0.28		0.24	0.48	1.25	3d	15	2 ± 0.5
$\beta$	0.32		0.19		0.49	1.25	1d	28	1.5 ± 0.5
$\beta$		0.29	0.23		0.48	1.25	8d	10	1.0 ± 0.5

PHASE EQUILIBRIA IN FATS  
 - theory and experiments -

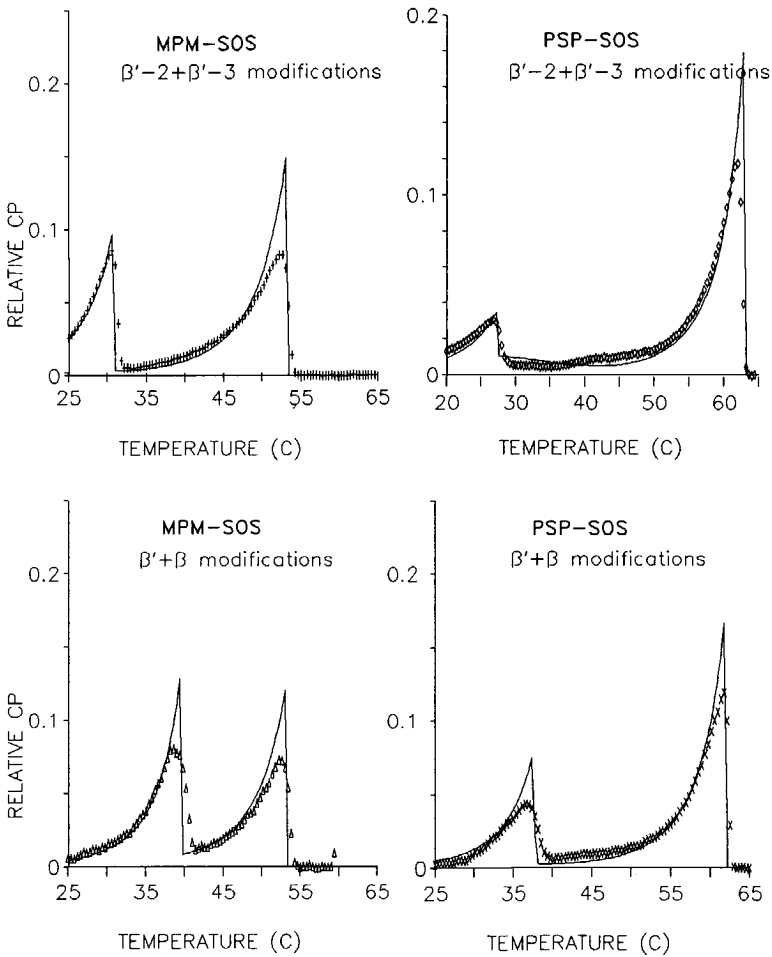


fig 7.27. Measured (dots) and fitted (lines) DSC-curves of ternary mixtures of  $\pm 25\%$  PSP or MPM% with  $\pm 25\%$  SOS and  $\pm 50\%$  OOO. The modification(s) in which crystallization has taken place is indicated.

DSC-CURVES

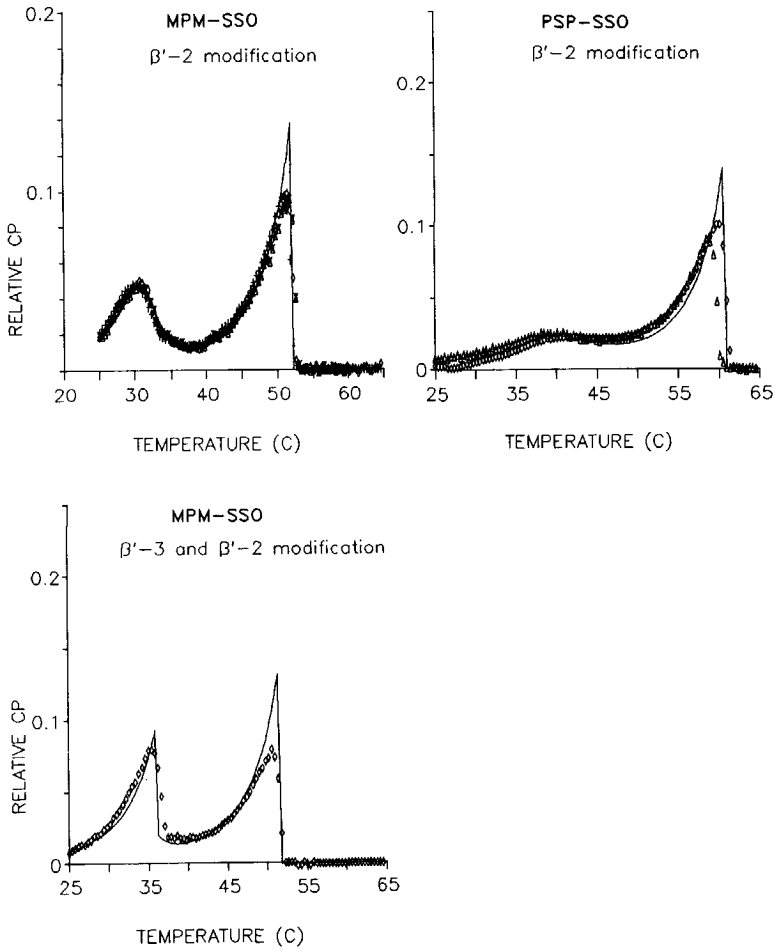


fig 7.28. Measured (dots) and fitted (lines) DSC-curves of ternary mixtures of  $\pm 25\%$  PSP or MPM% with  $\pm 25\%$  SSO and  $\pm 50\%$  OOO. The modification(s) in which crystallization has taken place is indicated.

PHASE EQUILIBRIA IN FATS  
- theory and experiments -

From the work of de Jong (30) it can be concluded that the melting point of a hypothetical  $\beta$ -3 modification of PSP and MPM is about 3 degrees less than the melting point of a hypothetical  $\beta$ -2 form of these TAGS. In analogy to the  $\beta$  modification, we assume that the  $\beta'$ -3 melting points of MPM and PSP also lie 3°C below their experimental  $\beta'$ -2 melting points. Based on the enthalpy of fusion data of chapter 4 we conclude that the heat of fusion of the  $\beta'$ -3 form is about 90% of that of the  $\beta'$ -2 modification.

Similarly it is assumed that the heat of fusion of the hypothetical  $\beta'$ -2 form of SSO, PPO and SOS is 90% of that of the  $\beta'$ -3 modification. If the 2-suffix Margules equation is used, the melting points of the  $\beta'$ -2 modification of these TAGs can be calculated from the  $\beta'$ -2 DSC curves of the mixtures with MPM:

$$\text{SSO} : T_f(\beta'-2) = 39 \pm 0.5 \text{ } ^\circ\text{C} \quad (T_f(\beta'-3) = 42^\circ\text{C} )$$

$$\text{SOS} : T_f(\beta'-2) = 29 \pm 2 \text{ } ^\circ\text{C} \quad (T_f(\beta'-3) = 36.5^\circ\text{C} )$$

$$\text{PPO} : T_f(\beta'-2) = 31 \pm 0.5 \text{ } ^\circ\text{C} \quad (T_f(\beta'-3) = 34^\circ\text{C} )$$

The measurements that were carried out and the results of the fitting procedure are given in table 7.12 and 7.13 and figures 7.27-7.30

*table 7.13. DSC measurements and 2-suffix Margules parameters for the highest melting binary pair determined from these measurements. (composition in mole fractions, temperatures in °C, time in minutes, unless otherwise indicated : d = days)*

modification	PSP	MPM	POP	PPO	OOO	scan rate (K/min)	stabilisation time (min)	stabilisation temp. (°C)	A/RT
$\beta'$ -2	0.26		0.26		0.48	1.25	15-7d	10	no fit
$\beta'$ -2	-	0.29	0.23		0.48	2.5	1	5	$0.8 \pm 0.2$
$\beta'$ -2	0.25			0.28	0.47	1.25	7d	15	-1.5 ?
$\beta'$ -2		0.28		0.25	0.47	1.25-2.5	1 - 60	10	$0.8 \pm 0.4$
$\beta'$ -3	0.25			0.28	0.47	1.25	26d	5	-
$\beta'$ -3		0.28		0.25	0.47	1.25-2.5	7d	10	$-0.2 \pm 0.4$
$\beta$	0.26		0.26		0.48	-	-	15	no $\beta$
$\beta$		0.29	0.23		0.48	1.25	7d	5	$3.5 \pm 1$

PHASE EQUILIBRIA IN FATS  
 - theory and experiments -

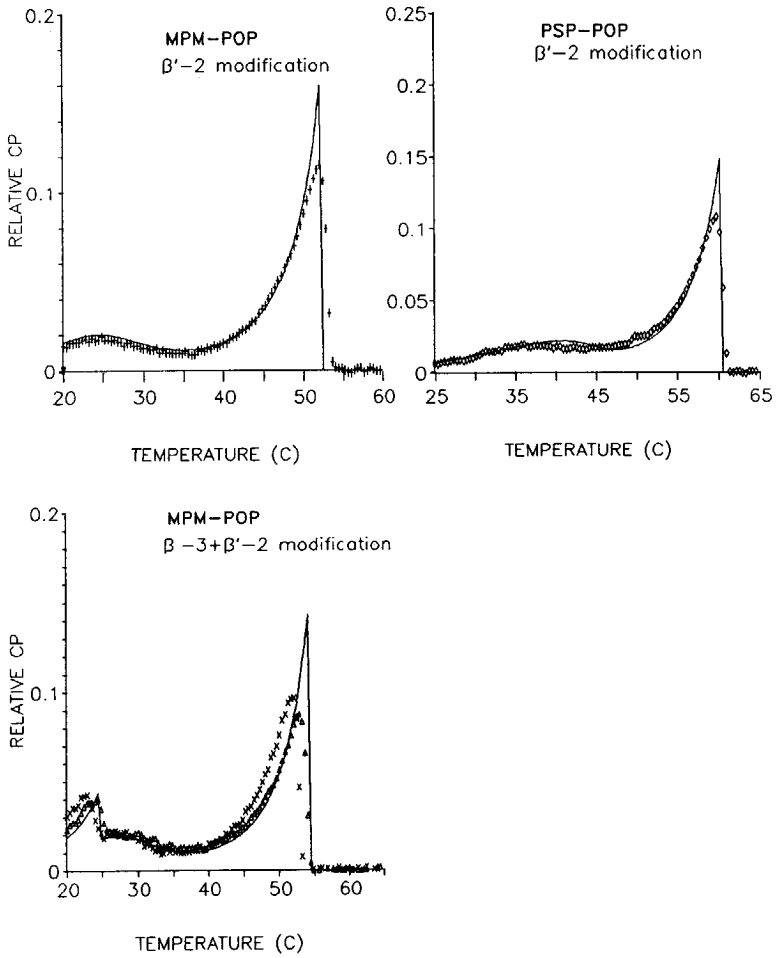


fig 7.29. Measured (dots) and fitted (lines) DSC-curves of ternary mixtures of  $\pm 25\%$  PSP or MPM% with  $\pm 25\%$  POP and  $\pm 50\%$  OOO. The modification(s) in which crystallization has taken place is indicated.

DSC-CURVES

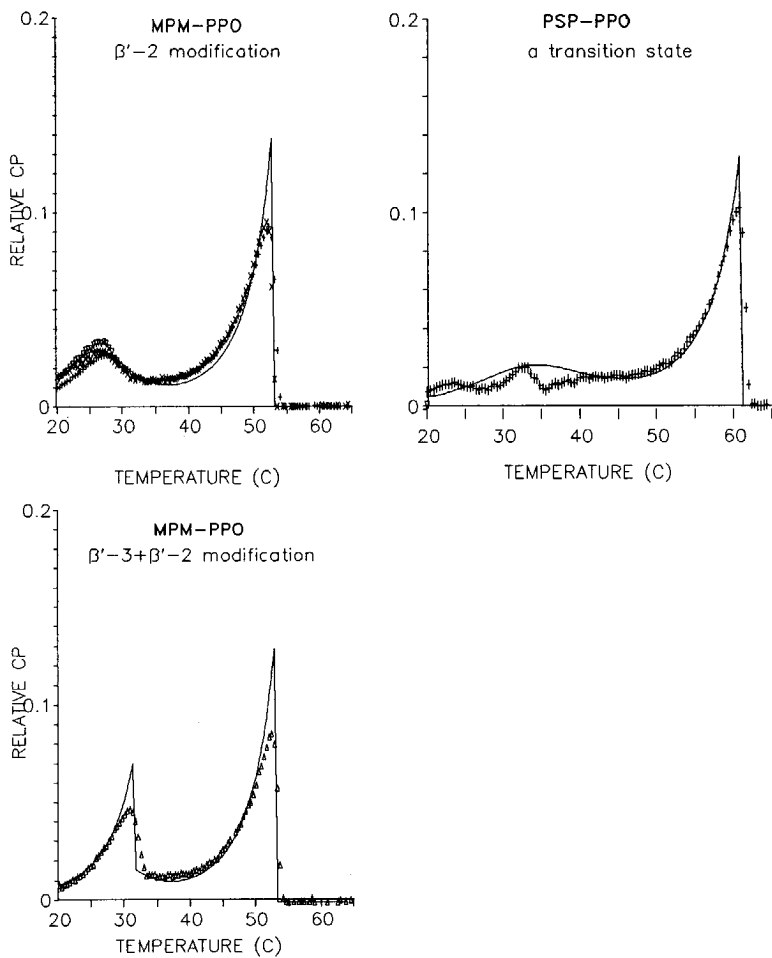


fig 7.30. Measured (dots) and fitted (lines) DSC-curves of ternary mixtures of  $\pm 25\%$  PSP or MPM% with  $\pm 25\%$  PPO and  $\pm 50\%$  OOO. The modification(s) in which crystallization has taken place is indicated.



## RESULTS

The broad first melting peaks in the  $\beta'$ -2 DSC curves of PSP-POP and PSP-SSO have maxima, that lie several degrees above the temperature where these maxima should be situated when  $A/RT = 0$ . These DSC curves could only be fitted with the 3-suffix Margules equation, using negative values for  $A_{PSP\_POP}$  and  $A_{PSP\_SSO}$  (table 7.14). Apparently the  $\beta'$ -2 form of POP and SSO is enormously stabilised by the presence of PSP, their almost exact saturated counterpart. Calculations show that this stabilizing effect makes the mixture  $\beta'$ -2 stable. Indeed no transition to the  $\beta$ -modification (POP) or the  $\beta'$ -3 modification (SSO) was observed, even after long stabilisation.

The stabilising effect seems also present in the curves of PSP-PPO and PSP-SOS. In these case an exact determination of the  $\beta'$ -2 state was not possible: a  $\beta'$ -2/ $\beta'$ -3 transition always disturbed the DSC curve. The shape of the PSP-PPO-000 melting curves above 35°C suggest  $A/RT = -1.5$ .

table 7.14: 2 and 3 -suffix Margules parameters for some of the systems of table 7.12 and 7.13.

system	modification	$A/RT$	$A_{12}/RT$	$A_{21}/RT$
PSP-POP	$\beta'$ -2	-	$-3 \pm 1$	$0 \pm 0.5$
PSP-SSO	$\beta'$ -2	-	$-2 \pm 1$	$0 \pm 0.5$
PSP-SOS	$\beta$	$1.5 \pm 0.5$	$1.5 \pm 0.5$	$3 \pm 1.5$
MPM-SOS	$\beta$	$1.0 \pm 0.5$	$0.5 \pm 1$	$3 \pm 2$

The 2-suffix parameters for the  $\beta$ -modification of the mixtures with SOS are very low, compared to those for the  $\beta'$ -modification. It is possible to use 3-suffix Margules  $\beta$ -interaction parameters that are more in line with the results for the  $\beta'$ -modification for the description of the curve (table 7.14). However, they have no statistical significance.

## 7.6 DISCUSSION

### 7.6.1 The use of DSC-melting curves

The results show that it is possible to use DSC melting curves of ternary mixtures to determine binary interaction parameters. This method is much quicker and more reliable than the determination of a phase diagram. It allows the study of phase behaviour in unstable modifications. Thus we have obtained a new, powerful and versatile method for studying the solid liquid phase behaviour.

#### The 3-suffix Margules equation.

The 3-suffix Margules interaction parameters can be obtained from the combination of peak shape and peak position in the DSC melting curve. This dependency on exact peak position implies that the uncertainty in the melting points of the pure components of about 1°C will translate itself into an error in the 3-suffix Margules parameters of about 0.5. Due to this uncertainty in the parameters, asymmetric behaviour in systems that show only small differences in the two parameters cannot be detected. In those cases the 2-suffix Margules equation performs equally well. In this work TAGs were studied that show considerable differences in stereochemical nature. Yet only in the most extreme case, for TAGs with oleic acid, which crystallize in very different lattices, clear asymmetric behaviour and the need for using the 3-suffix Margules equation was apparent.

### 7.6.2 Binary interaction parameters

#### The $\beta'$ -modification

For the first time reliable information about mixing behaviour in the  $\beta'$ -modification has been obtained. On average solid solubility in the  $\beta'$ -modification is higher than in the  $\beta$ -modification, but contrary to the  $\alpha$ -modification non ideal mixing can occur.

The influence of size differences is clear: none of the unsaturated TAGs mixes very well with the smaller TAG MPM, while often even ideal miscibility is found with PSP, which is about similar in size. The position of the fatty acid chains on the glycerol influences the mixing behaviour with MPM only very slightly, the size difference

## DISCUSSION

dominates. But when the size difference is small, the chain position is of great influence, as can be seen from the data on PSP-PEE vs PSP-EPE, PSP-SSO vs PSP-SOS and PSP-PPO vs PSP-POP. It is not clear why these relatively small differences can have such large effects on mixing behaviour. Simulation of the disturbance of a crystal lattice by insertion of another TAG using molecular mechanics, may help to create understanding. This will be attempted in chapter 8.

### The $\beta$ -modification

Due to the use of  $\beta'$ -stable TAGs as the highest melting component in the systems that were studied by DSC,  $\beta$ -interaction parameters could only be determined very roughly from the position of the first melting peak. That means that the uncertainty in the melting points already has to be taken into account in the 2-suffix Margules parameters, while the determination of statistically significant 3-suffix Margules parameters is impossible.

However, as illustrated for the system SSS and EEE, determination of accurate interaction parameters for the  $\beta$ -modification from DSC-curves is very well possible if a  $\beta$ -stable TAG is used as highest melting component.

In the survey of the binary phase diagrams complete solid miscibility was only found for pairs of TAGs that are very similar in size, like SSS and PSS. Our DSC results are in line with this finding. In chapter 8 we will use the data in an attempt to find a relation between the influence of structural differences of TAGs and the magnitude of the interaction parameters.

### 7.6.3 Kinetics

It is striking how strongly the kinetics of transformation from  $\beta'$  to  $\beta$  depend on the miscibility in the  $\beta'$ -modification: if the components mix very well in the  $\beta'$ -modification, the transformation takes at least several days, while if solid phase immiscibility occurs, it takes only a few seconds to an hour to complete the transformation.

The explanation is twofold:

The combination of poor  $\beta$ -phase miscibility and nearly ideal mixing in the  $\beta'$ -modification reduces the Gibbs energy difference between the two modifications, which is the driving force for recrystallization.

It also leads to a  $\beta'$ -solid phase composition that is completely different from that in the demixed  $\beta$ -modification, which makes the transformation kinetically much more difficult. In the case of poor  $\beta'$ -phase miscibility the solid phase composition is nearly equal to that in the  $\beta$ -modification, so that the barrier for the transformation is much smaller.

### 7.7 TERNARY SOLIDS

Although the DSC melting curves of section 7.6 were measured using ternary mixtures, the composition of the mixture and the temperature range of the experiment were selected such, that only a binary solid phase was present. This enabled the determination of binary interaction parameters in the solid phase.

Crystallized fats are normally multicomponent solid phases. The binary interaction parameters that were determined in this work can only be used for prediction of multicomponent phase behaviour if ternary, quaternary and higher interaction terms can be neglected. A way of checking this is comparing measured ternary phase diagrams with phase diagrams predicted from binary interaction parameters. In literature there are only a few ternary phase diagrams available: that of the Cocoa Butter (CB) TAGs SOS/POS/POP from Smith (15) and those of the palm oil TAGs PPP/POP/POO and PPP/PPO/POO from Gibon (16). The data from Gibon are not very reliable, due to the very poor stabilisation procedure and the high DSC-scan rates that were used (section 7.2). Calculated and measured ternary clear point curves for the three systems are given in figures 7.31 and 7.32. For SOS-POS-POP also a diagram is given with the isotherms for 25% solids.

As can be seen the agreement between theory and experiment is very good for the SOS/POS/POP ternary, taking into account the error in the measurements of 1°C. Also the temperatures at which a mixture contains 25% solids are predicted within 1°C.

TERNARY SOLIDS

calculated

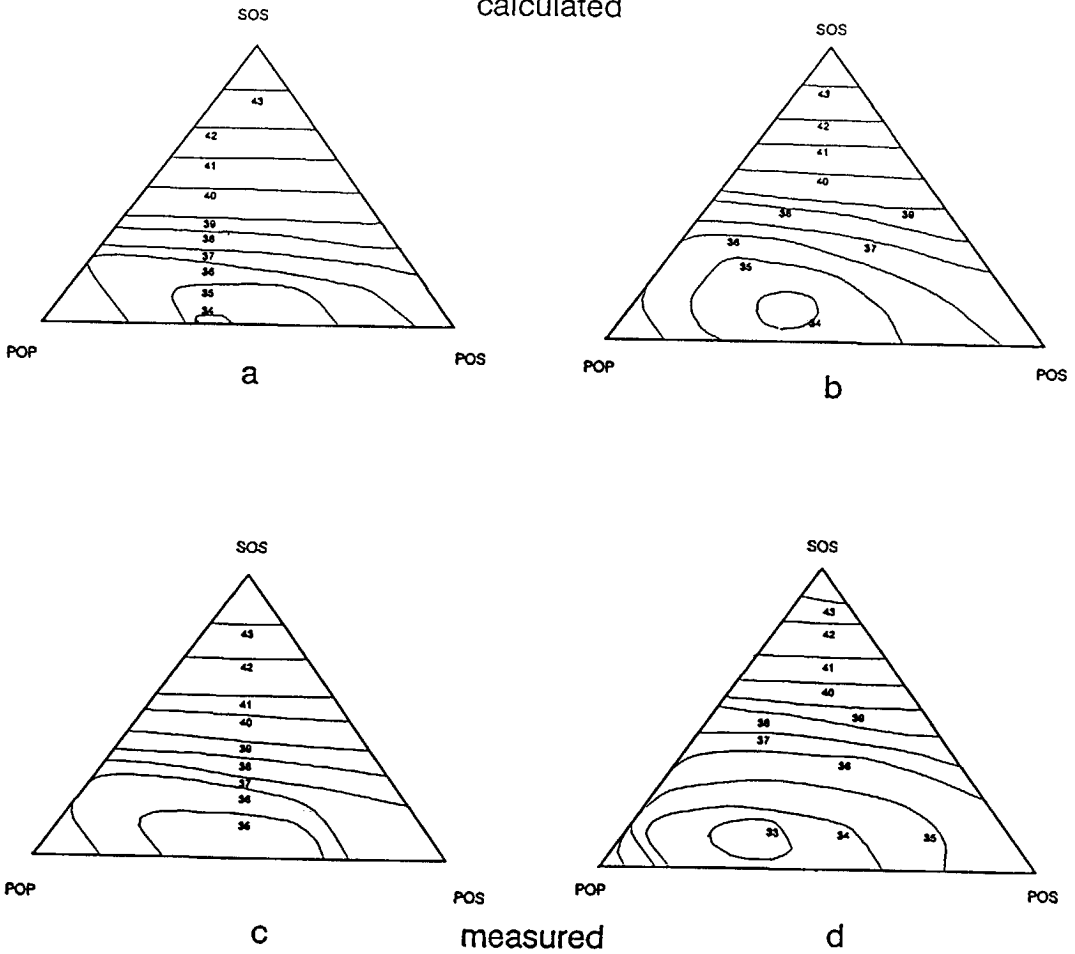
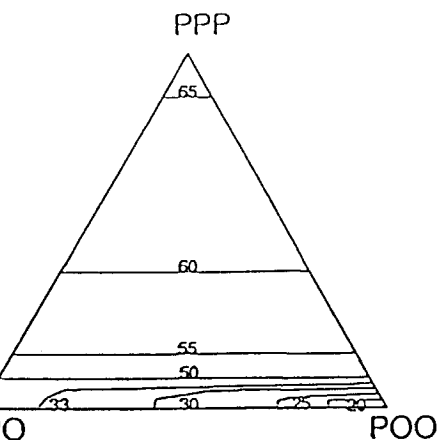


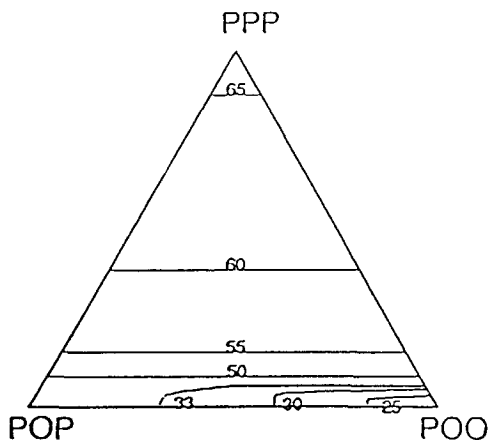
figure 7.31: Calculated and measured ternary isosolids diagrams of SOS-POS-POP. Measured by Smith (15). a and c: Clear point diagrams, b and d: isotherms with 25% solid fat.

The PPP/POP/POO and PPP/PPO/POO ternaries also show good agreement between measurements and calculations. The agreement near the PPP corner at the PPP-POO side of the diagrams is somewhat less good.

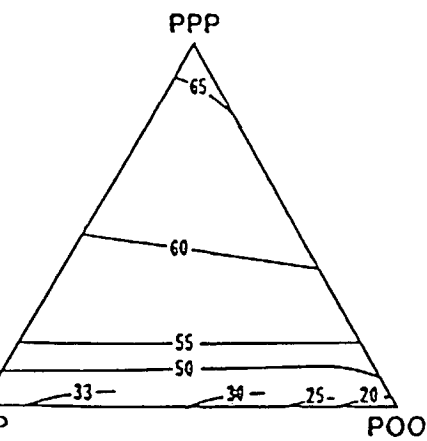
PHASE EQUILIBRIA IN FATS  
 - theory and experiments -



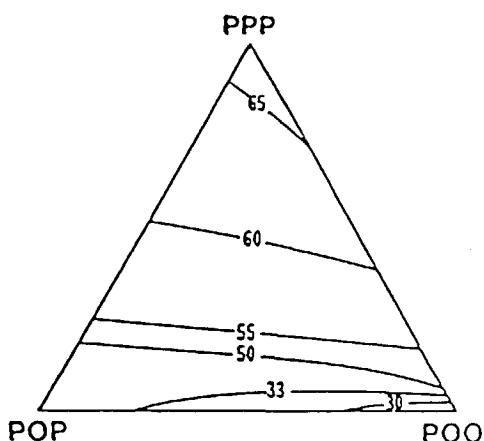
a



c



b



d

figure 7.32: Calculated and experimental clear point diagrams of TAGS from palm oil. a and c: calculated, b and d: measured by Gibon (16).

## CONCLUSION

However, the clear points that are given by Gibon for this PPP/POO binary are probably not correct as they lie well below the eutectic liquidus.

The results suggest that indeed the use of binary interaction parameters is sufficient for the description of multicomponent TAG systems. In our later work good predictions were also obtained using only binary interaction parameters (chapter 9).

The clear point diagram for the CB-TAGs SOS/POS/POP may be used to define the possible compositions of CBEs (Cocoa Butter Equivalents). CBE's must have the same clear point as CB, and so all possible CBE compositions will be restricted to the isotherm through the CB composition. The 25% isosolids diagram demonstrates that even for such difficult systems as SOS-POS-POP solids content can be predicted by application of solid-liquid equilibrium thermodynamics.

### 7.8 CONCLUSION

In the  $\beta$  and  $\beta'$  modification TAGs show limited solid miscibility that can be described with rather simple models for the excess Gibbs energy: the 2 and 3-suffix Margules equation.

84 of the 120 binary phase diagrams of TAGs, that are available in literature are rejected because they are clearly not correct. The solidus lines of most of the remaining 36 phase diagrams show large inconsistencies. The majority of these phase diagrams was measured after 1971. The 36 phase diagrams can be described within experimental error both by the 2- and by the 3-suffix Margules equations.

The excess Gibbs energy models contain binary interaction parameters. The large experimental errors in the binary phase diagrams lead to a very large inaccuracy in the interaction parameters that are determined from these diagrams.

Due to the serious drawbacks in the use and determination of binary phase diagrams, a new method for the study of solid-liquid phase behaviour has been defined. It is possible to obtain quantitative information about mixed crystal formation from a single, complete DSC melting curve of a ternary system, consisting of two crystallizing TAGs and one liquid TAG.

PHASE EQUILIBRIA IN FATS  
- theory and experiments -

The method is much quicker, more reliable and more versatile than the traditional study of phase behaviour of TAGs via binary phase diagrams.

For the first time accurate information was obtained about the degree of mixed crystal formation in the  $\beta'$ -modification. Generally solid phase miscibility is higher in the  $\beta'$ -modification than in the  $\beta$ -modification. Large differences in molecular size reduce solid phase miscibility. Also the position of the fatty acid on the glyceryl-group has a great influence on solid phase miscibility.

Surprisingly the mixing behaviour of TAGs in the solid phase can usually be described with sufficient accuracy by the very simple regular solution model or 2-suffix Margules equation. Only in a few cases the use of the more complex 3-suffix Margules equation was required.

Ternary systems could be described with binary interaction parameters only.

Kinetics of recrystallization showed a clear relation with the calculated thermodynamic driving force and the degree of rearrangement of the solid phase that is required.

LIST OF SYMBOLS

A	interaction coefficient.
a	$A/RT$ .
$c_p$	heat capacity (J/mol,K)
g	molar Gibbs free energy (J/mol)
G	Gibbs free energy (J)
k, K	constants
$K^{AB}$	distribution coefficient
N	number of components
n	number of moles (mol)
P	number of phases
R	Gas constant (J/mol,K)
T	Temperature (K)
$T_f$	normal melting point (K)
x,y	mole fractions



## REFERENCES

z	overall mole fraction
$\gamma$	activity coefficient
$\Delta H_f$	heat of fusion at $T_f$ . (kJ/mol)
$\Phi$	phase fraction
$\mu$	chemical potential (J/mol)

## REFERENCES

1. J.M. Prausnitz Molecular Thermodynamics of Fluid Phase Equilibria. Prentice Hall 1986
2. K.W. Won 4th Int Conf. on Fluid Properties and Phase Equilibria for Chem. Process Design, Helsingør Denmark (May 1986)
3. K.W. Won 5th Int Conf. on Fluid Properties and Phase Equilibria for Chem. Process Design, Banff Canada (May 1989)
4. J.H. Hansen, A. Fredenslund et al, A thermodynamic model for predicting wax formation in crude oils. SEP8716, Danmark Tekniske Højskole (1987).
5. A.I. Kitaigorodskii, Molecular crystals and molecules, Academic press (1973)
6. Y. Haget et al, 2nd Codata symp. on prediction of phase equilibria in multicomponent systems vol I, 170 (Sept 1985).
7. Y. Haget et al, 2nd Codata symp. on prediction of phase equilibria in multicomponent systems vol II, 636 (Sept 1985).
8. J.Fischer, D.Moeller , ibid vol I, 246 (Sept 1985).
9. L. Janelli, ibid, vol II, 631 (Sept 1985).
10. H.R. Null, Phase Equilibria in Process Design 2nd Ed,239, Krieger New York (1980)
11. M. Maroncelli et al., J. Phys Chem 89, 5260 (1985)
12. J.B Rossell, Adv. Lip. Res. 5, 353 (1967)
13. P. de Bruyne et al, Chem Phys Lipids 9, 309 (1972)
14. P.A.M Grootcholten, Unilever Research Vlaardingen, private communication, (1987)
15. K. Smith, Unilever Research Colworth House, private communication (1989)
16. V. Gibon, Thèse, Université de Notre Dame de la paix, Namur (1984)
17. P. de Bruyne, F. Reckweg, P VD 72 3275
18. P. de Bruyne, F. Reckweg, P VD 71 3637.
19. A. DeSmedt, V.Gibon, private communication, (Jan 1990)
20. R.E. Timms, Progr. Lip. Res. 23, 1 (1984)
21. P.A.M Grootcholten, Calculation of solid liquid equilibria in fats LP VD 84 3074

PHASE EQUILIBRIA IN FATS  
- theory and experiments -

22. I.T. Norton et al, *JAOCS* 62, 1237 (1985)
23. Numerical recipes ( )
24. R. Perron, J. Petit, A. Matthieu, *Chem. Phys. Lipids* 6, 58 (1971).
25. M. Ollivon, R.Perron, *Chem. Phys. Lipids* 25, 395 (1979)
26. J. Krautwurst, *Kieler. Milchw. Forsch. Ber.* 22, 255 (1972)
27. P. Barbano, J.W Sherbon, *JAOCS* 55, 478 (1977)
28. N.V. Lovegren, M.S. Gray, R.O Fuege, *JAOCS* 53, 519 (1976)
29. E.S. Lutton, *JAOCS* 32, 49 (1955)
30. S. de Jong, Thesis, Rijksuniversiteit Utrecht. (1980)
31. E.E. Brumbaugh, M.L Johnson, C. Huang, *Chem. Phys of Lipids* 52,69 (1990)
32. K.Sato, *JAOCS* 66, 664 (1989)
33. R. Vazquez Ladron, R. de Castro Ramos, *Grasas y Aceites* 22, 401 (1971)
34. H.W. Hagemann, *JAOCS* 52, 204 (1975)
35. T. Malkin, M.G.R. Carter, *J. Chem. Soc.*, 554 (1947)
36. M. Zief, W.R. Wilcox, *Fractional Solidification*, Marcel Dekker inc (New York) 1967.
37. K.v.Putte, Unilever Research Vlaardingen, private communication (1986)



## CHAPTER 8 PREDICTING INTERACTION PARAMETERS

*Now that it has been shown that the mixing behaviour of TAGs in the  $\alpha$ ,  $\beta'$  and  $\beta$ -modification can be described with rather simple excess Gibbs energy models, there remains only one step to be taken: finding a procedure for predicting the binary interaction parameters for any pair of TAGs. Therefore the relation between geometrical differences and the magnitude of the interaction parameter is studied. Molecular mechanics are used to obtain an impression of the lattice distortions that are brought about by incorporation of guest TAGs in a lattice of a host TAG. Finally a first, empirical, set of rules is given for prediction of the binary interaction parameters.*

### 8.1 ARE INTERACTION PARAMETERS RELATED TO STRUCTURAL DIFFERENCES?

In the conclusion of chapter 2, we mentioned four steps that had to be taken to obtain a description of the liquid-multiple solid phase equilibria in fats. Those four steps were the subject of the preceding chapters. It was concluded that the solid-liquid phase equilibrium in a TAG mixture can be described, provided the binary interaction parameters for all possible pairs of TAGs in the mixture are known. The large number of TAGs in a natural oil makes it impossible to determine the parameters experimentally. Therefore a method must be developed for predicting these binary parameters. Fortunately TAGs are chemically very similar, so the degree of non-ideal mixing will only be determined by sterical effects. In the next sections it will be attempted to find a relation between the binary interaction parameters and structural differences.

#### 8.1.1 Degree of isomorphism

In his work on mixed crystals (1) Kitaigorodskii investigated the solid miscibility of several hundreds of pairs of organic compounds. Based on this investigation he formulated his 'major rule of substitutional solid solubility' of organic compounds:

1. Solid solubility is determined by geometric factors if:

- there is no electron transfer between the two components to be mixed,
- the components to be mixed have no permanent dipole moments and

ARE INTERACTION PARAMETERS  
RELATED TO STRUCTURAL DIFFER-  
ENCES?

- the components to be mixed do not form strong hydrogen bridges.
- 2. If solid solubility is solely determined by geometrical factors, then two components will only mix in the solid state if their 'degree of isomorphism' exceeds 0.85.

The degree of isomorphism  $\epsilon$  is defined as follows: superimpose the molecules of the components so as to maximize the intermolecular overlap. Let the volume of the non-overlapping parts be  $v_{\text{non}}$  and the volume of the overlapping parts  $v_0$ . Then the 'degree of isomorphism' or 'coefficient of geometrical similarity' is given by:

eq. 8.1

$$\epsilon = 1 - \frac{v_{\text{non}}}{v_0}$$

- 3. In addition to this second condition, complete solid state miscibility in any proportion is only possible if the molecular packing in the crystal of the pure components is similar, the crystals have the same symmetry and the atoms occupy the same crystallographic positions.

Generally, Kitaigorodskii's rule gives a correct prediction of the occurrence of fully eutectic behaviour and the presence of a miscibility gap. However, the reverse is not true: sometimes a miscibility gap is found, even though Kitaigorodskii's rule has predicted a good solid state miscibility. The reason for this is that when a guest molecule is inserted in a host lattice, then, depending on the nature of the guest molecule, its protruding part may occupy a lattice site in an area where packing is very dense. Obviously, solid solubility will be considerably less than in the case of a guest molecule of the same size that protrudes into a loosely packed area. Therefore, generally, Kitaigorodskii's rule can only be used for qualitative statements on solid phase miscibility.

According to Kitaigorodskii quantitative predictions of solid solubility can be obtained by calculating the lattice distortion:

- 1. An impurity is placed in an undistorted lattice of the pure component.

2. The difference in interaction energy of the impurity with the lattice and of the host with the lattice is calculated.

The simplest approach is to leave the host lattice completely undisturbed and calculate the conformation of the impurity that gives minimal interaction energy.

A more sophisticated approach is to allow also some conformational changes in the host lattice near the impurity ('crystal elasticity'). Unfortunately, this increases computing time enormously.

The lattice distortion obtained in this way can be used to calculate the excess Gibbs energy and hence the maximum solid solubility. The results are reasonable estimates of the maximum solid solubility. Surprisingly, Kitaigorodskii only calculates the maximal solid solubility and does not use this information to calculate a complete binary phase diagram. Most of these complex computer calculations were carried out for relatively simple atomic crystals. Only one example of molecular crystals is mentioned (diphenyl-dipyridyl).

In mixtures of TAGs, the lattice distortion always occurs on the same lattice sites, the methyl-end-plane region, and is always caused by the same functional group:  $\text{CH}_2\text{-CH}_3$ . Because of this, it may very well be that the degree of isomorphism correlates much better with the solid solubility of TAGs than with that of an arbitrary pair of organic substances.

The condition for complete solid state miscibility of Kitaigorodskii's rule implies that complete solid solubility in the equilibrium state cannot occur when two TAGs differ in their most stable polymorphic form, like PSP and SSS. This was already implicitly assumed in all previous calculations by treating the polymorphic forms as different states of the substance, equivalent to the liquid and gas state. However, this condition also implies that complete miscibility cannot occur in mixtures of two TAGs that crystallize in different submodifications, as is the case in a mixture of a  $\beta$ -3 forming TAG and a  $\beta$ -2 forming TAG.

In the next sections we will investigate to what extent the simple parameter  $\epsilon$  correlates with the interaction parameters of TAGs,

ARE INTERACTION PARAMETERS  
RELATED TO STRUCTURAL DIFFER-  
ENCES?

whether it is possible to calculate the lattice distortion by impurities in TAG crystals and whether this lattice distortion can be used for prediction of interaction coefficients.

8.1.2 TAGs and the degree of isomorphism  $\epsilon$

There are two major lattice distortions that occur in TAG mixtures: those caused by differences in chain length and those caused by cis-unsaturated double bonds. We assume that the distortion in the lattice of a saturated TAG that is caused by a trans-double bond is negligible, in line with the nearly ideal miscibility that was found for SSS, SES, SSE, SEE and EEE. The two major distortions will be considered separately.

The  $\beta'$ -modification

In table 8.1 the binary interaction parameters for the  $\beta'$ -modification of saturated and trans-unsaturated TAGs are listed together with the degree of isomorphism. As a matter of convenience we used for  $v_{\text{non}}$  the sum of the absolute differences in carbon number of each of three chains and for  $v_0$  the sum of the carbon numbers of the smallest chain on each glyceryl position.

The correlation between the degree of isomorphism  $\epsilon$  and the binary interaction parameter is striking. In agreement with the results of Kitaigorodskii, we find that the limit of complete miscibility, corresponding to  $A/RT = 2$ , is reached at  $\epsilon = 0.85$ . Moreover ideal miscibility is found if  $\epsilon \geq 0.92$ . The degree of isomorphism explains the large difference in miscibility with PSP that has been found for PEE and EPE in chapter 7. Although the number of data is too small for a decisive statement, it seems possible to use  $\epsilon$  for predicting the binary interaction parameters of pairs of these TAGs.

The correlation for cis-unsaturated TAGs will be less simple, as the cis-double bond disturbs the regular zigzag (trans configuration) of the saturated chains in the crystal lattice. From the cis-unsaturated TAGs that were studied in chapter 7, only POP crystallizes in the  $\beta'$ -2 modification, while SOS, SSO and PPO are reported to crystallize in the  $\beta'$ -3 modification (2,3,4). In chapter 7 we have

PHASE EQUILIBRIA IN FATS  
- theory and experiments -

table 8.1 Two suffix Margules parameters for the  $\beta'$ -modification and the degree of isomorphism of saturated and trans-unsaturated TAGs. (from chapter 7)

binary pair	A/RT	$\epsilon$
PSP-PEE	$0 \pm 0.2$	0.96
PSP-SEE	$0 \pm 0.2$	0.92
PSP-ESE	$0 \pm 0.2$	0.92
PSP-EEE	$0 \pm 2$	0.92
PSP-EPE	$2 \pm 0.5$	0.88
MPM-PEE	$1.8 \pm 0.5$	0.82
MPM-EPE	$2.3 \pm 0.5$	0.82
MPM-SEE	$3 \pm 0.2$	0.77
MPM-ESE	$3 \pm 0.2$	0.77
MPM-EEE	$3 \pm 2$	0.77

found that SSO and PPO initially seem to crystallize in a  $\beta'$ -2 form that does not exist in pure PPO and SSO. The values of the two or three suffix Margules equation interaction parameters for the  $\beta'$ -2 and  $\beta'$ -3 forms are listed in table 8.2 together with  $\epsilon$ . The extra contribution of a cis-double bond to  $\epsilon$  is not incorporated in the number, but indicated by - (minus).

Here again, the limited amount of data for both  $\beta'$ -forms indicate that the degree of isomorphism is related to the magnitude of the binary interaction parameters. Surprisingly the miscibility of saturated and cis-unsaturated TAGs seems to be slightly better than that of saturated and trans-unsaturated TAGs with the same degree of isomorphism.



ARE INTERACTION PARAMETERS  
RELATED TO STRUCTURAL DIFFER-  
ENCES?

table 8.2 Two or three suffix Margules parameters for the  $\beta'$ -modification and the degree of isomorphism of saturated and cis-unsaturated TAGs. The modification in which the cis-unsaturated TAG has crystallized is given. A - behind the value of  $\epsilon$  indicates, that the contribution of the cis-double bond is not incorporated in the value of  $\epsilon$ .

binary pair	modification	$A_{12}/RT$	$A_{21}/RT$	$\epsilon$
PSP-POP	$\beta'$ -2	$-3 \pm 1$	$0 \pm 0.5$	1-
PSP-PPO	$\beta'$ -2	$-1.5 \pm 1.5$	$-1.5 \pm 2$	0.92-
PSP-SSO	$\beta'$ -2	$-2 \pm 1$	$0 \pm 0.5$	0.92-
MPM-POP	$\beta'$ -2	$0.8 \pm 0.4$	$0.8 \pm 0.2$	0.86-
MPM-PPO	$\beta'$ -2	$0.8 \pm 0.5$	$0.8 \pm 0.3$	0.86-
MPM-SSO	$\beta'$ -2	$2 \pm 0.7$	$2 \pm 0.2$	0.77-
binary pair	modification	A/RT		
PSP-SOS	$\beta'$ -3	$0 \pm 0.5$		0.92-
MPM-PPO	$\beta'$ -3	$-0.2 \pm 0.4$		0.86-
MPM-SOS	$\beta'$ -3	$1.7 \pm 0.7$		0.77-
MPM-SSO	$\beta'$ -3	$2 \pm 0.5$		0.77-

**The  $\beta$ -modification.**

Most data for the  $\beta$ -modification that are available have a considerable error margin. Yet, as appears from the table below, a correlation between degree of isomorphism and the binary interaction parameters seems present.

In line with expectations, the degree of isomorphism that is required for complete miscibility in the  $\beta$ -modification is higher than for the less densely packed  $\beta'$ -modification: in the  $\beta$ -modification  $A/RT = 2$  is already reached when  $\epsilon = 0.94$ , while miscibility in the  $\beta'$ -modification at  $\epsilon = 0.94$  is still ideal. The few data for the  $\beta$ -3 modification agree with those for the  $\beta$ -2 modification.

PHASE EQUILIBRIA IN FATS  
- theory and experiments -

table 8.3: Two- and three-suffix Margules interaction parameters and the degree of isomorphism for binary pairs of  $\beta$ -2 or  $\beta$ -3 forming TAGs

binary pair	modification	A/RT	A <sub>12</sub> /RT	A <sub>21</sub> /RT	ε
SSS-SES	β-2	0.4 ± 0.5	0 ± 0.5	0.8 ± 0.5	1
SSS-SSE	β-2	0.4 ± 0.5	0.1 ± 0.5	0.7 ± 0.5	1
SSS-SEE	β-2	0 ± 1	0 ± 1	0 ± 1	1
SSS-EEE	β-2	0 ± 0.2	0 ± 0.2	0 ± 0.2	1
SES-SSE	β-2	0 ± 0.5	0 ± 0.5	0 ± 0.5	1
SSS-PSS	β-2	1.6 ± 0.5	1.1 ± 0.5	2.3 ± 0.5	0.96
SSS-SPS	β-2	> 3	> 3	> 2	0.96
PSS-PPS	β-2	1.6 ± 0.5	1.4 ± 0.5	1.8 ± 0.5	0.96
SPS-PPS	β-2	2 ± 0.5	3 - 5	0.4	0.96
PSP-PPP	β-2	> 3	> 3	> 1	0.96
PPS-PPP	β-2	1.9 ± 0.5	1.6 ± 0.5	2.3 ± 0.5	0.96
SSS-PSP	β-2	> 3	-	-	0.92
SSS-PPS	β-2	> 2.2 ?	-	-	0.92
PSS-SPS	β-2	2 ± 0.5	1.4 ± 0.5	2.6 ± 0.5	0.92
PSS-PPP	β-2	2.2 ± 0.5	2.8 ± 0.5	2.1 ± 0.5	0.92
SPS-PPP	β-2	> 5	> 5	> 5	0.92
PSP-PPS	β-2	> 3	> 3	> 1	0.92
PSP-SEE	β-2	> 2.5	-	-	0.92
PSP-ESE	β-2	> 2	-	-	0.92
PSP-EEE	β-2	> 2	-	-	0.92
SSS-PPP	β-2	3 ± 0.5	5.8 ± 1	1.4 ± 1	0.88
SPS-PSP	β-2	1.4 ± 0.5	> 1	1.8 ± 0.5	0.88
PSP-EPE	β-2	> 2.5	-	-	0.88
PPP-MMM	β-2	> 3	-	-	0.86
MPM-PEE	β-2	> 2.5	-	-	0.82
MPM-EPE	β-2	> 3	-	-	0.82
BBB-SSS	β-2	> 3	-	-	0.77
MPM-SEE	β-2	> 2.5	-	-	0.77
MPM-ESE	β-2	2 ± 1	-	-	0.77
PPP-LLL	β-2	> 3	-	-	0.67
BBB-PPP	β-2	> 3	-	-	0.63
SSS-LLL	β-2	> 3	-	-	0.50
SSS-888	β-2	> 3	-	-	0
SOS-POS	β-3	1.3 ± 0.5	1.5 ± 0.5	1.1 ± 0.5	0.96
POS-POP	β-3	1.6 ± 0.5	2.2 ± 0.5	1.0 ± 0.5	0.96
SOS-POP	β-3	> 3.6	5 ± 1	1.5 ± 1	0.92

ARE INTERACTION PARAMETERS  
RELATED TO STRUCTURAL DIFFER-  
ENCES?

There are a few noticeable exceptions in the data set, all concerning SPS and PSP: in combination with each other the miscibility is better than could be expected from their low degree of isomorphism, while in combination with other saturated TAGs that have a high degree of isomorphism with these two TAGs, miscibility seems much less than expected.

Although SSS and SPS both crystallize in a  $\beta$ -2 lattice, according to de Jong (5), they crystallize into different  $\beta$ -2 submodifications. SSS, PSS, PPS and PPP crystallize into the  $\beta$ -2A submodification, while PSP and SPS both crystallize into the  $\beta$ -2B submodification. Although these submodifications are very similar, apparently the condition for complete solid miscibility of Kitaigorodskii's rule is not fulfilled. The  $\beta$ -2 submodifications should have been treated as independent polymorphs. The effect of treating the submodifications as independent polymorphs is illustrated in figure 8.1 for  $A/RT=1.8$ , a value in agreement with the other data of TAGs with a degree of isomorphism  $\epsilon = 0.96$ . It is clear that the treatment as independent polymorphs gives a much better fit to the data.

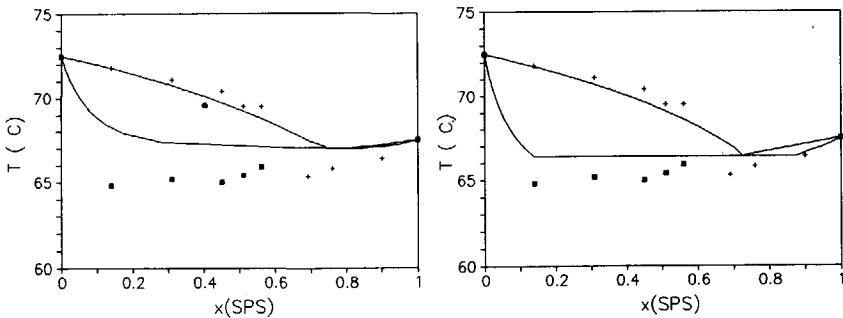


fig. 8.1 The influence of discontinuous miscibility in the  $\beta$ -2A and  $\beta$ -2B submodifications on the phase diagram of SSS-SPS.

Left: continuous miscibility with  $A/RT = 1.8$

Right: discontinuous miscibility with  $A/RT = 1.8$  for both submodifications.

Out of the four  $\beta$ -2 submodifications that occur, the  $\beta$ -2B submodification has the lowest packing density in the methyl terrace area. This could explain the 'too large' miscibility that was experimentally found for SPS-PSP.

### Conclusions

Kitaigorodskii's major rule of substitutional solubility applies to TAGs.

Within one submodification, the degree of isomorphism correlates very well with the binary interaction parameters. Contrary to the general case of organic compounds, the use of the degree of isomorphism for an empirical prediction of interaction parameters between TAGs seems feasible.

It turns out that in the description of phase equilibria in TAGs not only the three basic modifications have to be considered as separate states, but also each subform of these three modifications. A practical problem in doing so, is the fact that only the heat of fusion and melting point of the most stable subform can be determined experimentally.

### 8.2 CALCULATION OF LATTICE DISTORTION

When the degree of isomorphism is used for predicting binary interaction parameters, it is implicitly assumed that the two suffix Margules equation gives an adequate description of the phase behaviour of TAGs. Although this is quite often true, it is not always the case. Moreover, the validity of the 2-suffix Margules equation is theoretically unlikely. There is no reason why an impurity with a protuberance will lead to a lattice distortion of the same magnitude as an impurity that causes a hole in the lattice, or why a protuberance of a constant size should cause a lattice distortion of the same magnitude regardless whether it is a protuberance of the fatty acid on 1, 2 or 3 position of the glycerol group. To get a clearer insight into this matter more sophisticated molecular considerations are required.

8.2.1 Equivalent distortions in the  $\beta$ -2 modification

All saturated TAGs and trans-unsaturated TAGs that were considered in this work crystallize in the  $\beta$ -2 modification. According to de Jong (5) and using his nomenclature, all mono-acid TAGs, PSS, PPS, SES, SSE, SEE and EEE crystallize in the  $\beta$ -2A submodification, while PSP, SPS and probably also PEP crystallize into the  $\beta$ -2B submodification. These two submodifications have the same angle of tilt,  $60^\circ$ , of the fatty acid chains, but differ in the shape of their methyl end plane. The  $\beta$ -2B modification is somewhat less densely packed in this area. Within one submodification the shape of the methyl terrace does not change, but the position of the 'steps' in the terrace is shifted (fig 8.2).

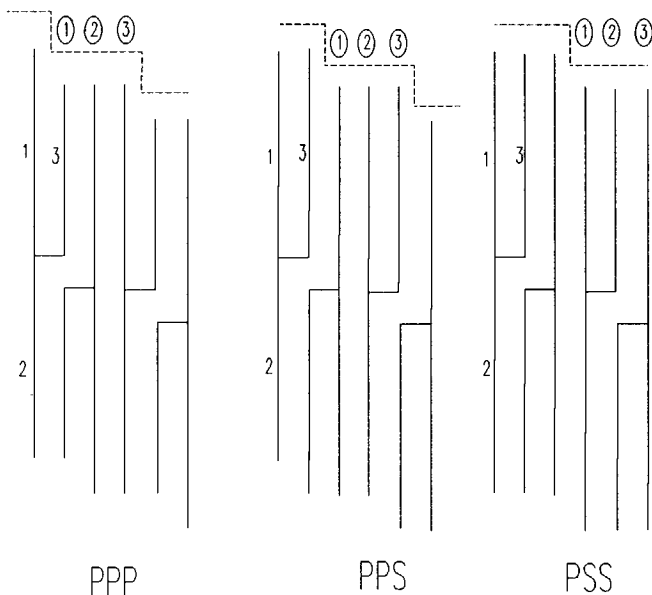


fig 8.2 Equivalent positions on the methyl terraces of PPP, PPS and PSS (marked by a circled number).

In fig 8.2 equivalent positions on the methyl terrace are marked by a circled 1, 2, or 3. Exchanging a molecule by a molecule of another TAG will corrupt the methyl end plane. If a PPP molecule is exchanged by PPS then an ethyl group is added to the first chain of a 'step'

of the methyl terrace. The distortion of the lattice caused by this addition will be called a  $(1,0,0)$  distortion, while that caused by removing an ethyl group from the same chain will be denoted as a  $(-1,0,0)$  distortion. A  $(0,1,0)$  distortion is in this nomenclature the addition of an ethyl group to the chain in the middle of a 'step' in the methyl terrace. It is also possible to bring about a  $(1,0,0)$  distortion in a PPS crystal: by exchanging PPS with PSS. As the distortion to the lattice is exactly the same, the activity coefficients at infinite dilution of PPS in PPP and PSS in PPS must be equal. Therefore, according to equation 7.6, the 3-suffix Margules parameters  $A_{PPS-PPP}$  and  $A_{PSS-PPS}$  should be identical as well, which was found indeed ( $A_{PPS-PPP} = 1.6$ ,  $A_{PSS-PPS} = 1.4$ ). Table 8.4 lists all 26 different distortions to the lattice of  $\beta$ -2A and  $\beta$ -2B TAGs that can be caused by addition or removal of ethyl groups.

These 26 different distortions occur at only three levels of the degree of isomorphism.

A complicating factor is the asymmetry of the TAGs PPS and PSS: PPS causes a  $(1,0,0)$  distortion in PPP, while its mirror image SPP leads to a  $(0,0,1)$  disturbance. These 2 distortions are not necessarily equivalent.

Notwithstanding the fact that sometimes asymmetric TAGs are involved, a good agreement is found between the values of the three suffix Margules parameters of equivalent distortions (table 8.5).

CALCULATION OF LATTICE DISTORTION

table 8.4: TAGs that cause equivalent distortions when inserted in the crystal lattice of the six TAGs that can be formed from P and S.

disturbance of methyl terrace		TAGs crystallizing in the $\beta$ -2A modification				TAGs in the $\beta$ -2B modification		$\epsilon$
		PPP	SSS	PPS	PSS	PSP	SPS	
A	-1 -1 -1	MMM	PPP	MMP	MPP	MPM	PMP	0.88
B	-1 -1 0	PHM	SPP	MMS	MSP	MPP	PPP	0.92
C	-1 -1 1	SMM	APP	MMA	MAP	MPS	PSP	0.88
D	-1 0 -1	MPM	PSP	PMP	MPS	PPM	PMS	0.92
E	-1 0 0	PPM	SSP	PMS	MSS	PPP	PPS	0.96
F	-1 0 1	SPM	ASP	PMA	MAS	PPS	PSS	0.92
G	-1 1 -1	MSM	PAP	SMP	MPA	SPM	PMA	0.88
H	-1 1 0	PSM	SAP	SMS	MSA	SPP	PPA	0.92
I	-1 1 1	SSM	AAP	SMA	MAA	SPS	PSA	0.88
J	0 -1 -1	MMP	PPS	MPP	PPP	MSM	SMP	0.92
K	0 -1 0	PMP	SPS	MPS	PSP	MSP	SPP	0.96
L	0 -1 1	SMP	APS	MPA	PAP	MSS	SSP	0.92
M	0 0 -1	MPP	PSS	PPP	PPS	PSM	SMS	0.96
N	0 0 1	SPP	ASS	PPA	PAS	PSS	SSS	0.96
O	0 1 -1	MSP	PAS	SPP	PPA	SSM	SMA	0.92
P	0 1 0	PSP	SAS	SPS	PSA	SSP	SPA	0.96
Q	0 1 1	SSP	AAS	SPA	PAA	SSS	SSA	0.92
R	1 -1 -1	MMS	PPA	MSP	SPP	MAM	AMP	0.88
S	1 -1 0	PMS	SPA	MSS	SSP	MAP	APP	0.92
T	1 -1 1	SMS	APA	MSA	SAP	MAS	ASP	0.88
U	1 0 -1	MPS	PSA	PSP	SPS	PAM	AMS	0.92
V	1 0 0	PPS	SSA	PSS	SSS	PAP	APS	0.96
W	1 0 1	SPS	ASA	PSA	SAS	PAS	ASS	0.92
X	1 1 -1	MSS	PAA	SSP	SPA	SAM	AMA	0.88
Y	1 1 0	PSS	SAA	SSS	SSA	SAP	APA	0.92
Z	1 1 1	SSS	AAA	SSA	SAA	SAS	ASA	0.88

The 3-suffix Margules parameters for the binary SSS-PPS could not be determined because of poor data quality. If the effects of chirality are negligible, they should be the same as those of PSS-PPP.

The distortions of table 8.4 are arbitrarily marked from A-Z for the  $\beta$ -2A submodification and from A' - Z' for the  $\beta$ -2B submodification. Using these markers, the phase diagrams can be classified: for

PHASE EQUILIBRIA IN FATS  
- theory and experiments -

table 8.5: Three suffix Margules parameters for some equivalent distortions. ( $a = A/RT$ )

code	distortion			
P	(0,1,0)	$a_{PSP-PPP} = > 3$	$a_{SPS-PPS} = > 3$	
U	(1,0,-1)	$a_{PSP-PPS} = > 3$	$a_{SPS-PPS} = 2.6$	
J	(0,-1,-1)	$a_{PPS-SSS} = 2.3$	$a_{PPP-PSS} = 2.1$	
M	(0,0,-1)	$a_{PSS-SSS} = 2.3 ?$	$a_{PPP-PSS} = 2.3$	$a_{PPS-PSS} = 1.8$
V	(1,0,0)	$a_{SSS-PSS} = 1.1$	$a_{PPS-PPP} = 1.6$	$a_{PSS-PPS} = 1.4$
Y	(1,1,0)	$a_{PSS-PPP} = 2.8$	$a_{SSS-PSS} = 2.3 ?$	

example SSS-PPP is a Z/A phase diagram. The binary interaction parameters for all Z/A phase diagrams should be the same, regardless of the excess Gibbs energy model used. The classification of all 15 P-S binary phase diagrams is given in table 9.

table 8.6. The P/S binaries classified in the types defined in table 8.4, together with the 2 -suffix Margules parameters. Where asymmetric TAGs are involved, a three or four letter code is used, indicating the distortions caused by both mirror images.

binary	type	A/RT	binary	type	A/RT
SSS-PSS	V/ME	1.6	SSS-PPP	Z/A	3
PSS-PPS	VX/MS	1.6			
PPS-PPP	VN/M	1.9	PSP-SPS	C'/I'	1.4
SSS-PSP	Q'/D	> 3	PSS-SPS	F'L/U	2
			PSP-PPS	U/F'H'	$\beta'$
SSS-SPS	N'/K	$\geq 3$			
PSS-PSP	N'/K'	$\beta'$	PSP-PPP	P/E'	$\beta'$
			SPS-PPS	P/E'	2
SSS-PPS	Y/BJ	$\geq 2.3 ?$			
PSS-PPP	QY/J	2.2	SPS-PPP	W/B'	> 5

If chirality is neglected, the 15 phase diagrams can be classified into nine different groups. The value of the binary interaction parameter within a group seems to be constant.



## CALCULATION OF LATTICE DISTORTION

These structural considerations show clearly that there is no reason at all for the assumption that the interaction parameters for the binary pairs PSP-PPP (type P/E') and PPS-PPP (type VN/M) should be the same, in spite of the fact that the degree of isomorphism of both pairs is 0.96. In the previous section it was found that the binaries with PSP and SPS are exceptions to the empirical 'rule' that the degree of isomorphism is related to the magnitude of the 2-suffix Margules parameter. This was explained by assuming that continuous miscibility cannot exist between the  $\beta$ -2A and  $\beta$ -2B modification, in spite of the close resemblance between the two  $\beta$  modifications. An alternative explanation is simply that the (0,1,0) distortion caused by PSP in PPP is not equivalent to the (1,0,0) distortion of PPS in PPP. This alternative explanation implies that the degree of isomorphism is too coarse a measure to correlate the interaction parameters.

Only calculation of the magnitude of the lattice distortions can decide which of the explanations is most likely.

### 8.2.2 $\beta$ -2A lattice distortion calculations

The calculations were carried out using the programs Insight and Discover from Biosym. The program calculates the molecular configuration with minimal energy. The molecular energy is the sum of the internal energy from bond length stretching, bond angle stretching and torsion and the non-bond-associated energy due to Coulomb and van der Waals forces.

The magnitude of a (1,0,0), a (0,1,0) and a (0,0,1) distortion to LLL have been calculated by comparison of the lattice energy of a pure LLL crystal with the lattice energy of an LLL crystal in which one molecule of an impurity [I] has been inserted per 54 molecules of LLL.

In the latter calculations we allowed the impurity to obtain the conformation with minimal energy, while the LLL molecules were fixed to the conformation that they have in a pure crystal. Calculations in which the complete impure crystal was allowed to rearrange went beyond the capacity of the program. The results are given in table 8.7.

PHASE EQUILIBRIA IN FATS  
- theory and experiments -

table 8.7 Lattice distortions  $U/RT$  to a  $\beta$ -2A crystal of LLL caused by impurities at infinite dilution in LLL.

type	caused by	distortion $U/RT$	U (distorted crystal) kJ/mol	U (pure 'im- purity') kJ/mol
(1,0,0)	LLM	1.0	258.9	270.1
(0,1,0)	LML	1.9	251.9	268.8
(0,0,1)	MML	3.6	255.0	270.1
(0,0,0)	LLL	0	253.8	253.8

The order of magnitude of the crystal energy corresponds very well with the data of de Jong (5) for CCC.

The (0,1,0) lattice distortion, which is brought about by the  $\beta$ -2B-forming TAG LML, has the same order of magnitude as those caused by the two  $\beta$ -2A forming TAGs LLM and MLL. The very poor miscibility in the solid phase that was found experimentally for TAGs equivalent to LML and LLL can therefore only be explained by assuming that continuous miscibility between the  $\beta$ -2A and  $\beta$ -2B submodification is not possible, in line with the findings in the previous section. The magnitude of the lattice distortion  $U/RT$  agrees strikingly well with the magnitude of the interaction parameter  $A/RT = 1.8$  that we obtained from the experimental data (fig 8.1).

The (1,0,0) distortion caused by LLM is much smaller than the (0,0,1) distortion caused by its mirror image MLL. The effects of chirality may clearly not be disregarded. Here again, the average value of the distortions  $U/RT$  corresponds reasonably well to the values of the interaction parameter  $A/RT$  of 1.6 - 2.3 that were found experimentally.

The order of magnitude of the calculated distortions corresponds with that expected from the value of the interaction parameters. However, we would expect that the distortions calculated in this way would lead to a systematic overestimate of the interaction parameters. The actual distortion is smaller, because in reality some relaxation of the LLL lattice near the distortion will occur. Moreover, entropy effects are neglected. Apparently both effects are relatively small.

## AN EMPIRICAL METHOD

It has become evident that the lattice distortion calculations can be used to obtain good insight into the influence of structural differences on the solid state miscibility. We will continue this approach in future work. In view of the results obtained, the good performance of the 2-suffix Margules equation and the good correlation of the interaction parameter with the degree of isomorphism remain very surprising.

### 8.3 AN EMPIRICAL METHOD

Although Larsson and Hernqvist (6) have announced a detailed analysis of the crystal structure of the  $\beta'$ -modification, similar to that of de Jong for the  $\beta$ -modification, at present the  $\beta'$ -crystal structure of TAGs is still not exactly known. The instability of the  $\beta'$ -modification and the inability to grow large single crystals are the main obstacles to be taken. The crystal structure of cis-unsaturated TAGs has not been unambiguously revealed either. This implies that it is not yet possible to study the influence of impurities on the  $\beta'$ -crystal lattice by molecular modelling. Fundamental insight in the relation between non-ideal miscibility of TAGs and structural differences can probably best be obtained from these lattice distortion calculations. While this is impossible, a semi-empirical approach to the problem of this chapter, finding a method to predict binary interaction parameters, has to be followed.

#### 8.3.1 The method

The correlation between the degree of isomorphism,  $\epsilon$ , and the two suffix Margules parameter within one submodification can serve as basis for such a semi-empirical predictive method. It is assumed that:

1. Within one submodification the 2-suffix Margules binary interaction parameter  $A/RT$  is:

for a  $\beta'$ -modification:

eq. 8.2

$$\epsilon > 0.93 : \frac{A}{RT} = 0$$

PHASE EQUILIBRIA IN FATS  
- theory and experiments -

eq. 8.3  $\epsilon \leq 0.93 : \frac{A}{RT} = -19.5\epsilon + 18.2$

and for a  $\beta$ -modification:

eq. 8.4  $\epsilon > 0.98 : \frac{A}{RT} = 0$

eq. 8.5  $\epsilon \leq 0.98 : \frac{A}{RT} = -35.8\epsilon + 35.9$

2. Both three suffix Margules parameters are also given by equations 8.2 - 8.5, except for the  $\beta'$ -2 modification of a binary pair of which one of the TAGs belongs to the  $h_{2u}$  TAG-group. If the  $h_{2u}$ -type TAG is indicated by 2, then  $A_{21}$  is given by equations 8.2 and 8.3, while  $A_{12}$  follows from:

eq. 8.6  $\frac{A_{12}}{RT} = -21.7\epsilon + 18.7$

3. If  $A/RT > 8$ ,  $A/RT = 8$  can be used in calculations.

The relations were obtained by linear regression through the data of tables 8.1-8.3. The correlation coefficient is 0.9, while the standard error in the estimated interaction parameters is 0.3 - 0.5. The values of the regression constants clearly illustrate the better solid miscibility in the less densely packed  $\beta'$ -modification.

Interaction parameters within a submodification are useless if the pure component properties of the TAG, crystallized in that submodification, are not known. Often these properties cannot be measured, because the pure components do not occur in the desired submodification. Therefore the following additional assumptions are made in line with our observations in chapter 4 and those of de Jong:

4. The melting point of a hypothetical -3 form of a TAG that crystallizes into the  $\beta'$ -2 or  $\beta$ -2 form, is 3°C less than the melting point of the corresponding -2 form. The heat of fusion is 90% of that of the corresponding -2 form. Similarly the melting point of

AN EMPIRICAL METHOD

a hypothetical -2 forms of a TAG that crystallizes into the  $\beta'$ -3 of  $\beta$ -3 form is 3°C less than that of the corresponding -3 form, while the heat of fusion is 90% of that of the -3 form.

5. Submodifications in the  $\beta'$ -modification are, if they exist, continuously miscible
6. It is only possible to form continuous solid solutions of two TAGs in the  $\beta$ -2 modification when they both crystallize in the same  $\beta$ -2 submodification. Table 8.7 lists the 4 different  $\beta$ -2 submodifications that occur in practice, using de Jong's nomenclature, representing a TAG according to the method defined in chapter 4 as (p.p+x.p+y) and thus indicating TAG-families by (x,y).

table 8.7: Summary of the  $\beta$ -2 submodifications in which different TAG-families (x,y) crystallize

$\beta$ -2 submodification			
A	B	C	D
(0,0)	(-2,0)	(4,2)	(2,2)
(0,2)	(2,0)	(4,4)	
(2,2)	(2,4)		

7. The melting point and heat of fusion of the hypothetical  $\beta$ -2 forms, which do not occur in the pure TAG, are assumed to lie 3°C below that of the stable  $\beta$ -2 form, while the heat of fusion is 90% of that of the stable form.

Thermodynamic calculations now become extremely complicated, as the number of independent polymorphs that have to be considered, has increased with each extra assumption from 3 to 8. Because most binary pairs of TAGs that crystallize into different  $\beta$ -2 modifications are not completely miscible even when they would crystallize in the same submodification, often equivalent calculation results are obtained if assumption 7 is replaced by the following assumption:

8. In calculations only one  $\beta$ -2 polymorph can be used. However, if the two TAGs of a binary crystallize in different submodifications, the two suffix Margules parameter that is obtained from eq. 8.4 and 8.5 is augmented by 1.

The phase diagram of SSS-SPS (fig 8.1) that was calculated allowing the occurrence of 2  $\beta$ -2 modifications and  $A/RT = 1.8$  in each submodification is nearly the same as the phase diagram given in chapter 7 using only one  $\beta$ -modification and  $A/RT = 3$ .

The difference of 3°C between the melting point of the stable and hypothetical  $\beta'$ - and  $\beta$ -forms is a best guess, based on de Jong's findings for the melting points of saturated mono-acid TAGs in different submodifications. The value of 90% for the heat of fusion of hypothetical submodifications is a best guess that is based on the data, given in chapter 4.

### 8.3.2 Discussion

It is obvious that the empirical method given is far from perfect, as it is based on a small number of data, which necessitated a number of speculative assumptions. However, the underlying notion that only TAGs with a high degree of geometric similarity will mix well in a densely packed solid phase is most likely correct. Therefore, the main effects of structural differences on solid phase miscibility are covered by the method, although not always very precise. In order to improve the method, more data are required and a number of issues need to be solved:

1. There is still a lack of reliable data on binary interaction parameters of TAGs, both for the  $\beta'$ -modification and for the  $\beta$ -modification. Especially on mixtures with cis-mono- and di-unsaturated TAGs more information is required.
2. The crystal structure of the  $\beta'$ -modification and its possible submodifications as well as the structure of the polymorphic forms of cis-unsaturated TAGs have to be known.

## CONCLUSION

3. It must be established to what extent the structure of two submodifications must be different before continuous miscibility of the two submodifications cannot occur, so that treatment as independent polymorphs is necessary
4. If two submodifications need to be treated as independent polymorphs, a method must be developed to estimate the thermodynamic properties of those polymorphs that do not occur in the pure component.
5. To obtain insight in the magnitude of different lattice distortions more mixtures have to be studied by molecular modelling, not only in the  $\beta$ -modification, but also in the  $\beta'$ -modification.

In spite of its serious limitations, we will test the empirical method in chapter 9 to see how it performs in practical situations.

### 8.4 CONCLUSION

The non-ideal mixing behaviour of TAGs in the solid phase can be explained by geometrical considerations.

Within one (sub)modification the binary interaction parameters show a clear correlation with the degree of isomorphism, as defined by Kitaigorodskii.

Based on the good correlation between degree of isomorphism and the 2-suffix Margules interaction parameter, a method has been defined that predicts the binary interaction parameters from structural differences.

The work that is required to improve this predictive method was outlined.

### LIST OF SYMBOLS

A	interaction parameter
v	volume of a molecule
$\epsilon$	degree of isomorphism

### REFERENCES

1. A.I. Kitaigorodskii, *Mixed Crystals, Solid State Sciences* 33, Springer Verlag, Berlin (1984).
2. K. Sato, *JAOCs* 66, 664 (1989)

PHASE EQUILIBRIA IN FATS  
- theory and experiments -

3. R. Vazquez Ladron, R. de Castro Ramos, *Grasas y Aceites* 22, 401 (1971).
4. V. Gibon, Thèse, Université de Notre Dame de la Paix, Namur (1984)
5. S. de Jong, Thesis, Rijksuniversiteit Utrecht (1980)
6. L. Hernqvist, K. Larsson, *Fette, Seife, Anstrichmittel* 84, 349 (1982)





## CHAPTER 9. PRACTICAL APPLICATIONS

*In the previous chapters, all steps that are required to meet the objective of this work: prediction of melting ranges and solid phase composition of fats, have been taken. In this chapter, the method developed will be used for predictions in a number of practical situations: the prediction of melting ranges of margarine fat blends, the prediction of the composition of fat fractions obtained from fractional crystallization and the understanding of recrystallization phenomena. Some examples outside the area of edible fats are considered as well. Finally the conclusions of this work are summarized.*

### 9.1 PREDICTION OF MELTING RANGES

The primary objective of this work is the development of a general method to predict the melting range of a fat blend from its composition. In this section we will investigate to what extent this objective has been attained.

In chapter 6 it was shown that the  $\alpha$ -melting ranges, or ' $\alpha$ -lines' of the fat blends of nine different commercial fat spreads could be predicted very well.

If the binary interaction parameters for the  $\beta'$ -modification are estimated with the procedure outlined in section 8.3, it is in principle possible to calculate the  $\beta'$ -melting ranges of these fats as well. A complicating factor in the calculations is the large number of components, usually between 30 and 400 in these fats. Even if only 4 coexisting  $\beta'$ -phases are formed, the flash calculation of chapter 3 must already handle matrices with a 2000 X 2000 dimension, which will make the calculation procedure too slow for practical use.

To keep the calculations manageable, pseudocomponents are defined as follows: all components that are nearly isomorphous ( $\epsilon > 0.95$ ) and that differ 5°C or less in their  $\beta'$ -2 melting point are taken together as a new pseudocomponent that has the polymorphic behaviour and the size of the component that contributes most to the pseudocomponent. Components and pseudocomponents with a concentration less than 0.1% are neglected.

PREDICTION OF MELTING RANGES

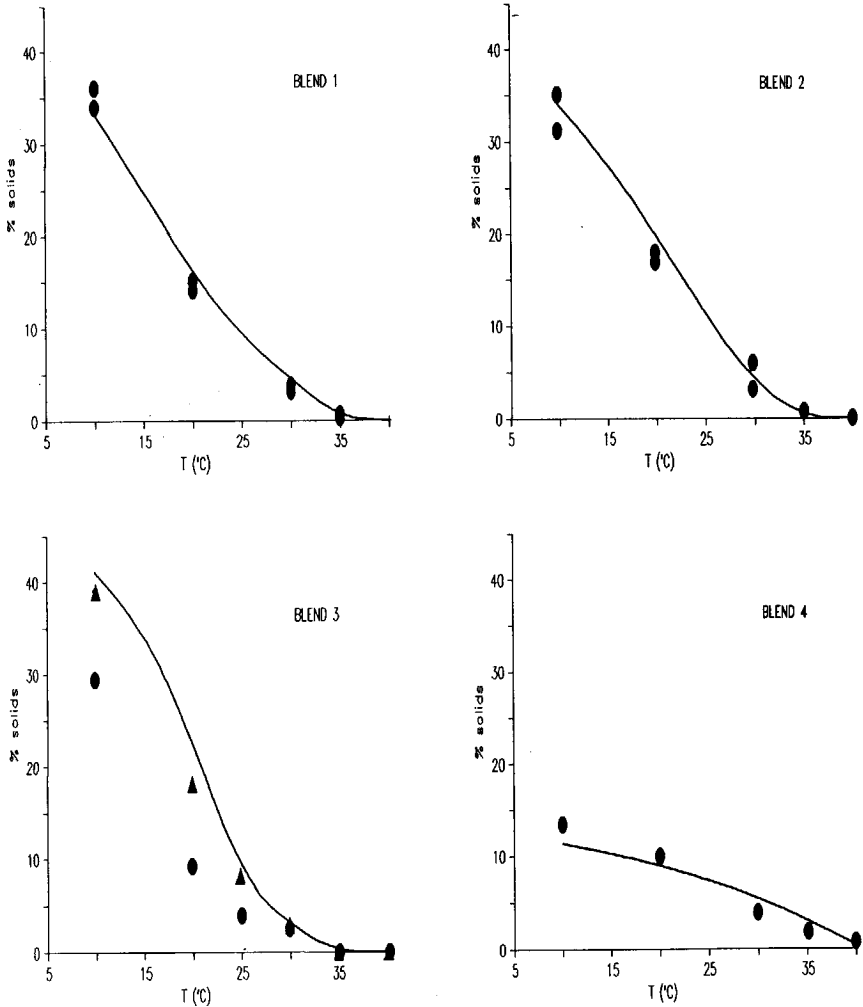


figure 9.1a Predicted (lines) and experimental (points)  $\beta'$ -melting ranges of several commercial fat blends. The numbers refer to the composition of the fat blend, given in table 6.2. The 2-suffix Margules equation was used for the excess Gibbs energy.  
 dots : solid phase measured with standard procedure  
 triangles (blend 3 only): determined in a week old margarine

PHASE EQUILIBRIA IN FATS  
- theory and experiments -

In this way blend 1 - 8 from table 6.2 were reduced to 15-20 component mixtures. Only blend 9 remained too complex. The  $\beta'$ -melting ranges of these 15-20 component mixtures were calculated and plotted in figure 9.1, together with the experimental values. The experimental values were obtained with wide range NMR of samples that were molten, kept for 1 hour at 80°C, rapidly cooled to 0 °C, stabilised for 16 hours at 0°C and for 30 minutes at the temperature of measurement. With this procedure, one of the Unilever standard methods, most normal fat blends have crystallized completely.

Although the predictions show a larger deviation than those for the  $\alpha$ -melting ranges, the agreement with the experimental data is still very good, in spite of the large simplifications that were made in the composition and in the estimation of the interaction parameters. The standard error of 3% solids compares well with the experimental error of 1% solids and the effects of kinetics of crystallization, that are normally estimated to be in the order of a few percent of solids.

Out of the empirical methods, mentioned in chapter 1, only the multiple linear regression/linear programming method performs better, but only within the limited range of compositions for which this method is valid. As it is based on interpolations within a finely meshed raster of experimental data points, this is not too surprising.

Only for blend 3, which contains 23% of POP, the experimental points, determined with the standard method, lie far below the calculated line. Blend 3 is a typical example of a fat blend that shows extreme 'post-crystallization'. Post crystallization means that in the first week after production still a considerable amount of solid fat crystallizes. The solid fat content that was determined in a margarine sample of a week old is also plotted in figure 9.1. Now the agreement with the calculated data is very good. Obviously, blend 3 has not crystallized completely when the standard procedure is used.

Thus we have demonstrated that indeed melting ranges of the practically relevant polymorphic forms of fat blends can be predicted by application of solid-liquid phase equilibrium thermodynamics.

## FRACTIONAL CRYSTALLIZATION

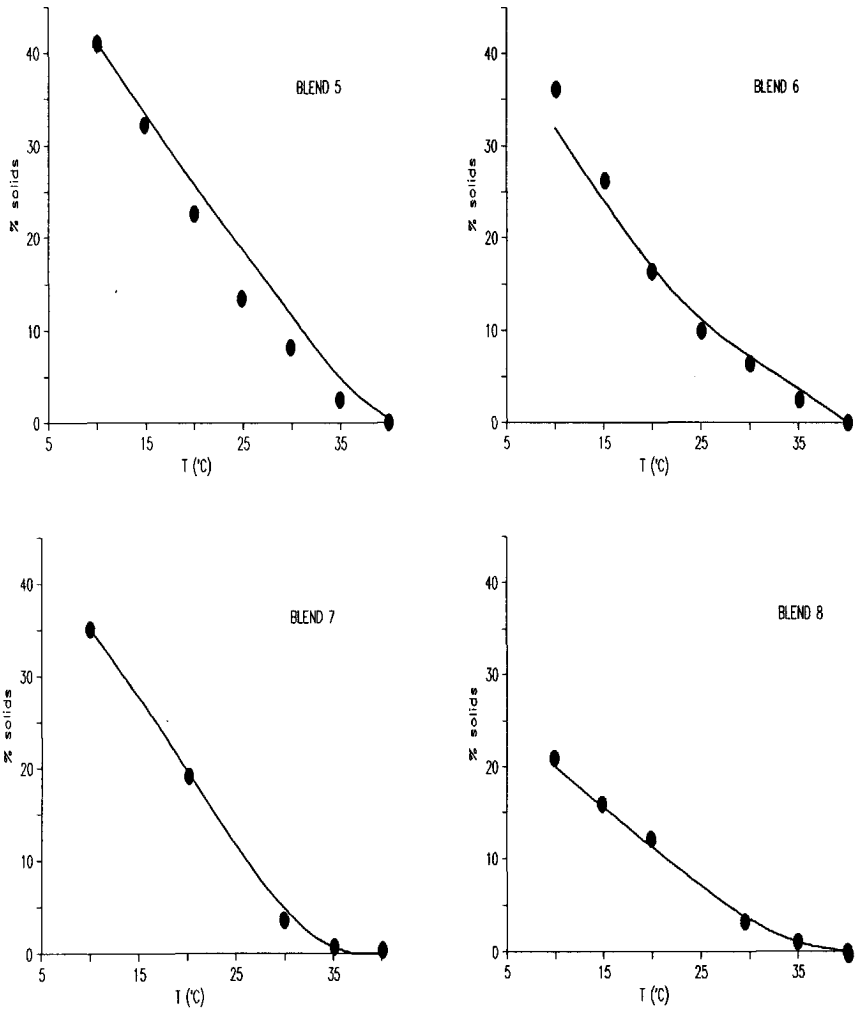


figure 9.1b Predicted (lines) and experimental (points)  $\beta'$ -melting ranges of several commercial fat blends. The numbers refer to the composition of the fat blend, given in table 6.2. The 2-suffix Margules equation was used for the excess Gibbs energy

## 9.2 FRACTIONAL CRYSTALLIZATION

The second objective of this work is the development of a method that predicts the solid phase composition of a fat at a certain

PHASE EQUILIBRIA IN FATS  
- theory and experiments -

temperature, in order to enable modelling of a fractional crystallization process. At present fractional crystallization is primarily used for fractionation of palm oil into palm olein, a liquid fraction of palm oil and palm stearin, a solid fraction.

*table 9.1 Experimental and predicted compositions of palm oil fractions. (Calculated for the most stable state, the  $\beta$ -modification)*

	fract. at 29 °C		fract. at 32°C	
	measured	calc.	measured	calc.
palm oil				
h <sub>3</sub>	8.8			
hOh	33.0			
hhO	7.1			
h <sub>1</sub> h	9.5			
rest	41.7			
stearin				
h <sub>3</sub>	45.3	46.2	54.7	53.3
hOh	25.4	29.3	21.5	17.2
hhO	6.1	4.1	5.5	4.3
h <sub>1</sub> h	5.3	4.9	4.3	4.7
rest	17.9	15.4	14.0	20.1
olein				
h <sub>3</sub>	2.2	0.1	2.8	0.2
hOh	34.4	33.7	34.7	35.8
hhO	6.1	7.8	5.9	7.6
h <sub>1</sub> h	10.6	10.5	10.1	10.3
rest	46.7	47.7	46.4	46.0

Palm oil was heated to 80°C for 1 hour and subsequently cooled to the fractionation temperature. Five hour after the appearance of the first turbidity the palm olein was filtered off in a filter press at 12 bar. The separation efficiency (amount of olein that is obtained over the total amount of liquid phase that is present in palm oil) was determined. NMR showed that crystallization had taken place into the  $\beta$ -modification. The TAG compositions of the palm oil, the olein and the stearin were analyzed by AgNO<sub>3</sub>-HPLC (3). The results are

## RECRYSTALLIZATION PHENOMENA

given in table 9.1, together with the composition that was calculated, using the procedure as outlined above and the measured separation efficiency

The calculated data agree very well with the experimental ones.

v. Putte (1) states that palm oil crystallizes into the  $\beta'$ -modification when the crystallization takes place at 27°C or less, while above this temperature the  $\beta$ -modification is observed. In line with this observation, our calculations show that in palm oil up to 25-26°C a stable  $\beta'$ -solid phase coexists with 2  $\beta$ -solid phases, while above this temperature only  $\beta$ -solid phases remain.

This example shows clearly that application of solid liquid phase equilibrium thermodynamics to fat fractionation processes is feasible.

### 9.3 RECRYSTALLIZATION PHENOMENA

#### 9.3.1 The influence of precrystallization and temperature cycling

In chapter 7, we determined DSC-curves of mixtures of a crystallizing binary pair of TAGs in a surplus of a liquid TAG. The samples were stabilised by rapid cooling to a stabilisation temperature. In those experiments, stabilisation at temperatures below the onset of the first melting peak in the DSC thermogram in the end always resulted in the same DSC-curve, regardless of the stabilisation procedure that was followed. However, if a well stabilised sample was subjected to temperature cyclisation by increasing the temperature from the stabilisation temperature to a cycling temperature well above the onset of the first melting peak and backwards, then the DSC-curves that were measured directly after the cycling step often had a completely different shape. The effect even occurred at cycling rates as low as 0.6°C/min. It was not possible to fit such DSC-curves with the 2 or the 3 suffix Margules equation.

The shape of the curves of the cycled samples could be obtained using the well known concept of shell formation (2), which was already mentioned in chapter 2. Upon heating the sample part of the solid phase dissolves. It is assumed that upon cooling the remaining crystals are covered with a layer of solid fat that is in equilibrium

with the liquid phase that is present. This shell effectively keeps the inner part of the crystals from gaining the equilibrium composition.

The resulting DSC melting curve will be the sum of that of a sample that has an overall composition equal to that of the liquid phase at the cyclisation temperature and the curve of the solid phase that remained at the cyclisation temperature. This DSC curve will deviate from the equilibrium curve at temperatures below the cyclisation temperature. Figure 9.2a shows that this is exactly what is observed, while the curves in figure 9.2b., which are calculated assuming shell formation, confirm that shell formation can describe the observations.

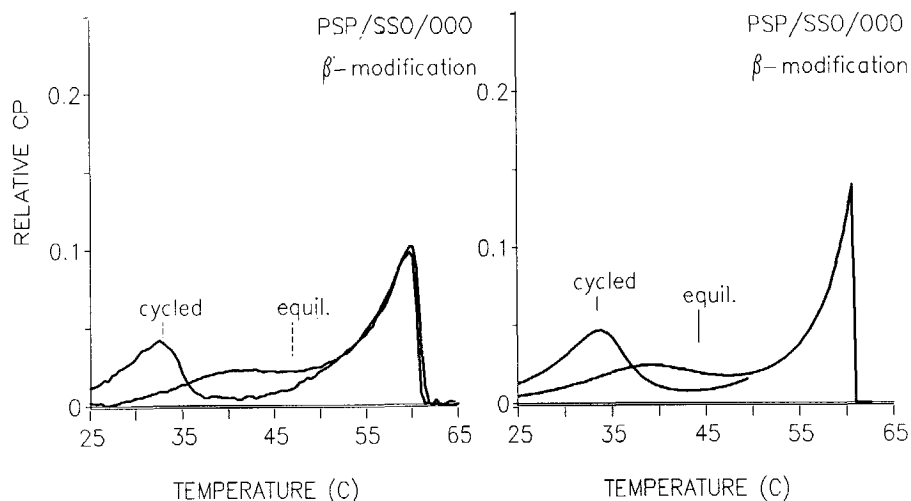


fig 9.2a: 25 PSP/25 SSO/50 000. Effect of cycling to 50°C on the DSC melting curve. Experimental curves, taken at 2.5°C/min.

fig 9.2b: Simulation of the effect of cycling to 50°C on the DSC melting curve of the system of fig 13 a.

Shell formation is much less likely with the isothermal stabilisation procedure that is followed in this work: always a completely liquid sample is very quickly supercooled to the stabilisation temperature. Therefore all solids are formed at the stabilisation temperature.



### RECRYSTALLIZATION PHENOMENA

Elaborate cyclisation procedures were followed in order to obtain the binary phase diagrams given chapter 7. The cycling effect described here offers another explanation for the large discrepancies between solidus and liquidus that were found: cyclisation leads to the formation of a solid phase that starts to melt off at lower temperatures. After initial melting a solid phase that is enriched in the highest melting component remains.

Shell formation also offers the explanation for the differences in fraction composition that are obtained with fractional crystallization of oils and fats when different cooling rates are used (3): slow cooling to the fractionation temperature causes shell formation and so results in a solid phase that is enriched in the higher melting components, while quick cooling results in the equilibrium composition. This work enables the quantification of the magnitude of these effects.

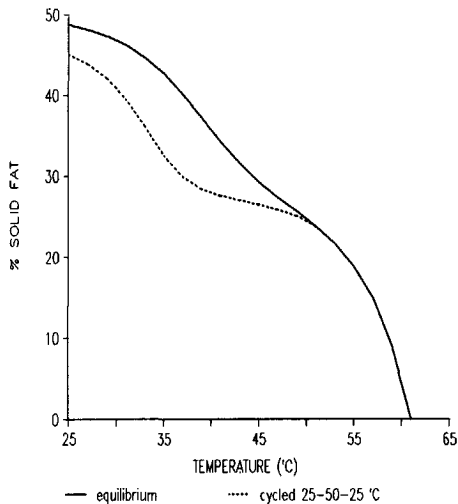


fig 9.3: Calculated solids-temperature lines of the TAG-blend of fig 9.2 (25 PSP/25 SSO/50 OOO). solid line = equilibrium line, dashed line = after precrystallization at 50°C.

Shell formation also plays a role in the normal margarine 'votator' process. Fat spreads are usually prepared by quickly cooling and emulsifying a mixture of a molten fat blend and milk or water in a

scraped surface heat exchanger or 'A-unit'. The supercooled emulsion is subsequently crystallized in a pin stirrer, or 'C-unit'. In many cases this is followed by further cooling and crystallization in second series of A and C-units (4), so that the complete votator process sequence becomes A-C<sub>1</sub>-A-C<sub>2</sub>. It is often impossible to complete crystallization in this second C-unit to the  $\beta'$ -equilibrium, even when a very long residence time is provided. Upon storage, eventually the equilibrium solids content will be reached, resulting in a considerable posthardening and change of rheological properties. In fact, the two-step crystallization in this votator process is a 'build in' cyclisation step: in the first C-unit a solid phase is formed, which is encapsulated in the second C-unit with a solid phase of different composition.

The effect of this precrystallization on solids content can be quite dramatic, as is illustrated in figure 9.3 for the PSP/SSO/000 model blend that was used in chapter 7: the difference in solid content between precrystallized and equilibrium situation can be as large as 10-15% solids. After the A-C<sub>1</sub>-A-C<sub>2</sub> votator process the fat can only crystallize to a point on the lower solids line. But upon storage it will recrystallize to the equilibrium composition in several weeks, which explains the increase in solids content and the rise in product hardness.

Fat blends in which the TAGs show considerable solid phase miscibility will be more sensitive to precrystallization effects than blends in which the TAGs show no solid phase miscibility.

### 9.3.2 Sandiness

A well known phenomenon is the development of 'sandiness' in fat spreads with a fat blend containing only liquid oils and hydrogenated low erucic acid rape seed oil (5,6). Sandiness is the development upon storage of large  $\beta$ -fat crystals in a product that initially had crystallized into the  $\beta'$ -modification. Those large crystals give a sensation to the consumer as if sand has been erroneously added to the product.

## RECRYSTALLIZATION PHENOMENA

Hydrogenated rape seed oil consists for 95% out of TAGs from C18 fatty acids (E,O and S). The degree of isomorphism between these TAGs is 1, which implies ideal solid solubility both in the  $\beta'$  and in the  $\beta$ -modification. In chapter 7 we found that the rate of recrystallization from  $\beta'$  to the  $\beta$ -modification depends on the thermodynamic driving force and on the degree of rearrangement of the solid phase that is required. Because the rape seed TAGs mix ideally in both modifications, the thermodynamic driving force is the full stability difference between the two modifications, while virtually no change in solid phase composition has to take place.

In this reasoning, the tendency to develop sandiness can be reduced by additions of TAGs that reduce the thermodynamic driving force and increase the degree of rearrangement in the solid phase that is required. Such TAGs should mix nearly ideally with the TAGs from rape seed oil in the  $\beta'$ -modification, but must demix in the  $\beta$ -modification. TAGs that have a degree of isomorphism with the rape seed TAGs of about 0.92 and a melting point above 30°C fulfil this criterion. Candidates are therefore the TAGs  $P_2S$ ,  $P_2E$ ,  $P_2O$ ,  $A_2S$ ,  $A_2S$ ,  $A_2O$  and also  $BS_2$ ,  $B_2E$  and  $B_2O$ . The solubility of these inhibiting TAGs in the  $\beta$ -modification of the rape seed TAGs is according to the findings in chapter 8 nearly 10%. Therefore we may expect that the  $\beta'$ - $\beta$  transition in hydrogenated rape seed oil mixtures will be retarded considerably if the crystallizing TAGs in the fat blend consist for more than 10% of inhibiting TAGs. Hydrogenated rape seed oil already contains 5% of those TAGs, so that addition of only 5% of an inhibiting fat is required to retard sandiness.

TAGs with a degree of isomorphism with the rape seed TAGs of less than 0.86 are expected to have much less effect: they do not even co-crystallize with the rape seed TAGs in the  $\beta'$ -modification, so that still hardly any solid phase rearrangement is required for the formation of the  $\beta$ -modification.

Hydrogenated soybean oil has a TAG composition that is very similar to that of hydrogenated rape seed oils, but the concentration of sandiness inhibiting TAGs is higher: it varies from batch to batch around the critical value of 10%, which implies that depending on

the batch of oil sandiness can occur. And indeed from time to time we have observed sandiness in products based on hydrogenated soybean oil.

Hydrogenated high erucic rape seed oil, contains depending on the hydrogenation procedure followed, more than 10% of inhibiting TAGs. Therefore sandiness is not so often observed in products of this rape seed oil breed (5,6)

Hernqvist already mentioned the possibility of addition of inhibiting TAGs, but he followed another reasoning and is not able to specify which TAGs and what amounts are required. By trial and error Hernqvist found no sandiness in a mixture of TAGs from rape seed and 20% PSP and he suggests that other inhibiting TAGs may exist. Indeed PSP belongs to the inhibiting TAGs mentioned.

### 9.3.3 Conclusion

The examples in this section have made clear that, although quantitative predictions are not always possible, the methods of this work help create understanding of recrystallization phenomena, which can directly be translated into practical methods to influence recrystallization.

## 9.4 APPLICATIONS OUTSIDE EDIBLE OILS AND FATS

### 9.4.1 Solid liquid phase behaviour of n-alkanes

Contrary to TAGs, which have only one thermodynamically stable polymorph ('monotropic polymorphism'), each polymorphic form of medium to long chain odd numbered n-alkanes is stable within a certain temperature and pressure region ('enantiotropic polymorphism'). Far below the melting point the  $\beta'$ -form is stable. However, from about 10°C below to melting point upwards the  $\alpha$ -modification ('rotator phase') is the stable polymorph. Upon heating a  $\beta'$ -form of an odd numbered n-alkane, it will first transform to the  $\alpha$ -modification at the so called transition temperature and finally melt at the  $\alpha$ -melting point.

The enantiotropic polymorphism gives rise to most peculiar solid-liquid phase diagrams, of which an example is depicted in fig 9.4a.

APPLICATIONS OUTSIDE EDIBLE  
OILS AND FATS

The phase diagram consists of three single phase regions, a liquid, an  $\alpha$ - and a  $\beta'$ -region. The regions are separated by two two phase domains, a cigar-shaped  $\alpha$ -L and a  $\beta'$ - $\alpha$  region with a minimum transition temperature (7,8). Although on first sight the phase behaviour seems completely different, remarkable agreement exists between the phase behaviour of TAGs and these n-alkanes.

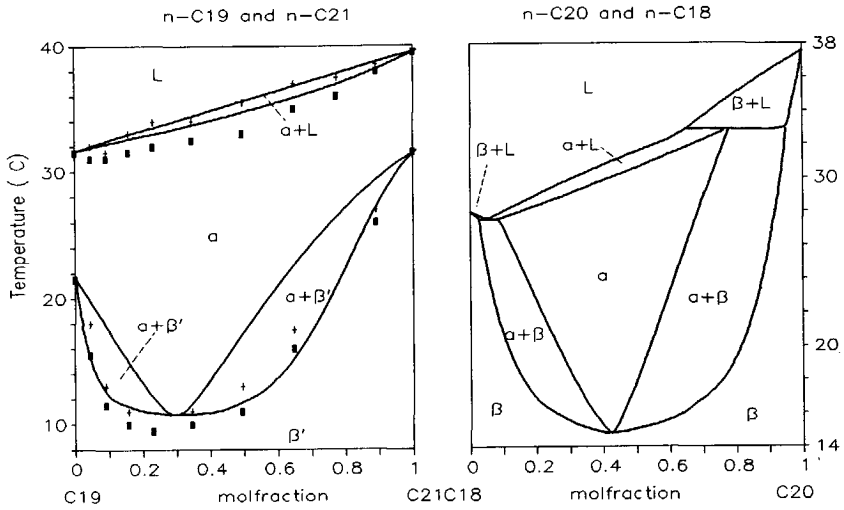


fig 9.4 Phase diagrams of binary n-alkane mixtures.

- a. (left): n-C19 with n-C21, points: data from Würflinger (7)  
lines : calculated with ideal  $\alpha$  and liquid phase miscibility and non-ideal mixing in the  $\beta'$ -modification with 3-suffix Margules parameters  $A_{19\_21}/RT = 0.4$  and  $A_{21\_19}/RT = 1.7$
- b. (right): n-C18 with n-C20. Calculated assuming ideal miscibility in the  $\alpha$ -modification and liquid phase and non ideal miscibility in the  $\beta'$ -modification with regular solution parameter  $A/RT=1.6$ . The  $\alpha$ -melting points were taken  $1.5^\circ\text{C}$  below the  $\beta$ -melting points.

The cigar-shape of the  $\alpha$ -L region indicates that miscibility in the  $\alpha$ -modification of these n-alkanes must be nearly ideal. This is in agreement with our findings for the  $\alpha$ -modification of TAGs.

The shape of the  $\beta'$ - $\alpha$  region and the existence of a single phase  $\beta'$ -region suggest non ideal mixing in the  $\beta'$ -modification, with a value for a regular solution binary interaction parameter in the  $\beta'$ -modification around 1.3-1.8. This is the same order of magnitude of the interaction parameters that have been found for the  $\beta'$ -modification of a binary pair of TAGs with a degree of isomorphism of 0.89.

When these values are used to describe the mixing behaviour in the  $\alpha$ - and  $\beta'$ -modification, the phase diagram of fig 9.4 is obtained easily, applying the models and techniques used in this work for TAGs.

The main problem in the calculations is the absence of values for the  $\beta'$ -melting points. The enantiotropic behaviour of these n-alkanes makes an experimental determination of  $\beta'$ -melting point impossible. However, they can be calculated from the measured  $\beta'$ - $\alpha$ -transition temperatures using the following expression:

eq. 9.1

$$T_{f,\beta'} = T_{\text{transition}} \cdot \frac{\Delta H_{\beta'}}{\Delta H_{\beta'} + \Delta H_{\alpha} \left( \frac{T_{\text{transition}}}{T_{f,\alpha}} - 1 \right)}$$

The expression follows from the fact that at the transition temperature the Gibbs energy of the 2 polymorphs must be equal. The differences in heat capacity are neglected. Calculated  $\beta'$ -melting points are listed in table 9.1. Although the transition temperatures lie 10°C or more below the  $\alpha$ -melting point, the calculated  $\beta'$ -melting points lie only 1 or 2 degrees below the  $\alpha$ -melting point.

The table also shows that, in spite of the higher melting point, entropy and heat of fusion of the  $\alpha$ -modification are only 70% of the  $\beta$ -values, which is in agreement with the values found for TAGs. In fact, a rise of only 5% in  $\alpha$ -melting entropy would change the enantiotropic polymorphism into the normal monotropic behaviour that is observed for TAGs.

APPLICATIONS OUTSIDE EDIBLE  
OILS AND FATS

table 9.3 Thermodynamic data of some odd-chain n-alkanes. (Calculated from data of Würflinger (7) ).  $T$  in °C,  $H$  in kJ/mol and  $S$  in J/K,mol.

carbon number	$T_{f,\alpha}$	$T_{f,\beta'}$	$\Delta H_{\alpha}$	$\Delta H_{\beta'}$	$\Delta S_{\alpha}$	$\Delta S_{\beta'}$	$T_{trans}$
9	-53.5	-54.2	16	22	71	100	-56.0
11	-25.5	-28.1	22	29	90	118	-36.5
13	-5.4	-8.1	28	36	106	136	-18.0
15	9.9	7.3	35	44	123	157	-2.3
17	21.9	19.4	41	52	138	176	10.5
19	32.0	29.6	46	59	150	197	22.0
21	40.2	38.3	48	63	152	203	32.5
23	47.5	45.5	54	76	169	238	40.5
25	53.5	51.5	58	84	177	258	47.0
27	58.8	56.9	60	89	182	270	53.0
29	61.2	60.2	66	98	198	293	58.0

The phase diagram that is calculated from the values of table 9.3 and the assumptions about the mixing behaviour in the various polymorphic forms is plotted in fig 9.4a, together with the data of Würflinger. The agreement is striking, especially when taking into account that it must be almost impossible to determine the equilibrium  $\alpha$ - $\beta'$ -coexistence region correctly by experiment. It would require large rearrangements in the solid state within the time of measurement, while solid state diffusion is extremely slow.

Some even chain n-alkanes are 'just' monotropic: the  $\alpha$ -melting point lies just below the  $\beta$  melting point. Binary mixtures of those components are enantiotropic, which gives rise to interesting phase diagrams (7). This type of phase diagrams, too, is obtained without problems, assuming ideal mixing in the  $\alpha$ -modification and non ideal mixing in the  $\beta'$ -modification with  $A_{12}/RT= 1.3-1.8$ . (fig 9.4b).

Thus it is illustrated that very simple excess Gibbs energy models, when combined with a proper treatment of polymorphism, can describe the main features of the complex solid-liquid phase behaviour of n-alkanes.

#### 9.4.2 Petroleum waxes

In parallel with this work a number of articles appeared from Won (9,10) and Hansen (11) on petroleum waxes. If mineral oils are brought from reservoir temperature and pressure to atmospheric conditions, sometimes a solid wax phase crystallizes, which causes fouling of the equipment and pipelines.

This wax phase is amorphous, so it is in complete rotational disorder. In line with our findings for the  $\alpha$ -modification of TAGs and the rotator phase of alkanes, it can be expected that these wax phases behave like ideal solid solutions. Consequently it is possible to calculate the wax appearance point of these oils.

Indeed, Won and Hansen found that the melting range of these complex petroleum waxes was predicted correctly by assuming ideal solid phase miscibility.

#### 9.4.3 $\beta$ -substituted naphthalenes

Another class of components that show polymorphism are the  $\beta$ -substituted naphthalenes. Like the odd-chain alkanes, the polymorphism is enantiotropic, with a high temperature polymorph that shows some rotational disorder and more densely packed lower temperature polymorphs. Consequently the phase diagrams are very similar to those of the enantiotropic odd-chain n-alkanes. An extensive study of binary phase diagrams of these components has been made by Chanh and Haget (12-15). Contrary to the n-alkanes, the rotational disorder in the high temperature  $\alpha$ -polymorph is not very large, so that a fairly high degree of isomorphism is required for ideal  $\alpha$ -miscibility. In the more densely packed lower temperature polymorphs miscibility is even less ideal than in the  $\alpha$ -modification, which in mixtures will lead to an extension towards lower temperatures of the region where the  $\alpha$ -modification is stable. This is illustrated in fig 9.5 for  $\beta$ -thionaphthalene and  $\beta$ -bromonaphthalene with a degree of isomorphism of 0.97. These components mix nearly ideally in the  $\alpha$ -modification and highly non ideally in the other modifications.  $\beta$ -thionaphthalene and  $\beta$ -fluoronaphthalene, with a degree isomorphism of only 0.87 already show non ideal mixing in the  $\alpha$ -modification.



CONCLUSION OF THIS WORK

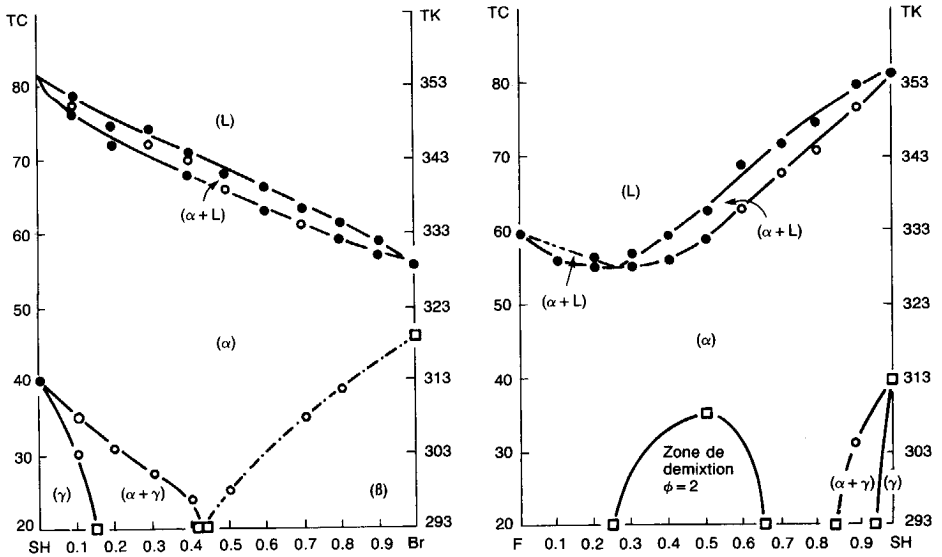


figure 9.5:  $T,x,y$  binary phase diagrams of some  $\beta$ -substituted naphthalenes.

Left:  $\beta$ -thionaphthalene and  $\beta$ -bromonaphthalene.

Right:  $\beta$ -thionaphthalene and  $\beta$ -fluoronaphthalene.

Although Chanh et al. do not report pure component properties for each polymorphic form, so that calculation of the phase diagrams from their data is not possible, it is clear that the approach of this work offers a good starting point for the development of a description of the complex solid phase behaviour of this class of compounds.

9.5 CONCLUSION OF THIS WORK

The objective of this work is the development of a predictive method for the melting range and the solid phase composition of edible oils and fats. We have shown that this objective can be attained by application of solid-liquid phase equilibrium thermodynamics to all three basic polymorphic forms in which TAGs crystallize.

In order to develop this thermodynamic description

PHASE EQUILIBRIA IN FATS  
- theory and experiments -

- Existing multicomponent multiphase vapour liquid flash calculation algorithms have been adapted to deal with a number of mixed solid phases that show polymorphism.
- The heat of fusion and the melting points of TAGs have been correlated with a number of structural parameters.
- Liquid TAG mixtures and TAG mixtures in the  $\alpha$ -modification have been treated as ideal mixtures.
- The deviation from ideal miscibility in the  $\beta'$  and  $\beta$ -modification has been described by the two and the three suffix Margules equations.
- A new method for the determination of the binary interaction parameters that occur in the two or three suffix Margules equation has been developed. The method is based upon the interpretation of the complete DSC melting curve of a mixture of the binary pair and a surplus of a liquid TAG. It is quicker, more versatile and more reliable than the use of binary T,x,y solid liquid phase diagrams.
- The binary interaction parameters that occur in the two or the three suffix Margules equation have been correlated with the degree of isomorphism of the binary pair, a parameter that indicates geometrical similarity.

Now the thermodynamic framework has been set up, the main scope of future research in this area should be the development of a more refined method to predict binary interaction parameters from structural differences.

LIST OF SYMBOLS

T	Temperature (K)
$T_f$	Normal melting point (K)
$\Delta H_f$	Heat of fusion (kJ/mol)
$\Delta S_f$	Entropy of fusion (kJ/mol)
$\epsilon$	Degree of isomorphism

## REFERENCES

### REFERENCES

1. K.P.A.M. v. Putte, B.H. Bakker, *JAACS* 64, 1138 (1987)
2. M. Zief, W.R. Wilcox, *Fractional Solidification*, Marcel Dekker inc (New York) 1967.
3. K. Keulemans, Unilever Research Vlaardingen, private communication (1986)
4. C. Poot, G. Biernoth, *The Lipids Handbook*, F. Padley et al. ed. Chapman & Hall, London (1986).
5. L. Hernqvist, K. Larsson et al., *J. Sci Food Agric* 32, 1197 (1981).
6. L. Hernqvist, K. Anjou, *Fette Seife Anstrichmittel* 85, 64 (1983)
7. A. Würflinger, Thesis, University of Bochum (BDR), (1972)
8. M. Maroncelli, H.L. Strauss, R.G. Snijder, *J. Phys. Chem* 89, 5260 (1985)
9. K.W. Won, 4th Int. Conf. on Fluid Phase Properties and Phase Equilibria, Helsingør (May 1986).
10. K.W. Won, 5th Int. Conf. on Fluid Phase Properties and Phase Equilibria, Banff (May 1989).
11. J.H. Hansen. A. Fredenslund, A thermodynamic model for prediction of wax formation in crude oils, SEP 8717 Danmarkse Tekniske Højskole (1987)
12. N.B. Chanh, Y. Haget, *Acta Cryst* 28,3400 (1972)
13. N.B. Chanh, Y. Haget, *J. Chim. Phys* 72, 5 + 760 (1975)
14. Y. Haget, N.B. Chanh, Second Codata symposium on critical evaluation and prediction of phase equilibria in multicomponent systems, Paris (sept 1985), 170
15. Y. Haget, N.B. Chanh, Second Codata symposium on critical evaluation and prediction of phase equilibria in multicomponent systems, Paris (sept 1985), 637

## SAMENVATTING

Het is voor de levensmiddelenindustrie van groot belang het smelten en stolgedrag van spijsoliën en -vetten te kunnen beïnvloeden. De eigenschappen van veel voedingsmiddelen zoals margarine, halvarine, koekjes, ijs, chocolade en dressings worden voor een belangrijk deel bepaald door het smelttraject van het vet in deze producten. Het is het doel van dit proefschrift om een methode te ontwikkelen om het smelttraject en de samenstelling van de vetkristallen in een mengsel van oliën en vetten te voorspellen uit de samenstelling van het mengsel. Momenteel bestaan daarvoor slechts enkele empirische methoden met een zeer beperkt toepassingsgebied. De hoeveelheid vast vet, die uiteindelijk kan uitkristalliseren, wordt uitsluitend bepaald door de ligging van het thermodynamisch evenwicht tussen vloeistof en vaste fase, alhoewel de manier waarop men het vet laat kristalliseren in de praktijk tot duidelijke afwijkingen van de evenwichtssituatie kan leiden. In de eerste hoofdstukken wordt duidelijk dat het startpunt voor elke algemeen geldige methode om het gehalte aan vast vet te voorspellen een beschrijving van het vast-vloeistof evenwicht in vetten is.

Vetten bestaan uit honderden verschillende triacylglycerolen (TAGs), die in verschillende kristalvormen kunnen uitkristalliseren, de onstabiele  $\alpha$ -modificatie, de metastabiele  $\beta'$ -modificatie en de stabiele  $\beta$ -modificatie. Het blijkt nodig de ligging van het vast-vloeistof evenwicht voor elk van deze drie kristalvormen te beschrijven. Dergelijke vast-vloeistof fasenevenwichten in multi-componentsystemen waarbij mengkristalvorming optreedt, zijn niet eerder beschreven.

De thermodynamische vergelijkingen, die een vast-vloeistof fasenevenwicht beschrijven worden in hoofdstuk 2 uitgewerkt. Om dit stelsel vergelijkingen te kunnen oplossen om zo het gehalte aan vast vet en de samenstelling daarvan te verkrijgen, moeten de volgende zaken bekend zijn:

1. de smeltwarmten en smeltpunten van zuivere TAGs.
2. het menggedrag van TAGs in de vloeibare fase.

## SAMENVATTING

3. de mate van mengkristalvorming in de vaste fasen. Ook moet nog een efficiënte oplosmethode voor het stelsel vergelijkingen worden gevonden.

In hoofdstuk 3 wordt verder op deze oplosmethode ingegaan. Een aantal methoden voor gas-vloeistof evenwichtsberekeningen aan systemen met meer fasen en veel componenten wordt aangepast, zodat vaste stoffen die polymorfie vertonen gehanteerd kunnen worden. Na vergelijking blijkt dat Michelsens methode voor beginwaarde schattingen in combinatie met een Gibbs vrije energie minimalisering volgens Murray het beste voldoen.

De smeltwarmtes en smeltpunten van de diverse polymorfe vormen van zuivere TAGs worden verkregen uit een aantal empirische relaties, die zijn ontwikkeld door data uit de literatuur, aangevuld met eigen metingen, te correleren met enkele kengetallen van de structuur van een TAG.

Het menggedrag van TAGs in de vloeistoffase wordt bestudeerd in hoofdstuk 5. Uit modelberekeningen, literatuurdata en een bepaling van enkele activiteitscoëfficiënten in vloeibare TAG-mengsels door middel van gas-vloeistof chromatografie blijkt dat mengsels van vloeibare TAGs in de praktijk veelal als ideaal kunnen worden beschouwd.

In de onstabiele  $\alpha$ -vorm blijken de vetzuurketens van de TAGs nog een hoge mate van beweeglijkheid te bezitten. Dit vormt aanleiding om naar analogie van de vloeistoffase ideaal menggedrag in de  $\alpha$ -modificatie te veronderstellen. Zeer verrassend blijkt dat de  $\alpha$ -smelttrajecten van een groot aantal industriële vetten met behulp van deze veronderstelling goed worden voorspeld.

Het menggedrag in de  $\beta'$ - en  $\beta$ -modificatie is duidelijk niet ideaal. Aan de hand van, deels voor het eerst gepubliceerde, binaire T,x,y fasendiagrammen laten we zien dat de niet ideale menging in deze polymorfe vormen beschreven kan worden met de relatief eenvoudige 2- en 3-suffix Margules vergelijkingen. Omdat fasendiagrammen alleen informatie geven over de  $\beta$ -vorm en niet over de veel belangrijker  $\beta'$ -modificatie en bovendien het merendeel van de bestaande binaire fasendiagrammen inconsistent is, wordt een nieuwe methode ontwikkeld voor de bepaling van de binaire interactieparameters die in de

modellen voor niet ideale menging voorkomen. Deze methode berust op de interpretatie van één volledige DSC smeltcurve van een mengsel van de twee te bestuderen TAGs en een overmaat van een derde, vloeibare TAG. Voor het eerst worden zo betrouwbare gegevens verkregen over het menggedrag in de  $\beta'$ -modificatie.

In hoofdstuk 8 blijkt dat de binaire interactieparameters, die zijn bepaald, een correlatie vertonen met een parameter, die de mate van geometrische gelijkvormigheid van twee TAGs aangeeft. Op grond hiervan wordt een praktische methode geformuleerd om de grootte van de interactieparameters te schatten.

In hoofdstuk 9 laten we zien dat met de in dit proefschrift ontwikkelde methodiek het smelttraject van vetten en de samenstelling van de vetkristallen kan worden voorspeld. Ook is meer inzicht verkregen in het optreden en voorkomen van allerlei ongewenste rekristallisatieverschijnselen in vetten. De methoden blijken verder ook buiten de wereld van de spijsvetten toepasbaar.



## SUMMARY

It is important for the production of fat containing food products to control the melting and solidification behaviour of edible oils and fats. The properties of many food products, like margarine, reduced fat spreads, cake, ice-cream and chocolate are to large extent determined by the melting range of the fat that they contain. The objective of this work is to develop a method to predict the melting range and solid phase composition of fats from their overall composition. Unfortunately at present only empirical calculation methods are available, that have only limited use. The ultimate amount and composition of the solid phase in a fat are determined by the position of the thermodynamic equilibrium solely, but the crystallization process may lead to significant deviations from the equilibrium composition in practical situations. Yet, it appears that the starting point for any general predictive method of the solid phase content is a description of the solid-liquid phase equilibrium.

Fats consist out of hundreds of different triacylglycerols (TAGs) that can basically crystallize in three forms: the unstable  $\alpha$ -modification, the metastable  $\beta'$ -modification and the stable  $\beta$ -modification. The objective of this work requires the description of the solid-liquid phase equilibrium for all three polymorphic forms.

The thermodynamic equations that describe these equilibria are worked out in chapter 2. To solve this set of equations to obtain the solid phase content and the solid phase composition, the following things must be known:

1. the melting enthalpies and melting points of pure TAGs.
2. the mixing behaviour in the liquid phase.
3. the degree of mixed crystal formation in the solid phases.

A method to solve the set of equations must be found as well.

In chapter 3 the way to solve the thermodynamic equations is worked out. Several methods for flash calculations in multicomponent, multiphase gas-liquid systems are adapted for use with solid phases



#### SUMMARY

that show polymorphism. Michelsen's method for the initial estimate combined with a Gibbs free energy minimisation according to Murray perform best.

The melting enthalpies and melting points of pure TAGs are obtained from empirical relations, which are developed by correlating literature data and experimental data with a set of parameters that represent the TAG structure.

The mixing behaviour of TAGs in the liquid phase is studied in chapter 5. From model calculations, literature data and determination of some liquid phase activity coefficients by means of gas liquid chromatography it appears that the TAGs mix essentially ideally in the liquid phase.

The fatty acid chains of the TAGs still possess considerable mobility in the unstable  $\alpha$ -modification. This suggested the hypothesis of ideal miscibility in the  $\alpha$ -modification. To our surprise the  $\alpha$ -melting ranges of a large number of commercial fats is predicted very well using this hypothesis.

Miscibility is clearly not ideal in the  $\beta'$  and  $\beta$ -modification. Using binary T,x,y phase diagrams, of which some have never been published before, we show that it is possible to describe non ideal mixing in these polymorphic forms with the relatively simple 2- and 3 suffix Margules equations. As binary phase diagrams only give information about the  $\beta$ -modification and not about the much more important  $\beta'$ -modification, and as the majority of the existing phase diagrams is inconsistent, a new method is developed for quick determination of the binary interaction parameters in the models for non-ideal behaviour. This method is based upon the interpretation of a single, complete DSC melting curve of a mixture of the two TAGs to be studied and a surplus of a liquid TAG. In this way, reliable data concerning the mixing behaviour in the  $\beta'$ -modification have been obtained for the first time.

The binary interaction parameters that occur in the models for non ideal mixing show a correlation with a parameter, that indicates the degree of geometrical similarity. This correlation is used to develop a practical method to predict the binary interaction parameters of two TAGs.

PHASE EQUILIBRIA IN FATS  
- theory and experiments -

In chapter 9 we show that the methods developed in this thesis can be used for predicting melting ranges and the composition of the solid phase of fats. A better insight is obtained in the occurrence and prevention of undesired recrystallization phenomena that occur in fats. Also applications outside the world of edible fats are feasible.



PHASE EQUILIBRIA IN FATS  
- theory and experiments -

APPENDIX 1 PURE COMPONENT DATA

SATURATED TAGs

TABLE A1.1 : Enthalpy of fusion for the  $\alpha$ -modification of saturated TAGs. Data marked by a \* include measurements from this work. FREQ indicates the number of measurements that has been averaged.

X	Y	TAG	n	$\Delta H_f$ (kJ/mol)	predicted	residual	FREQ
-6	0	SLS	48	70.0	85.1	-15.1	1*
-6	2	PCS	44	80.0	71.8	8.2	1*
-4	0	PLP	44	65.0	76.6	-11.6	1*
-4	0	SMS	50	90.0	92.8	-2.8	1*
-4	2	PLS	46	70.0	79.5	-9.5	1*
-4	4	MCS	42	67.0	63.7	3.3	1*
-2	0	PMP	46	79.0	86.5	-7.5	1*
-2	0	SPS	52	103.0	102.7	0.3	1*
-2	2	PMS	48	93.0	89.4	3.6	1*
0	0	888	24	18.4	31.8	-13.4	3*
0	0	CCC	30	57.3	47.9	9.4	2*
0	0	LLL	36	69.8	64.1	5.7	3*
0	0	MMM	42	81.9	80.3	1.6	3*
0	0	PPP	48	95.8	96.5	-0.7	3*
0	0	SSS	54	108.5	112.7	-4.2	3*
0	0	BBB	66	143.2	145.1	-1.9	1
0	0	24.24.24	72	160.9	161.3	-0.4	1
0	2	88C	26	26.0	34.7	-8.7	1*
0	2	MMP	44	82.0	83.2	-1.2	1*
0	2	PPS	50	100.0	99.4	0.6	1*
0	4	LLP	40	67.0	67.4	-0.4	1*
0	4	MMS	46	87.0	83.6	3.4	1*
2	0	8C8	26	51.0	37.8	13.2	1*
2	0	CLC	32	67.0	54.0	13.0	1*
2	0	LML	38	83.0	70.2	12.8	1*
2	0	MPM	44	93.0	86.4	6.6	1*
2	0	PSP	50	112.2	102.6	9.7	2*

APPENDIX 1 PURE COMPONENT  
DATA

X	Y	TAG	n	$\Delta H_f$ (kJ/mol)	predicted	residual	FREQ
2	2	MPP	46	89.0	89.3	-0.3	1*
2	2	PSS	52	106.0	105.5	0.5	1*
2	4	LMP	42	74.0	73.5	0.5	1*
2	4	MPS	48	86.0	89.7	-3.7	1*
2	6	CLP	38	57.0	59.0	-2.0	1*
2	6	MPA	50	72.0	91.3	-19.3	1
4	0	MSM	46	99.0	87.8	11.2	1*
4	0	SBS	58	128.0	120.2	7.8	1*
4	2	MSP	48	91.0	90.7	0.3	1*
4	4	LPP	44	83.0	75.0	8.0	1*
4	4	MSS	50	92.0	91.1	0.9	1*
6	0	LSL	42	66.0	72.2	-6.2	1*
6	0	MAM	48	88.0	88.4	-0.4	1*
6	4	LSP	46	76.0	75.5	0.5	1*
6	6	CPP	42	53.0	61.0	-8.0	1*
6	6	LSS	48	70.0	77.2	-7.2	1*

PHASE EQUILIBRIA IN FATS  
- theory and experiments -

TABLE A1.2 : Enthalpy of fusion for the  $\beta'$ -modification of saturated TAGs. Data marked by a \* include measurements from this work. FREQ indicates the number of measurements that has been averaged.

X	Y	TAG	n	$\Delta H_f$ (kJ/mol)	predicted	residual	FREQ
0	0	LLL	36	86.0	88.0	-2.0	1
0	0	MMM	42	106.0	111.1	-5.1	3*
0	0	PPP	48	126.5	134.3	-7.8	2*
0	0	SSS	54	156.5	157.5	-1.0	2*
0	2	MMP	44	100.0	106.5	-6.5	1*
0	2	PPS	50	124.0	129.7	-5.7	1*
0	4	LLP	40	90.0	84.4	5.6	1*
0	4	MMS	46	93.0	107.6	-14.6	1*
2	0	8CB	26	62.0	63.5	-1.5	1*
2	0	CLC	32	87.5	86.7	0.8	2*
2	0	LML	38	112.0	109.9	2.1	1*
2	0	MPM	44	127.0	133.0	-6.0	1*
2	0	PSP	50	165.5	156.2	9.3	4*
2	4	LMP	42	94.0	106.3	-12.3	1*
2	4	MPS	48	111.0	129.5	-18.5	1*
4	0	MSM	46	148.0	133.0	15.0	1*
4	0	SBS	58	189.0	179.4	9.6	1*
4	2	MSP	48	143.5	128.4	15.1	2*
4	4	LPP	44	110.0	106.3	3.7	1*
4	4	MSS	50	128.0	129.5	-1.5	1*
6	0	LSL	42	87.0	107.8	-20.8	0*
6	0	NAM	48	117.0	130.9	-13.9	1*
6	4	LSP	46	107.0	104.2	2.8	1*
6	6	LSS	48	104.0	111.6	-7.6	1*

APPENDIX 1 PURE COMPONENT  
DATA

TABLE A1.3 : Enthalpy of fusion for the  $\beta$ -modification of saturated TAGs. Data marked by a \* include measurements from this work. FREQ indicates the number of measurements that has been averaged.

X	Y	TAG	n	$\Delta H_f$ (kJ/mol)	predicted	residual	FREQ
-10	0	SBS	44	141.0	131.7	9.3	1
-8	0	PBP	40	122.0	116.2	5.8	3
-8	0	SCS	46	143.0	139.5	3.5	2
-6	0	PCP	42	122.5	124.0	-1.5	2
-6	0	SLS	48	132.0	147.4	-15.4	2*
-6	2	PCS	44	125.0	123.3	1.7	1*
-4	0	PLP	44	121.5	133.1	-11.6	2*
-4	0	SMS	50	146.5	156.5	-10.0	2*
-4	2	PLS	46	123.0	132.4	-9.4	1*
-4	4	MCS	42	88.0	106.3	-18.3	1*
-2	0	PMP	46	137.0	148.3	-11.3	2*
-2	0	SPS	52	170.3	171.7	-1.4	4*
-2	2	PMS	48	152.0	147.6	4.4	1*
0	0	888	24	69.2	74.7	-5.4	4*
0	0	CCC	30	95.0	98.0	-3.0	5*
0	0	LLL	36	122.2	121.3	0.9	9*
0	0	MMM	42	146.8	144.7	2.1	8*
0	0	PPP	48	171.3	168.0	3.3	16*
0	0	SSS	54	194.2	191.3	2.8	20*
0	2	88C	26	59.0	73.9	-14.9	1*
0	2	LLM	38	116.0	120.6	-4.6	1
0	2	MMP	44	131.0	143.9	-12.9	1*
0	2	PPS	50	166.3	167.3	-1.0	4*
0	4	LLP	40	117.0	117.8	-0.8	1*
0	4	MMS	46	145.0	141.2	3.8	1*
2	0	PSP	50	166.0	173.6	-7.6	1
2	2	LMM	40	118.0	126.2	-8.2	1
2	2	MPP	46	140.0	149.6	-9.6	1*
2	2	PSS	52	175.0	172.9	2.1	3*
2	4	LMP	42	125.0	123.5	1.5	1*
2	4	MPS	48	137.0	146.8	-9.8	1*
2	6	CLP	38	95.0	105.0	-10.0	1*
2	6	MPA	50	122.0	151.6	-29.6	0*

PHASE EQUILIBRIA IN FATS  
- theory and experiments -

X	Y	TAG	n	$\Delta H_f$ (kJ/mol)	predicted	residual	FREQ
4	4	LPP	44	146.0	119.0	27.0	0*
4	4	MSS	50	139.0	142.4	-3.4	1*
6	0	LSL	42	131.0	124.8	6.2	1*
6	0	MAM	48	157.0	148.1	8.9	1*
6	4	LSP	46	124.0	121.3	2.7	1*
6	6	CPP	42	89.0	102.8	-13.8	1*
6	6	LSS	48	123.0	126.1	-3.1	1*



APPENDIX 1 PURE COMPONENT  
DATA

TABLE A1.4 : Melting points of the  $\alpha$ -modification of saturated TAGs.  
FREQ indicates the number of measurements that has been averaged.

X	Y	TAG	n	T <sub>f</sub> (kJ/mol)	predicted	residual	FREQ
-12	0	S6S	42	27.8	23.7	4.1	2
-10	0	P6P	38	14.6	10.2	4.4	2
-8	0	SCS	46	30.0	34.4	-4.4	2
-6	0	PCP	42	20.0	24.3	-4.3	2
-6	0	SLS	48	36.0	39.3	-3.3	2
-4	0	MCM	38	16.0	13.4	2.6	1
-4	0	PLP	44	32.6	31.4	1.2	2
-4	0	SMS	50	43.8	44.3	-0.5	4
-4	0	BSB	62	61.1	61.7	-0.6	1
-2	0	LCL	34	5.0	2.9	2.1	2
-2	0	MLM	40	24.0	23.7	0.3	1
-2	0	PMP	46	39.1	38.5	0.6	5
-2	0	SPS	52	50.7	49.4	1.3	6
-2	2	PMS	48	40.9	41.3	-0.4	2
-1	0	P.15.P	47	43.4	41.7	1.7	1
-1	0	S.17.S	53	53.1	51.8	1.3	1
0	0	888	24	-51.0	-47.8	-3.2	1
0	0	9.9.9	27	-26.0	-26.1	0.1	1
0	0	CCC	30	-11.5	-9.3	-2.2	2
0	0	11.11.11	33	2.0	4.2	-2.2	2
0	0	LLL	36	15.6	15.2	0.4	4
0	0	13.13.13	39	24.5	24.3	0.2	3
0	0	MMM	42	32.6	32.0	0.6	6
0	0	15.15.15	45	39.5	38.7	0.8	4
0	0	PPP	48	44.7	44.4	0.3	5
0	0	17.17.17	51	49.9	49.4	0.5	4
0	0	SSS	54	54.7	53.8	0.9	8
0	0	19.19.19	57	59.1	57.7	1.4	2
0	0	AAA	60	62.9	61.3	1.6	2
0	0	21.21.21	63	65.0	64.4	0.6	1
0	0	BBB	66	69.1	67.3	1.8	2
0	1	11.11.L	34	7.5	7.3	0.2	1
0	2	CCL	32	0.0	-3.2	3.2	1
0	2	LLM	38	19.0	19.4	-0.4	1
0	2	MMP	44	34.5	35.2	-0.7	3
0	2	PPS	50	46.4	46.9	-0.5	5

PHASE EQUILIBRIA IN FATS  
- theory and experiments -

X	Y	TAG	n	T <sub>f</sub> (kJ/mol)	predicted	residual	FREQ
0	4	CCM	34	3.0	-0.8	3.8	2
0	4	LLP	40	20.0	21.4	-1.4	1
0	4	MMS	46	35.6	37.0	-1.4	3
0	4	SSB	58	56.7	57.2	-0.5	2
0	6	CCP	36	2.0	3.2	-1.2	1
0	6	LLS	42	20.5	24.5	-4.0	2
0	8	CCS	38	32.0	9.6	22.4	0
0	10	66P	28	-7.4	-50.2	42.8	0
0	10	88S	34	5.0	-9.0	14.0	0
0	12	66S	30	6.8	-34.1	40.9	0
0	14	88B	38	26.0	9.0	17.0	0
0	16	66B	34	31.0	-9.1	40.1	0
1	0	P.17.P	49	48.2	46.5	1.7	1
1	0	S.19.S	55	55.5	55.4	0.1	1
2	0	CLC	32	6.0	0.8	5.2	1
2	0	LML	38	24.0	22.0	2.0	1
2	0	MPM	44	36.2	36.9	-0.7	3
2	0	PSP	50	47.2	48.0	-0.8	5
2	2	CLL	34	5.0	6.1	-1.1	1
2	2	LMM	40	22.0	25.7	-3.7	1
2	2	MPP	46	36.0	39.8	-3.8	1
2	2	PSS	52	50.1	50.4	-0.3	5
2	4	MPS	48	41.9	41.5	0.4	3
4	0	CMC	34	3.0	4.4	-1.4	1
4	0	LPL	40	19.0	24.7	-5.7	1
4	0	MSM	46	33.0	39.1	-6.1	1
4	0	SBS	58	56.0	58.2	-2.2	1
4	4	CMM	38	15.0	11.7	3.3	1
4	4	LPP	44	32.0	30.3	1.7	1
4	4	MSS	50	44.0	43.6	0.4	1
4	4	SBB	62	61.3	61.4	-0.1	1
6	0	CPC	36	6.0	6.9	-0.9	1
6	0	LSL	42	21.0	26.8	-5.8	1
6	0	PBP	54	47.4	51.4	-4.0	1
6	6	CPP	42	23.0	17.6	5.4	1
6	6	LSS	48	36.0	34.9	1.1	1
6	6	PBB	60	55.9	56.8	-0.9	1
8	0	CSC	38	34.0	11.5	22.5	0
8	8	CSS	46	42.5	26.6	15.9	0
12	0	6S6	30	0.0	-31.6	31.6	0

APPENDIX 1 PURE COMPONENT  
DATA

TABLE A1.5 : Melting points of the  $\beta'$ -modification of saturated TAGs.  
FREQ indicates the number of measurements that has been averaged.

X	Y	TAG	n	T <sub>f</sub> (kJ/mol)	predicted	residual	FREQ
-8	0	SCS	46	53.0	54.3	-1.3	1
-6	0	PCP	42	44.5	47.7	-3.2	2
-6	0	SLS	48	57.3	57.0	0.3	2
-4	0	NCM	38	40.0	39.4	0.6	1
-4	0	PLP	44	49.6	51.2	-1.6	2
-4	0	SMS	50	58.8	59.5	-0.7	3
-4	0	BSB	62	71.8	70.5	1.3	2
-2	2	PMS	48	56.1	53.5	2.6	1
0	0	888	24	-19.5	-16.7	-2.8	2
0	0	9.9.9	27	4.0	3.0	1.0	1
0	0	CCC	30	16.8	17.3	-0.5	2
0	0	11.11.11	33	27.9	28.2	-0.3	4
0	0	LLL	36	35.1	36.7	-1.6	9
0	0	13.13.13	39	41.8	43.6	-1.8	4
0	0	MMM	42	45.9	49.3	-3.4	5
0	0	15.15.15	45	50.8	54.1	-3.3	2
0	0	PPP	48	55.7	58.1	-2.4	6
0	0	17.17.17	51	61.5	61.6	-0.1	4
0	0	SSS	54	64.3	64.6	-0.3	7
0	0	19.19.19	57	65.6	67.3	-1.7	2
0	0	AAA	60	69.5	69.6	-0.1	2
0	0	21.21.21	63	71.0	71.7	-0.7	1
0	0	BBB	66	74.8	73.6	1.2	2
0	1	11.11.L	34	28.5	28.3	0.2	1
0	2	88C	26	5.5	-24.9	30.4	0
0	2	CCL	32	26.0	13.6	12.4	0
0	2	LLM	38	37.8	34.8	3.0	3
0	2	MMP	44	48.5	48.2	0.3	2
0	2	PPS	50	58.7	57.5	1.2	3
0	4	CCM	34	31.0	15.6	15.4	0
0	4	LLP	40	43.0	36.2	6.8	1
0	4	MMS	46	49.3	49.3	0.0	2
0	4	SSB	58	69.7	65.0	4.7	1
0	6	LLS	42	39.8	41.0	-1.2	2
0	8	CCS	38	38.0	30.2	7.8	1
0	10	66P	28	12.0	-22.2	34.2	0
0	10	88S	34	25.0	15.3	9.7	1
0	12	66S	30	17.0	-6.7	23.7	0

PHASE EQUILIBRIA IN FATS  
- theory and experiments -

X	Y	TAG	n	T <sub>f</sub> (kJ/mol)	predicted	residual	FREQ
1	0	P17P	49	61.2	60.9	0.3	2
1	0	S19S	55	69.8	66.7	3.1	1
2	0	8CB	26	18.5	14.3	4.2	1
2	0	CLC	32	37.7	34.5	3.2	2
2	0	LML	38	49.8	47.5	2.3	3
2	0	MPM	44	59.5	56.6	2.9	5
2	0	PSP	50	67.7	63.4	4.3	10
2	0	11.13.11	35	42.6	41.6	1.0	1
2	2	8CC	28	12.8	10.3	2.5	2
2	2	CLL	34	31.0	32.4	-1.4	1
2	2	LMM	40	42.0	46.4	-4.4	1
2	2	MPP	46	52.0	56.0	-4.0	1
2	2	PSS	52	61.8	63.0	-1.2	3
2	4	CLM	36	36.7	33.9	2.8	1
2	6	LMS	44	45.5	50.8	-5.3	1
2	8	CLS	40	40.0	43.4	-3.4	1
4	0	CMC	34	30.0	35.2	-5.2	1
4	0	LPL	40	46.7	48.2	-1.5	2
4	0	LPL	40	42.5	48.2	-5.7	1
4	0	MSM	46	55.2	57.2	-2.0	3
4	0	SBS	58	64.0	69.0	-5.0	1
4	4	CMM	38	38.0	34.7	3.3	1
4	4	LPP	44	49.5	48.1	1.4	1
4	4	MSS	50	58.3	57.4	0.9	2
4	4	SBB	62	71.5	69.4	2.1	1
4	6	LPS	46	47.0	51.5	-4.5	1
4	8	CMS	42	42.0	44.1	-2.1	1
6	0	CPC	36	36.0	34.8	1.2	1
6	0	LSL	42	43.0	48.0	-5.0	1
6	0	PBP	54	61.5	64.0	-2.5	1
6	6	CPP	42	41.0	39.3	1.7	1
6	6	LSS	48	51.4	51.4	0.0	8
6	6	PBB	60	66.1	66.2	-0.1	1
8	0	CSC	38	40.0	39.4	0.6	1
8	8	CSS	46	46.0	47.6	-1.6	1

APPENDIX 1 PURE COMPONENT  
DATA

TABLE A1.6 : Melting points of the  $\beta$ -modification of saturated TAGs.  
FREQ indicates the number of measurements that has been averaged.

X	Y	TAG	n	T <sub>f</sub> (kJ/mol)	predicted	residual	FREQ
-12	0	S6S	42	53.1	53.6	-0.5	2
-10	0	P6P	38	45.4	45.7	-0.3	3
-10	0	SBS	44	54.0	57.0	-3.0	5
-8	0	P8P	40	48.5	49.9	-1.4	1
-8	0	SCS	46	57.4	60.1	-2.7	4
-6	0	PCP	42	51.8	53.7	-1.9	2
-6	0	SLS	48	60.3	62.9	-2.6	3
-6	2	PCS	44	54.2	51.2	3.0	3
-4	0	MCM	38	43.5	46.0	-2.5	1
-4	0	PLP	44	53.9	57.2	-3.3	4
-4	0	SMS	50	63.3	65.6	-2.3	9
-4	2	PLS	46	57.0	54.9	2.1	2
-4	4	MCS	42	51.7	45.3	6.4	3
-2	0	CBC	28	20.0	19.9	0.1	1
-2	0	LCL	34	37.4	38.5	-1.1	3
-2	0	MLM	40	49.8	51.4	-1.6	2
-2	0	PMP	46	59.9	60.8	-0.9	6
-2	0	SPS	52	68.0	68.1	-0.1	8
-2	2	PMS	48	59.6	58.7	0.9	3
-2	4	MLS	44	54.5	50.9	3.6	2
-2	6	LCS	40	41.8	41.7	0.1	1
-1	0	P.15.P	47	56.5	57.7	-1.2	1
-1	0	S.17.S	53	65.7	64.9	0.8	2
0	0	888	24	9.1	11.4	-2.3	6
0	0	CCC	30	31.6	31.8	-0.2	8
0	0	LLL	36	45.7	45.9	-0.2	9
0	0	13.13.13	39	44.1	45.8	-1.7	5
0	0	MMM	42	57.1	56.2	0.9	10
0	0	15.15.15	45	54.6	55.5	-0.9	4
0	0	PPP	48	65.9	64.0	1.9	9
0	0	17.17.17	51	63.9	63.0	0.9	6
0	0	SSS	54	72.5	70.2	2.3	9
0	0	19.19.19	57	70.6	69.0	1.6	3
0	0	AAA	60	77.8	75.3	2.5	4
0	0	21.21.21	63	77.0	73.9	3.1	2
0	0	BBB	66	81.7	79.4	2.3	7
0	0	24.24.24	72	86.0	82.9	3.1	1

PHASE EQUILIBRIA IN FATS  
 - theory and experiments -

X	Y	TAG	n	T <sub>f</sub> (kJ/mol)	predicted	residual	FREQ
0	1	11.11.L	34	29.2	29.8	-0.6	2
0	2	88C	26	11.5	7.9	3.6	1
0	2	CCL	32	30.0	28.9	1.1	1
0	2	LLM	38	42.3	43.4	-1.1	4
0	2	MMP	44	53.3	54.1	-0.8	5
0	2	PPS	50	62.6	62.2	0.4	10
0	2	15.15.17	47	54.0	53.5	0.5	1
0	4	CCM	34	34.5	30.6	3.9	1
0	4	LLP	40	45.6	45.3	0.3	5
0	4	MMS	46	56.6	55.9	0.7	4
0	4	SSB	58	70.7	70.3	0.4	1
0	6	CCP	36	35.0	35.1	-0.1	1
0	6	LLS	42	45.1	48.7	-3.6	8
0	8	CCS	38	42.5	40.1	2.4	2
0	10	88S	34	31.0	29.3	1.7	2
0	12	66S	30	22.6	15.4	7.2	2
0	14	88B	38	38.0	40.1	-2.1	1
0	16	66B	34	34.0	29.3	4.7	1
2	0	8CB	26	20.5	17.9	2.6	1
2	0	CLC	32	34.0	36.4	-2.4	1
2	0	MPM	44	55.0	58.8	-3.8	1
2	0	PSP	50	65.3	66.2	-0.9	2
2	2	8CC	28	19.0	14.6	4.4	2
2	2	CLL	34	34.1	33.6	0.5	2
2	2	LMM	40	47.5	46.9	0.6	2
2	2	MPP	46	55.8	56.8	-1.0	4
2	2	PSS	52	64.4	64.4	0.0	9
2	4	LMP	42	48.5	48.8	-0.3	3
2	4	MPS	48	58.5	58.7	-0.2	5
2	6	LMS	44	49.0	52.0	-3.0	2
2	8	CLS	40	44.0	44.1	-0.1	1
4	0	CMC	34	34.0	37.7	-3.7	1
4	0	SBS	58	69.9	73.8	-3.9	2
4	4	CMM	38	43.5	36.7	6.8	1
4	4	LPP	44	54.4	50.5	3.9	4
4	4	MSS	50	60.9	60.5	0.4	6
4	4	SBB	62	73.5	73.9	-0.4	1
4	6	LPS	46	52.0	53.8	-1.8	1
4	8	CMS	42	45.0	45.7	-0.7	1

APPENDIX 1 PURE COMPONENT  
DATA

X	Y	TAG	n	T <sub>f</sub> (kJ/mol)	predicted	residual	FREQ
6	0	CPC	36	40.0	41.2	-1.2	1
6	0	LSL	42	49.8	53.8	-4.0	3
6	0	MAM	48	59.0	63.0	-4.0	1
6	0	PBP	54	65.5	70.0	-4.5	2
6	6	CPP	42	45.5	44.5	1.0	1
8	0	CSC	38	44.5	45.7	-1.2	1
8	8	CSS	46	48.3	52.8	-4.5	3
10	0	8S8	34	41.0	35.6	5.4	1
12	0	6S6	30	32.0	22.5	9.5	1

PHASE EQUILIBRIA IN FATS  
- theory and experiments -

UNSATURATED TAGs

TABLE A1.7 : Enthalpy of fusion for the  $\alpha$ -modification of unsaturated TAGs. Data marked by a \* include measurements from this work. FREQ indicates the number of measurements that has been averaged.

X	Y	TAG	n	$\Delta H_f$ (kJ/mol)	predicted	residual	FREQ
-2	0	EPE	52	79	79	0	2*
0	0	SSO	54	71	81	-10	2*
0	0	SOS	54	73	81	-8	1
0	0	OOO	54	37	18	19	1
0	0	SEE	54	89	89	0	1*
0	0	EEE	54	78	78	0	1*
0	0	ESE	54	92	89	3	2*
0	2	PPE	50	118	88	30	0
0	2	PPO	50	53	68	-15	2*
2	0	PEP	50	122	91	31	0
2	0	POP	50	70	71	1	4*
2	2	POS	52	78	74	4	2
2	2	PEE	52	81	82	-1	2*



APPENDIX 1 PURE COMPONENT  
DATA

TABLE A1.8 : Enthalpy of fusion for the  $\beta'$ -modification of unsaturated TAGs. Data marked by a \* include measurements from this work. FREQ indicates the number of measurements that has been averaged.

X	Y	TAG	n	$\Delta H_f$ (kJ/mol)	predicted	residual	FREQ
-2	0	SPO	52	126	117	9	1
0	0	SOS	54	111	129	-18	2
0	0	SOO	54	110	101	9	1
0	0	SSO	54	125	129	-4	2*
0	0	OOO	54	79	73	6	1
0	2	PPO	50	111	101	10	2*
2	0	PEP	50	135	140	-5	1*
2	0	POP	50	104	128	-24	6
2	2	PSO	52	111	123	-12	1
2	2	POS	52	114	123	-9	1
2	2	POO	52	95	95	0	1

PHASE EQUILIBRIA IN FATS  
- theory and experiments -

TABLE A1.9 : Enthalpy of fusion for the  $\beta$ -modification of unsaturated TAGs. Data marked by a \* include measurements from this work. FREQ indicates the number of measurements that has been averaged.

X	Y	TAG	n	$\Delta H_f$ (kJ/mol)	predicted	residual	FREQ
-2	0	EPE	52	130	140	10	2
-2	0	OPO	52	126	111	14	1
0	0	EEE	54	148	144	4	11
0	0	ESE	54	155	160	-5	3
0	0	lll	54	84	78	6	1
0	0	SES	54	163	175	-12	2
0	0	SEE	54	155	160	-5	1
0	0	SOS	54	154	161	-7	5
0	0	OOO	54	100	101	1	5
0	2	PPE	50	157	151	6	3
0	2	SOA	56	158	160	-2	1
2	0	POP	50	140	143	-3	4
2	0	PlP	50	100	136	-36	0
2	0	PEP	50	150	158	-8	1
2	2	POS	52	150	143	7	2
2	2	PEE	52	134	141	-7	2

APPENDIX 1 PURE COMPONENT  
DATA

TABLE A1.10 : Melting points of the  $\alpha$ -modification of unsaturated TAGs. FREQ indicates the number of measurements that has been averaged, OMOD indicates the modification that was originally reported for the melting point.

TAG	T <sub>f</sub> (kJ/mol)	predicted	residual	FREQ	OMOD
CCE	15	8.9	6.1	1	?
COC	-16.4	-22.8	6.4	1	alpha
LLI	15.5	17	-1.5	1	?
LLL	-11.5	-15.6	4.1	1	?
MML	20.5	22.2	-1.7	1	?
MLL	-8.5	-7.6	-0.9	1	?
MOM	11.7	4.8	6.9	2	alpha
PPO	18.4	16.8	1.6	4	alpha
PSI	36.5	32.6	3.9	1	?
PSO	25.9	21.3	4.6	2	alpha
PEP	39.4	35.6	3.8	2	alpha
PEE	22.8	26.1	-3.3	1	?
PIO	13.2	11.2	2	1	?
POP	16.6	17.6	-1	6	alpha
POS	19.6	21.3	-1.7	4	alpha
POI	13.3	11.2	2.1	1	?
SES	41.5	44	-2.5	2	alpha
SES	46.5	44	2.5	0	$\beta'$
SIS	37.9	37.3	0.6	3	?
SOS	22.9	27.2	-4.3	8	alpha
88E	3	5.4	-2.4	1	?
EPE	26	27	-1	1	alpha
EPE	32	27	5	0	$\beta'$
ESS	43	44	-1	1	?
ESE	34	32	2	1	alpha
EES	28.8	32	-3.2	1	alpha
EEE	15.8	19.1	-3.3	4	alpha
LPS	34.2	33.1	1.1	1	?
LPO	11.7	11.1	0.6	1	?
LSI	-3	0.2	-3.2	1	?
LSO	16.5	15.8	0.7	1	?
LLO	-16.4	-15.6	-0.8	2	?
LLeO	-24.7	-22.5	-2.2	1	?
LOO	-2.2	-5.7	3.5	1	?

PHASE EQUILIBRIA IN FATS  
 - theory and experiments -

TAG	T <sub>f</sub> (kJ/mol)	predicted	residual	FREQ	OMOD
leSl	-9.2	-7.9	-1.3	1	?
leSO	5.2	6.1	-0.9	1	?
lelS	-8.3	-7.9	-0.4	2	?
lelO	-22.4	-22.5	0.1	2	?
lelele	-44.6	-42.8	-1.8	1	alpha
leleO	-17.8	-19.9	2.1	2	?
leOS	-2.5	6.1	-8.6	1	?
OPS	17.9	22.1	-4.2	2	alpha
OSS	30.3	27.2	3.1	6	alpha
OSO	1	-0.7	1.7	1	alpha
OleO	-15	-14.3	-0.7	1	?
OOO	-33.7	-28.8	-4.9	4	alpha

APPENDIX 1 PURE COMPONENT  
DATA

TABLE A1.11 : Melting points of the  $\beta'$ -modification of unsaturated TAGs. FREQ indicates the number of measurements that has been averaged, OMOD indicates the modification that was originally reported for the melting point.

TAG	T <sub>f</sub> (kJ/mol)	predicted	residual	FREQ	OMOD
CCO	4.4	2.7	1.7	2	?
CEE	25	20.1	4.9	1	?
LLO	18	15.7	2.3	2	?
MOM	26.4	26.4	0	2	$\beta'$
PPL	26.5	24.9	1.6	1	?
PPO	34.6	34.2	0.4	8	$\beta'$
PSO	40	38	2	6	$\beta'$
PES	48.5	51.4	-2.9	1	?
PLL	-4.2	-2.9	-1.3	3	?
PlEl	-7.5	-6.2	-1.3	1	?
PlEle	-10.5	-10.2	-0.3	1	?
POP	33.2	34.8	-1.6	8	$\beta'$
SOS	37	42.2	-5.2	9	$\beta'$
SOS	43	42.2	0.8	0	$\beta$
ESS	56.7	54.9	1.8	1	?
ESE	43.2	45.1	-1.9	0	$\beta$
EEE	37	35.7	1.3	1	$\beta'$
lPl	-3	-2.3	-0.7	1	?
lls	2.5	3.8	-1.3	2	?
lll	-25.3	-25	-0.3	3	$\beta'$
lOS	-3.5	-1.2	-2.3	1	?
lOl	-39	-46.5	7.5	1	?
lePl	-4	-4	0	1	?
leSS	27.8	28.1	-0.3	2	?
lelle	-15.5	-15.5	0	1	?
lelel	-16.5	-15.5	-1	1	?
leOl	-28.5	-31.7	3.2	1	?
leOle	-11.1	-14.9	3.8	2	?
OSS	41.9	42.2	-0.3	10	$\beta'$
OSO	20.5	19.3	1.2	1	$\beta'$
Ols	-10.4	-1.2	-9.2	2	?
OleS	14.2	7.6	6.6	1	?
OOA	29.2	23	6.2	1	?
OOB	33.3	25.8	7.5	1	?
O.O.24	36.1	27.4	8.7	1	?
OOO	-10	-3.4	-6.6	5	$\beta'$

PHASE EQUILIBRIA IN FATS  
- theory and experiments -

TABLE A1.12 : Melting points of the  $\beta$ -modification of unsaturated TAGs. FREQ indicates the number of measurements that has been averaged, OMOD indicates the modification that was originally reported for the melting point.

TAG	T <sub>f</sub> (kJ/mol)	predicted	residual	FREQ	OMOD
CCl	-0.5	-9.7	9.2	1	?
CMO	13.9	16.8	-2.9	1	?
COC	-4.8	1.6	-6.4	0	$\beta'$
COC	5.9	1.6	4.3	2	$\beta$
COO	-0.3	5	-5.3	2	?
LLE	27	31.6	-4.6	1	?
LPO	29.5	24.6	4.9	1	?
LEE	35.5	38	-2.5	1	?
LOL	16.5	15.8	0.7	0	$\beta'$
LOO	5.1	4.7	0.4	3	?
MME	39.5	40.9	-1.4	1	?
MMO	23.9	22.4	1.5	2	?
MEE	40	39.8	0.2	1	?
MOM	28	28	0	2	$\beta$
MOP	27	30	-3	1	?
MOS	27	32.7	-5.7	1	?
MOO	12.8	8.3	4.5	4	?
PPE	50.2	50.1	0.1	3	?
PEP	55.3	53.7	1.6	4	$\beta$
PEP	53.9	53.7	0.2	0	$\beta'$
PEE	44.2	44.1	0.1	3	?
PlP	27.1	27.6	-0.5	2	$\beta$
PLS	24.5	28.8	-4.3	1	?
POP	37.2	37.6	-0.4	10	$\beta$
POS	31	38	-7	0	$\beta'$
POS	37.1	38	-0.9	8	$\beta$
POO	18.5	14.6	3.9	0	$\beta'$
SES	60.5	59.3	1.2	3	$\beta$
SlEs	35.8	31.4	4.4	2	?
SOA	41.5	44	-2.5	1	$\beta$

APPENDIX 1 PURE COMPONENT  
DATA

TAG	T <sub>f</sub> (kJ/mol)	predicted	residual	FREQ	OMOD
EPE	44.5	46.9	-2.4	1	$\beta$
ESS	61.1	59.3	1.8	4	$\beta$
ESE	49.7	50.2	-0.5	2	$\beta$
EES	49.7	50.2	-0.5	5	$\beta$
EEE	42.2	44	-1.8	9	$\beta$
LSS	35.8	35.4	0.4	4	?
LLL	-12.3	-14	1.7	6	$\beta$
leleS	-0.5	-0.5	0	1	?
lelele	-24.2	-23.5	-0.7	3	$\beta$
leOO	-13.1	-12	-1.1	2	?
OPS	40.2	41	-0.8	0	$\beta'$
OPO	19.6	17.9	1.7	3	$\beta$
OSO	23.9	22.7	1.2	4	$\beta$
OLO	-9.5	-7	-2.5	1	?
OOS	23.5	22.7	0.8	0	$\beta'$
OOO	4.8	6.1	-1.3	9	$\beta$
PEP	54	51.2	2.8	0	?

APPENDIX 2. SPECIFIC RETENTION VOLUMES OF SEVERAL PROBES IN STATIONARY PHASES OF LIQUID TAGs

APPENDIX 2. SPECIFIC RETENTION VOLUMES OF SEVERAL PROBES IN STATIONARY PHASES OF LIQUID TAGs

Specific retention volume in ml/g. Stationary phase: SSS

T (°C)	82	92	102	112	123	133
n-pentane	16.856	13.332	10.611	8.567		
n-hexane	38.053	29.16	22.595	18.307	14.618	11.571
n-heptane	88.048	64.449	48.319	39.669	29.083	22.295
2-methyl-pent.	28.852	23.087	18.014	14.722	11.722	9.36
3-methyl-pent.	33.438	26.465	20.88	16.188	13.428	10.789
benzene	88.658	65.532	50.591	39.684	31.332	24.767
toluene	218.379	154.476	114.394	85.939	64.479	50.534
cyclohexane	73.4	55.932	42.915	33.832	26.582	20.903

Specific retention volume in ml/g. Stationary phase: MMM

T (°C)	82	92	102	112	123	133
n-pentane	16.448	13.525	11.09	8.323		
n-hexane	39.175	30.356	23.319	18.389	14.449	11.715
n-heptane	90.897	66.559	50.618	38.246	29.328	23.399
2-methyl-pent.	30.691	23.922	18.619	14.482	12.019	9.926
3-methyl-pent.	34.607	27.125	21.358	16.77	13.487	11.41
benzene	97.106	72.451	54.744	42.351	33.476	26.445
toluene	235.44	169.84	123.941	91.414	69.741	53.632
cyclohexane	74.389	57.106	44.007	34.218	26.791	21.699



PHASE EQUILIBRIA IN FATS  
- theory and experiments -

Specific retention volume in ml/g. Stationary phase: 8C8

T (°C)	82	92	102	112	123	133
n-pentane	15.803	12.58	10.341	8.067		
n-hexane	37.093	28.536	22.103	17.575	14.291	11.052
n-heptane	84.266	61.824	47.214	36.302	28.01	22.596
2-methyl-pent.	28.69	22.432	17.473	13.829	11.433	9.33
3-methyl-pent.	33.008	25.125	19.726	15.558	12.576	10.561
benzene	105.237	77.315	59	46.098	34.87	27.754
toluene	250.008	177.156	130.416	97.67	72.598	55.754
cyclohexane	68.781	52.18	40.569	31.692	24.866	20.14

Specific retention volume in ml/g. Stationary phase: 0.4487 SSS, 0.5513 MMM

T (°C)	82	92	102	112	123	133
n-pentane	15.772	12.92	10.023	8.432		
n-hexane	38.571	29.43	22.959	18.083	14.644	11.976
n-heptane	88.55	65.675	49.205	37.647	29.347	23.427
2-methyl-pent.	29.374	22.84	18.173	14.563	11.875	9.806
3-methyl-pent.	33.769	26.388	20.544	16.667	13.366	11.047
benzene	93.42	69.591	53.302	41.705	32.528	25.958
toluene	226.576	162.709	119.042	89.083	67.384	52.15
cyclohexane	73.139	56.066	43.033	34.312	26.868	21.905

Specific retention volume in ml/g. Stationary phase: 0.7116 SSS, 0.2884 MMM

T (°C)	82	92	102	112	123	133
n-pentane	15.637	12.695	10.335	8.961		
n-hexane	37.808	29.054	22.138	18.762	14.216	11.513
n-heptane	87.566	64.7	48.113	38.308	28.667	22.664
2-methyl-pent.	29.191	22.873	17.671	14.681	11.656	9.642
3-methyl-pent.	33.639	26.154	20.204	16.969	13.17	10.806
benzene	89.447	67.982	51.08	41.244	31.129	24.872
toluene	216.024	157.377	114.093	88.601	65.358	50.193
cyclohexane	71.81	55.042	42.012	34.242	26.328	21.026

APPENDIX 2. SPECIFIC RETENTION VOLUMES OF SEVERAL PROBES IN STATIONARY PHASES OF LIQUID TAGs

Specific retention volume in ml/g. Stationary phase: 0.1557 SSS, 0.8443 8C8

T (°C)	82	92	102	112	123	133
n-pentane	16.106	12.78	10.684	7.576		
n-hexane	38.33	29.045	23.253	18.239	15.18	11.53
n-heptane	89.874	65.641	49.02	37.321	29.777	22.787
2-methyl-pent.	29.958	22.945	18.225	14.872	12.261	9.598
3-methyl-pent.	34.145	26.14	20.739	16.836	13.721	10.981
benzene	103.725	76.097	58.447	44.336	35.324	27.454
toluene	249.649	176.011	129.15	95.406	73.275	56.006
cyclohexane	72.801	54.314	41.793	33.111	26.712	20.865

Specific retention volume in ml/g. Stationary phase: 0.3593 SSS, 0.6407 8C8

T (°C)	82	92	102	112	123	133
n-pentane	15.707	12.973	10.513	8.432		
n-hexane	38.224	29.198	22.737	18.077	14.426	11.369
n-heptane	88.634	63.696	48.437	37.146	28.879	22.157
2-methyl-pent.	29.616	22.65	17.992	14.799	11.769	9.388
3-methyl-pent.	33.493	25.654	20.25	16.368	12.962	10.658
benzene	98.094	71.955	54.47	42.629	33.273	26.636
toluene	235.818	166.864	121.852	91.705	68.986	52.84
cyclohexane	72.015	53.896	41.858	32.677	26.331	21.08

Specific retention volume in ml/g. Stationary phase: 0.6023 SSS, 0.3977 8C8

T (°C)	82	92	102	112	123	133
n-pentane	16.053	12.907	10.38	8.446		
n-hexane	38.167	28.82	23.03	18.049	14.425	11.9
n-heptane	88.696	65.02	49.16	37.255	28.732	23.11
2-methyl-pent.	29.275	23.16	18.376	14.462	11.607	9.706
3-methyl-pent.	33.845	26.658	20.643	16.313	13.603	11.093
benzene	93.481	70.449	53.696	41.189	32.5	26.462
toluene	226.756	162.489	119.081	88.857	67.427	52.692
cyclohexane	72.627	55.369	42.955	33.206	26.383	21.492



PHASE EQUILIBRIA IN FATS  
- theory and experiments -

APPENDIX 3. PURITY OF THE TAGS USED IN CHAPTER 7

TAG	purity (%)	main impurities
SSS	99.6	-
PSP	99.3	-
MPM	>99.6	-
SEE	91.4	SES 8%
ESE	94.3	4.5% SSE, 1% SEO
PEE	91.1	8.6% PEP, PPE, EPE
EPE	89.8	9.1% PEP, PPE, PEE, 1.1% PEO
EEE	96.8	1.7% ESE, SEE
SOS	99.5	-
SSO	90.7	4% SOS, 3% SSE
POP	99.0	1% PEP
PPO	98.5	1.5% PPO



PHASE EQUILIBRIA IN FATS  
- theory and experiments -

APPENDIX 4. BINARY PHASE DIAGRAMS OF TAGs -data

(x in mol fraction, solidus and liquidus in °C)

<p>SSS-PSS</p> <table border="1"> <thead> <tr> <th>x</th> <th>solidus</th> <th>liquidus</th> </tr> </thead> <tbody> <tr><td>0.00</td><td>72.5</td><td>72.5</td></tr> <tr><td>0.11</td><td>67.7</td><td>71.8</td></tr> <tr><td>0.29</td><td>67.5</td><td>71.2</td></tr> <tr><td>0.46</td><td>67.4</td><td>70.4</td></tr> <tr><td>0.58</td><td></td><td>68.5</td></tr> <tr><td>0.74</td><td></td><td>67.3</td></tr> <tr><td>0.85</td><td></td><td>67.1</td></tr> <tr><td>1.00</td><td>67.2</td><td>67.2</td></tr> </tbody> </table>	x	solidus	liquidus	0.00	72.5	72.5	0.11	67.7	71.8	0.29	67.5	71.2	0.46	67.4	70.4	0.58		68.5	0.74		67.3	0.85		67.1	1.00	67.2	67.2	<p>SSS-PSP</p> <table border="1"> <thead> <tr> <th>x</th> <th>solidus</th> <th>liquidus</th> </tr> </thead> <tbody> <tr><td>0.00</td><td>72.5</td><td>72.7</td></tr> <tr><td>0.19</td><td>65.2</td><td>71.6</td></tr> <tr><td>0.20</td><td></td><td>71.4</td></tr> <tr><td>0.32</td><td>65.4</td><td>71.3</td></tr> <tr><td>0.40</td><td></td><td>69.9</td></tr> <tr><td>0.50</td><td></td><td>68.6</td></tr> <tr><td>0.50</td><td>65.6</td><td>69.0</td></tr> <tr><td>0.62</td><td>65.4</td><td>68.2</td></tr> <tr><td>0.70</td><td></td><td>66.0</td></tr> <tr><td>0.80</td><td>66.1</td><td>67.3</td></tr> <tr><td>0.88</td><td>65.7</td><td>67.8</td></tr> <tr><td>1.00</td><td>68.4</td><td>68.4</td></tr> <tr><td>1.00</td><td></td><td>68.7</td></tr> </tbody> </table>	x	solidus	liquidus	0.00	72.5	72.7	0.19	65.2	71.6	0.20		71.4	0.32	65.4	71.3	0.40		69.9	0.50		68.6	0.50	65.6	69.0	0.62	65.4	68.2	0.70		66.0	0.80	66.1	67.3	0.88	65.7	67.8	1.00	68.4	68.4	1.00		68.7	<p>SSS-SPS</p> <table border="1"> <thead> <tr> <th>x</th> <th>solidus</th> <th>liquidus</th> </tr> </thead> <tbody> <tr><td>0.00</td><td>72.5</td><td>72.5</td></tr> <tr><td>0.14</td><td>64.8</td><td>71.8</td></tr> <tr><td>0.31</td><td>65.2</td><td>71.1</td></tr> <tr><td>0.45</td><td>65.0</td><td>70.4</td></tr> <tr><td>0.51</td><td>65.4</td><td>69.5</td></tr> <tr><td>0.56</td><td>65.9</td><td>69.5</td></tr> <tr><td>0.69</td><td></td><td>65.3</td></tr> <tr><td>0.76</td><td></td><td>65.8</td></tr> <tr><td>0.90</td><td></td><td>66.4</td></tr> <tr><td>1.00</td><td>67.5</td><td>67.5</td></tr> </tbody> </table>	x	solidus	liquidus	0.00	72.5	72.5	0.14	64.8	71.8	0.31	65.2	71.1	0.45	65.0	70.4	0.51	65.4	69.5	0.56	65.9	69.5	0.69		65.3	0.76		65.8	0.90		66.4	1.00	67.5	67.5																																																																																										
x	solidus	liquidus																																																																																																																																																																																																
0.00	72.5	72.5																																																																																																																																																																																																
0.11	67.7	71.8																																																																																																																																																																																																
0.29	67.5	71.2																																																																																																																																																																																																
0.46	67.4	70.4																																																																																																																																																																																																
0.58		68.5																																																																																																																																																																																																
0.74		67.3																																																																																																																																																																																																
0.85		67.1																																																																																																																																																																																																
1.00	67.2	67.2																																																																																																																																																																																																
x	solidus	liquidus																																																																																																																																																																																																
0.00	72.5	72.7																																																																																																																																																																																																
0.19	65.2	71.6																																																																																																																																																																																																
0.20		71.4																																																																																																																																																																																																
0.32	65.4	71.3																																																																																																																																																																																																
0.40		69.9																																																																																																																																																																																																
0.50		68.6																																																																																																																																																																																																
0.50	65.6	69.0																																																																																																																																																																																																
0.62	65.4	68.2																																																																																																																																																																																																
0.70		66.0																																																																																																																																																																																																
0.80	66.1	67.3																																																																																																																																																																																																
0.88	65.7	67.8																																																																																																																																																																																																
1.00	68.4	68.4																																																																																																																																																																																																
1.00		68.7																																																																																																																																																																																																
x	solidus	liquidus																																																																																																																																																																																																
0.00	72.5	72.5																																																																																																																																																																																																
0.14	64.8	71.8																																																																																																																																																																																																
0.31	65.2	71.1																																																																																																																																																																																																
0.45	65.0	70.4																																																																																																																																																																																																
0.51	65.4	69.5																																																																																																																																																																																																
0.56	65.9	69.5																																																																																																																																																																																																
0.69		65.3																																																																																																																																																																																																
0.76		65.8																																																																																																																																																																																																
0.90		66.4																																																																																																																																																																																																
1.00	67.5	67.5																																																																																																																																																																																																
<p>SSS-PPS</p> <table border="1"> <thead> <tr> <th>x</th> <th>solidus</th> <th>liquidus</th> </tr> </thead> <tbody> <tr><td>0.00</td><td></td><td>72.3</td></tr> <tr><td>0.10</td><td>68.8</td><td>71.8</td></tr> <tr><td>0.18</td><td>61.9</td><td>71.8</td></tr> <tr><td>0.20</td><td>65.4</td><td>70.8</td></tr> <tr><td>0.20</td><td></td><td>70.9</td></tr> <tr><td>0.30</td><td>61.2</td><td>69.9</td></tr> <tr><td>0.30</td><td>60.8</td><td>70.7</td></tr> <tr><td>0.30</td><td></td><td>70.2</td></tr> <tr><td>0.33</td><td>61.0</td><td>71.4</td></tr> <tr><td>0.40</td><td>61.1</td><td>69.6</td></tr> <tr><td>0.40</td><td></td><td>60.9</td></tr> <tr><td>0.50</td><td>61.0</td><td>68.9</td></tr> <tr><td>0.50</td><td>60.8</td><td>68.3</td></tr> <tr><td>0.50</td><td></td><td>60.6</td></tr> <tr><td>0.55</td><td>61.0</td><td>70.3</td></tr> <tr><td>0.59</td><td>60.8</td><td>67.3</td></tr> <tr><td>0.60</td><td>61.0</td><td>67.8</td></tr> <tr><td>0.65</td><td>60.9</td><td>66.2</td></tr> <tr><td>0.67</td><td>60.8</td><td>65.7</td></tr> <tr><td>0.67</td><td>61.1</td><td></td></tr> <tr><td>0.70</td><td>59.5</td><td>61.0</td></tr> <tr><td>0.70</td><td>60.2</td><td>61.2</td></tr> <tr><td>0.71</td><td>59.6</td><td>60.7</td></tr> <tr><td>0.73</td><td>62.3</td><td>69.3</td></tr> <tr><td>0.75</td><td>59.7</td><td>60.4</td></tr> <tr><td>0.75</td><td>59.7</td><td>60.8</td></tr> <tr><td>0.79</td><td>61.0</td><td>62.5</td></tr> <tr><td>0.80</td><td>59.8</td><td>60.4</td></tr> <tr><td>0.80</td><td>59.6</td><td>60.8</td></tr> <tr><td>0.85</td><td></td><td>60.7</td></tr> <tr><td>0.85</td><td></td><td>60.0</td></tr> <tr><td>0.85</td><td></td><td>60.4</td></tr> <tr><td>0.91</td><td></td><td>60.8</td></tr> <tr><td>0.91</td><td></td><td>60.5</td></tr> <tr><td>0.91</td><td></td><td>60.2</td></tr> <tr><td>0.94</td><td></td><td>61.6</td></tr> <tr><td>0.95</td><td></td><td>60.6</td></tr> <tr><td>0.95</td><td></td><td>61.1</td></tr> <tr><td>0.99</td><td></td><td>60.2</td></tr> <tr><td>0.99</td><td></td><td>61.7</td></tr> <tr><td>1.00</td><td>63.4</td><td>63.4</td></tr> <tr><td>1.00</td><td></td><td>62.5</td></tr> </tbody> </table>	x	solidus	liquidus	0.00		72.3	0.10	68.8	71.8	0.18	61.9	71.8	0.20	65.4	70.8	0.20		70.9	0.30	61.2	69.9	0.30	60.8	70.7	0.30		70.2	0.33	61.0	71.4	0.40	61.1	69.6	0.40		60.9	0.50	61.0	68.9	0.50	60.8	68.3	0.50		60.6	0.55	61.0	70.3	0.59	60.8	67.3	0.60	61.0	67.8	0.65	60.9	66.2	0.67	60.8	65.7	0.67	61.1		0.70	59.5	61.0	0.70	60.2	61.2	0.71	59.6	60.7	0.73	62.3	69.3	0.75	59.7	60.4	0.75	59.7	60.8	0.79	61.0	62.5	0.80	59.8	60.4	0.80	59.6	60.8	0.85		60.7	0.85		60.0	0.85		60.4	0.91		60.8	0.91		60.5	0.91		60.2	0.94		61.6	0.95		60.6	0.95		61.1	0.99		60.2	0.99		61.7	1.00	63.4	63.4	1.00		62.5	<p>SSS-PPP</p> <table border="1"> <thead> <tr> <th>x</th> <th>solidus</th> <th>liquidus</th> </tr> </thead> <tbody> <tr><td>0.00</td><td>72.5</td><td>72.5</td></tr> <tr><td>0.14</td><td>63.8</td><td>72.4</td></tr> <tr><td>0.19</td><td>64.0</td><td>72.0</td></tr> <tr><td>0.39</td><td>63.7</td><td>71.1</td></tr> <tr><td>0.49</td><td>64.0</td><td>70.6</td></tr> <tr><td>0.59</td><td>63.8</td><td>69.5</td></tr> <tr><td>0.73</td><td>63.7</td><td>66.3</td></tr> <tr><td>0.80</td><td>63.7</td><td>64.7</td></tr> <tr><td>0.87</td><td>63.8</td><td>65.1</td></tr> <tr><td>0.94</td><td>63.8</td><td>65.2</td></tr> <tr><td>1.00</td><td>65.7</td><td>65.7</td></tr> </tbody> </table>	x	solidus	liquidus	0.00	72.5	72.5	0.14	63.8	72.4	0.19	64.0	72.0	0.39	63.7	71.1	0.49	64.0	70.6	0.59	63.8	69.5	0.73	63.7	66.3	0.80	63.7	64.7	0.87	63.8	65.1	0.94	63.8	65.2	1.00	65.7	65.7	<p>PSS-PPS</p> <table border="1"> <thead> <tr> <th>x</th> <th>solidus</th> <th>liquidus</th> </tr> </thead> <tbody> <tr><td>0.00</td><td>66.2</td><td>66.2</td></tr> <tr><td>0.15</td><td></td><td>66.1</td></tr> <tr><td>0.29</td><td></td><td>64.9</td></tr> <tr><td>0.46</td><td></td><td>64.5</td></tr> <tr><td>0.58</td><td>63.3</td><td>64.2</td></tr> <tr><td>0.72</td><td>64.7</td><td>65.4</td></tr> <tr><td>0.89</td><td>65.7</td><td>66.6</td></tr> <tr><td>1.00</td><td>68.7</td><td>68.7</td></tr> </tbody> </table>	x	solidus	liquidus	0.00	66.2	66.2	0.15		66.1	0.29		64.9	0.46		64.5	0.58	63.3	64.2	0.72	64.7	65.4	0.89	65.7	66.6	1.00	68.7	68.7
x	solidus	liquidus																																																																																																																																																																																																
0.00		72.3																																																																																																																																																																																																
0.10	68.8	71.8																																																																																																																																																																																																
0.18	61.9	71.8																																																																																																																																																																																																
0.20	65.4	70.8																																																																																																																																																																																																
0.20		70.9																																																																																																																																																																																																
0.30	61.2	69.9																																																																																																																																																																																																
0.30	60.8	70.7																																																																																																																																																																																																
0.30		70.2																																																																																																																																																																																																
0.33	61.0	71.4																																																																																																																																																																																																
0.40	61.1	69.6																																																																																																																																																																																																
0.40		60.9																																																																																																																																																																																																
0.50	61.0	68.9																																																																																																																																																																																																
0.50	60.8	68.3																																																																																																																																																																																																
0.50		60.6																																																																																																																																																																																																
0.55	61.0	70.3																																																																																																																																																																																																
0.59	60.8	67.3																																																																																																																																																																																																
0.60	61.0	67.8																																																																																																																																																																																																
0.65	60.9	66.2																																																																																																																																																																																																
0.67	60.8	65.7																																																																																																																																																																																																
0.67	61.1																																																																																																																																																																																																	
0.70	59.5	61.0																																																																																																																																																																																																
0.70	60.2	61.2																																																																																																																																																																																																
0.71	59.6	60.7																																																																																																																																																																																																
0.73	62.3	69.3																																																																																																																																																																																																
0.75	59.7	60.4																																																																																																																																																																																																
0.75	59.7	60.8																																																																																																																																																																																																
0.79	61.0	62.5																																																																																																																																																																																																
0.80	59.8	60.4																																																																																																																																																																																																
0.80	59.6	60.8																																																																																																																																																																																																
0.85		60.7																																																																																																																																																																																																
0.85		60.0																																																																																																																																																																																																
0.85		60.4																																																																																																																																																																																																
0.91		60.8																																																																																																																																																																																																
0.91		60.5																																																																																																																																																																																																
0.91		60.2																																																																																																																																																																																																
0.94		61.6																																																																																																																																																																																																
0.95		60.6																																																																																																																																																																																																
0.95		61.1																																																																																																																																																																																																
0.99		60.2																																																																																																																																																																																																
0.99		61.7																																																																																																																																																																																																
1.00	63.4	63.4																																																																																																																																																																																																
1.00		62.5																																																																																																																																																																																																
x	solidus	liquidus																																																																																																																																																																																																
0.00	72.5	72.5																																																																																																																																																																																																
0.14	63.8	72.4																																																																																																																																																																																																
0.19	64.0	72.0																																																																																																																																																																																																
0.39	63.7	71.1																																																																																																																																																																																																
0.49	64.0	70.6																																																																																																																																																																																																
0.59	63.8	69.5																																																																																																																																																																																																
0.73	63.7	66.3																																																																																																																																																																																																
0.80	63.7	64.7																																																																																																																																																																																																
0.87	63.8	65.1																																																																																																																																																																																																
0.94	63.8	65.2																																																																																																																																																																																																
1.00	65.7	65.7																																																																																																																																																																																																
x	solidus	liquidus																																																																																																																																																																																																
0.00	66.2	66.2																																																																																																																																																																																																
0.15		66.1																																																																																																																																																																																																
0.29		64.9																																																																																																																																																																																																
0.46		64.5																																																																																																																																																																																																
0.58	63.3	64.2																																																																																																																																																																																																
0.72	64.7	65.4																																																																																																																																																																																																
0.89	65.7	66.6																																																																																																																																																																																																
1.00	68.7	68.7																																																																																																																																																																																																
	<p>PSS-SPS</p> <table border="1"> <thead> <tr> <th>x</th> <th>solidus</th> <th>liquidus</th> </tr> </thead> <tbody> <tr><td>0.00</td><td>66.3</td><td>66.3</td></tr> <tr><td>0.15</td><td></td><td>64.9</td></tr> <tr><td>0.30</td><td></td><td>64.6</td></tr> <tr><td>0.45</td><td></td><td>64.9</td></tr> <tr><td>0.59</td><td></td><td>64.9</td></tr> <tr><td>0.72</td><td></td><td>66.6</td></tr> <tr><td>0.89</td><td>66.0</td><td>67.4</td></tr> <tr><td>1.00</td><td>67.9</td><td>67.9</td></tr> </tbody> </table>	x	solidus	liquidus	0.00	66.3	66.3	0.15		64.9	0.30		64.6	0.45		64.9	0.59		64.9	0.72		66.6	0.89	66.0	67.4	1.00	67.9	67.9	<p>SSS-SPS</p> <table border="1"> <thead> <tr> <th>x</th> <th>solidus</th> <th>liquidus</th> </tr> </thead> <tbody> <tr><td>0.00</td><td>66.1</td><td>66.1</td></tr> <tr><td>0.14</td><td></td><td>65.0</td></tr> <tr><td>0.24</td><td></td><td>64.3</td></tr> <tr><td>0.38</td><td></td><td>63.8</td></tr> <tr><td>0.51</td><td></td><td>63.2</td></tr> <tr><td>0.68</td><td></td><td>62.8</td></tr> <tr><td>0.87</td><td></td><td>62.3</td></tr> <tr><td>1.00</td><td>63.5</td><td>63.5</td></tr> </tbody> </table>	x	solidus	liquidus	0.00	66.1	66.1	0.14		65.0	0.24		64.3	0.38		63.8	0.51		63.2	0.68		62.8	0.87		62.3	1.00	63.5	63.5																																																																																																																																										
x	solidus	liquidus																																																																																																																																																																																																
0.00	66.3	66.3																																																																																																																																																																																																
0.15		64.9																																																																																																																																																																																																
0.30		64.6																																																																																																																																																																																																
0.45		64.9																																																																																																																																																																																																
0.59		64.9																																																																																																																																																																																																
0.72		66.6																																																																																																																																																																																																
0.89	66.0	67.4																																																																																																																																																																																																
1.00	67.9	67.9																																																																																																																																																																																																
x	solidus	liquidus																																																																																																																																																																																																
0.00	66.1	66.1																																																																																																																																																																																																
0.14		65.0																																																																																																																																																																																																
0.24		64.3																																																																																																																																																																																																
0.38		63.8																																																																																																																																																																																																
0.51		63.2																																																																																																																																																																																																
0.68		62.8																																																																																																																																																																																																
0.87		62.3																																																																																																																																																																																																
1.00	63.5	63.5																																																																																																																																																																																																
	<p>PSS-PPP</p> <table border="1"> <thead> <tr> <th>x</th> <th>solidus</th> <th>liquidus</th> </tr> </thead> <tbody> <tr><td>0.00</td><td>66.1</td><td>66.1</td></tr> <tr><td>0.17</td><td>63.0</td><td>65.3</td></tr> <tr><td>0.25</td><td>62.4</td><td>64.9</td></tr> <tr><td>0.42</td><td>62.9</td><td>64.2</td></tr> <tr><td>0.53</td><td></td><td>62.7</td></tr> <tr><td>0.68</td><td>62.8</td><td>65.0</td></tr> <tr><td>0.90</td><td>62.8</td><td>66.0</td></tr> <tr><td>1.00</td><td>66.0</td><td>66.0</td></tr> </tbody> </table>	x	solidus	liquidus	0.00	66.1	66.1	0.17	63.0	65.3	0.25	62.4	64.9	0.42	62.9	64.2	0.53		62.7	0.68	62.8	65.0	0.90	62.8	66.0	1.00	66.0	66.0	<p>PSP-SPS</p> <table border="1"> <thead> <tr> <th>x</th> <th>solidus</th> <th>liquidus</th> </tr> </thead> <tbody> <tr><td>0.00</td><td>68.5</td><td>68.5</td></tr> <tr><td>0.20</td><td>65.2</td><td>68.1</td></tr> <tr><td>0.26</td><td>65.2</td><td>67.4</td></tr> <tr><td>0.37</td><td>65.3</td><td>66.1</td></tr> <tr><td>0.48</td><td></td><td>65.6</td></tr> <tr><td>0.53</td><td></td><td>65.2</td></tr> <tr><td>0.66</td><td>64.6</td><td>66.1</td></tr> <tr><td>0.79</td><td>64.6</td><td>66.7</td></tr> <tr><td>0.91</td><td>64.4</td><td>67.5</td></tr> <tr><td>1.00</td><td>67.6</td><td>67.6</td></tr> </tbody> </table>	x	solidus	liquidus	0.00	68.5	68.5	0.20	65.2	68.1	0.26	65.2	67.4	0.37	65.3	66.1	0.48		65.6	0.53		65.2	0.66	64.6	66.1	0.79	64.6	66.7	0.91	64.4	67.5	1.00	67.6	67.6																																																																																																																																				
x	solidus	liquidus																																																																																																																																																																																																
0.00	66.1	66.1																																																																																																																																																																																																
0.17	63.0	65.3																																																																																																																																																																																																
0.25	62.4	64.9																																																																																																																																																																																																
0.42	62.9	64.2																																																																																																																																																																																																
0.53		62.7																																																																																																																																																																																																
0.68	62.8	65.0																																																																																																																																																																																																
0.90	62.8	66.0																																																																																																																																																																																																
1.00	66.0	66.0																																																																																																																																																																																																
x	solidus	liquidus																																																																																																																																																																																																
0.00	68.5	68.5																																																																																																																																																																																																
0.20	65.2	68.1																																																																																																																																																																																																
0.26	65.2	67.4																																																																																																																																																																																																
0.37	65.3	66.1																																																																																																																																																																																																
0.48		65.6																																																																																																																																																																																																
0.53		65.2																																																																																																																																																																																																
0.66	64.6	66.1																																																																																																																																																																																																
0.79	64.6	66.7																																																																																																																																																																																																
0.91	64.4	67.5																																																																																																																																																																																																
1.00	67.6	67.6																																																																																																																																																																																																

APPENDIX 4

(x in mol fraction, solidus and liquidus in °C)

<p>PSP-PPS (De Bruyne)</p> <table border="1"> <thead> <tr> <th>x</th> <th>solidus</th> <th>liquidus</th> </tr> </thead> <tbody> <tr><td>0.00</td><td>68.6</td><td>68.6</td></tr> <tr><td>0.10</td><td>60.6</td><td>67.1</td></tr> <tr><td>0.21</td><td>60.4</td><td>66.2</td></tr> <tr><td>0.30</td><td>60.8</td><td>65.7</td></tr> <tr><td>0.40</td><td>60.8</td><td>64.8</td></tr> <tr><td>0.50</td><td>61.1</td><td>63.5</td></tr> <tr><td>0.60</td><td>60.7</td><td>62.7</td></tr> <tr><td>0.71</td><td>61.2</td><td>61.2</td></tr> <tr><td>0.9</td><td>61.3</td><td>62.4</td></tr> <tr><td>1.0</td><td>63.4</td><td>63.4</td></tr> </tbody> </table>	x	solidus	liquidus	0.00	68.6	68.6	0.10	60.6	67.1	0.21	60.4	66.2	0.30	60.8	65.7	0.40	60.8	64.8	0.50	61.1	63.5	0.60	60.7	62.7	0.71	61.2	61.2	0.9	61.3	62.4	1.0	63.4	63.4	<p>PSP-PPP</p> <table border="1"> <thead> <tr> <th>x</th> <th>solidus</th> <th>liquidus</th> </tr> </thead> <tbody> <tr><td>0.00</td><td>68.6</td><td>68.6</td></tr> <tr><td>0.20</td><td>61.7</td><td>67.4</td></tr> <tr><td>0.46</td><td>61.5</td><td>65.1</td></tr> <tr><td>0.66</td><td>61.7</td><td>63.2</td></tr> <tr><td>0.80</td><td>61.7</td><td>63.3</td></tr> <tr><td>1.00</td><td>65.8</td><td>65.8</td></tr> </tbody> </table>	x	solidus	liquidus	0.00	68.6	68.6	0.20	61.7	67.4	0.46	61.5	65.1	0.66	61.7	63.2	0.80	61.7	63.3	1.00	65.8	65.8	<p>SPS-PPS</p> <table border="1"> <thead> <tr> <th>x</th> <th>solidus</th> <th>liquidus</th> </tr> </thead> <tbody> <tr><td>0.00</td><td>67.6</td><td>67.6</td></tr> <tr><td>0.20</td><td></td><td>66.3</td></tr> <tr><td>0.34</td><td>61.1</td><td>65.7</td></tr> <tr><td>0.40</td><td>60.8</td><td>65.3</td></tr> <tr><td>0.54</td><td>61.1</td><td>64.9</td></tr> <tr><td>0.60</td><td>61.3</td><td>64.2</td></tr> <tr><td>0.75</td><td></td><td>62.7</td></tr> <tr><td>0.86</td><td>60.6</td><td>61.9</td></tr> <tr><td>0.92</td><td>60.3</td><td>62.2</td></tr> <tr><td>1.00</td><td>63.3</td><td>63.3</td></tr> </tbody> </table>	x	solidus	liquidus	0.00	67.6	67.6	0.20		66.3	0.34	61.1	65.7	0.40	60.8	65.3	0.54	61.1	64.9	0.60	61.3	64.2	0.75		62.7	0.86	60.6	61.9	0.92	60.3	62.2	1.00	63.3	63.3																																				
x	solidus	liquidus																																																																																																																											
0.00	68.6	68.6																																																																																																																											
0.10	60.6	67.1																																																																																																																											
0.21	60.4	66.2																																																																																																																											
0.30	60.8	65.7																																																																																																																											
0.40	60.8	64.8																																																																																																																											
0.50	61.1	63.5																																																																																																																											
0.60	60.7	62.7																																																																																																																											
0.71	61.2	61.2																																																																																																																											
0.9	61.3	62.4																																																																																																																											
1.0	63.4	63.4																																																																																																																											
x	solidus	liquidus																																																																																																																											
0.00	68.6	68.6																																																																																																																											
0.20	61.7	67.4																																																																																																																											
0.46	61.5	65.1																																																																																																																											
0.66	61.7	63.2																																																																																																																											
0.80	61.7	63.3																																																																																																																											
1.00	65.8	65.8																																																																																																																											
x	solidus	liquidus																																																																																																																											
0.00	67.6	67.6																																																																																																																											
0.20		66.3																																																																																																																											
0.34	61.1	65.7																																																																																																																											
0.40	60.8	65.3																																																																																																																											
0.54	61.1	64.9																																																																																																																											
0.60	61.3	64.2																																																																																																																											
0.75		62.7																																																																																																																											
0.86	60.6	61.9																																																																																																																											
0.92	60.3	62.2																																																																																																																											
1.00	63.3	63.3																																																																																																																											
<p>PSP-PPS (Perron)</p> <table border="1"> <thead> <tr> <th>x</th> <th>solidus</th> <th>liquidus</th> </tr> </thead> <tbody> <tr><td>0.00</td><td></td><td>68.2</td></tr> <tr><td>0.05</td><td>65.6</td><td>67.8</td></tr> <tr><td>0.10</td><td>64.1</td><td>67.5</td></tr> <tr><td>0.15</td><td>62.5</td><td>66.9</td></tr> <tr><td>0.20</td><td>62.9</td><td>66.4</td></tr> <tr><td>0.25</td><td>61.9</td><td>66.2</td></tr> <tr><td>0.30</td><td>61.6</td><td>65.6</td></tr> <tr><td>0.35</td><td>61.8</td><td>64.7</td></tr> <tr><td>0.40</td><td>60.6</td><td>64.1</td></tr> <tr><td>0.50</td><td>60.9</td><td>63.5</td></tr> <tr><td>0.60</td><td>60.9</td><td>61.9</td></tr> <tr><td>0.65</td><td>60.7</td><td>61.3</td></tr> <tr><td>0.71</td><td>60.9</td><td>61.8</td></tr> <tr><td>0.75</td><td>60.4</td><td>61.3</td></tr> <tr><td>0.80</td><td>60.6</td><td>61.5</td></tr> <tr><td>0.85</td><td>60.9</td><td>61.6</td></tr> <tr><td>0.90</td><td>60.4</td><td>61.5</td></tr> <tr><td>0.95</td><td>60.7</td><td>61.8</td></tr> <tr><td>1.00</td><td>62.2</td><td>62.2</td></tr> </tbody> </table>	x	solidus	liquidus	0.00		68.2	0.05	65.6	67.8	0.10	64.1	67.5	0.15	62.5	66.9	0.20	62.9	66.4	0.25	61.9	66.2	0.30	61.6	65.6	0.35	61.8	64.7	0.40	60.6	64.1	0.50	60.9	63.5	0.60	60.9	61.9	0.65	60.7	61.3	0.71	60.9	61.8	0.75	60.4	61.3	0.80	60.6	61.5	0.85	60.9	61.6	0.90	60.4	61.5	0.95	60.7	61.8	1.00	62.2	62.2	<p>SPS-PPP</p> <table border="1"> <thead> <tr> <th>x</th> <th>solidus</th> <th>liquidus</th> </tr> </thead> <tbody> <tr><td>0.00</td><td>67.7</td><td>67.7</td></tr> <tr><td>0.18</td><td>61.0</td><td>66.5</td></tr> <tr><td>0.51</td><td>60.2</td><td>63.8</td></tr> <tr><td>0.61</td><td></td><td>62.0</td></tr> <tr><td>0.79</td><td>60.8</td><td>63.3</td></tr> <tr><td>0.84</td><td>60.6</td><td>63.6</td></tr> <tr><td>1.00</td><td>66.0</td><td>66.0</td></tr> </tbody> </table>	x	solidus	liquidus	0.00	67.7	67.7	0.18	61.0	66.5	0.51	60.2	63.8	0.61		62.0	0.79	60.8	63.3	0.84	60.6	63.6	1.00	66.0	66.0	<p>PPS-PPP</p> <table border="1"> <thead> <tr> <th>x</th> <th>solidus</th> <th>liquidus</th> </tr> </thead> <tbody> <tr><td>0.00</td><td>63.2</td><td>63.2</td></tr> <tr><td>0.14</td><td></td><td>62.7</td></tr> <tr><td>0.29</td><td></td><td>61.6</td></tr> <tr><td>0.45</td><td></td><td>62.3</td></tr> <tr><td>0.63</td><td></td><td>62.0</td></tr> <tr><td>0.75</td><td>61.1</td><td>63.0</td></tr> <tr><td>0.83</td><td>61.4</td><td>64.4</td></tr> <tr><td>0.90</td><td>61.4</td><td>65.1</td></tr> <tr><td>1.0</td><td>63.7</td><td>65.7</td></tr> </tbody> </table>	x	solidus	liquidus	0.00	63.2	63.2	0.14		62.7	0.29		61.6	0.45		62.3	0.63		62.0	0.75	61.1	63.0	0.83	61.4	64.4	0.90	61.4	65.1	1.0	63.7	65.7									
x	solidus	liquidus																																																																																																																											
0.00		68.2																																																																																																																											
0.05	65.6	67.8																																																																																																																											
0.10	64.1	67.5																																																																																																																											
0.15	62.5	66.9																																																																																																																											
0.20	62.9	66.4																																																																																																																											
0.25	61.9	66.2																																																																																																																											
0.30	61.6	65.6																																																																																																																											
0.35	61.8	64.7																																																																																																																											
0.40	60.6	64.1																																																																																																																											
0.50	60.9	63.5																																																																																																																											
0.60	60.9	61.9																																																																																																																											
0.65	60.7	61.3																																																																																																																											
0.71	60.9	61.8																																																																																																																											
0.75	60.4	61.3																																																																																																																											
0.80	60.6	61.5																																																																																																																											
0.85	60.9	61.6																																																																																																																											
0.90	60.4	61.5																																																																																																																											
0.95	60.7	61.8																																																																																																																											
1.00	62.2	62.2																																																																																																																											
x	solidus	liquidus																																																																																																																											
0.00	67.7	67.7																																																																																																																											
0.18	61.0	66.5																																																																																																																											
0.51	60.2	63.8																																																																																																																											
0.61		62.0																																																																																																																											
0.79	60.8	63.3																																																																																																																											
0.84	60.6	63.6																																																																																																																											
1.00	66.0	66.0																																																																																																																											
x	solidus	liquidus																																																																																																																											
0.00	63.2	63.2																																																																																																																											
0.14		62.7																																																																																																																											
0.29		61.6																																																																																																																											
0.45		62.3																																																																																																																											
0.63		62.0																																																																																																																											
0.75	61.1	63.0																																																																																																																											
0.83	61.4	64.4																																																																																																																											
0.90	61.4	65.1																																																																																																																											
1.0	63.7	65.7																																																																																																																											
<p>SSS-III</p> <table border="1"> <thead> <tr> <th>x</th> <th>solidus</th> <th>liquidus</th> </tr> </thead> <tbody> <tr><td>0.00</td><td>72.6</td><td>72.6</td></tr> <tr><td>0.15</td><td>45.7</td><td></td></tr> <tr><td>0.25</td><td>66.7</td><td>71.0</td></tr> <tr><td>0.39</td><td>59.9</td><td>70.1</td></tr> <tr><td>0.48</td><td>45.7</td><td>69.2</td></tr> <tr><td>0.59</td><td>45.7</td><td>68.0</td></tr> <tr><td>0.68</td><td>45.7</td><td>66.9</td></tr> <tr><td>0.79</td><td>45.7</td><td>65.1</td></tr> <tr><td>0.85</td><td>45.7</td><td>63.6</td></tr> <tr><td>0.937</td><td>45.7</td><td>60.0</td></tr> <tr><td>0.955</td><td>45.7</td><td>58.4</td></tr> <tr><td>0.975</td><td></td><td>56.4</td></tr> <tr><td>0.980</td><td>45.7</td><td>56.1</td></tr> <tr><td>0.983</td><td></td><td>54.6</td></tr> <tr><td>0.988</td><td>53.4</td><td>53.4</td></tr> <tr><td>0.993</td><td>51.6</td><td>51.6</td></tr> <tr><td>0.995</td><td>47.6</td><td>47.6</td></tr> <tr><td>1.000</td><td>46.4</td><td>46.4</td></tr> </tbody> </table>	x	solidus	liquidus	0.00	72.6	72.6	0.15	45.7		0.25	66.7	71.0	0.39	59.9	70.1	0.48	45.7	69.2	0.59	45.7	68.0	0.68	45.7	66.9	0.79	45.7	65.1	0.85	45.7	63.6	0.937	45.7	60.0	0.955	45.7	58.4	0.975		56.4	0.980	45.7	56.1	0.983		54.6	0.988	53.4	53.4	0.993	51.6	51.6	0.995	47.6	47.6	1.000	46.4	46.4	<p>SSS-888</p> <table border="1"> <thead> <tr> <th>x</th> <th>solidus</th> <th>liquidus</th> </tr> </thead> <tbody> <tr><td>0.00</td><td>72.5</td><td>72.5</td></tr> <tr><td>0.23</td><td>50.2</td><td></td></tr> <tr><td>0.52</td><td>8.4</td><td>67.0</td></tr> <tr><td>0.78</td><td>8.4</td><td>65.9</td></tr> <tr><td>0.94</td><td>8.4</td><td>60.6</td></tr> <tr><td>0.96</td><td>7.0</td><td>59.1</td></tr> <tr><td>0.97</td><td>8.4</td><td>57.7</td></tr> <tr><td>0.99</td><td>8.4</td><td>54.1</td></tr> <tr><td>1.00</td><td>8.4</td><td>8.4</td></tr> </tbody> </table>	x	solidus	liquidus	0.00	72.5	72.5	0.23	50.2		0.52	8.4	67.0	0.78	8.4	65.9	0.94	8.4	60.6	0.96	7.0	59.1	0.97	8.4	57.7	0.99	8.4	54.1	1.00	8.4	8.4	<p>PPP-MMM</p> <table border="1"> <thead> <tr> <th>x</th> <th>solidus</th> <th>liquidus</th> </tr> </thead> <tbody> <tr><td>0.00</td><td>64.3</td><td>64.3</td></tr> <tr><td>0.11</td><td>64.0</td><td>64.0</td></tr> <tr><td>0.22</td><td>64.0</td><td>64.0</td></tr> <tr><td>0.32</td><td>61.8</td><td>61.8</td></tr> <tr><td>0.43</td><td>61.4</td><td>61.4</td></tr> <tr><td>0.53</td><td>60.1</td><td>60.1</td></tr> <tr><td>0.63</td><td>59.8</td><td>59.8</td></tr> <tr><td>0.72</td><td>57.2</td><td>57.2</td></tr> <tr><td>0.82</td><td>52.9</td><td>52.9</td></tr> <tr><td>0.91</td><td>53.2</td><td>53.2</td></tr> <tr><td>1.00</td><td>54.5</td><td>54.5</td></tr> </tbody> </table>	x	solidus	liquidus	0.00	64.3	64.3	0.11	64.0	64.0	0.22	64.0	64.0	0.32	61.8	61.8	0.43	61.4	61.4	0.53	60.1	60.1	0.63	59.8	59.8	0.72	57.2	57.2	0.82	52.9	52.9	0.91	53.2	53.2	1.00	54.5	54.5
x	solidus	liquidus																																																																																																																											
0.00	72.6	72.6																																																																																																																											
0.15	45.7																																																																																																																												
0.25	66.7	71.0																																																																																																																											
0.39	59.9	70.1																																																																																																																											
0.48	45.7	69.2																																																																																																																											
0.59	45.7	68.0																																																																																																																											
0.68	45.7	66.9																																																																																																																											
0.79	45.7	65.1																																																																																																																											
0.85	45.7	63.6																																																																																																																											
0.937	45.7	60.0																																																																																																																											
0.955	45.7	58.4																																																																																																																											
0.975		56.4																																																																																																																											
0.980	45.7	56.1																																																																																																																											
0.983		54.6																																																																																																																											
0.988	53.4	53.4																																																																																																																											
0.993	51.6	51.6																																																																																																																											
0.995	47.6	47.6																																																																																																																											
1.000	46.4	46.4																																																																																																																											
x	solidus	liquidus																																																																																																																											
0.00	72.5	72.5																																																																																																																											
0.23	50.2																																																																																																																												
0.52	8.4	67.0																																																																																																																											
0.78	8.4	65.9																																																																																																																											
0.94	8.4	60.6																																																																																																																											
0.96	7.0	59.1																																																																																																																											
0.97	8.4	57.7																																																																																																																											
0.99	8.4	54.1																																																																																																																											
1.00	8.4	8.4																																																																																																																											
x	solidus	liquidus																																																																																																																											
0.00	64.3	64.3																																																																																																																											
0.11	64.0	64.0																																																																																																																											
0.22	64.0	64.0																																																																																																																											
0.32	61.8	61.8																																																																																																																											
0.43	61.4	61.4																																																																																																																											
0.53	60.1	60.1																																																																																																																											
0.63	59.8	59.8																																																																																																																											
0.72	57.2	57.2																																																																																																																											
0.82	52.9	52.9																																																																																																																											
0.91	53.2	53.2																																																																																																																											
1.00	54.5	54.5																																																																																																																											

PHASE EQUILIBRIA IN FATS  
- theory and experiments -

Phase diagrams of TAGs

(x in mol fraction, solidus and liquidus in °C)

PPP-LLL			SSS-SES			SSS-SSE		
x	solidus	liquidus	x	solidus	liquidus	x	solidus	liquidus
0.00	65.1	65.1	0.00		72.2	0.00	72.2	72.2
0.12	63.9	64.9	0.10		71.7	0.10	69.8	71.9
0.17	59.7	64.2	0.20		71.2	0.20		71.2
0.25	56.0	63.8	0.30		70.6	0.2	68.0	71.5
0.31	55.6	63.5	0.40		69.9	0.3	67.3	71.2
0.32	53.6		0.50		69.5	0.30		70.6
0.33	46.1		0.60		69.0	0.40		70.0
0.36		63.1	0.70		68.3	0.4	65.6	70.9
0.37	45.7	62.9	0.80		67.5	0.50		69.2
0.44		62.4	0.90		66.6	0.5	64.6	70.2
0.46		61.9	1.0		65.5	0.60		68.4
0.49	45.7	61.7				0.6	64.1	68.6
0.66	45.7	59.6				0.69	63.1	66.5
0.75	45.7					0.70		67.4
0.80		56.5	SSS-SEE			0.80	62.5	65.5
0.82		55.7	x	solidus	liquidus	0.80		66.2
0.84		55.1	0.00		72.2	0.89	62.1	64.6
0.89		52.8	0.20		71.2	0.90		65.8
0.92	45.7		0.30		70.6	0.94	62.1	63.4
0.94		50.1	0.40		70.0	1.00	62.1	62.1
0.95		49.6	0.50		69.2			
0.967		47.1	0.60		68.4			
0.970		46.7	0.70		67.4			
0.973	45.7	45.7	0.80		66.2			
0.989		46.3	0.90		65.8			
0.995		46.4	1.00		63.4			
1.000	45.7	45.7						
PPP-SSE			PPP-EEE			LLL-EEE		
x	solidus	liquidus	x	solidus	liquidus	x	solidus	liquidus
0.00	65.8	65.8	0.00	65.4	65.4	0.00	46.0	46.0
0.05	60.8	64.5	0.05	64.2	65.1	0.05	44.8	46.0
0.10	59.5	64.2	0.09	64.2	65.0	0.15	43.5	46.0
0.14		63.0	0.14	63.7	65.1	0.21	42.6	45.9
0.21	57.6	62.9	0.19	62.9	64.7	0.30	41.5	44.8
0.29	56.4	62.3	0.23	61.6	64.5	0.36	40.4	45.1
0.41	55.6	61.3	0.28	61.4	64.2	0.40	39.3	44.3
0.50		59.8	0.33	61.0	64.3	0.45	38.9	44.1
0.54	56.2	58.7	0.38	60.0	65.0	0.50	38.9	44.1
0.56		58.3	0.43	59.0	64.6	0.55	38.1	43.3
0.59	55.7	58.6	0.48	55.9	64.6	0.60	40.0	42.5
0.61		59.3	0.53	55.4	64.7	0.67	37.7	42.6
0.64	56.2	59.8	0.58	52.2	64.4	0.70	37.3	39.6
0.67	56.1	60.4	0.63	50.6	63.0	0.74	37.1	38.2
0.70	56.0		0.68	46.9	62.5	0.80	37.8	39.1
0.76		61.3	0.73	43.9	61.3	0.84	37.8	39.7
0.81	56.0		0.78	40.3	61.2	0.89	38.4	40.2
0.87	57.1	61.6	0.84	40.0	60.0	0.95	38.9	40.0
0.92	59.3	61.9	0.89	39.8	58.0	1.00	39.5	40.3
1.00	61.9	61.9	0.95	39.3	55.0			
			1.00	40.3	40.3			



## APPENDIX 4

## Phase diagrams of TAGs

(x in mol fraction, solidus and liquidus in °C)

<p>SSS-SOS</p> <table> <thead> <tr> <th>x</th> <th>solidus</th> <th>liquidus</th> </tr> </thead> <tbody> <tr><td>0.00</td><td>72.8</td><td>72.8</td></tr> <tr><td>0.06</td><td>65.5</td><td></td></tr> <tr><td>0.17</td><td>53.6</td><td></td></tr> <tr><td>0.23</td><td>44.3</td><td></td></tr> <tr><td>0.27</td><td></td><td>70.9</td></tr> <tr><td>0.51</td><td>44.3</td><td>69.3</td></tr> <tr><td>0.61</td><td>44.3</td><td>68.3</td></tr> <tr><td>0.75</td><td>44.3</td><td>66.1</td></tr> <tr><td>0.83</td><td>44.3</td><td>64.5</td></tr> <tr><td>0.91</td><td>44.3</td><td>61.3</td></tr> <tr><td>0.95</td><td>44.3</td><td>57.8</td></tr> <tr><td>0.97</td><td>44.3</td><td>52.0</td></tr> <tr><td>0.99</td><td>44.3</td><td>44.8</td></tr> <tr><td>1.00</td><td>44.3</td><td>44.3</td></tr> </tbody> </table>	x	solidus	liquidus	0.00	72.8	72.8	0.06	65.5		0.17	53.6		0.23	44.3		0.27		70.9	0.51	44.3	69.3	0.61	44.3	68.3	0.75	44.3	66.1	0.83	44.3	64.5	0.91	44.3	61.3	0.95	44.3	57.8	0.97	44.3	52.0	0.99	44.3	44.8	1.00	44.3	44.3	<p>PPP-SOS</p> <table> <thead> <tr> <th>x</th> <th>solidus</th> <th>liquidus</th> </tr> </thead> <tbody> <tr><td>0.00</td><td>65.8</td><td>65.8</td></tr> <tr><td>0.09</td><td>61.6</td><td>65.5</td></tr> <tr><td>0.19</td><td>54.5</td><td>64.7</td></tr> <tr><td>0.26</td><td>50.0</td><td>64.2</td></tr> <tr><td>0.35</td><td>44.0</td><td>63.7</td></tr> <tr><td>0.47</td><td>40.6</td><td>62.6</td></tr> <tr><td>0.57</td><td>41.0</td><td>61.1</td></tr> <tr><td>0.69</td><td>41.2</td><td>59.0</td></tr> <tr><td>0.79</td><td>41.0</td><td>56.1</td></tr> <tr><td>0.88</td><td>41.6</td><td>49.5</td></tr> <tr><td>0.93</td><td>41.0</td><td>44.0</td></tr> <tr><td>0.94</td><td>41.6</td><td>41.3</td></tr> <tr><td>0.97</td><td>41.8</td><td>41.8</td></tr> <tr><td>1.00</td><td>42.3</td><td>42.3</td></tr> </tbody> </table>	x	solidus	liquidus	0.00	65.8	65.8	0.09	61.6	65.5	0.19	54.5	64.7	0.26	50.0	64.2	0.35	44.0	63.7	0.47	40.6	62.6	0.57	41.0	61.1	0.69	41.2	59.0	0.79	41.0	56.1	0.88	41.6	49.5	0.93	41.0	44.0	0.94	41.6	41.3	0.97	41.8	41.8	1.00	42.3	42.3	<p>PPP-POP</p> <table> <thead> <tr> <th>x</th> <th>solidus</th> <th>liquidus</th> </tr> </thead> <tbody> <tr><td>0.00</td><td>65.9</td><td>65.9</td></tr> <tr><td>0.06</td><td></td><td>65.4</td></tr> <tr><td>0.10</td><td>58.4</td><td>65.0</td></tr> <tr><td>0.13</td><td>49.6</td><td>64.6</td></tr> <tr><td>0.25</td><td>44.8</td><td>63.6</td></tr> <tr><td>0.35</td><td>35.2</td><td>62.7</td></tr> <tr><td>0.45</td><td></td><td>61.6</td></tr> <tr><td>0.56</td><td>35.2</td><td>60.5</td></tr> <tr><td>0.63</td><td>35.2</td><td>59.5</td></tr> <tr><td>0.80</td><td>34.5</td><td>56.4</td></tr> <tr><td>0.85</td><td></td><td>53.6</td></tr> <tr><td>0.88</td><td>34.7</td><td>50.7</td></tr> <tr><td>0.95</td><td></td><td>43.0</td></tr> <tr><td>0.97</td><td></td><td>39.5</td></tr> <tr><td>0.98</td><td></td><td>37.9</td></tr> <tr><td>0.99</td><td></td><td>37.1</td></tr> <tr><td>1.00</td><td>34.6</td><td>34.6</td></tr> </tbody> </table>	x	solidus	liquidus	0.00	65.9	65.9	0.06		65.4	0.10	58.4	65.0	0.13	49.6	64.6	0.25	44.8	63.6	0.35	35.2	62.7	0.45		61.6	0.56	35.2	60.5	0.63	35.2	59.5	0.80	34.5	56.4	0.85		53.6	0.88	34.7	50.7	0.95		43.0	0.97		39.5	0.98		37.9	0.99		37.1	1.00	34.6	34.6
x	solidus	liquidus																																																																																																																																																
0.00	72.8	72.8																																																																																																																																																
0.06	65.5																																																																																																																																																	
0.17	53.6																																																																																																																																																	
0.23	44.3																																																																																																																																																	
0.27		70.9																																																																																																																																																
0.51	44.3	69.3																																																																																																																																																
0.61	44.3	68.3																																																																																																																																																
0.75	44.3	66.1																																																																																																																																																
0.83	44.3	64.5																																																																																																																																																
0.91	44.3	61.3																																																																																																																																																
0.95	44.3	57.8																																																																																																																																																
0.97	44.3	52.0																																																																																																																																																
0.99	44.3	44.8																																																																																																																																																
1.00	44.3	44.3																																																																																																																																																
x	solidus	liquidus																																																																																																																																																
0.00	65.8	65.8																																																																																																																																																
0.09	61.6	65.5																																																																																																																																																
0.19	54.5	64.7																																																																																																																																																
0.26	50.0	64.2																																																																																																																																																
0.35	44.0	63.7																																																																																																																																																
0.47	40.6	62.6																																																																																																																																																
0.57	41.0	61.1																																																																																																																																																
0.69	41.2	59.0																																																																																																																																																
0.79	41.0	56.1																																																																																																																																																
0.88	41.6	49.5																																																																																																																																																
0.93	41.0	44.0																																																																																																																																																
0.94	41.6	41.3																																																																																																																																																
0.97	41.8	41.8																																																																																																																																																
1.00	42.3	42.3																																																																																																																																																
x	solidus	liquidus																																																																																																																																																
0.00	65.9	65.9																																																																																																																																																
0.06		65.4																																																																																																																																																
0.10	58.4	65.0																																																																																																																																																
0.13	49.6	64.6																																																																																																																																																
0.25	44.8	63.6																																																																																																																																																
0.35	35.2	62.7																																																																																																																																																
0.45		61.6																																																																																																																																																
0.56	35.2	60.5																																																																																																																																																
0.63	35.2	59.5																																																																																																																																																
0.80	34.5	56.4																																																																																																																																																
0.85		53.6																																																																																																																																																
0.88	34.7	50.7																																																																																																																																																
0.95		43.0																																																																																																																																																
0.97		39.5																																																																																																																																																
0.98		37.9																																																																																																																																																
0.99		37.1																																																																																																																																																
1.00	34.6	34.6																																																																																																																																																
<p>PPP-POO</p> <table> <thead> <tr> <th>x</th> <th>solidus</th> <th>liquidus</th> </tr> </thead> <tbody> <tr><td>0.00</td><td>65.7</td><td>65.7</td></tr> <tr><td>0.06</td><td>65.3</td><td>65.3</td></tr> <tr><td>0.08</td><td>64.5</td><td>64.5</td></tr> <tr><td>0.15</td><td>13.6</td><td>64.7</td></tr> <tr><td>0.32</td><td>14.7</td><td>63.3</td></tr> <tr><td>0.49</td><td>17.1</td><td>61.3</td></tr> <tr><td>0.68</td><td>17.7</td><td>58.1</td></tr> <tr><td>0.83</td><td>17.9</td><td>54.5</td></tr> <tr><td>0.92</td><td>18.5</td><td>50.0</td></tr> <tr><td>1.00</td><td>18.6</td><td>18.6</td></tr> </tbody> </table>	x	solidus	liquidus	0.00	65.7	65.7	0.06	65.3	65.3	0.08	64.5	64.5	0.15	13.6	64.7	0.32	14.7	63.3	0.49	17.1	61.3	0.68	17.7	58.1	0.83	17.9	54.5	0.92	18.5	50.0	1.00	18.6	18.6	<p>SES-SSE</p> <table> <thead> <tr> <th>x</th> <th>solidus</th> <th>liquidus</th> </tr> </thead> <tbody> <tr><td>0.00</td><td>65.4</td><td>65.4</td></tr> <tr><td>0.10</td><td>65.3</td><td>65.3</td></tr> <tr><td>0.20</td><td>65.2</td><td>65.2</td></tr> <tr><td>0.30</td><td>65.0</td><td>65.0</td></tr> <tr><td>0.40</td><td>64.9</td><td>64.9</td></tr> <tr><td>0.50</td><td>64.7</td><td>64.7</td></tr> <tr><td>0.60</td><td>64.5</td><td>64.5</td></tr> <tr><td>0.70</td><td>64.2</td><td>64.2</td></tr> <tr><td>0.80</td><td>64.0</td><td>64.0</td></tr> <tr><td>0.90</td><td>63.6</td><td>63.6</td></tr> <tr><td>1.00</td><td>63.3</td><td>63.3</td></tr> </tbody> </table>	x	solidus	liquidus	0.00	65.4	65.4	0.10	65.3	65.3	0.20	65.2	65.2	0.30	65.0	65.0	0.40	64.9	64.9	0.50	64.7	64.7	0.60	64.5	64.5	0.70	64.2	64.2	0.80	64.0	64.0	0.90	63.6	63.6	1.00	63.3	63.3	<p>SOS-POS</p> <table> <thead> <tr> <th>x</th> <th>solidus</th> <th>liquidus</th> </tr> </thead> <tbody> <tr><td>0.00</td><td>36.5</td><td>36.5</td></tr> <tr><td>0.10</td><td>34.2</td><td>36.5</td></tr> <tr><td>0.20</td><td>34.2</td><td>37.0</td></tr> <tr><td>0.30</td><td>34.5</td><td>38.5</td></tr> <tr><td>0.40</td><td>35.0</td><td>39.0</td></tr> <tr><td>0.50</td><td>35.5</td><td>40.5</td></tr> <tr><td>0.60</td><td>35.5</td><td>41.8</td></tr> <tr><td>0.70</td><td>36.5</td><td>42.5</td></tr> <tr><td>0.80</td><td>38.0</td><td>43.0</td></tr> <tr><td>0.90</td><td>40.5</td><td>43.5</td></tr> <tr><td>1.00</td><td>44.0</td><td>44.0</td></tr> </tbody> </table>	x	solidus	liquidus	0.00	36.5	36.5	0.10	34.2	36.5	0.20	34.2	37.0	0.30	34.5	38.5	0.40	35.0	39.0	0.50	35.5	40.5	0.60	35.5	41.8	0.70	36.5	42.5	0.80	38.0	43.0	0.90	40.5	43.5	1.00	44.0	44.0																																							
x	solidus	liquidus																																																																																																																																																
0.00	65.7	65.7																																																																																																																																																
0.06	65.3	65.3																																																																																																																																																
0.08	64.5	64.5																																																																																																																																																
0.15	13.6	64.7																																																																																																																																																
0.32	14.7	63.3																																																																																																																																																
0.49	17.1	61.3																																																																																																																																																
0.68	17.7	58.1																																																																																																																																																
0.83	17.9	54.5																																																																																																																																																
0.92	18.5	50.0																																																																																																																																																
1.00	18.6	18.6																																																																																																																																																
x	solidus	liquidus																																																																																																																																																
0.00	65.4	65.4																																																																																																																																																
0.10	65.3	65.3																																																																																																																																																
0.20	65.2	65.2																																																																																																																																																
0.30	65.0	65.0																																																																																																																																																
0.40	64.9	64.9																																																																																																																																																
0.50	64.7	64.7																																																																																																																																																
0.60	64.5	64.5																																																																																																																																																
0.70	64.2	64.2																																																																																																																																																
0.80	64.0	64.0																																																																																																																																																
0.90	63.6	63.6																																																																																																																																																
1.00	63.3	63.3																																																																																																																																																
x	solidus	liquidus																																																																																																																																																
0.00	36.5	36.5																																																																																																																																																
0.10	34.2	36.5																																																																																																																																																
0.20	34.2	37.0																																																																																																																																																
0.30	34.5	38.5																																																																																																																																																
0.40	35.0	39.0																																																																																																																																																
0.50	35.5	40.5																																																																																																																																																
0.60	35.5	41.8																																																																																																																																																
0.70	36.5	42.5																																																																																																																																																
0.80	38.0	43.0																																																																																																																																																
0.90	40.5	43.5																																																																																																																																																
1.00	44.0	44.0																																																																																																																																																
<p>SOS-POP</p> <table> <thead> <tr> <th>x</th> <th>solidus</th> <th>liquidus</th> </tr> </thead> <tbody> <tr><td>0.00</td><td>44.0</td><td>44.0</td></tr> <tr><td>0.10</td><td>38.5</td><td>43.5</td></tr> <tr><td>0.20</td><td>35.5</td><td>43.0</td></tr> <tr><td>0.30</td><td>35.0</td><td>42.5</td></tr> <tr><td>0.40</td><td>35.0</td><td>41.5</td></tr> <tr><td>0.50</td><td>34.0</td><td>40.0</td></tr> <tr><td>0.60</td><td>34.0</td><td>39.0</td></tr> <tr><td>0.70</td><td>33.5</td><td>37.0</td></tr> <tr><td>0.80</td><td>33.5</td><td>36.0</td></tr> <tr><td>0.90</td><td>33.5</td><td>36.5</td></tr> <tr><td>1.00</td><td>37.2</td><td>37.2</td></tr> </tbody> </table>	x	solidus	liquidus	0.00	44.0	44.0	0.10	38.5	43.5	0.20	35.5	43.0	0.30	35.0	42.5	0.40	35.0	41.5	0.50	34.0	40.0	0.60	34.0	39.0	0.70	33.5	37.0	0.80	33.5	36.0	0.90	33.5	36.5	1.00	37.2	37.2	<p>POS-POP</p> <table> <thead> <tr> <th>x</th> <th>solidus</th> <th>liquidus</th> </tr> </thead> <tbody> <tr><td>0.00</td><td>36.5</td><td>36.5</td></tr> <tr><td>0.10</td><td>34.0</td><td>36.2</td></tr> <tr><td>0.20</td><td>32.0</td><td>36.0</td></tr> <tr><td>0.30</td><td>31.0</td><td>35.5</td></tr> <tr><td>0.40</td><td>31.8</td><td>35.2</td></tr> <tr><td>0.50</td><td>31.5</td><td>34.0</td></tr> <tr><td>0.60</td><td>31.5</td><td>34.5</td></tr> <tr><td>0.70</td><td>31.5</td><td>35.5</td></tr> <tr><td>0.80</td><td>31.5</td><td>35.5</td></tr> <tr><td>0.90</td><td>34.0</td><td>37.0</td></tr> <tr><td>1.00</td><td>37.2</td><td>37.2</td></tr> </tbody> </table>	x	solidus	liquidus	0.00	36.5	36.5	0.10	34.0	36.2	0.20	32.0	36.0	0.30	31.0	35.5	0.40	31.8	35.2	0.50	31.5	34.0	0.60	31.5	34.5	0.70	31.5	35.5	0.80	31.5	35.5	0.90	34.0	37.0	1.00	37.2	37.2	<p>POP-PEP</p> <table> <thead> <tr> <th>x</th> <th>solidus</th> <th>liquidus</th> </tr> </thead> <tbody> <tr><td>0.00</td><td>33.0</td><td>33.0</td></tr> <tr><td>0.08</td><td>31.1</td><td>41.7</td></tr> <tr><td>0.16</td><td>31.5</td><td>45.3</td></tr> <tr><td>0.25</td><td>31.1</td><td>47.1</td></tr> <tr><td>0.50</td><td>31.1</td><td>52.9</td></tr> <tr><td>0.75</td><td>36.0</td><td>54.4</td></tr> <tr><td>1.00</td><td>57.0</td><td>57.0</td></tr> </tbody> </table>	x	solidus	liquidus	0.00	33.0	33.0	0.08	31.1	41.7	0.16	31.5	45.3	0.25	31.1	47.1	0.50	31.1	52.9	0.75	36.0	54.4	1.00	57.0	57.0																																																
x	solidus	liquidus																																																																																																																																																
0.00	44.0	44.0																																																																																																																																																
0.10	38.5	43.5																																																																																																																																																
0.20	35.5	43.0																																																																																																																																																
0.30	35.0	42.5																																																																																																																																																
0.40	35.0	41.5																																																																																																																																																
0.50	34.0	40.0																																																																																																																																																
0.60	34.0	39.0																																																																																																																																																
0.70	33.5	37.0																																																																																																																																																
0.80	33.5	36.0																																																																																																																																																
0.90	33.5	36.5																																																																																																																																																
1.00	37.2	37.2																																																																																																																																																
x	solidus	liquidus																																																																																																																																																
0.00	36.5	36.5																																																																																																																																																
0.10	34.0	36.2																																																																																																																																																
0.20	32.0	36.0																																																																																																																																																
0.30	31.0	35.5																																																																																																																																																
0.40	31.8	35.2																																																																																																																																																
0.50	31.5	34.0																																																																																																																																																
0.60	31.5	34.5																																																																																																																																																
0.70	31.5	35.5																																																																																																																																																
0.80	31.5	35.5																																																																																																																																																
0.90	34.0	37.0																																																																																																																																																
1.00	37.2	37.2																																																																																																																																																
x	solidus	liquidus																																																																																																																																																
0.00	33.0	33.0																																																																																																																																																
0.08	31.1	41.7																																																																																																																																																
0.16	31.5	45.3																																																																																																																																																
0.25	31.1	47.1																																																																																																																																																
0.50	31.1	52.9																																																																																																																																																
0.75	36.0	54.4																																																																																																																																																
1.00	57.0	57.0																																																																																																																																																

PHASE EQUILIBRIA IN FATS  
- theory and experiments -

Phase diagrams of TAGs

(x in mol fraction, solidus and liquidus in °C)

PPO-POO			PPO-OPO			POO-OPO		
x	solidus	liquidus	x	solidus	liquidus	x	solidus	liquidus
0.00	32.6	32.6	0.00	34.7	34.7	0.00	19.3	20.0
0.17	11.8	32.7	0.11	28.9	33.1	0.04	18.7	19.8
0.29	12.3	32.0	0.25	25.3	31.1	0.08	17.6	19.4
0.40	12.2	31.0	0.40	22.7	29.6	0.23	14.0	18.4
0.47	12.1	29.7	0.50	21.1	29.1	0.38	12.0	17.6
0.62	12.8	28.0	0.55	19.3	28.7	0.52	11.2	15.6
0.78	13.1	26.3	0.60	18.2	28.0	0.62	11.1	16.3
0.84	14.6	18.3	0.70	17.8	26.2	0.77	11.6	18.4
1.00	18.6	18.6	0.80	18.2	23.1	0.91	14.0	18.9
			0.85	17.8	20.2	1.00	19.8	19.8
			0.87	17.6	19.8			
			0.90	17.6	18.7			
			0.95	17.8	19.1			
			0.98	18.2	19.2			
			1.00	19.3	19.3			
SSS-OOO			PPP-OOO			SOS-OOO		
x	solidus	liquidus	x	solidus	liquidus	x	solidus	liquidus
0.00	73.9	73.9	0.00	64.5	64.5	0.00	42.8	42.8
0.01		72.5	0.10			0.12	42.4	42.4
0.11		71.9	0.20			0.33	41.3	41.3
0.29		70.3	0.30			0.52	40.3	40.3
0.33	5.4	68.9	0.40			0.81	35.3	35.3
0.51		68.4	0.50			0.90	32.1	32.1
0.54		64.5	0.60			0.96	30.0	30.0
0.58		64.2	0.70			0.98	28.2	28.2
0.62		65.4	0.80			1.00	5.4	5.4
0.71		64.9	0.83		54.3			
0.80		64.1	0.88		52.3			
0.83	5.4	65.4	0.90					
0.84		62.7	0.91		50.3			
0.84		60.7	0.93		49.0			
0.85		66.1	0.942		47.3			
0.88		60.0	0.956		44.7			
0.89	4.9	62.4	0.971		42.7			
0.89		66.6	0.978		41.0			
0.899		61.9	0.989		38.0			
0.907		57.3	0.991		35.7			
0.920		56.0	0.993		34.3			
0.920		54.0	0.996		32.7			
0.947		54.7	1.000	6.7	6.7			
0.949		57.8						
0.960		52.0						
0.960		51.3						
0.974		47.3						
0.974		44.7						
0.975		55.0						
0.980		50.0						
0.987		41.3						
1.000	5.4	5.4						



#### CURRICULUM VITAE

De schrijver van dit proefschrift volgde van 1971 to 1977 de VWO-opleiding aan het Christelijk College Nassau-Veluwe te Harderwijk. In 1980 legde hij het kandidaatsexamen Scheikunde af aan de Vrije Universiteit te Amsterdam. In 1981/82 was hij werkzaam bij het 'Lesotho Science Pre-entry Course' project in Lesotho (Afrika). In 1984 legde hij het doctoraalexamen Scheikunde cum laude af aan de Universiteit van Amsterdam, met als hoofdvakken Chemische Technologie (katalytische vorming van methanol) en Fysische Chemie (de elektrische dubbellaag in het grensvlak van kwik en een waterige KBr oplossing). Vervolgens trad hij in dienst van Unilever Research Vlaardingen, waar hij als projectleider deel uitmaakt van de groep 'Edible Fat Products'.





